



2808915697

REFERENCE ONLY

UNIVERSITY OF LONDON THESIS

Degree PHD Year 2006 Name of Author ALQASIM,
Abdulmonium

COPYRIGHT

This is a thesis accepted for a Higher Degree of the University of London. It is an unpublished typescript and the copyright is held by the author. All persons consulting the thesis must read and abide by the Copyright Declaration below.

COPYRIGHT DECLARATION

I recognise that the copyright of the above-described thesis rests with the author and that no quotation from it or information derived from it may be published without the prior written consent of the author.

LOANS

Theses may not be lent to individuals, but the Senate House Library may lend a copy to approved libraries within the United Kingdom, for consultation solely on the premises of those libraries. Application should be made to: Inter-Library Loans, Senate House Library, Senate House, Malet Street, London WC1E 7HU.

REPRODUCTION

University of London theses may not be reproduced without explicit written permission from the Senate House Library. Enquiries should be addressed to the Theses Section of the Library. Regulations concerning reproduction vary according to the date of acceptance of the thesis and are listed below as guidelines.

- A. Before 1962. Permission granted only upon the prior written consent of the author. (The Senate House Library will provide addresses where possible).
- B. 1962 - 1974. In many cases the author has agreed to permit copying upon completion of a Copyright Declaration.
- C. 1975 - 1988. Most theses may be copied upon completion of a Copyright Declaration.
- D. 1989 onwards. Most theses may be copied.

This thesis comes within category D.



This copy has been deposited in the Library of _____



This copy has been deposited in the Senate House Library, Senate House, Malet Street, London WC1E 7HU.

DETERMINANTS OF VASCULAR
RESPONSIVENESS TO ENDOGENOUS
AND EXOGENOUS ACTIVATORS OF
GUANYLATE CYCLASES

ABDULMONIM A. ALQASIM

A thesis submitted to the University of London for
the degree of Doctor of Philosophy

April 2006

Centre for Clinical Pharmacology
Department of Medicine
University College London

UMI Number: U592579

All rights reserved

INFORMATION TO ALL USERS

The quality of this reproduction is dependent upon the quality of the copy submitted.

In the unlikely event that the author did not send a complete manuscript and there are missing pages, these will be noted. Also, if material had to be removed, a note will indicate the deletion.



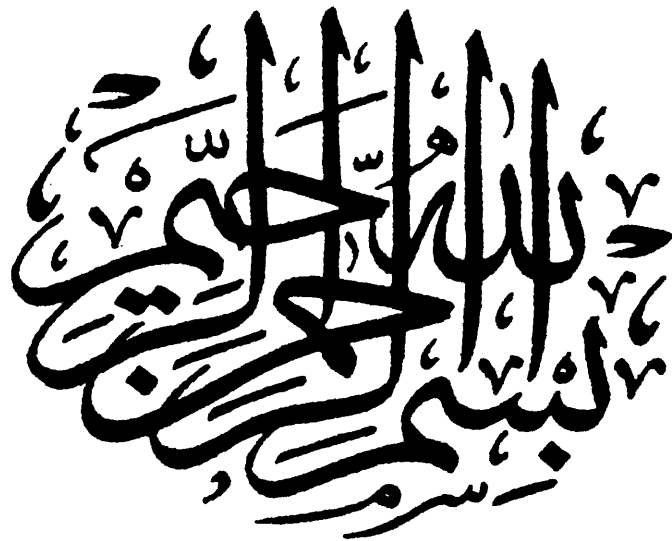
UMI U592579

Published by ProQuest LLC 2013. Copyright in the Dissertation held by the Author.
Microform Edition © ProQuest LLC.

All rights reserved. This work is protected against
unauthorized copying under Title 17, United States Code.



ProQuest LLC
789 East Eisenhower Parkway
P.O. Box 1346
Ann Arbor, MI 48106-1346



ABSTRACT

This thesis describes studies to investigate the regulation of guanylate cyclases pathways in blood vessels. Endogenous *S*-nitrosothiols have been implicated in the regulation of soluble guanylate cyclase (sGC), by modulating nitric oxide (NO) bioactivity. To determine whether the biotransformation of *S*-nitrosothiols by isolated rat aorta is enzyme-dependent, stereoisomers of *S*-nitrosoglutathione (GSNO), *S*-nitrosocysteine (CYSNO) and *S*-nitroso-*N*-acetyl-penicillamine (SNAP) were synthesised and their decomposition and relaxant effects characterised. Decomposition of these *S*-nitrosothiol stereoisomers by Cu(I), Cu(II), Cu/Zn superoxide dismutase (Cu/Zn SOD) or rat aorta was equivalent ($P>0.05$). Similarly, the vasorelaxant activity of *S*-nitrosothiol stereoisomers was equipotent ($P>0.05$). The selective Cu(I) chelator, bathocuproine disulfonic acid (BCS), blocked the decomposition of *S*-nitrosothiol stereoisomers by Cu(I), Cu(II), Cu/Zn SOD and rat aorta ($P<0.05$) and significantly inhibited their relaxant effects ($P<0.05$). These studies suggest that in rat aorta, there are no stereospecific vasorelaxant effects of *S*-nitrosothiols, consistent with non-enzymatic release of NO. Biotransformation of *S*-nitrosothiols is, in part, dependent on Cu(I) ions.

The sensitivity of sGC to NO and particulate guanylate cyclase (pGC) to atrial natriuretic peptide (ANP) regulates vasodilatation in response to these mediators. To determine the role of endogenous NO as a feedback regulator of sGC and pGC, rat aorta was incubated *in vitro* with bacterial lipopolysaccharide (LPS) to mimic many aspects of sepsis. LPS produced “high output” NO from inducible nitric oxide synthase (iNOS) and reduced the potency of the direct (SPER-NONOate, sodium nitroprusside, GSNO and BAY 58-2667) and indirect (acetylcholine and histamine) sGC activators. iNOS (1400W) but not cyclooxygenase (indomethacin) inhibition, preserved acetylcholine- and SPER-NONOate-dependent relaxations in LPS-treated vessels ($P<0.05$). LPS reduced the potency of 8-bromo-cyclic guanosine-3',5'-monophosphate ($P<0.05$), but not forskolin (adenylate cyclase activator) or 8-bromo-cyclic adenosine-3',5'-monophosphate ($P>0.05$). LPS also reduced the potency of the pGC activators C-type natriuretic peptide and ANP. 1400W, the sGC inhibitor 1H-[1,2,4]Oxadiazolo[4,3-a]quinoxalin-1-one (ODQ) or both, preserved relaxations to ANP in LPS-treated vessels. 1400W and/or ODQ also reversed established desensitisation to ANP within minutes (all $P<0.05$ versus LPS alone). These results

indicate that sGC and pGC signalling are desensitised following exposure to LPS, consistent with a compensatory mechanism offsetting high-output NO production by iNOS. This effect is specific to cGMP-dependent pathways since the cAMP pathway was unaltered. The mechanism of desensitisation is likely to involve a reversible biochemical change, since the responsiveness was restored immediately following removal of excess NO (by 1400W) or cGMP (by ODQ). These observations suggest that inflammatory cardiovascular disorders associated with excessive NO production (i.e. septic shock) are characterised by specific impairment of GC-cGMP-mediated vasorelaxation that is mediated, at least in part by cGMP, and readily reversible.

To investigate the mechanism(s) of iNOS-derived NO-mediated desensitisation of sGC and pGC, pharmacological inhibition of phosphodiesterases (type 5 (sildenafil), 1A1 (vinpocetine), and 3 (milrinone)), protein phosphatase 2A (okadaic acid and cantharidic acid), superoxide anion (SOD) and myeloperoxidase (4-aminobenzoic hydrazide) were used to probe the role of these enzymes. Desensitisation of ANP- and NO-mediated dilatation by iNOS-derived NO was unaffected by inhibition of these enzymes (all $P > 0.05$ versus LPS alone). However, activation of protein kinase C by phorbol 12-myristate 13-acetate and thymeleatoxin caused desensitisation of both guanylate and adenylate cyclases. If PKC activation causes LPS-induced desensitisation of sGC and pGC, then other mechanisms must preserve cAMP-mediated relaxation.

ACKNOWLEDGEMENTS

Special thanks to Dr Raymond MacAllister and Dr Adrian Hobbs for their constructive supervision and continuous support throughout this project.

Great thanks go to the Government of Saudi Arabia for sponsoring this work.

Special thanks to Catherine Panayiotou for showing me how to do western blotting.

My love and gratitude goes to all members of my family for their support and sacrifices.

Above all, thanks and praise are due to the almighty Allah for his great mercy and bounty throughout my life.

DECLARATION

All the work presented in this thesis is the work of Abdulmonim A. Alqasim. Contributions by others are acknowledged in the text (see page 177).

PUBLICATIONS

Alqasim, A., MacAllister, R.J. & Hobbs, A.J. (2003). Selective desensitisation of soluble and particulate guanylate cyclases in rat aorta treated with endotoxin. *Br. J. Pharmacol.*, **141**, 79P.

Section	Table of Contents	Page
	Abstract.....	3
	Acknowledgment.....	5
	Declaration.....	5
	Publications	6
	Table of Contents.....	7
	List of Figures	15
	List of Tables	20
	Abbreviations	21
	Chapter One: Introduction.....	24
1.	INTRODUCTION	25
1.1	Nitric oxide	25
1.1.1	Neuronal nitric oxide synthase	26
1.1.2	Endothelial nitric oxide synthase	26
1.1.3	Inducible nitric oxide synthase	27
1.1.4	Structure of NOS.....	28
1.1.5	Synthesis of NO.....	29
1.1.6	Soluble guanylate cyclase (NO receptor)	30
1.1.6.1	Structure of sGC.....	30
1.1.6.2	Mechanisms of activation	32
1.1.6.3	Activators of sGC.....	33
1.1.6.4	Inhibitors of sGC.....	34
1.1.7	Physiology of NO-cGMP signalling.....	34
1.1.7.1	Regulation of vascular tone	34
1.1.7.2	Regulation of platelet activity.....	35
1.1.7.3	Regulation of circulating cells.....	35
1.1.7.4	Regulation of smooth muscle proliferation	36
1.1.7.5	Regulation of endothelial cell apoptosis.....	36
1.1.8	Pathophysiology of NO-cGMP.....	36
1.1.8.1	Hypertension.....	37

1.1.8.2	Diabetes.....	37
1.1.8.3	Cardiovascular inflammation	38
1.1.8.4	Atherosclerosis	39
1.1.8.5	Septic shock.....	40
1.2	Natriuretic peptides	41
1.2.1	Natriuretic peptide receptors (particulate guanylate cyclases).....	42
1.2.1.1	Extracellular domain	42
1.2.1.2	Transmembrane domain.....	43
1.2.1.3	Intracellular domain	43
1.2.2	Mechanisms of pGC activation and cGMP-dependent relaxation.....	45
1.2.3	Physiological functions of natriuretic peptides	47
1.2.3.1	Regulation of vascular tone and blood pressure.....	47
1.2.3.2	Regulation of renal function	47
1.2.3.3	Effects on coagulation, adhesion and inflammatory cells.....	48
1.2.4	Pathophysiological roles of natriuretic peptides.....	48
1.2.5	Therapeutics of natriuretic peptides.....	50
1.3	Aspects of cGMP-mediated vasodilatation to be addressed in this thesis.....	51
1.4	Modulation of NO biology by the formation of S-nitrosothiols.....	51
1.4.1	S-nitrosothiols in biological systems.....	51
1.4.2	Formation of S-nitrosothiols.....	52
1.4.3	Formation of S-nitrosoproteins.....	53
1.4.4	Biotransformation of S-nitrosothiols	54
1.4.4.1	Role of metal ions.....	54
1.4.4.2	Role of reducing agents.....	55
1.4.4.3	Enzymatic decomposition.....	55
1.4.5	Biological roles of S-nitrosothiols.....	57
1.4.6	Pathophysiological aspects of S-nitrosothiols.....	60
1.4.7	Therapeutic implications of NO and S-nitrosothiols.....	60
1.4.8	Exploring the mechanisms of S-nitrosothiols biotransformation....	62
1.5	Desensitisation of GC-cGMP pathway.....	62

1.5.1	Evidence for desensitisation of sGC and pGC pathways.....	62
1.5.2	Mechanisms of desensitisation affecting GC-cGMP pathways.....	63
1.5.2.1	Role of phosphodiesterases.....	63
1.5.2.2	Role of protein kinase C.....	64
1.5.2.3	Desensitisation specific for NO: role of free radicals.....	65
1.5.2.4	Desensitisation affecting NPRs pathway: role of protein phosphatase 2A.....	67
1.5.3	Importance of GC desensitisation.....	67
1.6	Research questions addressed in this thesis.....	68
	 Chapter Two: Materials and Methods.....	70
2.1	Saville assay for <i>S</i>-nitrosothiols.....	71
2.1.1	Basic principle.....	71
2.1.2	Basic protocol.....	72
2.2	Stereoisomers of <i>S</i>-nitrosothiols	72
2.2.1	Basic Principles	72
2.2.2	Synthesis of <i>S</i> -nitrosothiols.....	73
2.2.3	Assessment of enzyme-dependent and independent decomposition of <i>S</i> -nitrosothiols.....	74
2.2.3.1	Non-enzymatic (chemical) decomposition.....	74
2.2.3.2	Enzymatic decomposition	74
2.3	Organ bath pharmacology.....	75
2.3.1	Rationale.....	75
2.3.2	Vessel harvesting.....	75
2.3.3	Basic Protocol.....	76
2.4	<i>In vitro</i> animal model of sepsis	77
2.5	Pharmacological interventions.....	79
2.6	Western blotting	81
2.6.1	Rationale.....	81
2.6.2	Protocols.....	81
2.6.2.1	Samples preparation.....	81
2.6.2.2	Protein separation.....	83
2.6.2.3	Protein identification.....	84

2.7	Materials.....	85
2.8	Data analysis.....	86
	Chapter Three: Biotransformation of <i>S</i>-nitrosothiols.....	87
3.1	Introduction.....	88
3.2	Experimental Protocols and statistics.....	89
3.2.1	Decomposition of <i>S</i> -nitrosothiols; effects of Cu(I), Cu(II) and copper chelation	89
3.2.2	Decomposition of L-and D-GSNO and DL-and D-SNAP by Cu/Zn SOD.....	89
3.2.3	Decomposition of L-and D-GSNO by rat aorta in the presence of BCS.....	89
3.2.4	Effects of the stereoisomers of <i>S</i> -nitrosothiols on rat aorta.....	90
3.2.5	Effect Cu(I) ions on the intracellular content of <i>S</i> -nitrosothiols.....	90
3.2.6	Calculation and statistics.....	90
3.3	Results.....	91
3.3.1	Decomposition of <i>S</i> -nitrosothiols by copper ions.....	91
3.3.1.1	Decomposition of DL-SNAP by copper ions.....	91
3.3.1.2	Decomposition of D-SNAP by copper ions.....	92
3.3.1.3	Decomposition of L-GSNO by copper ions.....	93
3.3.1.4	Decomposition of D-GSNO by copper ions.....	94
3.3.1.5	Decomposition of L-CYSNO by copper ions.....	96
3.3.1.6	Decomposition of D-CYSNO by copper ions.....	97
3.3.2	Effect of Cu/Zn SOD on the stability of <i>S</i> -nitrosothiols.....	98
3.3.2.1	Decomposition of L-GSNO by Cu/Zn SOD.....	98
3.3.2.2	Decomposition of D-GSNO by Cu/Zn SOD.....	99
3.3.2.3	Decomposition of DL-SNAP by Cu/Zn SOD.....	101
3.3.2.4	Decomposition of D-SNAP by Cu/Zn SOD.....	101
3.3.3	Decomposition of L-and D-GSNO by rat aorta.....	103
3.3.4	Responses of rat aorta to L-and D-isomers of <i>S</i> -nitrosothiols.....	105
3.3.4.1	Responses of rat aorta to DL-and D-SNAP.....	105
3.3.4.2	Responses of rat aorta to L-and D-GSNO.....	105
3.3.4.3	Responses of rat aorta to L-and D-CYSNO.....	106

3.3.4.4	Effects of BCS on the responses of rat aorta to SPER-NO.....	108
3.3.5	Effects of BCS and Cu(I) on endogenous NO-mediated responses of rat aorta.....	108
3.4	Discussion	111
3.4.1	Decomposition of <i>S</i> -nitrosothiols by copper ions	111
3.4.2	Decomposition of stereoisomers of <i>S</i> -nitrosothiols by Cu/Zn SOD.....	112
3.4.3	Decomposition of stereoisomers of <i>S</i> -nitrosothiols by rat aorta.....	113
3.4.4	Non-stereospecific relaxation of rat aorta by <i>S</i> -nitrosothiols.....	114
3.4.5	Effect of metal chelation on the response of rat aorta to <i>S</i> -nitrosothiols.....	115
3.4.6	Endogenous <i>S</i> -nitrosothiols.....	116
3.4.7	Summary and conclusions.....	116
	 Chapter Four: Desensitisation of soluble and particulate guanylate cyclases by lipopolysaccharide.....	 117
4.1	Introduction	118
4.2	Experimental Protocols and statistics.....	119
4.2.1	Organ bath studies	119
4.2.1.1	Characterisation of the effect of LPS on contraction.....	119
4.2.1.2	Effect of LPS on sGC-mediated relaxation.....	119
4.2.1.3	Effect of LPS on pGC-mediated relaxation.....	119
4.2.1.4	Effect of LPS on the sensitivity of vessels to cGMP.....	120
4.2.1.5	Effect of LPS on cAMP-mediated relaxation.....	120
4.2.1.6	Reversibility of desensitisation of cGMP-mediated relaxation.....	120
4.2.2	Western blotting	121
4.2.3	Statistics	121
4.3	Results.....	122
4.3.1	Effect of LPS on contraction.....	122
4.3.2	Effect of LPS on relaxation.....	122
4.3.2.1	Effect of LPS on sGC-mediated relaxation.....	122
4.3.2.2	Effect of LPS on pGC-mediated relaxation.....	128

4.3.2.2.1	Reversibility of desensitisation of ANP-mediated relaxation.....	129
4.3.2.3	Effect of LPS on the sensitivity of vessels to cGMP.....	130
4.3.2.4	Effect of LPS on cAMP-mediated relaxation.....	132
4.3.3	Detection of iNOS protein in LPS treated vessels	133
4.4	Discussion	134

Chapter Five: Mechanisms of Desensitisation of Guanylate Cyclase by Lipopolysaccharide

5.1	Introduction	139
5.2	Experimental Protocols and statistics.....	140
5.2.1	Effect of LPS on the sensitivity of GC in the presence of sildenafil.....	140
5.2.2	Effect of LPS on the sensitivity of GC in the presence of vinpocetine.....	140
5.2.3	Effect of LPS on the sensitivity of GC in the presence of milrinone.....	141
5.2.4	Effect of LPS on the sensitivity of sGC in the presence of SOD...	141
5.2.5	Effect of LPS on the sensitivity of sGC in the presence of 4-aminobenzoic hydrazide	141
5.2.6	Effect of the PKC activators on the sensitivity of GC and AC.....	141
5.2.7	Effect of LPS on the sensitivity of GC and AC in the presence protein phosphatase 2A inhibitors	142
5.2.8	Statistics.....	142
5.3	Results	143
5.3.1	Effect of LPS on sGC-mediated relaxation in the presence of sildenafil	143
5.3.2	Effect of LPS on pGC-mediated relaxation in the presence of sildenafil.....	143
5.3.3	Effect of LPS on sGC-mediated relaxation in the presence of vinpocetine	144
5.3.4	Effect of LPS on pGC-mediated relaxation in the presence of vinpocetine	145

5.3.5	Effect of LPS on sGC-mediated relaxation in the presence of milrinone.....	146
5.3.6	Effect of LPS on pGC-mediated relaxation in the presence of milrinone	147
5.3.7	Effect of LPS on sGC-mediated relaxation in the presence of superoxide dismutase	148
5.3.8	Effect of LPS on sGC-mediated relaxation in the presence of aminobenzoic hydrazide.....	150
5.3.9	Responses to sGC-mediated vasorelaxation in tissue precontracted with phorbol myristate acetate (PMA)	151
5.3.10	Responses to pGC-mediated vasorelaxation in tissue precontracted with PMA.....	152
5.3.11	Responses to cGMP-mediated vasorelaxation in tissue precontracted with PMA.....	153
5.3.12	Responses to AC-mediated vasorelaxation in tissue precontracted with PMA.....	154
5.3.13	Responses to sGC-mediated vasorelaxation in tissue precontracted with thymeleatoxin	155
5.3.14	Responses to pGC -mediated vasorelaxation in tissue precontracted with thymeleatoxin.....	157
5.3.15	Responses to AC-mediated vasorelaxation in tissue precontracted with thymeleatoxin	157
5.3.16	Effect of okadaic acid on the sensitivity of GC and AC-mediated relaxation	158
5.3.17	Effect of LPS on pGC-mediated relaxation in the presence of cantharidic acid.....	160
5.4	Discussion	162
5.4.1	Phosphodiesterases	162
5.4.2	Protein kinase C.....	163
5.4.3	Protein phosphatase 2A.....	165
5.4.4	Role of superoxide	166
5.4.5	Myeloperoxidase.....	166
5.4.6	Summary.....	167

	Chapter six: Summary.....	168
6	Summary.....	169
6.1	Enzymatic or non-enzymatic?	169
6.2	Feedback regulatory mechanism.....	171
6.3	What is causing the desensitisation?.....	172
6.4	Future studies.....	174
	 Contributions to this work	 177
	References List.....	178

	List of Figures	Page
	Chapter One	
Figure 1.1	Schematic representation of a NOS dimer.....	29
Figure 1.2	Biosynthesis of NO from L-arginine.....	30
Figure 1.3	Illustration showing different domains of soluble guanylate cyclase.....	32
Figure 1.4	Illustration showing different domains of NPRs.....	44
Figure 1.5	The mechanism of cGMP-mediated relaxation.....	46
	Chapter Two	
Figure 2.1	Diagram showing the steps in the Saville's assay.....	71
Figure 2.2	Illustration showing different parts of the organ bath chamber.....	78
Figure 2.3	Illustration showing the process of iNOS detection by western blotting	82
	Chapter Three	
Figure 3.1	Time-dependent decomposition of DL-SNAP in the presence or absence of Cu(I), Cu(II) and BCS.....	91
Figure 3.2	Time-dependent decomposition of D-SNAP in the presence or absence of Cu(I), Cu(II) and BCS.....	92
Figure 3.3	Time-dependent decomposition of L-GSNO in the presence or absence of Cu(I), Cu(II) and BCS.....	94
Figure 3.4	Time-dependent decomposition of D-GSNO in the presence or absence of Cu(I), Cu(II) and BCS.....	95
Figure 3.5	Time-dependent decomposition of L-CYSNO in the presence or absence of Cu(I), Cu(II) and BCS.....	96
Figure 3.6	Time-dependent decomposition of D-CYSNO in the presence or absence of Cu(I), Cu(II) and BCS.....	97
Figure 3.7	Time-dependent decomposition of L-GSNO in the presence or absence of Cu/Zn SOD, GSH, Cu/Zn SOD plus GSH or a	

	combination of Cu/Zn SOD, GSH and BCS.....	99
Figure 3.8	Time-dependent decomposition of D-GSNO in the presence or absence of Cu/Zn SOD, GSH, Cu/Zn SOD plus GSH or a combination of Cu/Zn SOD, GSH and BCS.....	100
Figure 3.9	Time-dependent decomposition of DL-SNAP in the presence or absence of Cu/Zn SOD, GSH, Cu/Zn SOD plus GSH or a combination of Cu/Zn SOD, GSH and BCS.....	101
Figure 3.10	Time-dependent decomposition of D-SNAP in the presence or absence of Cu/Zn SOD, GSH, Cu/Zn SOD plus GSH or a combination of Cu/Zn SOD, GSH and BCS.....	102
Figure 3.11	Time-dependent decomposition of L-GSNO and D-GSNO in the absence and presence of aortic tissue and BCS.....	104
Figure 3.12	Concentration-response curves to DL-SNAP and D-SNAP following 30 mins incubation with vehicle or BCS.....	105
Figure 3.13	Concentration-response curves to L- and D-GSNO following 30 mins incubation with vehicle or BCS.....	106
Figure 3.14	Concentration-response curves to L- and D-CYSNO following 30 mins incubation with vehicle or BCS.....	107
Figure 3.15	Concentration-response curves to SPER-NO following 30 mins incubation with vehicle or BCS.....	108
Figure 3.16	Concentration-response curves to ACh following 30 mins incubation with vehicle or BCS.....	109
Figure 3.17	Concentration response curves to Cu(I)-acetonitrile and acetonitrile in the presence and absence of endothelium, ODQ and L-NAME.....	110
Figure 3.18	Schematic representation showing the stereoisomers of S-nitrosothiols bind in a non-stereospecific manner to copper-containing enzymes on the cell membrane leading to decomposition and release of NO.....	115

Chapter Four

Figure 4.1	Concentration-response curves to (A) PE following 4hr incubation with vehicle or LPS and (B) U46619 following
-------------------	---

	4hr incubation with vehicle, LPS, LPS plus 1400W or LPS plus indomethacin	123
Figure 4.2	Concentration-response curves to (A) ACh and (B) histamine following 4hr incubation with vehicle or LPS.....	124
Figure 4.3	Concentration-response curves to (A) SPER-NO, (B) BAY 58-2667, (C) GSNO and (D) SNP following 4hr incubation with vehicle or LPS.....	126
Figure 4.4	Concentration-response curves to (A) ACh and (B) SPER-NO following 4hr incubation with vehicle, LPS, 1400W, LPS plus 1400W or LPS plus indomethacin.....	127
Figure 4.5	Concentration-response curves to CNP following 4hr incubation with vehicle or LPS.....	128
Figure 4.6	Concentration-response curves to ANP following 4hr incubation with vehicle, LPS, LPS plus 1400W, LPS plus ODQ or LPS plus both ODQ and 1400W.....	129
Figure 4.7	Concentration-response curves to ANP following 4hr incubation with vehicle or LPS. At 4hr, 1400W, ODQ or both ODQ plus 1400W were added to LPS-treated vessels.....	130
Figure 4.8	Concentration-response curves to (A) 8-Br-cGMP following 4hr incubation with vehicle, LPS, or LPS plus both 1400W and ODQ, or 4 hrs incubation with LPS and addition of 1400W plus ODQ at the 4hr timepoint; (B) 8-Br-cGMP following 4hr incubation with vehicle, GTN, or GTN plus ODQ.....	131
Figure 4.9	Concentration-response curves to (A) forskolin and (B) 8-Br-cAMP following 4hr incubation with vehicle or LPS.....	132
Figure 4.10	Detection of iNOS protein by western blotting following incubation of vessels with (A) vehicle and (B) LPS.....	133
 Chapter Five		
Figure 5.1	Concentration-response curves to SPER-NO following 4hr incubation with vehicle, LPS, sildenafil or LPS plus	

	sildenafil.....	143
Figure 5.2	Concentration-response curves to ANP following 4hr incubation with vehicle, LPS, sildenafil or LPS plus sildenafil.....	144
Figure 5.3	Concentration-response curves to SPER-NO following incubation with vehicle, LPS, vinpocetine or LPS plus vinpocetine.....	145
Figure 5.4	Concentration-response curves to ANP following incubation with vehicle, LPS, vinpocetine or LPS plus vinpocetine.....	146
Figure 5.5	Concentration-response curves to SPER-NO following incubation with vehicle, LPS, milrinone or LPS plus milrinone.....	147
Figure 5.6	Concentration-response curves to ANP following incubation with vehicle, LPS, milrinone or LPS plus milrinone.....	148
Figure 5.7	Concentration-response curves to (A) ACh and (B) SPER-NO following 4hr incubation with vehicle, LPS, SOD or LPS plus SOD.....	149
Figure 5.8	Concentration-response curves to SPER-NO following incubation with vehicle, LPS, ABAH or LPS plus ABAH....	150
Figure 5.9	Concentration-response curves to (A) ACh and (B) SPER-NO in vessels precontracted to an EC ₈₀ with PMA, U46619 and KCl.....	152
Figure 5.10	Concentration-response curves to ANP in vessels precontracted to an EC ₈₀ with PMA, U46619 and KCl.....	153
Figure 5.11	Concentration-response curves to 8-Br-cGMP in vessels precontracted to an EC ₈₀ with PMA and U46619.....	154
Figure 5.12	Concentration-response curves to forskolin in vessels precontracted to an EC ₈₀ with PMA, U46619 and KCl.....	155
Figure 5.13	Concentration-response curves to (A) ACh and (B) SPER-NO in vessels equipotently precontracted with thymeleatoxin and U46619.....	156

Figure 5.14	Concentration-response curves to ANP in vessels equipotently precontracted with thymeleatoxin and U46619.....	157
Figure 5.15	Concentration-response curves to forskolin in vessels equipotently precontracted with thymeleatoxin and U46619.....	158
Figure 5.16	Concentration-response curves to (A) ANP following incubation with vehicle, LPS, okadaic acid or LPS plus okadaic acid. (B) SPER-NO and (C) forskolin following 30 mins incubation with vehicle or okadaic acid.....	160
Figure 5.17	Concentration-response curves to ANP following incubation with vehicle, LPS, cantharidic acid or LPS plus cantharidic acid.....	161

	List of Tables	Page
Chapter One		
Table 1.1	Modulation of enzymes activity by <i>S</i> -nitrosothiols.....	59
Chapter Two		
Table 2.1	Specific inhibitors used to investigate enzymes involved in guanylate cyclase-cGMP signalling pathways.....	80
Chapter Three		
Table 3.1	Comparison of the decomposition of DL- and D-SNAP in the absence and presence of copper ions.....	93
Table 3.2	Comparison of the decomposition of L- and D-GSNO in the absence and presence of copper ions.....	95
Table 3.3	Comparison of the decomposition of L- and D-CYSNO in the absence and presence of copper ions.....	98
Table 3.4	Comparison of the decomposition of L-and D-GSNO in the absence and presence of Cu/Zn SOD, GSH and BCS	100
Table 3.5	Comparison of the decomposition of DL-and D-SNAP in the absence and presence of Cu/Zn SOD, GSH and BCS	102
Table 3.6	Comparison of the decomposition of L-and D-GSNO in the absence and presence of aortic tissue and BCS.....	103

Abbreviations

1400W	N-(3-(aminomethyl)benzyl) acetamidine
ABAH	4-Aminobenzoic hydrazide
AC	Adenylate cyclase
ACh	Acetylcholine
ADMA	Asymmetric dimethylarginine
ADP	Adenosine diphosphate
ANP	Atrial natriuretic peptide
AS	Ammonium sulphamate
BCS	Bathocuproinedisulfonic acid
BH ₄	Tetrahydrobiopterin
BNP	Brain natriuretic peptide
8-Br-cAMP	8-Bromoadenosine-3',5'-cyclic monophosphate
8-Br-cGMP	8-Bromoguanosine-3',5'-cyclic monophosphate
CaM	Calmodulin
cGMP	Cyclic guanosine-3',5'-monophosphate
CHF	Congestive heart failure
CNP	C-type natriuretic peptide
CO	Carbon monoxide
COX-2	Cyclooxygenase-2
Cu(I)	Copper(I)-acetonitrile
Cu(II)	Copper(II)-sulphate
Cu/Zn-SOD	Cu/Zn superoxide dismutase
CYSNO	S-nitrosocysteine
DAG	Diacylglycerol
ECL	Enhanced chemiluminescence
EDHF	Endothelium-derived hyperpolarizing factor
EDRF	Endothelial derived relaxing factor
EDTA	Ethylenediamine-tetraacetic Acid
EGTA	Ethylene glycol-bis-(2-aminoethyl)-N,N,N', N'-tetraacetic acid
eNOS	Endothelial nitric oxide synthase

FAD	Flavin adenine dinucleotide
FMN	Flavin mononucleotide
GC	Guanylate cyclase
GCD	Guanylate cyclase catalytic domain
GSH	Glutathione
GSNO	<i>S</i> -nitrosoglutathione
GSSG	Thiol disulfide
GTN	Glyceryl trinitrate
GTP	Guanosine-5'-triphosphate
HO-1	Haem-oxygenase-1
ICAM-1	Intercellular adhesion molecule-1
IL-1 β	Interleukin-1 β
IM	Indomethacin
iNOS	Inducible nitric oxide synthase
IP3R	Inositol triphosphate receptor
IRAG	Inositol triphosphate associated G-kinase
IRAK	Interleukin-1 receptor-associated kinase
KCl	Potassium chloride
KHD	Kinase-homologous regulatory domain
LBP	LPS-binding protein
LDL	Low density lipoprotein
L-NAME	N ^G -nitro-L-arginine methyl ester
L-NMMA	N ^G -monomethyl-L-arginine
LPS	Lipopolysaccharide
MPO	Myeloperoxidase
NADPH	Nicotinamide adenine dinucleotide phosphate
NED	N-(1-naphthyl) ethylenediamine dihydrochloride
NF- κ B	Nuclear factor-kappa β
nNOS	Neuronal nitric oxide synthase
NO	Nitric oxide
NPR	Natriuretic peptide receptor
NPs	Natriuretic peptides

O ₂ ⁻	Superoxide anion
ODQ	1H-[1,2,4]Oxadiazolo[4,3-a]quinoxalin-1-one
ONOO-	Peroxynitrite
PBS	Phosphate buffered saline
PDE	Phosphodiesterases
PDI	Protein disulfide isomerase
PE	Phenylephrine
pGC	Particulate guanylate cyclase
PKC	Protein kinase C
PKG	Protein kinase G
PMA	Phorbol 12-myristate 13-acetate
PP2A	Protein phosphatase 2A
ROS	Reactive oxygen species
RSNO	<i>S</i> -nitrosothiols
SA	Sulphanilamide
SDMA	Symmetric dimethylarginine
SDS	Sodium dodecyl sulphate
SEM	Standard error of the mean
sGC	Soluble guanylate cyclase
SNAP	<i>S</i> -nitroso- <i>N</i> -acetyl-penicillamine
SNOAlb	<i>S</i> -nitrosoalbumin
SNOHb	<i>S</i> -nitrosohaemoglobin
SNP	Sodium nitroprusside
SPER-NO	Spermine-NONOate
TEMED	Tetramethylethylenediamine
TLR4	Toll-like receptor 4
t-PA	Tissue-type plasminogen activator
TRAF6	TNF receptor-associated factor-6
TW-ANOVA	Two-way analysis of variance
U46619	9,11-Dideoxy-11 α ,9 α epoxymethano-prostaglandin
VCAM-1	Vascular cell adhesion molecule-1
VSMC	Vascular smooth muscle cell

CHAPTER ONE

INTRODUCTION

1. INTRODUCTION

Guanylate cyclases (GC) synthesise cyclic guanosine-3',5'-monophosphate (cGMP) in response to nitric oxide (NO) and natriuretic peptides (NPs). Two isoforms of GC are expressed in mammalian cells. Soluble guanylate cyclase (sGC), which is activated principally by NO, and a family of particulate guanylate cyclases (pGC) that act as receptors for the natriuretic peptide family (Lucas *et al.*, 2000). Upon production of intracellular cGMP, physiological effects via a variety of mechanisms. These include activation of protein kinases, opening of ion channels, and altering intracellular cyclic nucleotide concentrations through regulation of phosphodiesterases (PDEs) (Hobbs, 1997; Lucas *et al.*, 2000). Activation of these cellular targets contributes to the regulation of vascular tone, platelet function and cellular proliferation and trafficking (Vallance & Chan 2001 and Ahluwalia *et al.*, 2004a). In contrast, abnormalities of the GC-cGMP pathways occur in diseases such as hypertension, atherosclerosis, heart failure, diabetes and sepsis (MacAllister & Vallance, 1994; Vallance & Chan, 2001 and Han & Hasin, 2003), and contribute to the vascular phenotype of these conditions. Thus, regulation of GC-cGMP bioactivity is a fundamental physiological process, and a deeper understanding of this pathway is likely to lead to the development of novel therapeutics. This chapter describes current understanding of the molecular, biological, physiological and pathophysiological roles of the two GC-cGMP systems in the cardiovascular system. In section 1.1, the NO:sGC:cGMP is discussed, followed by section 1.2 describing the NP:pGC:cGMP. Later sections will focus on the specific research questions that were the focus of my experimental work.

1.1 Nitric oxide

Originally thought to act merely as an inert layer lining the luminal surface of blood vessels, it is now apparent that endothelial cells play important roles in the physiology and pathophysiology of the cardiovascular system (Vallance & Chan, 2001). Under normal physiological conditions, the vascular endothelium regulates vascular homeostasis through effects on vascular tone, circulating cell function, coagulation and cellular proliferation. It performs these functions through the release of endothelium-derived regulating factors such as endothelium-derived relaxing

factor (EDRF) (Furchgott & Zawadzki, 1980), prostacyclin and endothelium-derived hyperpolarising factors (Busse *et al.*, 2002; Chauhan *et al.*, 2003a). Aberrant function of these mediators can contribute to various cardiovascular diseases.

EDRF was discovered by Furchgott and Zawadzki in 1980 where they demonstrated the ability of the endothelium to release a potent, labile vasorelaxant factor (Furchgott & Zawadzki, 1980). Subsequently, Palmer *et al.* demonstrated that cultured endothelial cells from porcine aorta release NO, at a concentration sufficient to induce vasodilatation, thus demonstrating that EDRF was NO (Ignarro *et al.*, 1987; Palmer *et al.*, 1987). NO is synthesised by means of nitric oxide synthase (NOS). Three isoforms of NOS have been identified; constitutive, neuronal NOS (nNOS) (Knowles *et al.*, 1989) endothelial NOS (eNOS) (Palmer *et al.*, 1988), and inducible nitric oxide synthase (iNOS) (Busse & Mulsch, 1990).

1.1.1 Neuronal nitric oxide synthase

The gene encoding neuronal NOS (nNOS or NOS1; 160 kDa) is localised to chromosome 12 (Marsden *et al.*, 1993). nNOS is expressed in a variety of neuronal cells (Bredt & Snyder 1994) and other cells types such as the adventitia of blood vessels (Nozaki *et al.* 1993), skeletal myocytes (Kobzik *et al.*, 1994) and cardiac myocytes (Xu *et al.*, 1999). nNOS exists as a soluble and membrane bound isoform (Hecker *et al.*, 1994). It is regulated acutely through Ca^{2+} –calmodulin (CaM) binding (Abu-Soud *et al.*, 1994).

1.1.2 Endothelial nitric oxide synthase

The gene encoding endothelial NOS (eNOS or NOS3; 134 kDa) is localised to chromosome 7 and consists of 26 exons (Marsden *et al.*, 1993). eNOS is the major NOS isoform expressed in the cardiovascular system. Although eNOS expression occurs primarily in the vascular endothelium, this isoform is also expressed in a wide variety of other cell types such as cardiomyocytes, leukocytes, and neurons (Li *et al.*, 2002). The majority of eNOS is located in the membrane fraction of cells, with only a small fraction localised in the cytosol (Forstermann *et al.*, 1991). eNOS is directed to the plasma membrane by myristoylation (Pollock *et al.*, 1992), a co-translational

modification catalysed by *N*-myristoyltransferase in which an *N*-terminal glycine residue is modified by the formation of a fatty acyl amide bond (Boutin, 1997). This process helps to direct and anchor eNOS to the plasma membrane. eNOS is localised in the caveolae where it is bound and inhibited by caveolin (Michel *et al.*, 1997). Similar to nNOS, eNOS is largely dependent on the intracellular Ca^{2+} concentration and stimuli that increase intracellular Ca^{2+} (such as acetylcholine, histamine, thrombin, serotonin, adenosine diphosphate (ADP), bradykinin, norepinephrine, substance P, and isoproterenol) cause the formation of Ca^{2+} -CaM complexes, resulting in the binding to eNOS and consequently the dissociation of caveolin (Michel *et al.*, 1997). eNOS remains activated until intracellular Ca^{2+} levels drop. Activation of eNOS also occurs following phosphorylation of serine-1179 by protein kinase B (Fulton *et al.*, 1999).

Although eNOS is often considered to be a constitutive enzyme, there are numerous factors that have been shown to increase the basal expression and activity of the enzyme including shear stress (Uematsu *et al.*, 1995), hypoxia (Le Cras *et al.*, 1996), oxidised low-density lipoproteins (Ramasamy *et al.*, 1998) and hormones, such as oestrogen (Ruehlmann & Mann, 2000). Like nNOS, eNOS produces NO at nanomolar concentrations to exert its physiological effects.

1.1.3 Inducible nitric oxide synthase

Inducible nitric oxide synthase (iNOS or NOS2; 130 kDa) is expressed and activated in many types of cells, including vascular endothelial cells (Gross *et al.*, 1991), smooth muscle cells (Koide *et al.*, 1993) and macrophages (Xie *et al.*, 1993) following exposure to the cell wall components of gram negative bacteria, lipopolysaccharide (LPS) and the proinflammatory cytokines interleukin-1 β (IL-1 β), IL-2, IL-6, tumour necrosis factor (TNF) and interferon- γ (Kirkeboen & Strand, 1999). The gene encoding iNOS is localised to chromosome 17. An important distinctive feature of iNOS is that the enzyme is regulated in a Ca^{2+} -independent manner, as binding of calmodulin to iNOS is tight even at low Ca^{2+} (Busse & Mulsch, 1990). iNOS produces micromolar concentrations of NO; it is generally associated with the cytotoxic effects of NO and promoting cardiovascular pathophysiology (Shah, 2000).

LPS can trigger the expression of iNOS through interaction with a LPS-binding protein (LBP), which delivers LPS to CD14, a high-affinity LPS receptor on the cell membrane (Wright *et al.*, 1990; Choi & Lee, 2004). Toll-like receptor 4 (TLR4) in conjunction with the small extracellular protein named MD-2 interacts with the CD14-LPS complex, and then activates an intracellular signalling cascade, including interleukin (IL)-1 receptor-associated kinase (IRAK) and myeloid differentiation protein (MyD88). These in turn activate downstream molecules including TNF receptor-associated factor-6 (TRAF6) (Zhang *et al.*, 1999). Activation of nuclear factor-kappa β (NF- κ B) is crucial for induction of iNOS in vascular smooth muscle cells (VSMC) (Schini-Kerth *et al.*, 1997). NF- κ B is present in the cytosol as an inactive heterotrimer, which upon phosphorylation, dissociation and proteolytic degradation of its inhibitory I κ B α subunit, is activated and translocates to the nucleus where the p65/p50 heterodimer binds to the corresponding response element in the promoter of the iNOS gene (Xie *et al.*, 1994; Gomez *et al.*, 2005). Recent studies demonstrate a role for eNOS in the expression of iNOS via NF- κ B (Vo *et al.*, 2005, Connelly *et al.*, 2005). iNOS induction is associated with 'high output' production of NO (Thiemermann, 1997).

1.1.4 Structure of NOS

Although there are some structural differences between NOS isoforms, they share common structural features. NOS consists of two monomers (Figure 1.1), each monomer having two functionally distinct domains. The N-terminal oxygenase domain contains the catalytic site, a haem prosthetic group and binding sites for L-arginine and the redox cofactor, tetrahydrobiopterin (BH₄) (Ghosh & Stuehr, 1995). Two important residues for L-arginine binding have been located at amino acids residues Glu-371 and Asp-376 (these numbers refer to the location of the amino acid in the sequence in the enzyme) in iNOS (Gachhui *et al.*, 1997) and the analogous Glu-361 in eNOS (Chen *et al.*, 1997). BH₄ is bound to Cys-99 in eNOS (Chen *et al.*, 1995) and Gly-450 and Ala-453 in iNOS (Cho *et al.*, 1995). The C-terminal reductase domain has binding sites for nicotinamide adenine dinucleotide phosphate (NADPH), the flavin adenine dinucleotide (FAD), flavin mononucleotide (FMN) and CaM, which are required for electron transfer (Stuehr *et al.*, 1991). The reductase domain architecture is similar to that of cytochrome P450BM3 (Narhi & Fulco, 1987). All

NOS isoforms are only fully functional when dimeric. Dimerisation of eNOS occurs by the binding of haem, without which, NOS exists only as a monomer (Klatt *et al.*, 1996). Crystal structures of the NOS haem domain of all three isoforms (Fischmann *et al.*, 1999) show a tightly associated homodimer with the BH₄ binding sites sandwiched at the dimer interface. Stabilisation of the dimer requires Zn binding to two cysteine residues from each subunit (Hemmens *et al.*, 2000).

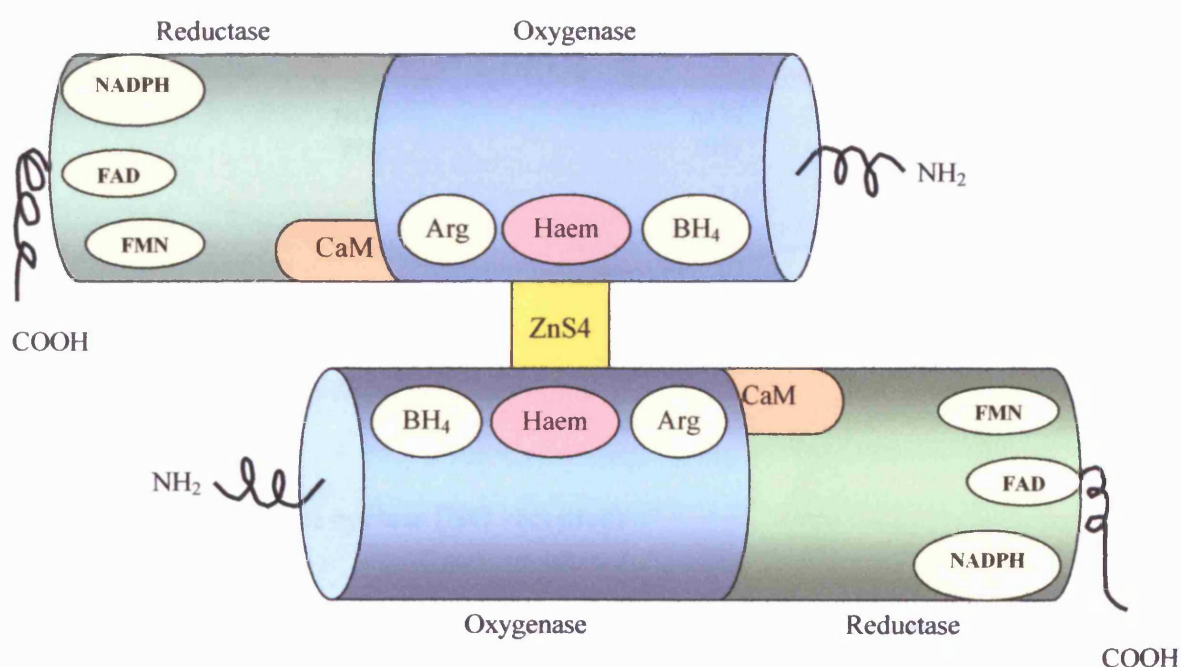


Figure 1.1 Schematic representation of a NOS dimer

1.1.5 Synthesis of NO

All three isoforms catalyse the oxidation of L-arginine to produce L-citrulline and NO (Figure 1.2). The reaction starts by hydroxylation of L-arginine to form *N*^G-hydroxy-L-arginine (L-OHArg) (Leone *et al.*, 1991). The reductase domain of one subunit catalyses the transfer of electrons from NADPH via FAD and FMN to CaM. CaM is essential for the transdomain transfer of electrons to the haem group in the oxygenase domain of the second subunit (Abu-Soud & Stuehr, 1993). Binding of O₂ to the oxygenase domain catalyses oxidative cleavage of L-OHArg leading to the formation of citrulline and NO (Marin & Rodriguez-Martinez, 1997). Once

synthesised, the NO diffuses across the endothelial cell membrane and enters the VSMC where it activates its main cellular target, sGC, leading to an increase in intracellular cGMP.

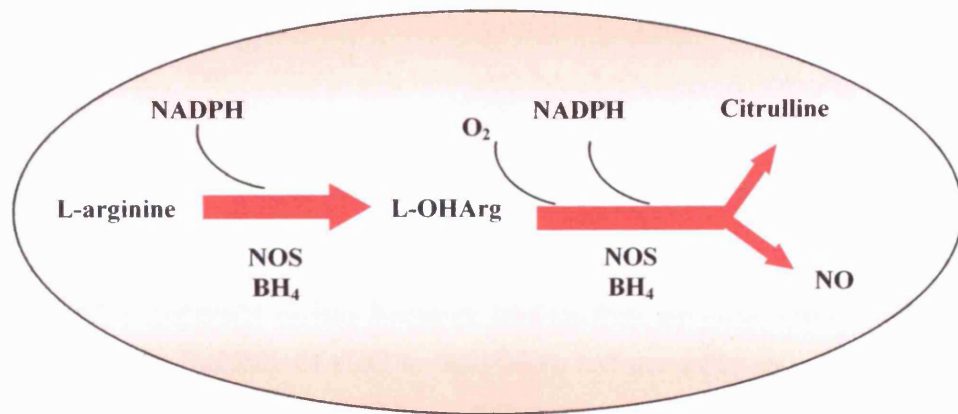


Figure 1.2 Biosynthesis of NO from L-arginine.

1.1.6 Soluble guanylate cyclase (NO receptor)

Although NO can react with other molecules (section 1.4.5), soluble guanylate cyclase (sGC) is considered as the principal physiological target for the freely diffusible intercellular messenger. Through sGC, the NO signals are coded into cytosolic cGMP accumulation. In turn, cGMP targets several classes of downstream effectors, principally cGMP-dependent kinase G, cyclic nucleotide-gated ion channels and cGMP-stimulated and-inhibited phosphodiesterases (a further description is found in section 1.2.2) (Hobbs, 1997).

1.1.6.1 Structure of sGC

Soluble guanylate cyclase is widely expressed in the cardiovascular system and other cell types. Originally, sGC was purified from bovine and rat lung and shown to exist as a heterodimer. Several isoforms of sGC have been cloned and characterised. In the rat, sGC consists of 82 kDa (α 1) and 70 kDa (β 1) subunits

(Kamisaki *et al.*, 1986). Further subunits have also been identified from human foetal brain; an 82 kDa subunit designated $\alpha 2$ and a 76 kDa subunit designated $\beta 2$ (Harteneck *et al.*, 1991; Yuen *et al.*, 1990). Each subunit consists of at least three domains: (i) Haem-binding domain, (ii) catalytic domain and (iii) dimerisation domain (Figure-1.3). The haem-binding domain is located at the N-terminus of each subunit. The presence of the haem prosthetic group is required for activation of sGC by NO (Ignarro *et al.*, 1982). Haem is a five-membered nitrogen-containing ring with four nitrogen atoms coordinated with a central iron that can be either Fe^{2+} (ferrous or the reduced form) or Fe^{3+} (ferric or the oxidised form). The fifth member of the ring in sGC is an imidazole axial ligand coordinated by the $\beta 1$ subunit at His-105 (Stone & Marletta, 1994). Mutation of this histidine located near the N-terminus of the $\beta 1$ subunit, results in the inability of sGC to bind haem and produces an enzyme that is unresponsive to NO (Ignarro *et al.*, 1982).

Catalytic domains are present in the C-terminus of both α and β subunits. The C-terminal of each subunit exhibits high homology not only among these subunits but also between the C-terminal domains of pGC and adenylate cyclase (AC) (Hobbs, 1997). Although both α and β subunits contain their own catalytic domains, sGC activity is dependent upon co-expression of both subunits. For example, expression of either the $\alpha 1$ or the $\beta 1$ subunit in L cell fibroblasts does not result in any measurable sGC activity (Buechler, *et al.*, 1991). The catalytic conversion of guanosine-5'-triphosphate (GTP) to cGMP by the catalytic domain relies on the presence of the divalent cations Mn^{2+} and Mg^{2+} as cofactors (Ohlstein *et al.*, 1982). The availability of the latter two cations can modulate enzyme activity by enhancing activation, as well as increasing substrate affinity for sGC (Wolin *et al.*, 1982).

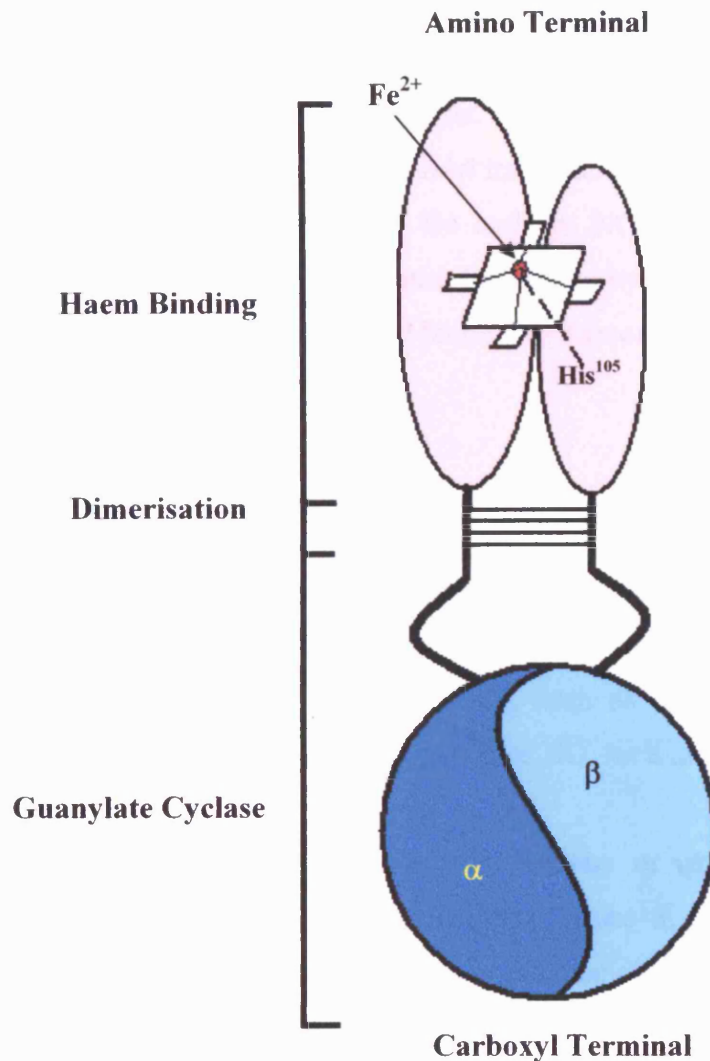


Figure 1.3 Illustration showing different domains of soluble guanylate cyclase.

1.1.6.2 Mechanisms of activation

Activation of sGC by NO involves the binding of NO to the prosthetic haem group, which leads to up to 200-fold activation of the enzyme (Stone & Marletta, 1994). Several models exist to explain the activation of sGC by NO; the simplest is thought to occur in two steps: first, NO binds to the sixth coordinated position of the haem and results in a six-coordinated NO- Fe^{2+} -histidine-complex. The subsequent step is the breakage of the histidine bond leading to the formation of a five-

coordinated nitrosyl-haem complex (Friebe & Koesling, 2003), the resulting conformational changes presumably propagates to the active site of the enzyme, and causes an increase in the rate of cGMP synthesis. A more complex model of NO activation of sGC has been suggested. In this model transition from the six-coordinate to the five-coordinate complex depends on the ambient NO concentration. This results in a scheme where NO not only activates the enzyme by binding to the haem but also regulates the velocity of activation via binding to a second non-haem binding site (Zhao *et al.*, 1999).

1.1.6.3 Activators of sGC

In addition to endogenously generated NO from the endothelium or released from *S*-nitrosothiols, sGC is activated by exogenous NO administered in the form of NO-donors. These agents release NO spontaneously, such as spermine-NONOate (SPER-NO) or, require metabolism by tissues to release NO, such as organic nitrates (Bennett *et al.*, 1994).

Carbon monoxide (CO) also increases sGC activity *in vitro*, but is less effective (4-fold increase) than NO (200-fold increase; Stone & Marletta, 1994). Endogenous CO generation stems primarily from the enzymatic degradation of haem by the haem oxygenase enzyme system. Its small effect *in vitro* may be amplified by *in vivo* factors; exogenous compounds such as YC-1 and BAY-41-2272 have been found to enhance the effect of CO *in vitro*, so that CO activates sGC to the same level as NO (Kim *et al.*, 2006). YC-1, a benzylindazol derivative, activates sGC independently of NO and CO (Ko *et al.*, 1994; Hobbs, 1997), but also potentiates the effect of NO, presumably by stabilisation of the enzyme's active configuration (Wu *et al.*, 1995). Other compounds activating sGC in a haem-dependent manner include BAY-41-2272 and BAY 41-8543 (Stasch *et al.*, 2002a). BAY 58-2667 increases the activity of sGC in a haem-deficient enzyme and in the presence of ODQ (Stasch *et al.*, 2002b; Hobbs, 2002). They are potent vasodilators and inhibitors of platelet activity (Hobbs & Moncada, 2003). Further investigations on the mechanism of action of this class of compound have shown that there is a regulatory binding site in the region of cysteines 238 and 243 in the α subunit (Stasch *et al.*, 2001).

1.1.6.4 Inhibitors of sGC

The most widely used inhibitor is ODQ, which is a potent and selective inhibitor of sGC in brain slices (Garthwaite *et al.*, 1995). ODQ does not lead to the inhibition of pGC or AC or lead to the inactivation of NO (Hobbs, 1997). ODQ has no effect on NOS activity at concentrations less than 30 μ M (Feelisch *et al.*, 1999), suggesting that this compound is suitable for differentiating between the cGMP-dependent and cGMP-independent effects of NO. sGC can also be inhibited by methylene blue and LY-83583, but these compounds are non-selective and interfere with NO synthesis by inhibition of NOS (Luo *et al.*, 1995).

1.1.7 Physiology of NO-cGMP signalling

In the vasculature, NO synthesised from endothelial cells plays critical roles in the regulation of vascular tone, platelet activity, smooth muscle proliferation and endothelial cell apoptosis. This section describes in more details the contribution of NO-cGMP pathway in the regulation of vascular homeostasis.

1.1.7.1 Regulation of vascular tone

Several lines of evidence indicate that there is a continuous basal synthesis of NO from the vascular endothelium to maintain resting vascular tone in animals and humans. In rings of rabbit aorta, inhibition of basal endothelial NO synthesis by N^G-monomethyl-L-arginine (L-NMMA), a specific inhibitor of endothelium-derived NO synthesis, causes significant endothelium dependent contraction (Rees *et al.*, 1989). Intravenous infusion of L-NMMA into experimental animals induces a dose dependent increase in blood pressure which is reversed by intravenous administration of L-arginine (Rees *et al.*, 1989). Mice with disruption of the eNOS gene are hypertensive and isolated blood vessels of these mice do not relax to endothelium-dependent vasodilators such as acetylcholine (ACh) (Huang *et al.*, 1995). In the human forearm vasculature, infusion of L-NMMA into the brachial artery causes substantial dose-dependent vasoconstriction, suggesting that generation of NO is crucial in maintaining peripheral vasodilatation in humans (Vallance *et al.*, 1989). Pharmacological inhibition of NO synthesis causes dose-dependent increases in blood

pressure, systemic and pulmonary vascular resistance in healthy human (Stamler *et al.*, 1994). Thus NO plays crucial role in the regulation of vascular tone.

1.1.7.2 Regulation of platelet activity

NO released by the endothelial cells towards the vascular lumen is a potent inhibitor of platelet aggregation and adhesion to the vascular wall, via activation of platelet sGC (Radomski *et al.*, 1987). *In vitro* studies have shown that stimulation of sGC inhibits aggregation of washed human platelets (Furlong *et al.*, 1987). It has been suggested that NO from endothelial cells diffuses into platelets and binds to sGC, leading to an increase in cGMP and a decrease in intracellular Ca^{2+} flux. This decrease in Ca^{2+} flux may decrease platelet association with fibrinogen (Mendelsohn *et al.*, 1990). In mice lacking eNOS there is a significant decrease in the bleeding times suggesting that sGC activation by NO regulates thrombus formation (Freedman *et al.*, 1999). These observations suggest that NO is important for regulation of platelet activity.

1.1.7.3 Regulation of circulating cells

Endothelium-derived NO plays important roles in the regulation of cellular trafficking in blood vessels. Inhibition of NO release enhances leukocyte adherence to the coronary endothelium (Lefer & Ma, 1993). Adhesion molecules regulate attachment and trans-endothelial migration of leukocytes. NO inhibits IL-1 β -mediated expression of intercellular adhesion molecule-1 (ICAM-1) and vascular cell adhesion molecule-1 (VCAM-1) (Takahashi *et al.*, 1996). NO decreases the expression of monocyte chemoattractant protein-1 (MCP-1), and of surface adhesion molecules such as CD11/CD18, thereby preventing leukocyte adhesion to vascular endothelium and leukocyte migration into the vascular wall (Li & Forstermann, 2000). Recent work has shown that leukocyte recruitment is enhanced in eNOS knockout mice and activation of sGC reduces leukocyte rolling and adhesion to levels observed in wild type animals by down-regulation of P-selectin expression (Ahluwalia *et al.*, 2004b). These findings suggest that NO is important anti-adhesive and anti-atherogenic agent.

1.1.7.4 Regulation of smooth muscle proliferation

Smooth muscle cells are normally quiescent in the vasculature, and their proliferation is associated with narrowing of the arterial lumen. Therefore, regulation of their growth is highly important. Activation of sGC by NO was shown to inhibit the proliferation of VSMC in a cGMP-dependent manner (Garg & Hassid, 1989). Mice lacking eNOS showed increased intimal hyperplasia following balloon injury compared with normal mice (Moroi *et al.*, 1998). NO can also inhibit smooth muscle proliferation in a cGMP-independent manner, by directly inhibiting the activity of arginase and ornithine decarboxylase to decrease the formation of polyamines that are key to cell proliferation (Ignarro *et al.*, 2002). Thus, by inhibiting the proliferation and migration of VSMC, NO may protect against cardiovascular diseases such as atherogenesis. This effect of NO in combination with its effects on cellular adhesion, platelets and vascular tone give rise to the thesis that endogenous NO is an important antiatherogenic, cytoprotective mediator.

1.1.7.5 Regulation of endothelial cell apoptosis

Increased endothelial cell apoptosis is associated with atherosclerosis. Activation of sGC by NO protects endothelial cells from apoptosis. Low concentrations of NO antagonise the apoptosis-inducing stimuli, such as TNF- α , but high concentrations of NO can induce apoptosis (Shen *et al.*, 1998). The protective effects of NO against apoptosis of endothelial cells might involve cGMP-dependent inhibition of cytochrome *c* release from mitochondria (Chung *et al.*, 2001). Thus NO plays a dual role in the regulation of apoptosis depending on its concentration.

1.1.8 Pathophysiology of NO-cGMP

A number of cardiovascular disorders are associated with endothelial dysfunction and/or abnormality in the NO-cGMP pathway such as hypertension (MacAllister & Vallance, 1994), diabetes and inflammatory vascular diseases such as septic shock and atherosclerosis (Vallance & Chan 2001). This section describes the role of NO-cGMP pathway in these diseases.

1.1.8.1 Hypertension

Physiologically, vascular tone is regulated by a balance between vasodilators and vasoconstrictors and any abnormality in this balance is likely to lead to abnormal vascular function. Substantial evidence from animal and human studies indicates that endothelial function is impaired in hypertension, with reduced NO production or bioactivity (Bolad & Delafontaine, 2005). Although many studies report normal smooth muscle dilator function, there is evidence that the activity of the downstream component of NO-cGMP pathway is reduced. In spontaneously hypertensive rats (SHR), the levels of both subunits of sGC are downregulated and the relaxation of aortic rings to the sGC activator YC-1 is also attenuated (Ruetten *et al.*, 1999). In lead-induced hypertension, relaxation to both ACh and sodium nitroprusside (SNP) is reduced, with reduced expression of both $\alpha 1$ and $\beta 1$ subunits of sGC (Marques *et al.*, 2001). Recent work has shown that the levels of sGC and cGMP were significantly lower in 4- and 8-week SHR compared with age-matched rats (Ndisang & Wang, 2003). In summary, these data suggest that in hypertension both upstream (endothelium) and downstream (smooth muscle) aspects of the NO-cGMP pathway are impaired.

1.1.8.2 Diabetes

A hallmark of diabetic vascular disease is endothelial dysfunction. Reduced endothelium-mediated vasodilation has been found in studies in arteries from diabetic animals and humans. In streptozotocin-induced diabetic rats, endothelium-dependent relaxation to ACh is impaired. Acute administration of L-arginine in these animals normalises the defective relaxation to ACh (Pieper & Peltier, 1995). Recent work in this animal model of diabetes also showed that the impaired endothelium-dependent relaxation to ACh is associated with increased levels of endogenous NOS inhibitors (asymmetric dimethyl L-arginine (ADMA)) suggesting the possible role of these substances in the endothelial dysfunction of type 1 diabetes mellitus (Xiong *et al.*, 2003).

In a model of type 2 diabetes mellitus (Goto-Kakizaki rats) relaxation of mesenteric arteries to ACh and SNP was blunted consistent with reduced activity and/or expression of sGC (Witte *et al.*, 2002). In men with type 2 diabetes mellitus, McNeill *et al* showed that the forearm blood flow responses to the endothelium-dependent vasodilator is significantly impaired in diabetic men compared with control subjects (McNeill *et al.*, 2000). Moreover, in patients with type 2 diabetes mellitus, the forearm blood flow responses to both methacholine chloride and SNP are significantly reduced suggesting either reduced sensitivity of smooth muscle sGC or increased breakdown of NO (Williams *et al.*, 1996). Taken together, these observations indicate that the NO-cGMP pathway is impaired in both types of diabetes mellitus.

1.1.8.3 Cardiovascular inflammation

In animals and humans there is evidence that acute inflammation causes endothelial dysfunction. This might provide a mechanism to link the association between acute systemic inflammation and the transiently elevated risk of cardiovascular events (Vallance *et al.*, 1997). Hingorani and co-workers demonstrated that systemic inflammation caused by *salmonella typhi* vaccine in healthy volunteers impairs endothelial but not smooth muscle responses in resistance and conduit vessels (Hingorani *et al.*, 2000). Similar findings were shown by Kharbanda *et al* in which systemic inflammation causes endothelial dysfunction that was prevented by pre-treatment with aspirin (possibly through modulation of the cytokine cascade) (Kharbanda *et al.*, 2002). In healthy volunteers, induction of acute systemic inflammation by low doses of *Escherichia coli* endotoxin impairs forearm blood flow responses to ACh but not glyceryl trinitrate (GTN). The anti-oxidant vitamin C counteracted this effect of endotoxin, suggesting that oxidative stress may play an important role in the pathogenesis of endothelial dysfunction during inflammation (Pleiner *et al.*, 2002). Recent studies by Clapp *et al* also demonstrated a role for oxidative stress in inflammation-induced endothelial dysfunction (Clapp *et al.*, 2004). In addition to the role of oxidative stress in causing endothelial dysfunction, Mittermayer and others examined the role of the cofactor BH₄ and found that forearm blood flow responses to ACh are impaired following 3.5 hr infusion of *Escherichia coli* endotoxin that was restored to baseline reactivity by BH₄ and vitamin C. The

authors suggested that vitamin C may exert some of its effects by increasing BH₄ concentrations (Mittermayer *et al.*, 2005). These findings demonstrate that acute inflammation in humans is associated with oxidative stress mediated-endothelial dysfunction.

1.1.8.4 Atherosclerosis

The NO-cGMP pathway plays a crucial role in the inhibition of smooth muscle proliferation, cellular adhesion and platelet aggregation as mentioned above. Endothelial dysfunction is likely to be involved in the initiation and development of atherosclerotic lesions, and contribute to the pathogenesis of plaque instability and thrombosis (Charakida *et al.*, 2006).

Abnormal endothelial function occurs in atherosclerotic animals and humans. Studies on arterial segments from hypercholesterolaemic rabbits demonstrated that there is accelerated inactivation of NO, probably due to enhanced formation of the superoxide anion (O₂⁻) (Minor *et al.*, 1990). In patients with hypercholesterolemia, endothelium-dependent vasodilatation to ACh is impaired in both coronary and peripheral vessels before the development of clinical atherosclerosis (Chowienczyk *et al.*, 1992). In human atherosclerosis, immunohistochemical measurement of the level of eNOS indicates reduced eNOS protein expression in carotid arteries obtained during surgery (Oemar *et al.*, 1998). Overproduction of the endogenous inhibitors of eNOS, ADMA, has been reported in patient with atherosclerosis, this increased level positively correlated with risk factors for atherosclerosis (Miyazaki *et al.*, 1998). These studies demonstrate different mechanisms that reduce the bioavailability of NO and contribute to atherogenesis.

Although much of the evidence points to endothelial dysfunction, there is also evidence of dysfunction in the sGC-cGMP pathway downstream from NO in atherosclerosis. Low density lipoprotein (LDL), which plays a key role in the development of atherosclerosis, reduces the responsiveness of sGC to nitrovasodilators (Schmidt *et al.*, 1992). A recent study has shown that hypercholesterolemia induces overexpression of dysfunctional vascular sGC, which may contribute to the pathogenesis of atherosclerosis (Laber *et al.*, 2002). In

summary, atherosclerosis is a multi-factorial vascular disease, in which impairment of the NO-cGMP pathway plays an important role in its pathogenesis.

1.1.8.5 Septic shock

Septic shock is a systemic inflammatory state characterised by vascular smooth muscle dysfunction, leading to hypotension, inadequate tissue perfusion, and multiple organ failure with a high mortality rate (Shah, 2000). It is generally accepted that the hyporeactivity to vasoconstrictors associated with septic shock is due to over-activation of the NO-cGMP pathway as a result of iNOS-derived NO (Shah, 2000). This was suggested by studies showing the reversal of endotoxin-induced hypotension through pharmacological inhibition of iNOS. In animal models of septic shock, administration of the NOS inhibitor (N^G-nitro-L-arginine methyl ester (L-NAME)) reverses endotoxin-induced hypotension suggesting the involvement of NO in the reduced blood pressure (Kilbourn *et al.*, 1990). Further evidence supporting the role of iNOS-derived NO in the reduced blood pressure, came from studies of iNOS gene knockout mice. In these animals, the hypotension caused by LPS is markedly attenuated (MacMicking *et al.*, 1995). Also, pretreatment of animals with dexamethasone inhibits the LPS-induced expression of iNOS and attenuates the circulatory failure and hyporeactivity to vasoconstrictor agents, further supporting the concept that excess NO production is pathogenic in circulatory failure in septic shock (Paya *et al.*, 1993).

In humans, pharmacological inhibition (L-NMMA) of NO synthesis by iNOS increases blood pressure in septic shock patients but decreases cardiac output (Petros *et al.*, 1994) and has no effect on mortality. It is possible that non-selective inhibitors of NOS have adverse effects on outcome through inhibition of eNOS causing excessive vasoconstriction in the microcirculation. Selective inhibitors of iNOS could represent a useful therapeutic approach for septic shock, whereas non-selective NOS inhibitors (although increasing blood pressure initially) may worsen the final outcome. Therefore, further experimental work by using a selective inhibitor directed only against iNOS is required. The most selective inhibitor of iNOS activity so far is 1400W (Garvey *et al.*, 1997). Inhibition of iNOS by 1400W has been shown to reverse hyporeactivity to vasoconstrictors in mesenteric arteries in experimental

model of septic shock in rats (O'Brien *et al.*, 2001). Recently, Miyamoto *et al.* demonstrated that inhibition of iNOS and sGC by 1400W and ODQ, respectively, restores the hyporeactivity to vasoconstrictors in rat aortic rings, further supporting the role of NO-cGMP pathway in septic shock (Miyamoto *et al.*, 2004). These observations indicate that “high output” iNOS-derived NO is likely to mediate the hypotension and hyporeactivity to vasoconstrictors in septic shock.

1.2 Natriuretic peptides

Natriuretic peptides (NPs) are a family of hormones that activate the particulate guanylate cyclase (also called natriuretic peptide receptors). These vasoactive hormones include atrial natriuretic peptide (ANP), brain natriuretic peptide (BNP), C-type natriuretic peptide (CNP) and urodilatin. NPs play important roles in the regulation of cardiovascular and renal physiology (section 1.2.3). The messenger RNA transcript for ANP is approximately 1 kb in size and encodes a precursor protein (pro-ANP) of 126 amino acids. Human pro-ANP is cleaved into a 98 amino acid amino-terminal fragment and a 28 amino acid carboxy-terminal fragment (by a serine protease named corin (Yan *et al.*, 2000)), which represents the biologically active hormone (Espiner *et al.*, 1995). The atrial myocyte is considered the main site of synthesis of ANP (Atlas *et al.*, 1984) and it is released in response to atrial distension. In addition, ANP expression is directly stimulated by angiotensin II, endothelin-1 or adrenomedullin (McFarlane *et al.*, 2003).

BNP was originally isolated from porcine brain, but in humans it is synthesised and secreted from the left ventricle (Yasue *et al.*, 1994). Human BNP is produced first as a 108 amino acid precursor (proBNP). Further processing is required to release a biologically active hormone, which consists of 32 amino acids (Yasue *et al.*, 1994) and an N-terminal fragment (NT-proBNP). CNP is primarily synthesised and stored in vascular endothelial cells in response to shear stress (Okahara *et al.*, 1995), where it is thought to act as an endothelium-derived hyperpolarising factor (Chauhan *et al.*, 2003a). CNP is also found in the kidney, and brain, including high concentrations in the human hypothalamus and midbrain (Komatsu *et al.*, 1991). CNP is produced first as a pro-CNP consisting of 126 amino acid peptide. Pro-CNP is further processed to generate 22 and 53-amino acid peptides by the serine protease

furin (Wu *et al.*, 2003). CNP-22 peptide is more widely and abundantly expressed and is more potent than CNP-53 peptide (Minamino *et al.*, 1990). Urodilatin or D-type natriuretic peptide is the fourth member of the natriuretic peptide system. Urodilatin, which binds to the ANP receptor, is synthesised mainly in the kidney and formed from the same ANP pro-hormone and consists of 32 amino acids. Urodilatin is a more potent natriuretic agent than ANP (Abassi *et al.*, 1992). Urodilatin regulates Na⁺ and H₂O handling in the kidney (Drummer *et al.*, 1997). Thus, NPs are a family of hormones including ANP, BNP, CNP and urodilatin that, upon generation, require further processing to generate the metabolically active hormone.

1.2.1 Natriuretic peptide receptors (particulate guanylate cyclases)

NPs exert their physiological effects by binding to high-affinity receptors on the surface of target cells. Three natriuretic peptide receptors (NPRs) subtypes have been isolated NPR-A, NPR-B, and NPR-C (Ahluwalia *et al.*, 2004a). Each of the NPs interacts with each of the NPR subtypes with differing kinetics. For NPR-A the affinity is ANP>BNP>>CNP whereas the affinity for NPR-B is CNP>>ANP>BNP (Koller & Goeddel, 1992). NPR-C interacts with all 3 NPs, although with slightly greater affinity for ANP. The non-selective affinity characteristics of NPR-C for all three NPs support its role as a clearance receptor to regulate circulating levels of NPs (Maack *et al.*, 1987). NPR-A and NPR-B consist of an extracellular ANP-binding domain, a single transmembrane sequence, and an intracellular domain consisting of a kinase-homologous regulatory domain (KHD) and a guanylate cyclase catalytic domain (GCD) (Figure-1.4) (Misono, 2002)

1.2.1.1 Extracellular domain

The ANP binding site at the extracellular domain has been characterised by mutagenesis experiments. Mutation at Glu-169 and His-185 caused significant loss of ANP binding, suggesting involvement of these residues in hormone interaction (Misono, 2002). Mutation at Phe-166, Arg-176 or Asn-180 demonstrated ANP binding comparable to the wild-type but significantly reduced cGMP stimulation, suggesting that these residues play a role in initiating or transferring the signal of hormone binding to activate the guanylate cyclase catalytic domain (Misono, 2002).

Miyagi et al found at least five potential glycosylation sites in the extracellular domain that seem to have no role in hormone binding but may be required for folding and transport of the receptor to the cell surface (Miyagi *et al.*, 2000). The binding of ANP to its receptor was found to require the presence of chloride in a concentration-dependent manner. The chloride-dependent ANP receptor regulation may work as a feedback mechanism regulating ANP natriuresis (Misono, 2000).

1.2.1.2 Transmembrane domain

All NPRs have a single transmembrane domain that is required for localisation to the membrane, but not for signal transduction. In addition to localisation, the transmembrane domains seem to facilitate receptor oligomerisation (Lemmon *et al.*, 1994). Beyond the transmembrane domain toward the cytoplasmic region, there is a juxtamembrane domain, which is a short region distal to the transmembrane domain that undergoes a significant conformational change responding to ANP binding and may mediate transmembrane signal transduction (Huo *et al.*, 1999). However, full understanding of the precise role of the transmembrane and juxtamembrane domain remains to be defined.

1.2.1.3 Intracellular domain

The intracellular domain of the ANP receptor consists of two subdomains, the KHD and GCD. Mutagenesis studies have shown that deletion of the KHD causes constitutive activation of the GCD, suggesting the KHD regulates the GCD by suppressing its activity (Chinkers & Garbers, 1989). Studies on the KHD have demonstrated that the binding of adenosine triphosphate (ATP) to the KHD is required for the responsiveness to ANP (Chinkers *et al.*, 1991). The KHD is phosphorylated at serine and threonine residues, and modulates responsiveness to ANP (Potter & Hunter, 1998a). Five residues (Ser-513, Thr-516, Ser-518, Ser-523, and Ser-526) within the KHD are phosphorylated when NPR-B is expressed in human 293 cells. Mutation of any of these residues to alanine reduces NPR-B phosphorylation state and guanylate cyclase activity (Potter & Hunter, 1998b).

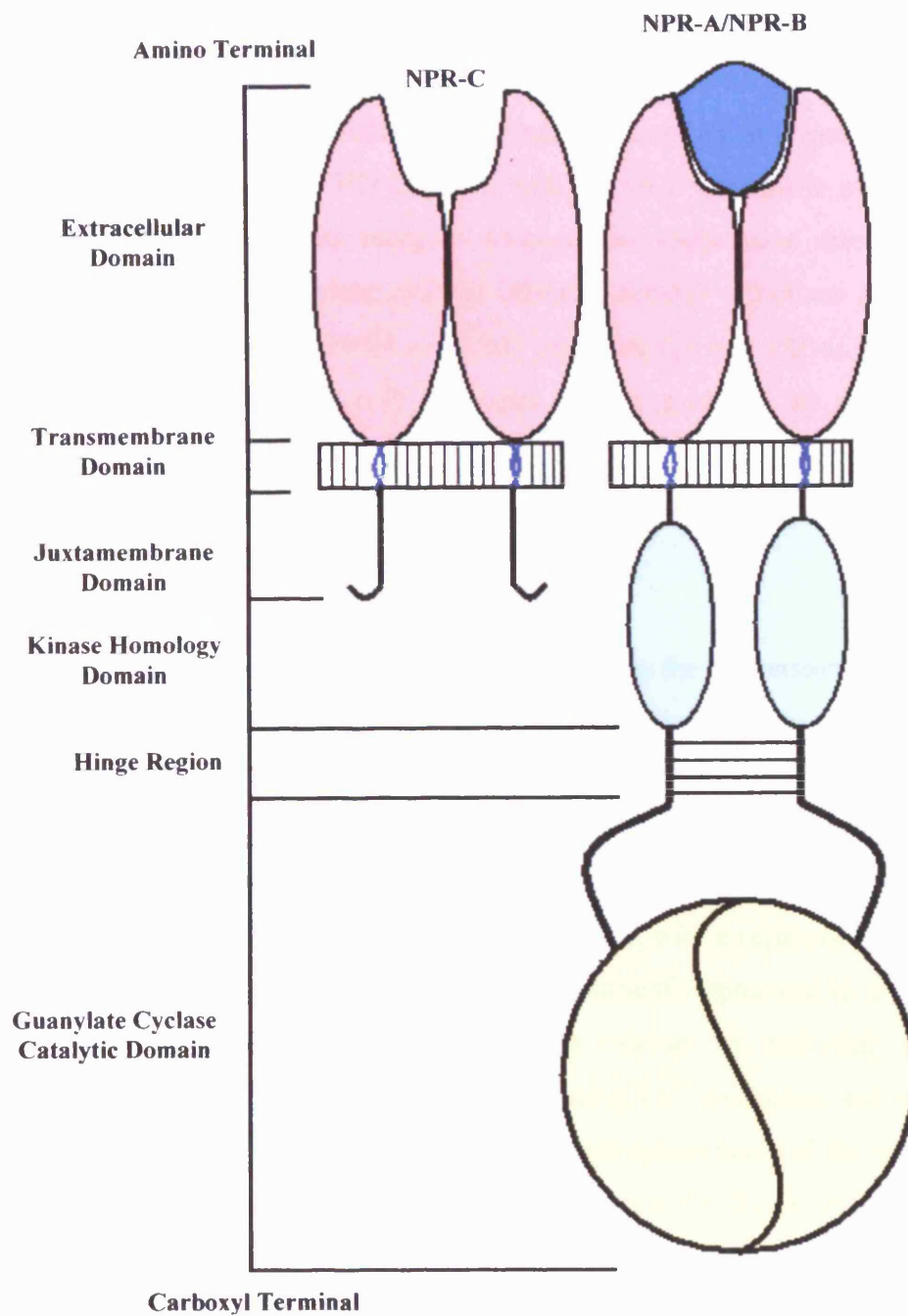


Figure 1.4 Illustration showing different domains of NPRs.

1.2.2 Mechanisms of pGC activation and cGMP-dependent relaxation

The mechanisms by which the signal is initiated by natriuretic peptide and translated into catalytic activation (i.e. cGMP formation), and the termination of that signal, have not been completely determined. However, it is generally accepted that, in its basal state, the KHD interacts with the GCD domain to suppress its activity. Binding of ANP to its receptor relieves this suppressive effect, leading to the elevation of the guanylate cyclase catalytic activity (Chinkers & Garbers, 1989). Binding of ATP to the KHD augments guanylate cyclase activation by ANP. Recent work demonstrated that ATP increases activity primarily by maintaining receptor phosphorylation status and also acts by stabilizing the enzyme function (Antos *et al.*, 2006). However, the entire process mediating this signalling mechanism is not completely understood.

Activation of guanylate cyclase stimulates the conversion of GTP into cGMP. It is widely accepted that the mechanism of relaxation is triggered by the formation of cGMP, which subsequently phosphorylates and activates protein kinase G (PKG) (Figure 1.5). PKG is a common final pathway for cGMP-derived from sGC or pGC. Stimulation of PKG leads to activation and inhibition of various proteins including ion channels, ions pump, receptors and enzymes, with a resultant effect to reduce the cytosolic Ca^{2+} level and the sensitivity of contractile apparatus to the Ca^{2+} (Carvajal *et al.*, 2000). PKG reduces intracellular calcium by activating membrane and sarcolemmal Ca^{2+} /ATPase pumps to increasing Ca^{2+} extrusion, and sequestration in the sarcoplasmic reticulum. PKG-dependent phosphorylation of the regulatory protein phospholamban, the inositol triphosphate receptor (IP3R) (Komalavilas & Lincoln, 1994) and inositol triphosphate associated G-kinase substrate (IRAG) (Geiselhoring *et al.*, 2004) also reduces intracellular Ca^{2+} concentration. PKG also phosphorylates and opens Ca^{2+} -activated K channels, which hyperpolarise the cell membrane and inhibit the influx of Ca^{2+} through voltage-gated Ca^{2+} channels. Reduction of Ca^{2+} influx leads to smooth muscle relaxation (Yamakage *et al.*, 1996). PKG inhibits voltage-gated Ca^{2+} channels probably through direct phosphorylation of the channel or nearby regulatory protein (Tewari & Simard, 1997). PKG also phosphorylates and activate myosin light chain phosphatase (MLCP). Since contraction is dependent on the activities of myosin light chain kinase, increased activity of myosin light chain

phosphatase produces relaxation by decreasing myosin light chain (MLC) phosphorylation and decreasing the sensitivity of the contractile apparatus to Ca^{2+} without altering intracellular Ca^{2+} concentration (Lee *et al.*, 1997).

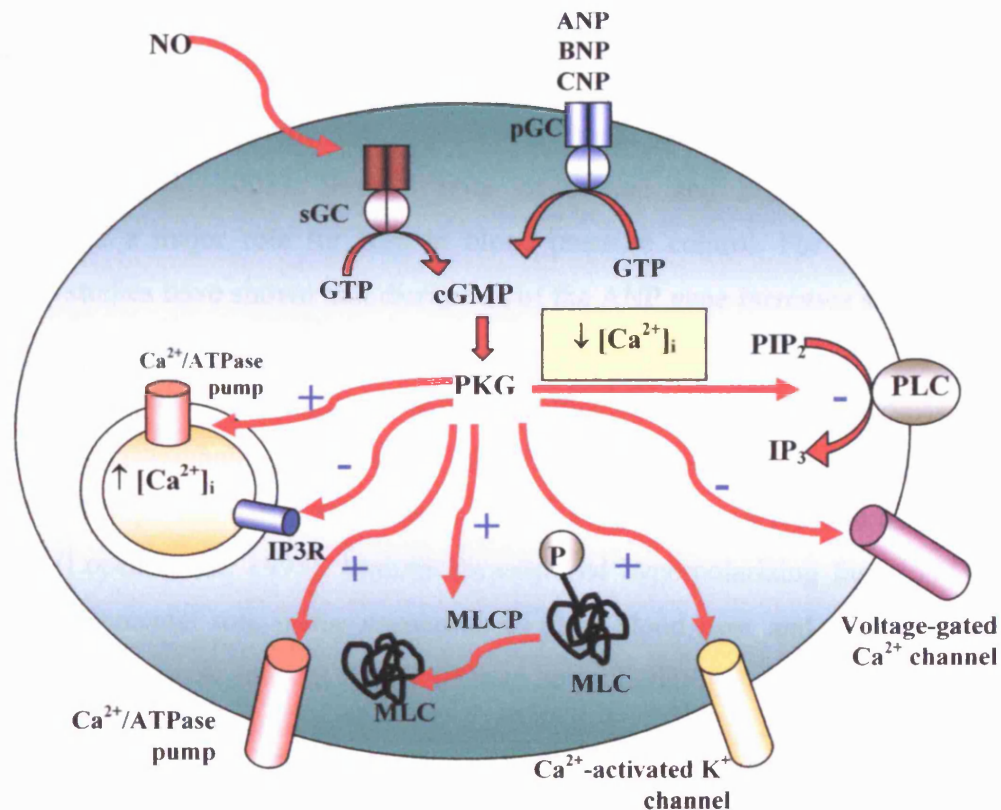


Figure 1.5 The mechanism of cGMP-mediated relaxation. Conversion of GTP into cGMP stimulates PKG. PKG activates or inhibits a wide range of cellular targets leading to a reduction in the cytosolic Ca^{2+} concentration and reduction in the sensitivity of the contractile apparatus to Ca^{2+} . Inositol triphosphate (IP_3), inositol triphosphate receptor (IP_3R), phosphatidylinositol biphosphate (PIP_2), phospholipase C (PLC), myosin light chain (MLC) and myosin light chain phosphatase (MLCP). Activation (+) and inhibition (-).

1.2.3 Physiological functions of natriuretic peptides

1.2.3.1 Regulation of vascular tone and blood pressure

NPs play important roles in the cardiovascular and renal systems, regulating their physiological function (Ahluwalia *et al.*, 2004a). ANP and BNP are secreted in response to atrial stretch and pressure. Once released into the circulation, NPs reach their targets, which include the vasculature, heart, kidneys and adrenal glands (McFarlane *et al.*, 2003). Several lines of animal and humans studies have demonstrated a major role for NPs in blood pressure control. For example, gene knockout studies have shown that disruption of the ANP gene increases sensitivity to high-salt diet, resulting in markedly increased blood pressure (John *et al.*, 1995). Overexpression of ANP genes resulted in a reduction of systolic blood pressure of 20–30 mmHg (Steinhilper *et al.*, 1990). In NPR-A gene knockout mice, although the sensitivity to high-salt diet is maintained, there is a significant increase in basal blood pressure (Lopez *et al.*, 1995). Endothelium-derived hyperpolarizing factor (EDHF) plays a fundamental role in the regulation of local blood flow and systemic blood pressure. Recent work showed that CNP may be an EDHF (Chauhan *et al.*, 2003a). These observations suggest that NPs are endocrine and paracrine agents that regulate blood pressure by natriuresis and vasodilatation.

1.2.3.2 Regulation of renal function

NPs regulate renal function; urodilatin is synthesised in the kidneys and can modify cardiovascular and renal function by decreasing blood pressure and increasing glomerular filtration rate (GFR) (Saxenhofer *et al.*, 1990). ANP regulates renal function by different mechanisms. ANP increases fluid and electrolyte excretion and opposes the renin-angiotensin-aldosterone system by inhibiting the synthesis and release of renin and aldosterone, and by antagonizing the biological effects of angiotensin (Tremblay *et al.*, 2002). In contrast, CNP does not seem to play role in the renal system, even when injected at high doses in the renal artery, and is therefore considered to be more a cardiovascular than renal peptide (Chen & Burnett, 1998).

1.2.3.3 Effects on coagulation, adhesion and inflammatory cells

Akin to NO, NPs also possess anti-atherogenic properties. ANP and CNP inhibit plasminogen activator inhibitor-1 mRNA expression in VSMC through a cGMP-dependent pathway (Bouchie *et al.*, 1998). Moreover, in rat cultured aortic endothelial cells, BNP and CNP reduce the expression of tissue factor (TF), and the expression of plasminogen activator inhibitor-1 (PAI-1) induced by angiotensin II (Yoshizumi *et al.*, 1999). Local CNP expression in balloon injured rabbit arteries suppresses expression of ICAM-1 and VCAM-1 through enhancement of NO production (Qian *et al.*, 2002). CNP inhibits leukocyte recruitment and platelet aggregation through suppression of P-selectin expression (Scotland *et al.*, 2005a). CNP also has a direct effect on inflammatory cells *in vivo*; exogenous CNP reduces cytokine or histamine-induced leukocyte rolling in mouse mesenteric circulation. This anti-adhesion effect is thought to occur through an NPR-C-mediated cGMP-independent mechanism (Scotland *et al.*, 2005b).

NPs also have anti-inflammatory properties. Inflammatory mediators such as IL-1 β , TNF and LPS increase endothelial CNP release. CNP and ANP attenuate the induction of the proinflammatory enzyme cyclooxygenase-2 (COX-2). Overexpression of CNP by adenoviral gene delivery reduces neointimal hyperplasia that develops when veins are grafted to the carotid artery (Scotland *et al.*, 2005b). Collectively, these studies show that NPs have substantial anti-atherogenic and anti-inflammatory properties by inhibiting recruitment and adhesion of inflammatory cells, together with inhibition of smooth muscle proliferation. These properties are thought to occur by cGMP-dependent and -independent pathways.

1.2.4 Pathophysiological roles of natriuretic peptides

NPs play important roles in a number of cardiovascular diseases. Several lines of evidence suggest the importance of NPs in congestive heart failure (CHF) in animals (Riegger *et al.*, 1988) and humans (Stoupakis & Klapholz, 2003). In CHF there is a significant increase in circulating ANP and BNP, and this correlates with the severity of the disease (Luchner *et al.*, 1998). Increased activation of NP pathways promote vasodilatation and natriuresis, and in so doing compensate for the effects of

neurohormonal activation that is a pathogenic in CHF. The plasma level of NPs has recently been used as a diagnostic tool and a measure of the response to treatment in patients with CHF (Stoupakis & Klapholz, 2003). In addition to their roles in CHF, NPs have been suggested to play a protective role in ischemic heart disease such as atherosclerosis and restenosis by inhibiting smooth muscle cells migration (Ikeda *et al.*, 1997). CNP inhibits growth factor-dependent DNA synthesis in smooth muscle cells suggesting that CNP regulates cellular proliferation (Porter *et al.*, 1992). CNP was also found in atherosclerotic lesions of different stages suggesting a regulatory role of this natriuretic peptide in atherogenesis (Naruko *et al.*, 1996).

In patients with acute myocardial infarction, there are high plasma levels of BNP with a positive correlation between plasma concentration and the size of infarction (Arakawa *et al.*, 1994). In cardiac hypertrophy, ANP is increased as a result of increased ventricular wall stress (McKenzie *et al.*, 1994). Kishimoto *et al.* demonstrated that in cardiac myocytes lacking the NPR-A receptor gene, the size of the cells is markedly increased and introduction of the NPR-A transgene inhibits cardiac ventricular myocyte hypertrophy (Kishimoto *et al.*, 2001). ANP-deficient mice exhibit an exaggerated increase in right and left ventricular weight in response to volume overload (Mori *et al.*, 2004). In humans with dilated cardiomyopathy, the increased levels of plasma ANP and BNP are associated with significant increases in ventricular ANP and BNP in both left and right ventricular tissue (Hasegawa *et al.*, 1993a). Raised levels of plasma BNP have also been found in patients with hypertrophic cardiomyopathy (Hasegawa *et al.*, 1993b). These findings suggest that NPs may be an important physiological modulator of cardiac hypertrophy. In pulmonary hypertension, circulating NPs concentrations are raised that may either directly reduce pulmonary arterial pressures or contribute to the vasodilatation induced by phosphodiesterase inhibitors (Sebkhi *et al.*, 2003).

NPs have a new emerging role in sepsis and septic shock. Hartemink *et al.* found that right and left systolic dysfunction correlated with an increase in plasma levels of ANP and its second messenger cGMP during the first 3 days after the diagnosis of septic shock (Hartemink *et al.*, 2001). The precursor of ANP, pro-ANP, has been studied as a novel hormone marker of cardiac depression caused by sepsis, (Mazul-Sunko *et al.*, 2001). CNP has also been implicated in sepsis, with markedly

elevated serum level of CNP seen in patients with severe infection compared to patients with congestive heart failure and hypertension (Hama *et al.*, 1994). These studies suggest that NPs might contribute to the hypotension associated with septic patient. Collectively these findings indicate that NPs are involved in various forms of cardiovascular pathophysiology.

1.2.5 Therapeutics of natriuretic peptides

The investigation of therapeutic values of NPs has been of great interest since NPs are regarded as beneficial in various cardiovascular disorders. For example, in patients with CHF, Crozier *et al.* demonstrated that infusion of ANP causes significant reductions in mean systemic arterial pressure, mean pulmonary artery pressure, pulmonary diastolic pressure, right atrial pressure, and increase of cardiac output (Crozier *et al.*, 1986). Though the haemodynamic improvements are significant, the effects of ANP infusion are transient so as to limit its practical use. In contrast, infusion of BNP, showed a sustained hemodynamic improvement in patients with CHF (Marcus *et al.*, 1996). The difference between the effective duration of ANP and BNP may be explained by the difference in their plasma half-life. Intravenous infusion of nesiritide (a recombinant human BNP) is effective in improving haemodynamics of patients with CHF. It decreases systemic vascular resistance, pulmonary-capillary wedge and pulmonary artery pressures and elevates cardiac index with improvement in CHF symptoms (Colucci *et al.*, 2000). However, recent concerns have been raised about the use of nesiritide, with reports of unexpected deaths in patients treated with this agent (Sackner-Bernstein *et al.*, 2005). I will revisit this and a possible mechanism to explain this phenomenon in section 1.5.3.

Further clinical benefits of NPs come from their diagnostic use. ANP and BNP levels are increased in patients with heart failure and in many patients with hypertension and chronic renal failure. Because BNP plasma levels correlate more closely than ANP levels with left ventricular function, BNP is considered a better diagnostic marker of CHF (Stoupakis & Klapholz, 2003). Campbell *et al.* showed that the plasma level of NT-proBNP is elevated in subjects with renal failure, myocardial infarction and heart failure. They suggested that NT-proBNP is a sensitive indicator of cardiac dysfunction and may prove to be a useful tool for the identification and

management of cardiac dysfunction (Campbell *et al.*, 2000). In a recent study of 1059 patients with chronic stable angina, Ndrepepa and co-workers showed that the plasma levels of NT-proBNP are correlated with mortality. They suggested that the circulating levels of NT-proBNP are a prognostic biomarker for patients with chronic stable angina (Ndrepepa *et al.*, 2005). Based on the discussion in section 1.2.4 it is unclear how increased NP activity is associated with an adverse cardiovascular outcome. I will discuss this further in section 1.5.3.

While much of the therapeutic roles for NPs have concentrated on the current and potential uses of ANP and BNP, the therapeutic uses of CNP have yet to be explored. CNP may hold promise as a cardiovascular drug because recent evidence indicates that CNP can regulate coronary blood flow and prevents myocardial ischemia/reperfusion injury in rat through an NPR-C-dependent pathway (Hobbs *et al.*, 2004). Also CNP can prevent cardiac remodeling following myocardial infarction in mice (Soeki *et al.*, 2005).

1.3 Aspects of cGMP-mediated vasodilatation to be addressed in this thesis

I have provided a brief review of the NO and NP systems in the above sections as a basis from which to describe the specific research areas that I investigated in this thesis. These are two-fold:

1. The role of endogenous adducts of NO, the *S*-nitrosothiols, as vasodilators which is described in section 1.4.
2. The interaction between the sGC and pGC systems, with specific emphasis on desensitisation of the guanylate cyclase pathways, described in section 1.5.

1.4 Modulation of NO biology by the formation of *S*-nitrosothiols

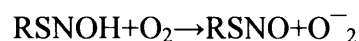
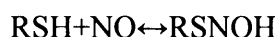
1.4.1 *S*-nitrosothiols in biological systems

It has been suggested that NO is stored and carried as *S*-nitrosothiol adducts, which preserve it from inactivation by several molecules like haemoglobin, molecular

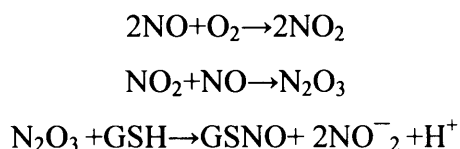
oxygen or superoxide (Stamler *et al.*, 1992a). *S*-nitrosothiols have been found endogenously in erythrocytes, polymorphonuclear leukocytes, and platelets, as well as tissues including brain and lung. The concentrations of *S*-nitrosothiols *in vivo* are a matter of debate. In the lining of human airways, *S*-nitrosothiols (predominantly *S*-nitrosoglutathione (GSNO)) has been detected at concentration of 0.25 μM (Gaston *et al.*, 1993). In the cerebellum, GSNO has been detected at concentration of 15.4 pmol/mg protein (Kluge *et al.*, 1997). Stamler *et al* found that human plasma contains approximately 7 μM *S*-nitrosothiols, 96% was in the form of *S*-nitrosoprotein, 82% of which was accounted for by *S*-nitrosoalbumin (SNOAlb) (Stamler *et al.*, 1992a). Tyurin *et al* found that the concentration of *S*-nitrosothiols was about 9.2 μM (Tyurin *et al.*, 2001). However, other studies reported lower plasma concentrations of *S*-nitrosothiols between 20-200 nM (Goldman *et al.*, 1998; Marley *et al.*, 2000). It is possible that the difference in the level of *S*-nitrosothiols observed in these studies is due to methodological differences in the analytical techniques.

1.4.2 Formation of *S*-nitrosothiols

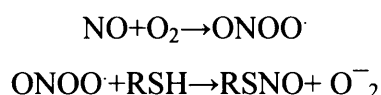
The mechanisms leading to formation of *S*-nitrosothiols in biological tissues are unclear. NO *per se* does not react directly with sulphydryl-containing compounds (RSH) such as glutathione (GSH) to form *S*-nitrosothiols (RSNO). Several mechanisms have been postulated for the formation of *S*-nitrosothiols in biological systems. Gow and colleagues proposed a mechanism for the formation of *S*-nitrosothiols that would proceed at physiologically relevant concentrations of NO. They suggested that NO reacts directly with a reduced thiol to produce a radical intermediate. In the presence of an electron acceptor, such as oxygen and NAD^+ this intermediate can be converted to an *S*-nitrosothiol by the reduction of the acceptor (Gow *et al.*, 1997) as follows:



Other studies have suggested alternate routes for the formation of *S*-nitrosothiols. *S*-nitrosothiols might be formed by the reaction of an *S*-nitrosating agent, such as dinitrogen trioxide (N₂O₃), with thiols as follows:



In this mechanism, the reaction of NO with oxygen yields nitrogen dioxide. Nitrogen dioxide can rapidly react with NO to form N₂O₃. The latter is a good nitrosating agent, which can nitrosate thiols (such as GSH and cysteine) to form *S*-nitrosothiols (Karitonov *et al.*, 1995). Another postulated mechanism includes nitrosyldioxy radical (ONOO[•]) as an intermediary in the formation of *S*-nitrosothiols within biological systems (Gow *et al.*, 1997). In this mechanism NO reacts with oxygen to form ONOO[•]. The latter reacts with reduced thiols to form an *S*-nitrosothiol and superoxide according to the following reaction:



However, whether one or more mechanisms are required for the formation of *S*-nitrosothiols in biological systems remains unclear.

1.4.3 Formation of *S*-nitrosoproteins

In addition to the low molecular weight *S*-nitrosothiols, high molecular weight *S*-nitrosothiols have been reported to exist endogenously in the form of *S*-nitrosoproteins. Formation of *S*-nitrosoproteins occurs when a specific cysteine residue reacts with NO in the presence of an electron acceptor. SNOAlb is the most abundant physiological circulating NO carrier regulating NO-dependent biological actions in humans (Stamler *et al.*, 1992a). The mechanisms of its formation is thought to occur through *S*-transnitrosation of the sulfhydryl group located at Cys-34 by the physiological *S*-nitroso-compounds, *S*-nitrosocysteine (CYSNO) and GSNO (Tsikas *et al.*, 2001). Marley *et al* demonstrated that significant amount of SNOAlb can be

generated in human plasma under aerobic conditions in a reaction involving two molecules of NO and one of O₂ (Marley *et al.*, 2001). *S*-nitrosohaemoglobin (SNOHb) is the product of the reaction between NO and haemoglobin, involving *S*-nitrosation of a specific cysteine residue at a position 93 of the β -chain (Jia, *et al.*, 1996). SNOHb has been proposed to regulate vascular tone under conditions of low oxygen tension. Other *S*-nitrosated proteins that have been described include tissue-type plasminogen activator (t-PA; *S*-nitrosated at Cys-83; Stamler *et al.*, 1992b) ornithine decarboxylase (at Cys-360; Bauer *et al.*, 2001), the cell signalling protein, p21^{ras} (*S*-nitrosated at Cys-118 leading to activation of downstream signalling pathways; Heo & Campbell, 2004).

1.4.4 Biotransformation of *S*-nitrosothiols

Several mechanisms have been reported to decompose *S*-nitrosothiols leading to the release of NO including metal ions, thiols, photochemical and enzymatic-mediated biotransformation.

1.4.4.1 Role of metal ions

Metal ions decompose *S*-nitrosothiols to release NO. One of the earliest descriptions of this is the action of mercury (Hg²⁺), which binds to the sulphur atom of the *S*-nitrosothiol, releasing nitrous acid (Saville 1958; Swift & Williams 1997). The presence of trace amount of copper ions strongly affects the stability of certain *S*-nitrosothiols (Williams, 1996). Cu(I) catalyses the decomposition of *S*-nitrosothiols probably by homolytic cleavage of the S-N bond resulting in the release of NO (Singh *et al.*, 1996). Likewise, the reaction between Cu(II) and *S*-nitrosothiols leads to the release of NO and the production of thiol disulfide. The decomposition of *S*-nitrosothiols by Cu(II) requires the reduction of Cu(II) into the active moiety, Cu(I), probably by thiols (Gorren *et al.*, 1996). Copper ions under physiological conditions are bound to proteins and enzymes. Dicks and Williams established that protein associated-Cu(II) (treated with thiol) catalyses the decomposition of *S*-nitrosothiols through the reduction of Cu(II) to Cu(I) (Dicks & Williams, 1996). This finding is important, as it implies that copper-associated enzymes in the body might metabolise *S*-nitrosothiols.

Kostka and co-workers reported that CYSNO degradation was enhanced several fold by millimolar concentrations of Mg^{2+} and Ca^{2+} ions in homogenates isolated from porcine aortic smooth muscle (Kostka *et al.*, 1999). Later, this group showed that the redox cycling of Fe^{2+} with the assistance of a protein factor catalyses decomposition of the S—NO bond of CYSNO (Sorenson *et al.*, 2000). However, other metal ions such as Zn^{2+} , Ni^{2+} , Co^{2+} , Mn^{2+} , Cr^{3+} , or Fe^{3+} have been shown to cause no measurable catalysis of *S*-nitrosothiols (Williams, 1996).

1.4.4.2 Role of reducing agents

Reducing agents such as ascorbic acid, cysteine and GSH, enhance the decomposition of *S*-nitrosothiols (Kashiba-Iwatsuki *et al.*, 1997). Wong *et al.* showed that the reaction of GSH with *S*-nitrosothiols results in the generation of nitroxyl (HNO). The subsequent reaction of HNO with the remaining *S*-nitrosothiols and thiols results in the generation of NO (Wong *et al.*, 1998). Thiols can cause decomposition of *S*-nitrosothiols by transnitrosation, in which the nitroso group is transferred from an *S*-nitrosothiol to a thiol (Hogg, 1999), although this does not release free NO. Thiols can also reduce metal ions which may then cause decomposition of *S*-nitrosothiols (Gorren *et al.*, 1996).

1.4.4.3 Enzymatic decomposition

Certain enzymes have been reported to breakdown *S*-nitrosothiols. Askew and co-workers demonstrated that the enzyme, γ -glutamyltranspeptidase, decomposes GSNO *in vitro* leading to the formation of unstable *S*-nitrosothiol called *S*-nitrosocysteinylglycine, which subsequently decomposes in the presence of metal ions leading to the release of NO (Askew *et al.*, 1995). Nikitovic and Holmgren showed that GSNO is a substrate for the enzyme thioredoxin reductase, which generates stoichiometric amounts of GSH and NO by homolytic cleavage (Nikitovic & Holmgren, 1996). Jourdain *et al.* reported that Cu/Zn superoxide dismutase (Cu/Zn SOD) causes decomposition of GSNO in a manner that is accelerated by the

presence of GSH (Jourdain *et al.*, 1999). It is unclear whether this is an enzymatic or chemical process, catalysed by exposure of bound copper to GSNO.

Additionally, it has been demonstrated that the intracellular enzyme glutathione-dependent formaldehyde dehydrogenase may have a role in the metabolism of GSNO (Liu *et al.*, 2001) and that xanthine oxidase might also catalyse the decomposition of *S*-nitrosothiols (Trujillo *et al.*, 1998). Further, recent studies have pointed to a possible role of the cell-surface protein disulfide isomerase (PDI) in the biotransformation of *S*-nitrosothiols. For instance, in human erythroleukaemia cells, inhibition of PDI decreases cGMP generation after *S*-nitrosothiol exposure (Zai *et al.*, 1999). Moreover, in platelets, PDI has been shown to catalyse the release of NO by denitrosation of GSNO (Root *et al.*, 2004). Importantly, since both xanthine oxidase (Roussos & Morrow, 1966) and PDI (Narindrasorasak *et al.*, 2003) are copper-binding enzymes, the inhibitory effects of copper chelators on *S*-nitrosothiol biotransformation should be interpreted with caution.

In the nervous system, Davisson *et al.* demonstrated that intracerebro-ventricular injection of the L-CYSNO produces greater hemodynamic changes than the D-isomer of CYSNO. They suggested that L-CYSNO may activate a specific recognition site on brain neurons (Davisson *et al.*, 1997). In the vasculature, Travis *et al.* showed that the L-isomer of *S*-nitrosopenicillamine generates more cGMP in porcine aortic smooth muscle cells than the D-isomer (Travis *et al.*, 1996). This group also suggested that a CYSNO recognition site may exist on the vascular smooth muscle of resistance arteries in the rat. They showed that in the conscious rat, intravenous injections of the L-CYSNO have greater vasodilator effect on mesenteric arteries than the D-isomers (Davisson *et al.*, 1996). However, this role of L-CYSNO was not observed by another group; Cavero *et al.* showed that responses to L- and D-isomers of CYSNO and *S*-nitroso-N-acetylpenicillamine (SNAP) were equipotent in rat aortic rings but L-GSNO is more potent vasorelaxant than D-GSNO (Cavero *et al.*, 2000). These observations suggest that there is no consensus on the relative contribution of enzyme-dependent biotransformation of *S*-nitrosothiols in the vasculature and more investigations are required to explore this mechanism.

1.4.5 Biological roles of *S*-nitrosothiols

S-nitrosothiols have been shown to cause NO-dependent regulation of vascular tone. In rat aortic rings, CYSNO, SNAP and GSNO cause concentration dependent relaxation that is inhibited by the NO scavengers, hydroxocobalamin and haemoglobin (Rand & Li 1993) and blocked by ODQ (Feelisch *et al.*, 1999). In rat pulmonary vasculature, administration of SNAP, causes vasodilatation. This action of SNAP was attributed to its ability to donate NO (Emery, 1995). Stamler *et al* demonstrated that the large molecular weight *S*-nitrosoprotein, SNOHb, also vasodilates in an NO-dependent manner (Stamler *et al.*, 1997). Megson *et al* reported that SNAP analogues cause NO-dependent vasorelaxation in isolated rat femoral artery and scavenging NO with haemoglobin, removed the vasodilator effect of SNAP (Megson *et al.*, 1999). Sogo and co-workers have also shown that *S*-nitrosothiols cause prolonged, NO-mediated relaxation in human saphenous vein and internal mammary artery (Sogo *et al.*, 2000). The vasorelaxation of vascular strips exposed to visible light suggest a possible role for endogenous NO store to act as photosensitive NO-donor within vascular smooth muscle (Megson *et al.*, 2000a; Chauhan *et al.*, 2003b). These studies demonstrate that *S*-nitrosothiols regulate vascular tone through the release of their bound NO.

S-nitrosothiols are also potent inhibitors of platelet aggregation. Mellion *et al* showed that CYSNO and SNAP inhibit platelet aggregation in a concentration-dependent manner through elevation of cGMP. The NO scavenger, methemoglobin partially reversed this anti-aggregatory effect (Mellion *et al.*, 1983). The ability of *S*-nitrosothiols to inhibit platelet aggregation is reduced in the presence of Cu(I) chelators (Gordge *et al.*, 1995). Pawloski *et al* showed that both cell-free and intra-erythrocytic SNOHb inhibit platelet aggregation (Pawloski *et al.*, 1998). Megson *et al* investigated the effect of two *S*-nitrosothiols, GSNO and RIG200, on platelet activity and found that these *S*-nitrosothiols are potent inhibitors of platelet aggregation. This effect was abolished in the presence of NO scavenger (Megson *et al.*, 2000b). Recently, Crane *et al* revealed that *S*-nitrosothiols inhibit platelet aggregation via cGMP-independent effects on Ca^{2+} signalling (Crane *et al.*, 2005). They showed that the *S*-nitrosothiol, *S*-nitroso-*N*-valerylpenicillamine (SNVP), displayed NO-mediated cGMP-independent inhibition of platelet aggregation in platelet-rich plasma in the

presence of the sGC inhibitor, ODQ. These studies support the thesis that NO synthesised by the endothelium or released from *S*-nitrosothiols might play important roles in the regulation of vascular homeostasis through their ability to inhibit platelet aggregation.

In addition to carrying and releasing NO, *S*-nitrosothiols might regulate cellular activities through *S*-thiolation and *S*-nitrosation (table 1.1). *S*-thiolation is a biological process that involves the nucleophilic attack of the sulphur group of *S*-nitrosothiols by a thiolate anion (Hogg, 1999). Protein *S*-thiolation has long been regarded as an intracellular response to oxidative stress. It has recently been shown that incubation of enzymes with *S*-nitrosothiols lead to both *S*-nitrosation and *S*-thiolation. GSNO thiolates glyceraldehyde-3-phosphate dehydrogenase and inhibits enzyme activity (Mohr *et al.*, 1999). Konorev and others reported that GSNO *S*-thiolates creatine kinase, which result in the inhibition of the enzyme (Konorev *et al.*, 2000). Incubation of papain with GSNO and SNAP, results in thiolation at Cys-25 with subsequent inhibition of this protein (Xian *et al.*, 2000).

S-nitrosothiols modify enzyme activity by *S*-nitrosation. Stamler *et al* found that *S*-nitrosation of t-PA made this protein a potent vasodilator and inhibitor of platelet activity (Stamler *et al.*, 1992b). Li and others found that NO reversibly inhibits seven members of the caspase family via *S*-nitrosation (Li *et al.*, 1997). SNAP and GSNO inhibit coagulation factor XIII activity in a concentration-dependent manner, in both purified enzyme and plasma preparations. The inhibition occurred through *S*-nitrosation of a highly reactive cysteine residue (Catani *et al.*, 1998). CYSNO inhibits the transcription factor, NF- κ B by *S*-nitrosation (Marshall & Stamler, 2001). The activity of ornithine decarboxylase, a rate-limiting enzyme in the polyamine biosynthetic pathway that is required for cell growth is inhibited by *S*-nitrosation by GSNO (Bauer *et al.*, 2001). Kwiecien *et al* showed that the catalytic activity of rhodanese, which catalyses the detoxification of cyanide, was inhibited on exposure to SNAP and GSNO as a result of *S*-nitrosation (Kwiecien *et al.*, 2003). Recent work suggests that *S*-nitrosothiols may have an effect on fibrinogen that is not due to either *S*-nitrosation or thiolation but rather due to interaction with an allosteric site leading to changes in the structure of fibrinogen (Akhter *et al.*, 2002). Thus, these

studies indicate that *S*-nitrosothiols are important biological mediators that modulate signalling pathways via activation or inhibition of many enzymes and proteins.

Nonetheless, it is not possible to determine if any of these effects of *S*-nitrosothiols are biologically relevant. So far, there is no specific inhibitor directed against *S*-nitrosothiols to allow investigation of their biology. Until it is possible to block specifically the action of *S*-nitrosothiols, there will be uncertainty about their biological roles.

Enzymes	Effect of <i>S</i> -nitrosothiols	Effect on the enzyme	Reference
Soluble guanylate cyclase	NO release	Activation	Craven & DeRubertis, 1983
Glyceraldehydes-3-phosphate dehydrogenase	Thiolation	Inhibition	Mohr <i>et al.</i> , 1999
Creatine kinase	Thiolation	Inhibition	Konorev <i>et al.</i> , 2000
Papain	Thiolation	Inhibition	Xian <i>et al.</i> , 2000
Tissue-type plasminogen activator	<i>S</i> -nitrosation	Activation	Stamler <i>et al.</i> , 1992b
Caspase	<i>S</i> -nitrosation	Inhibition	Li <i>et al.</i> , 1997
Coagulation factor XIII	<i>S</i> -nitrosation	Inhibition	Catani <i>et al.</i> , 1998
Nuclear factor-kappa β	<i>S</i> -nitrosation	Inhibition	Marshall & Stamler, 2001
Ornithine decarboxylase	<i>S</i> -nitrosation	Inhibition	Bauer <i>et al.</i> , 2001
p21 ^{ras}	<i>S</i> -nitrosation	Activation	Heo & Campbell, 2004
Rhodanese	<i>S</i> -nitrosation	Inhibition	Kwiecien <i>et al.</i> , 2003

Table 1.1 Modulation of enzymes activity by *S*-nitrosothiols.

1.4.6 Pathophysiological aspects of *S*-nitrosothiols

Abnormal levels of *S*-nitrosothiols are found to occur in numerous pathophysiological conditions suggesting that abnormal regulation of *S*-nitrosothiols may contribute to disease pathogenesis. For instance, GSNO was first described in human airways with an approximate concentration of 0.3 μ M in normal subjects (Gaston *et al.*, 1993), this concentration differs under pathological conditions with higher concentration in patients with pneumonia and lower concentration in patients with asthma (Gaston *et al.*, 1998). Circulating concentrations of SNOAlb and SNOHb increase in endotoxemia (Jourdain *et al.*, 2000), and cirrhosis (Ottesen *et al.*, 2001). In humans, increased *S*-nitrosothiols in exhaled breath has been reported in patients with chronic obstructive pulmonary disease (Corradi *et al.*, 2001) but decreased in children with cystic fibrosis (Grasemann *et al.*, 1999).

Increased plasma concentrations of *S*-nitrosothiols have been found in patients with preeclampsia (Tyurin *et al.*, 2001). Interestingly, a recent study demonstrated that the abnormal high level of *S*-nitrosothiols in women with preeclampsia may be due to deficient release of NO from SNOAlb (Gandley *et al.*, 2005), this suggests that the hypertension in preclampsia may be, at least in part, due to deficiency in NO release from endogenous *S*-nitrosothiols. High concentrations of *S*-nitrosothiols have also been observed in hypercholesterolemia (Moriel *et al.*, 2001) and patients on chronic haemodialysis (Massy *et al.*, 2003). Thus, these findings suggest that *S*-nitrosothiols are involved in the pathophysiology of various systems *in vivo*. Understanding of the regulation of their formation and biotransformation may be pathogenically important.

1.4.7 Therapeutic implications of NO and *S*-nitrosothiols

The use of glyceryl trinitrate (GTN) in cardiovascular disease is limited by the development of tolerance (Parker & Gori, 2001). The mechanism of nitrate tolerance is controversial, and it has been suggested that alternative NO donors might not be affected by tolerance to the same degree. In rat and rabbit aorta, the response to *S*-nitrosothiols was preserved in GTN-tolerant rings (Kowaluk *et al.*, 1987; Smith *et al.*, 1994). Administration of *S*-nitrosothiols to rats with congestive heart failure

showed reduced development of tolerance in comparison with GTN (Bauer & Fung 1991). Miller and colleagues found that the novel *S*-nitrosothiol, RIG200 did not cause vascular tolerance in an *ex vivo* study on rat femoral artery (Miller *et al.*, 2000). Sogo and others found that, in studies on human saphenous vein and internal mammary artery taken from patients undergoing coronary artery bypass grafting, *S*-nitrosothiols (RIG200 and GSNO) caused vasorelaxation that was sustained compared to GTN and SNP. They suggested that pretreatment of these vessels with *S*-nitrosothiols might improve their patency in the early post-operative period (Sogo *et al.*, 2000).

Balloon angioplasty is limited by the adhesion of platelets to the vascular wall. In rabbit models, *in vivo* administration of the *S*-nitrosothiol, SNVP, caused a remarkably prolonged and selective inhibition of platelet adhesion in the area of vascular injury with a negligible effect on blood pressure as compared to GTN (Miller *et al.*, 2003). An anti-platelet effect of GSNO has been documented in healthy volunteers, that is evident at doses with minimal vascular effects. This suggests a degree of platelet selectivity that might be useful clinically (De Belder *et al.*, 1994; Ramsay *et al.*, 1995).

In ischemia/reperfusion injury, *S*-nitrosothiols suppress endothelin-1 release, and subsequently inhibit the damaging effects of endothelin-1 during reperfusion (Brunner, 1997). SNOAlb inhibits intimal proliferation and platelet deposition following injury in rabbit femoral artery (Marks *et al.*, 1995). Moreover, SNOAlb provides significant protection of skeletal muscle from ischemia/reperfusion injury (Hallstrom *et al.*, 2002). In patients, intra-coronary infusion of GSNO during coronary balloon angioplasty prevents the angioplasty-induced increase in platelet expression of P-selectin and of glycoprotein IIb/IIIa, without altering blood pressure (Langford *et al.*, 1994). In humans, intravenous injection of GSNO reduces carotid emboli formation following angioplasty, suggesting that *S*-nitrosothiols may be clinically useful in the treatment of thromboembolic disease (Molloy *et al.*, 1998; Kaposzta *et al.*, 2001). In summary, *S*-nitrosothiols have wide therapeutic beneficial effects. They may not develop tolerance, exhibit a certain degree of platelet selectivity and show beneficial effects in the treatment of ischemia/reperfusion injury and thromboembolic disease.

1.4.8 Exploring the mechanisms of *S*-nitrosothiols biotransformation

Based on the above discussion of the biological, physiological (section 1.4.4 and 1.4.5), pathophysiological (section 1.4.6) and therapeutic (section 1.4.7) significance of *S*-nitrosothiols it is important to investigate the mechanisms by which these NO-donor are bio-transformed in the biological system. The relative contribution of enzymatic and non-enzymatic mechanisms of *S*-nitrosothiols biotransformation in vascular tissue and the role of free and enzyme-bound copper ions are explored in Chapter Three.

1.5 Desensitisation of GC-cGMP pathway

1.5.1 Evidence for desensitisation of sGC and pGC pathways

The sensitisation and desensitisation of GC can be described as changes in the responsiveness of GC-cGMP to a given stimulus. This process may be caused by changes in the activity, the amount of the enzyme and/or the factors that regulate the enzyme. The ambient concentration of NO has been shown to alter the responsiveness of guanylate cyclases. Studies have shown greater sensitivity to NO if endogenous synthesis of NO is reduced by NOS inhibitors or endothelial denudation (Moncada *et al.*, 1991). Vessels with reduced basal NO, as occurs in mice deficient in eNOS, show increased sensitivity to NO and NO donors (Hussain *et al.*, 1999). Desensitisation of the sGC-cGMP system also occurs after exposure of the tissues to high concentrations of NO (Hussain *et al.*, 1999). Overexpression of eNOS leads to reduced responses to endothelium-dependent and independent relaxation which can be attributed to reduced activity of sGC (Yamashita *et al.*, 2000). A cross-desensitisation between endogenously produced NO and exogenously administered NO donors has also been found to occur (Papapetropoulos *et al.*, 1998).

Cross-desensitisation between the sGC-cGMP and the pGC-cGMP systems has also been described, such that the changes in the sensitivity of one pathway are mirrored by the other cGMP-generating system. For example, murine aortic rings exposed to ANP show reduced responsiveness to the NO donor SPER-NO (Hussain *et al.*, 2001; Madhani *et al.*, 2003). Aorta from eNOS knockout (KO) mice are more

sensitive to ANP than tissues from WT animals. Moreover, the potency of ANP in aorta from WT animals is increased in the presence of NOS inhibitors (Madhani *et al.*, 2003). In contrast, the potency of ANP in aorta from eNOS KO animals is reduced following pre-treatment of tissues with high concentrations of the NO-donor, GTN.

1.5.2 Mechanisms of desensitisation affecting both GC-cGMP pathways

The mechanisms of sensitisation and desensitisation caused by changes in the ambient concentration of NO and ANP are yet to be identified. Some studies have suggested a reduction in the activity of sGC (Papapetropoulos *et al.*, 1996). Another study has suggested that the level and the activity of cGMP-dependent PKG is decreased (Yamashita *et al.*, 2000). The mechanism mediating the cross-desensitisation of NPR-A appears to involve cGMP, since administration of the sGC inhibitor, ODQ, significantly preserves relaxation to ANP (Hussain *et al.*, 2001; Madhani *et al.*, 2003). Enzyme systems that have been implicated in the regulation of the GC-cGMP pathways affecting the sensitivity of sGC and/or pGC-cGMP pathways will be discussed in detail below.

1.5.2.1 Role of phosphodiesterases

In VSMC, cGMP is regulated by cGMP-hydrolysing enzymes known as phosphodiesterases (PDEs). 11 different PDE isozymes have been identified; the predominant PDEs present in arterial smooth muscle are PDE1, PDE3 and PDE5 (Rybalkin *et al.*, 2003). PDE5 is considered the most important cGMP-hydrolysing PDE in VSMC. However, under conditions where calcium levels are elevated, PDE1 also plays a role in cGMP metabolism. PDEs degrade cGMP by transforming the active cyclic nucleotides into inactive 5'-nucleotide monophosphates (Rybalkin *et al.*, 2003).

Upregulation or downregulation of these cGMP-hydrolysing enzymes leads to a reduction or enhancement of the bioactivity of cGMP, respectively. De Garavilla *et al.* demonstrated in rats made tolerant following administration of GTN, that the vasorelaxation to GTN was restored following treatment with the phosphodiesterase

inhibitor zaprinast (De Garavilla *et al.*, 1996). In rats made tolerant by continuous infusion of GTN for 3 days, Kim and others demonstrated that the reduced responsiveness to further treatment with GTN was associated with upregulation of PDE1A1 activity and expression (Kim *et al.*, 2001). Oral administration of milrinone, a specific inhibitor of PDE3, suppressed intimal thickening in a mouse model of vascular injury (Kondo *et al.*, 1999), suggesting the possible involvement of PDE3 in inflammatory vascular diseases. These observations indicate that regulation of cGMP levels by PDEs are important factors in the determination of the activity of GC-cGMP pathway and have important implication in conditions associated with increased levels or activity of PDEs.

1.5.2.2 Role of protein kinase C

Protein kinase C (PKC) is a family of at least 12 isoforms that is expressed in various cell types, including VSMC, endothelial cells (Krotova *et al.*, 2003) and cardiac myocytes. PKC isoforms are divided into three subfamilies. The conventional-PKC isoforms (α , β I, β II and γ) are activated by the second messengers Ca^{2+} and diacylglycerol (DAG) in the presence of phosphatidylserine (PS) (Salamanca & Khalil, 2005). The novel-PKCs isoforms (ϵ , η , θ , δ and μ) require PS and DAG for full activation but are insensitive to Ca^{2+} . Finally, the atypical-PKC isoforms (λ , ν and ζ) are not activated by DAG or Ca^{2+} (Salamanca & Khalil, 2005). PKC isoforms that have been reported in VSMC include the conventional-PKC isoforms (α and β), the novel-PKC isoforms (ϵ , η , θ , δ and μ) and the atypical (ζ and λ) (Yano *et al.*, 1999; Itoh *et al.*, 2001; Salamanca & Khalil, 2005).

In VSMC, PKC has been shown to alter the sensitivity of sGC. Morrison and coworkers demonstrated that the responsiveness of rat aortic rings to endothelium-dependent and -independent vasodilators is reduced in vessels precontracted with phorbol 12-myristate 13-acetate (PMA) with reduced cGMP production compared to those precontracted with noradrenaline (Morrison & Pollock., 1990). The responsiveness of rat aortic rings to ACh, SNP, 8-Bromoguanosine-3',5'-cyclic monophosphate (8-Br-cGMP) but not the adenylate cyclase activator, forskolin, was significantly reduced in vessels precontracted with the PKC activators PMA and

phorbol 12, 13-dibutyrate compared to vessels precontracted with noradrenaline (Murphy *et al.*, 1994). Kamata *et al.* demonstrated in rat mesenteric vessels that precontraction with PMA reduces the responsiveness to ACh, SNP and forskolin compared to those vessels precontracted with methoxamine (Kamata *et al.*, 1995). These studies suggest that PKC desensitises sGC-cGMP pathway in blood vessels, but its effects on the AC pathway is controversial. However, they do not show which isoforms cause this desensitisation.

Desensitisation of NPRs by PKC has also been reported. In stable transfectants of NIH 3T3 fibroblasts with NPR-A, activation of PKC decreased cGMP accumulation by NPR-A (Potter & Garbers 1994). Exposure of HEK 293 cells to the PKC activator, PMA, results in a selective dephosphorylation of Ser-523 in NPR-B and reduces the accumulation of cGMP (Potter & Hunter 2000). Replacement of this amino acid with alanine or glutamate abolished the inhibition, suggesting that dephosphorylation of this serine residue accounts for desensitisation of NPR-B by PKC. These studies clearly demonstrate that PKC desensitise NPRs in cultured cells. However, it is not known which isoforms cause this desensitisation as these studies used PMA, which non-selectively activates both the conventional and the novel-PKC isoforms (Tsao & Wang, 1997; Kim *et al.*, 1997 and Krotova *et al.*, 2003).

1.5.2.3 Desensitisation specific for NO: role of free radicals

In general, relatively low concentrations of reactive oxygen species (ROS) such as superoxide anion (O_2^-) modulate cell signalling and contribute to other key functions, such as regulation of activity of transcription factors and gene expression. In contrast, higher levels of ROS contribute to vascular dysfunction (Faraci & Didion, 2004). Reduced responsiveness of sGC to NO may occur indirectly through scavenging of NO by free radicals. ROS such as O_2^- can react rapidly with NO, reducing its bioavailability and forming peroxynitrite $ONOO^-$ (Bouloumie *et al.*, 1997). $ONOO^-$ has cytotoxic effects and may account for endothelial injury (Bouloumie *et al.*, 1997). $ONOO^-$ can produce DNA strand breakage, initiate peroxidation of lipids and oxidise, nitrate or nitrosate a variety of proteins, thus modifying their function (Stoclet *et al.*, 1999). Several enzymes are involved in the generation of O_2^- , such as xanthine oxidase, NADH/NADPH oxidase, lipoxygenase

and NOS (Matsuoka, 2001). The scavenging properties of O_2^- , would affect both exogenously and endogenously applied NO. Therefore, increased production of O_2^- , as occurs in disease states associated with inflammation, may reduce the stimulation of sGC. Endogenously, cells are equipped with potent inactivators of O_2^- (i.e. antioxidants), one of the most important being superoxide dismutase (SOD). There are 3 isoforms of SOD, and each are products of distinct genes but catalyse the same reaction: two isoforms of Cu/Zn SOD, one cytosolic and the other is membrane bound, the third isoform is manganese SOD which is present in the mitochondria (Faraci & Didion, 2004). SOD plays an important role in the elimination of O_2^- by converting it into hydrogen peroxide (which is then converted to H_2O and O_2 by catalase). Because of the efficiency of the reaction, the local concentration of SOD may be a key determinant of bioactivity of NO (Faraci & Didion, 2004). Thus, a major function of SOD is to protect NO and NO-mediated signalling.

Myeloperoxidase (MPO) is an abundant haemoprotein synthesised by activated leukocytes such as neutrophils and monocytes (Heinecke, 1999). MPO-mediated mechanisms for NO consumption have been an area of intense recent interest. All members of the mammalian haem peroxidase superfamily, to which MPO belongs are capable of catalytically consuming NO under physiologically relevant conditions (Abu-Soud & Hazen, 2000). Accumulation of MPO within the subendothelium, and co-localisation within the subintima of atherosclerotic lesions, support the potential role for MPO in promoting oxidative consumption of NO. Evidence of an *in vivo* role for MPO in NO consumption within the vasculature was recently reported. Using an animal model of sepsis, Eiserich et al showed that MPO modulates NO responses in aorta from wild type versus MPO knockout mice through catalytic consumption of NO by MPO-generated free radicals (Eiserich *et al.*, 2002). In summary, NO bioavailability is crucial for vascular function and this bioavailability is affected during inflammation by free radicals. It is possible that oxidative stress could contribute to the mechanism of desensitisation of NO-sGC pathway.

1.5.2.4 Desensitisation affecting NPRs pathway: role of protein phosphatase 2A

Desensitisation of NPRs can occur as a result of receptor degradation, downregulation or changes in the phosphorylation status of the receptor (Potter *et al.*, 2006). Basally, NPRs exist in a phosphorylated state that is required for the acquisition of sensitivity towards NPs (Potter & Hunter, 1998a). In human embryonic kidney cells labelled with [³²P] orthophosphate, NPR-A is highly phosphorylated when unbound to ligand. Exposure to the ligand results in a time-dependent dephosphorylation and desensitisation of the receptor (Potter & Garbers, 1992). NPR-A can be dephosphorylated and desensitised by the addition of protein phosphatase 2A (PP2A), and blocked by the PP2A inhibitor, okadaic acid (Potter & Garbers., 1992). In a similar fashion to NPR-A, *in vitro* dephosphorylation of crude NPR-B membranes with purified PP2A resulted in marked losses in CNP-dependent NPR-B activity. The presence of PP2A inhibitor okadaic acid preserved the activity of NPR-B (Potter, 1998). To examine the absolute requirement of dephosphorylation-mediated desensitisation of NPR-A, Potter and Hunter generated a mutant version of NPR-A that is a fully phosphorylated receptor but is resistant to dephosphorylation. Although this mutant was less responsive to ANP than the wild type, it was resistant to the effects of a PP2A inhibitor (Potter & Hunter, 1999). In addition, Zhou *et al* demonstrated that PKG in vascular smooth muscle can activate PP2A (Zhou *et al.*, 1996). This suggests that desensitisation of NPRs could occur through a cGMP-dependent negative feedback mechanism. These data indicate that dephosphorylation is a mechanism of NPR-A and NPR-B desensitisation, with PP2A is strong candidate.

1.5.3 Importance of GC desensitisation

Most cellular signalling pathways possess regulatory feedback mechanisms in a positive and negative manner, which permit adaptation to changes in the degree of activation. The sGC- and pGC-cGMP systems share common roles in cardiovascular homeostasis. Therefore, an interaction between these two pathways to regulate cGMP levels might represent an important physiological phenomenon. An increase or decrease in one cGMP generating system could be compensated by the other cGMP system (Hussain *et al.*, 2001; Madhani *et al.*, 2003). This phenomenon may also have important pathophysiological and therapeutic implications. In cardiovascular disease,

it is possible that such integration provides a mean to compensate for dysfunction of either cGMP-dependent pathway. For instance, in cardiovascular diseases associated with endothelial dysfunction or deficiencies in NO production as in hypertension and atherosclerosis, pGC-cGMP pathways could supplement the reduced activity of the NO-cGMP pathway.

In contrast, the interaction may represent a negative-feedback mechanism that prevents overactivation of cGMP signalling. In disease states associated with excessive activation (such as sepsis) of one cGMP generating system might cause a downregulation of the other cGMP generating pathway. CHF is associated with increased circulating levels of NPs (Luchner *et al.*, 1998). This could lead to an increased generation of cGMP and possibly downregulation of both sGC and pGC-cGMP systems, contributing to the increased vasoconstriction seen in heart failure.

Therapeutically, the reciprocal interaction between sGC and pGC might also contribute to tachyphylaxis during chronic administration of NPs (Tsutamoto *et al.*, 1992; Komarek *et al.*, 2004) and organic nitrates (Parker & Gori, 2001). Indeed, therapies based on supplementing natriuretic peptides or NO are likely to result in reduced biological activity of sGC and pGC-cGMP. Down-regulation of vascular NO-sGC pathway activity might, therefore, explain the link between increased NP activity and increased cardiovascular risk (Wang *et al.*, 2004). This phenomenon might also underlie, at least in part, the increase in mortality rate observed in patients with heart failure treated with nesiritide (Sackner-Bernstein *et al.*, 2005); cGMP-induced resistance to NO could precipitate adverse cardiovascular events (i.e. stroke, myocardial infarction) as its cytoprotective influence on vascular tone, leukocytes and platelets is diminished. Therefore, a full understanding of this regulatory mechanism may have important therapeutic implications for conditions in which there is inappropriate activation of sGC or pGC-cGMP signalling pathways.

1.6 Research questions addressed in this thesis

This thesis has attempted to answer three main questions related to the endogenous regulation of NO-sGC and NP-pGC pathways that converge to govern cGMP signalling in the vasculature. Firstly, in chapter 3, I investigated the

mechanisms underlying Cu-mediated bioactivation of *S*-nitrosothiols (as NO-stores or NO-donors) and whether this might be facilitated by an endogenous enzyme/receptor –dependent or -independent process. Secondly, in chapter 4, I attempted to elucidate the effect of LPS, that mimics many aspects of inflammatory vascular disorders *in vitro*, on the sensitivity of GC-cGMP pathway. Finally, in chapter 5, I examined the potential mechanism(s) underlying the desensitisation of GC-cGMP pathway by LPS.

CHAPTER TWO

MATERIALS AND METHODS

2. MATERIALS AND METHODS

2.1 Saville assay for *S*-nitrosothiols

2.1.1 Basic principle

This assay was used for the measurement of the decomposition of *S*-nitrosothiols. The assay was established in 1958 by Saville (Saville, 1958) and depends on colourimetric determination of *S*-nitrosothiol concentration. *S*-nitrosothiols are known to undergo hydrolysis in the presence of certain metal ions, such as Hg^{2+} , yielding nitrous acid (HNO_2). The nitrous acid is detected by reaction with sulphanilamide and *N*-(1-naphthyl)ethylenediamine dihydrochloride. Before this hydrolytic process occurs, excess and free nitrous acid that may exist as a contaminant is removed from the solution with ammonium sulphamate (AS). Subsequent addition of Hg^{2+} results in an immediate liberation of nitrogen and the formation of a diazonium salt by reaction with sulphanilamide (SA). The reaction of the diazonium salt with *N*-(1-naphthyl) ethylenediamine dihydrochloride (NED) results in the production of an intensely coloured (purple) azo dye, which can be read spectrophotometrically (Abs_{540}) Figure 2.1.

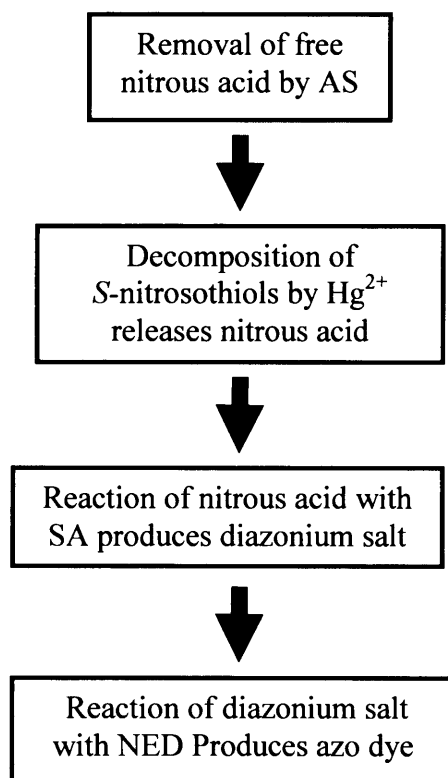


Figure 2.1 Diagram showing the steps in the Saville's assay

2.1.2 Basic protocol

S-nitrosothiols (50µl) treated with copper ions, Cu/Zn superoxide (Cu/Zn-SOD) or incubated with rat aorta, were mixed with 50µl ammonium sulphamate (0.1%; dissolved in 0.4N hydrochloric acid) for 5 mins (in a 96-well plate) to remove free nitrous acid/nitrite ($[H]NO_2$). In contrast, distilled water (50µl) was added to the standard (sodium nitrite). Standard and *S*-nitrosothiol samples were then mixed with a solution (50µl) containing sulphanilamide (3%) and Hg^{2+} (0.25%; both dissolved in 0.4N hydrochloric acid) to catalyse the release of NO. This step was immediately followed by addition of 50µl N-(1-naphthyl) ethylenediamine dihydrochloride (0.1%) into both standard and *S*-nitrosothiol samples to form a stable azo dye. After 10 mins incubation, absorbance of the purple colour produced was read (SpectraMAX 250, provided by Molecular Devices, USA) at 540nm. *S*-nitrosothiol concentration was calculated using a standard curve constructed with 0-200µM of sodium nitrite by using SoftMax Pro Software. All the readings of the standard curve were made in duplicate. The intensity of the colour (Abs_{540}) is directly proportional to the concentration of *S*-nitrosothiol.

2.2 Stereoisomers of *S*-nitrosothiols

2.2.1 Basic Principles

Two molecules may have exactly the same atoms arranged in exactly the same sequence yet differ with respect to the spatial orientation of a key functional group. Such molecules are called stereoisomers (Lamzin *et al.*, 1995). Depending on the direction in which the key functional group is orientated with respect to the molecules, stereoisomers are called either D-isomers (right-handed) or L-isomers (left-handed). These subtle differences in structure are extremely important biologically. They ensure enzymes, which interact with such molecules in a stereospecific way in chemical reactions, cannot combine with the opposite stereoisomer. The enzymes of all cells (human and others) can combine only with L-amino acids and D-sugars (Lamzin *et al.*, 1995). This approach is widely

recognised and was used in this work to examine whether the decomposition of *S*-nitrosothiols might involve enzyme dependent mechanisms.

2.2.2 Synthesis of *S*-nitrosothiols

Generally, the reaction between thiol groups and acidified nitrite in the presence of water results in the formation of *S*-nitrosothiols (Hogg, 2000). In this thesis, this reaction was used to synthesise the DL- and D-isomers of SNAP according to the method of Field et al (1978). Briefly, DL- and D-acetylpenicillamine were mixed with a two-fold molar excess of sodium nitrite under acidic conditions. The resulting fine, green precipitate was filtered and air-dried.

Synthesis of L- and D-isomers of CYSNO was also carried out in a similar fashion according to the method of Kowaluk & Fung (1990). Here, equimolar (20mM) volumes of L- or D-cysteine and sodium nitrite were added to sealed flasks and the pH adjusted to approximately 2 by the addition of 0.1M HCl. After shaking, the reaction mixture was kept at 4°C for 30mins and the pH re-adjusted to ~7.4 by addition of 0.1M NaOH. A characteristic red colour formed rapidly following acidification, indicative of the formation of CYSNO.

Synthesis of L- and D-GSNO was achieved by reaction of equimolar (20mM) concentrations of L- or D-GSH (synthesised by the Medicinal Chemistry Department, Wolfson Institute for Biomedical Research, University College London) and sodium nitrite in the presence of (1N) HCl, as adapted from the method of Hart (1985). After shaking, the reaction mixture was kept at 4°C for 30mins. The concentrations of L- and D-GSNO and CYSNO generated from the above reactions were measured by reading the absorbance of these solutions spectrophotometrically (CECIL, CE 2041, 2000 series, Cambridge, England) at 334nm and calculated by using this formula, $C = \frac{Abs_{334}}{\epsilon \cdot L}$, where C is the concentration, ϵ is the extinction coefficient (800M⁻¹cm⁻¹) (Mathews & Kerr, 1993), and L is the path length (1cm). To avoid premature decomposition, all *S*-nitrosothiols stock solutions were made fresh using deionised water (18 Omega Ω) just before use, kept on ice and protected

from light. To examine the decomposition by Cu/Zn-SOD (20 μ M) or rat aortic rings, all solutions and subsequent dilutions were prepared in Krebs' solution (composition (mM): NaCl 118, KCl 4.7, CaCl₂ 2.5, KH₂PO₄ 1.2, MgSO₄ 1.2, NaHCO₃ 2.5, glucose 11) to allow the reaction to occur in physiological media.

2.2.3 Assessment of enzyme-dependent and independent decomposition of *S*-nitrosothiols

Decomposition of L- and D-isomers of *S*-nitrosothiols was examined in the presence of free copper ions (copper(I)-acetonitrile and copper(II)-sulphate) or complex structures such as the copper containing enzyme, Cu/Zn-SOD and whole tissue (rat aorta). The abbreviations Cu(I) and Cu(II) will be used through the rest of the thesis to represent copper(I)-acetonitrile and copper(II)-sulphate, respectively.

2.2.3.1 Non-enzymatic (chemical) decomposition

Due to the insolubility and lack of commercial-availability of Cu(I) salts, most of the published works assessing the role of copper ions in *S*-nitrosothiol decomposition has been conducted using Cu(II) salts (in the presence of a reducing agent such as a thiol or ascorbate), and confirmed the role of Cu(I) ions only by using a specific chelator for Cu(I) (e.g. bathocuproine disulphonic acid (BCS) or neocuproine). In this thesis, I had access to a water soluble Cu(I)-acetonitrile complex (kind gift of Jon Fukuto, UCLA), that enabled direct determination of the role of Cu(I) ions on the decomposition rate of L- and D-isomers of GSNO, SNAP and CYSNO, and was also used to indirectly assess the role of endogenously stored *S*-nitrosothiols by using classical organ bath pharmacology. Confirmation of the role of Cu(I) ions in the decomposition of L- and D-isomers of *S*-nitrosothiols by Cu(I), Cu(II), Cu/Zn-SOD and rat aorta was made by using the specific Cu(I) chelator, BCS.

2.2.3.2 Enzymatic decomposition

To assess the role of endogenous (potentially enzymatic) breakdown of *S*-nitrosothiols, the vasorelaxant activity of L- and D- isomers of GSNO, SNAP and CYSNO were evaluated by using organ bath pharmacology (described in section 2.3) and confirmed by examining the decomposition of L- and D-GSNO by rat aortic rings

in vitro using the Saville assay (as described in section 2.1). This approach was used to show that if there is an enzyme-dependent decomposition of *S*-nitrosothiols then the decomposition rate of L-isomers of *S*-nitrosothiols by rat aorta will be faster than that of D-isomers due to the inability of the D-isomer to react stereospecifically with an endogenous enzyme. In the case of Cu/Zn-SOD, this enzyme (20 μ M) was used as an example of a copper-containing enzyme to show that such proteins could play an important role in the decomposition of *S*-nitrosothiols *in vivo*. The specific protocols that were used to examine the relaxant effect of L- and D-isomers of *S*-nitrosothiols on rat aorta and their decomposition by copper ions, Cu/Zn-SOD and rat aorta in the presence or absence of BCS are described in Chapter Three.

2.3 Organ bath pharmacology

2.3.1 Rationale

Measuring isometric tension of isolated vessels in an organ bath is a widely used technique to assess vascular function (Angus & Wright 2000). This technique allows the study of pharmacological interventions in the absence of the influence of other haemostatic mechanisms, the autonomic nervous system and physical influences, such as changes in shear stress. Tissues are suspended in a physiological oxygenated solution to allow preservation of function and can be stimulated with known concentrations of agonists and antagonists to explore changes in isometric force. As it is possible to treat multiple rings from the same vessel in different baths simultaneously, this technique lends itself to exploring the effects of different pre-treatments. In this work, the technique was used to study the vasorelaxant effect of the L- and D- isomers of GSNO, SNAP and CYSNO. This technique was also used to study the effects of LPS on the response to soluble and particulate guanylate cyclase-dependent vasorelaxants and to explore the mechanisms underlying these effects.

2.3.2 Vessel harvesting

Experiments were carried out using male Sprague-Dawley rats (200-250g) reared by the Central Biological Services Unit (University College London) on standard chow with water *ad libitum*. Male rats were used to avoid any discrepancies that might arise from differences in gender. Rats were killed by stunning and cervical

dislocation. The thoracic aorta was immediately exposed and removed in its entirety with minimal trauma to maintain tissue integrity. After removal the aorta was transferred to pre-oxygenated Krebs' solution (composition (mM): NaCl 118, KCl 4.7, CaCl₂ 1.25, KH₂PO₄ 1.2, MgSO₄ 1.2, NaHCO₃ 2.5, glucose 11) and extraneous fat and connective tissue were removed. The vessel was then cut into 2-3mm rings before suspension in the organ bath.

2.3.3 Basic Protocol

All organ baths were cleaned prior to studies with 10% hydrochloric acid and 30% ethanol followed by multiple washes with purified water (18 Ω). Organ baths were then filled with Krebs' solution that was heated to 37°C and bubbled with 95%O₂/5%CO₂. Each channel was calibrated with a standard 5g weight prior to mounting tissues. Vessel rings were suspended between a fixed stirrup and one connected to a force transducer (FT03, Grass Transducer, USA) connected to a Rikadenki chart recorder. Rat aorta was pre-tensioned to 1g and during a 60 mins equilibration period, this tension was adjusted, to maintain this level. The organ bath set up is shown in Figure 2.2. Following the equilibration period, vessels were primed by contraction with potassium chloride (KCl; 48mM) and vessels that did not generate active tension of at least 1g were discarded; this was repeated twice to ensure consistency of effect. Vessels were washed several times over at least 20 mins to restore baseline resting tension.

Endothelial integrity was examined by initially contracting the tissues with the alpha-adrenoceptor agonist phenylephrine (PE; 0.3μM), allowing a stable plateau to occur and then relaxation with ACh (1μM). In rat aorta, ACh acts by stimulating increased production of NO from the endothelium by eNOS following muscarinic receptor-mediated calcium influx (Furchgott & Zawadzki, 1980), which then acts in a paracrine fashion to decrease intracellular calcium in the vascular smooth muscle. Changes in sensitivity to ACh, therefore, act as a marker of changes in endothelial function. Relaxation by >50% in response to ACh indicated an intact endothelium; other vessels were discarded. Studies on denuded vessels were performed to assess the role of endothelial cells in endogenous S-nitrosothiol-mediated vasorelaxation.

Denudation of the endothelium was achieved by inserting forceps into the lumen of rat aortic rings and gently removing the endothelial cells without damaging VSMC. The endothelium was deemed denuded if the responses of precontracted (PE; 0.3 μ M) rings gave less than 5% relaxation to ACh (1 μ M). Vessels were washed several times and allowed to return to baseline over at least 30 minutes prior to the specific protocols that are described in the relevant data chapters.

Concentration-response curves to PE and U46619 (thromboxane A₂ mimetic) was achieved by cumulative addition of stock solutions of PE (10⁻⁶-10⁻²M) and U46619 (10⁻⁶-10⁻³M) to achieve half log unit changes in concentration at each step. This allowed the addition of 25-50 μ L at each step to a total volume of 25mL in the organ bath chamber– thus not significantly altering the total volume over a standard concentration-response curve. In LPS-treated vessels, the induction of iNOS caused hyporeactivity of the vessels to PE. However, unlike PE, U46619 caused stable contractions in vessels incubated with LPS and was therefore used in all experiments to pre-contract tissues (approximate EC₈₀: ~0.1 μ M in control tissues and ~0.3 μ M in LPS-treated tissues). Concentration-response curves to vasorelaxants were performed by pre-contracting the vessels with an EC₈₀ of PE or U46619 (where appropriate) and allowed to reach a plateau before incremental cumulative addition of stock solutions of the vasorelaxant of interest. The effect of the added concentration was allowed to reach a plateau before the addition of the subsequent concentration. On completion of each protocol, the vessels were removed and organ baths were again cleaned prior to further experimentation.

2.4 *In vitro* animal model of sepsis

In animal models, sepsis has been mimicked by administration of LPS. LPS contributes greatly to the structural integrity of the bacteria, and protects them from host immune defenses. LPS comprises of three parts: polysaccharide side chains, core polysaccharides and lipid A (Wright & Kanegasaki, 1971). Treatment with LPS is a widely used protocol to induce iNOS expression *in vitro* and thereby permit study of isolated vascular rings. In this work, LPS (0.3 μ g/ml) from *salmonella typhosa* (serotype: 0901) was incubated with rat aortic rings in the organ bath for 4 hours. Translation of iNOS mRNA and the subsequent assembly of iNOS protein is associated with ‘high output’ production of NO (Thiemermann, 1997). The cellular

mechanism by which LPS stimulates the induction of iNOS is described in details in Chapter One, section 1.1.3.

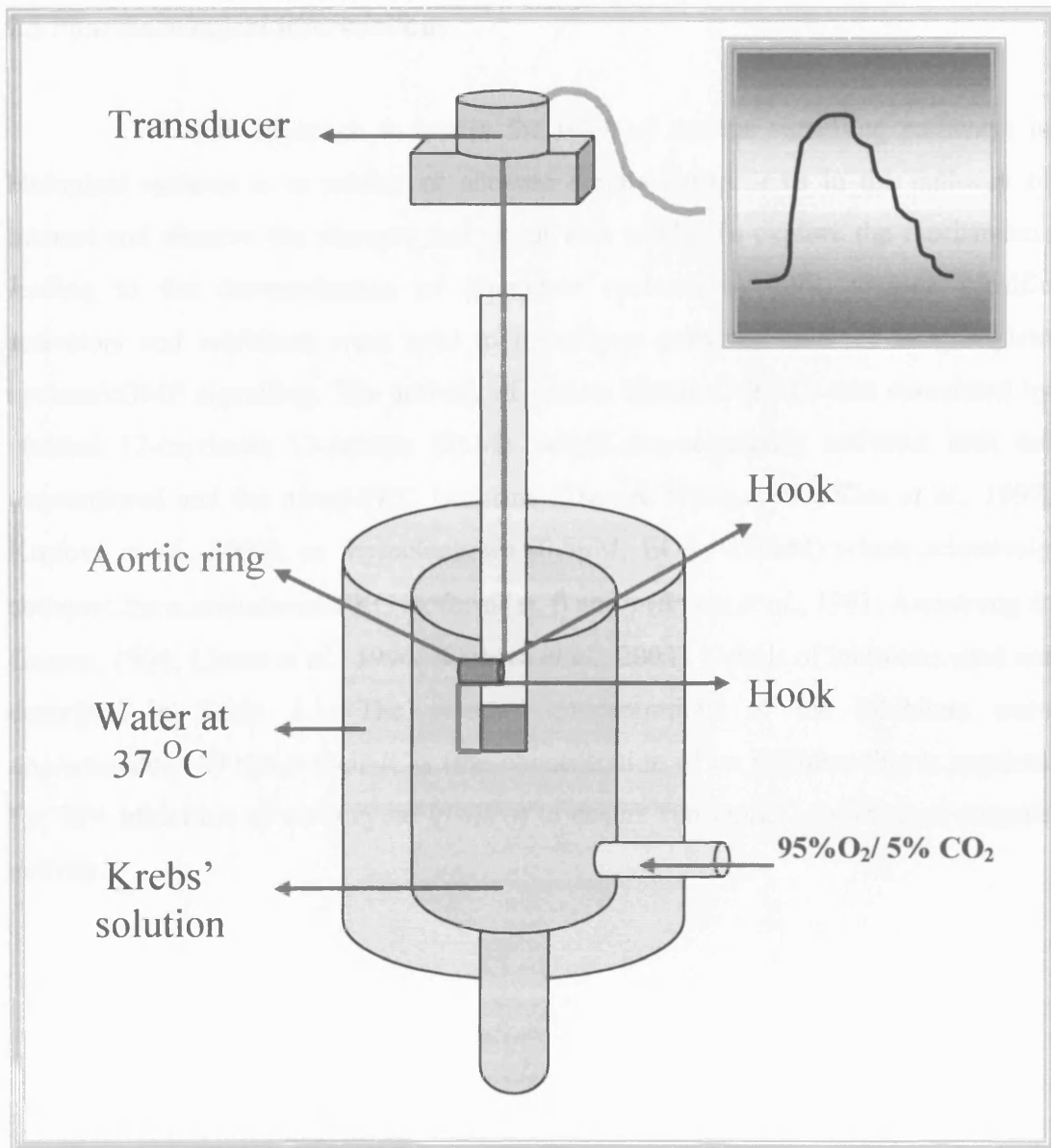


Figure 2.2 Illustration showing different parts of the organ bath chamber. Tissue is suspended between two hooks in 25 ml organ baths containing warmed (37°C), oxygenated Krebs' solution. The tissues were connected to a transducer for the measurement of isometric force.

2.5 Pharmacological interventions

One approach to assess the roles of various signalling pathways in biological systems is to inhibit or activate certain components in the pathway of interest and observe the changes that occur as a result. To explore the mechanisms leading to the desensitisation of guanylate cyclases by LPS, various specific activators and inhibitors were used to investigate enzymes involved in guanylate cyclase/cGMP signalling. The activity of protein kinase C (PKC) was stimulated by phorbol 12-myristate 13-acetate (5 μ M), which non-selectively activates both the conventional and the novel-PKC isoforms (Tsao & Wang, 1997; Kim *et al.*, 1997; Krotova *et al.*, 2003), or thymeleatoxin (0.5 μ M; EC₅₀ <100nM) which selectively activates the conventional-PKC isoforms α , β and γ (Ryves *et al.*, 1991; Armstrong & Ganote, 1994; Llosas *et al.*, 1996; Krotova *et al.*, 2003). Details of inhibitors used are described in Table 2.1. The selected concentrations of the inhibitors were approximately 10 times their IC₅₀ (the concentration of an inhibitor that is required for 50% inhibition of an enzyme *in vitro*) to ensure substantial inhibition of enzyme activity.

Inhibitor	Target enzyme	Concentration used	IC ₅₀
(1-[p-Chlorobenzoyl]-5-methoxy- 2-methylindole- 3-acetic acid) (Indomethacin)	Cyclooxygenase-2	10µM	970nM (Futaki <i>et al.</i> , 1994)
1H-[1,2,4]Oxadiazolo[4,3-a]quinoxalin-1-one (ODQ)	Soluble guanylate cyclase	5µM	20nM (Garthwaite <i>et al.</i> , 1995)
Aminobenzoic hydrazide	Myeloperoxidase	10µM	300nM (Kettle <i>et al.</i> , 1995)
Cantharidic acid	Protein phosphatase 2A	500nM	50nM (Li & Casida,1992)
Milrinone	Phosphodiesterase 3	10µM	300nM (Harrison <i>et al.</i> ,1986)
N-(3-(aminomethyl)benzyl) acetamidine (1400W)	Inducible nitric oxide synthase	10µM	0.8µM (Garvey <i>et al.</i> ,1997)
NG-nitro-L-arginine methyl ester (L-NAME)	Endothelial nitric oxide synthase	300µM	400nM (Moore <i>et al.</i> ,1990)
Okadaic acid	Protein phosphatase 2A	300nM	1nM (Ishihara <i>et al.</i> ,1989)
Sildenafil	Phosphodiesterase 5	3µM	3.5nM (Ballard <i>et al.</i> , 1998)
Vinpocetine	Phosphodiesterase 1A1	100µM	20µM (Hagiwara <i>et al.</i> ,1984)

Table 2.1 Specific inhibitors used to investigate enzymes involved in guanylate cyclase-cGMP signalling pathways

2.6 Western blotting

2.6.1 Rationale

Western Blotting (immunoblotting) allows the identification and semi-quantification of proteins within biological samples based on their electrophoretic properties. Equal quantities of protein are added under denaturing conditions to a polyacrylamide gel matrix and are separated according to their molecular weight as they move by one-dimensional electrophoresis towards the anode (Figure 2.3). By the use of a (coloured) protein ladder of known molecular weights it is possible to identify individual products. Specificity is improved by transferring the samples after separation to a nitrocellulose transfer membrane that fixes their relative position. This can then be stained with antibodies specific to the protein of interest. This process is generally performed in two stages, firstly a specific antibody (primary antibody) is used against a protein or enzyme such as iNOS and then a secondary antibody, tagged with horseradish peroxidase, is applied against the primary antibody. The presence of horseradish peroxidase allows the detection of the antibody by its emission of light, which is captured on radiographic film. Although only semi-quantitative the relative intensity of bands demonstrated by this technique indicate the degree on expression of the protein studied provided that equal quantities of total protein have been added to the system and complete and equal transfer has occurred for all samples.

2.6.2 Protocols

2.6.2.1 Samples preparation

Western blotting was used to detect iNOS protein following incubation of rat aorta with LPS (0.3µg/ml; 4hr) *in vitro*. Aortic rings were immediately removed from the organ bath. To preserve tissue proteins, aortic rings were wrapped in aluminium foil, immediately snap frozen by immersion in liquid nitrogen and then stored at -80°C before protein extraction. Prior to separation by electrophoresis,

samples were processed to ensure cellular disruption without degradation of the relevant protein.

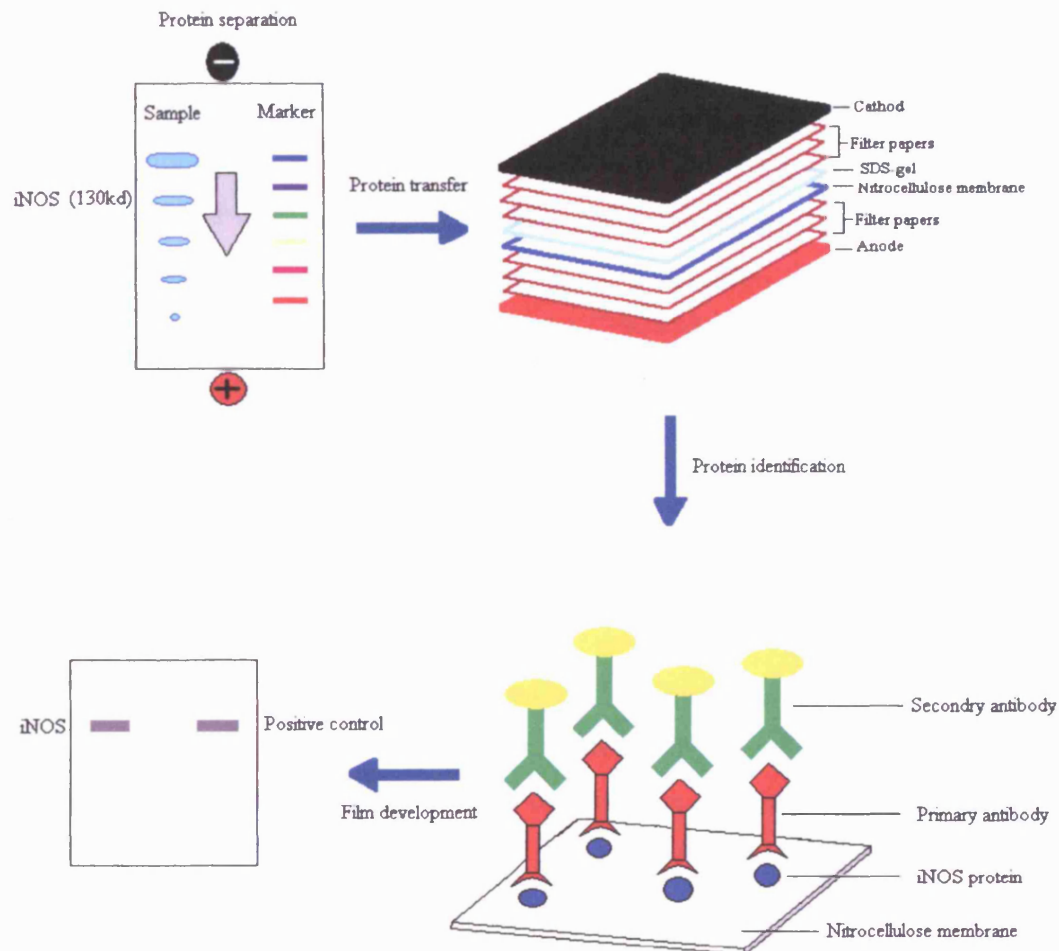


Figure 2.3 Illustration showing the process of iNOS detection by western blotting

To extract the proteins, vessels were placed in a metal receptacle (which itself had been cooled to -80°C) containing liquid nitrogen and smashed with a hammer into powder. The vessels were then removed immediately from the metal receptacle with clean forceps and kept in tubes containing (150 μl) whole cell homogenisation buffer (Tris-HCl (50mM), NaCl (150mM) and Triton X100 (1%) mixed with ethylenediamine-tetraacetic acid (EDTA) and ethylene glycol-bis-(2-aminoethyl)-

tetraacetic acid (EGTA) and adjusted to pH 7.4 with NaOH)) mixed with 1 tablet of protease inhibitors (complete, EDTA-free mini protease inhibitor cocktail; Roche) and incubated for 1 hr. The samples were vortexed every 15 min during this period to ensure complete tissue homogenisation. Tubes containing homogenised tissues were centrifuged at 13000 rpm for 5 min at 4 °C. The supernatant was collected and kept on ice for further analysis while the pellets were discarded (since iNOS is a cytosolic protein). Samples were then diluted 1:2 with the sample buffer (consists of Tris-HCl (20mM), EDTA (2mM), SDS (sodium dodecyl sulphate; 2%), mercaptoethanol (10%), glycerol (20%) and bromophenol blue (0.025%) stored at room temperature) by mixing 20µl of the sample with 20µl of the sample buffer. Before separation, protein was denatured by boiling at 95 °C for 5 min. Samples were then kept on ice for 5 min.

2.6.2.2 Protein separation

Separation of proteins was achieved by one-dimensional SDS-PAGE (sodium dodecyl sulphate-polyacrylamide gel electrophoresis). The separating gel (7.5% made by mixing separating gel buffer (consists of Tris-Base (1.875mM) and SDS (0.5%) and adjusted with concentrated HCl to pH 6.8) with acrylamide/bis-acrylamide (30%), ammonium persulphate (10%) and TEMED (NNNN-tetramethylethylenediamine)) was poured over the rig and overlaid with isopropanol (to prevent the formation of air bubbles). When gels had set, the isopropanol was poured off by inverting. The stacking gel (4% made by mixing stacking gel buffer (consists of Tris-Base (0.625mM) and SDS (0.5%) and adjusted with concentrated HCl to pH 6.8) with acrylamide/bis-acrylamide (30%), ammonium persulphate (10%) and TEMED) was poured over the separating gel. Combs (0.75mm in width) were inserted to produce the samples wells. After the gels had set, the combs were removed and the wells cleaned of excess material. The gels were mounted within the clamping frame and electrode assembly and placed in the buffer chamber. The chamber was then filled between the gels with running buffer (contains Tris base (50mM), glycine (0.384M) and SDS (0.1%)) until half full. The samples (20µl) and the marker (10µl; Precision

marker plus kaleidoscope was purchased from bio-Rad) were added to the appropriate wells within the stacking gel. In order to separate the proteins, the gel was run at a constant voltage of 100V until the proteins are completely separated according to their molecular weight.

Following separation, the gels were removed from the tanks and sandwiched between layers of filter papers and a nitrocellulose membrane to allow transfer of the samples. The filter papers and nitrocellulose sheet were prepared according to the size of the SDS-Gel. The layers were designed from the bottom to the top as follows: six filter papers were soaked in solution-1 (contains Tris-Base (0.3M) at pH 10.4 and 20% methanol), three filter papers were soaked in solution-2 (contains Tris-Base (0.025M) at pH 10.4 and 20% methanol), nitrocellulose paper was soaked in solution-2 and finally SDS-gel and nine filter papers were soaked in solution-3 (contains 6-Amino-n-Hexanoic Acid (0.04M) at pH 7.6 and 20% methanol). The graphic plate (anode and cathode) were moistened with distilled water to allow current conductance and a constant current of $0.8\text{mA}/\text{cm}^2$ passed across for 1 hr to achieve transfer. Transfer was verified by assessing the movement of pre-stained molecular weight markers from the gel to the membrane. The nitrocellulose membrane was stained with Ponceau S solution (1%) to visualise transferred proteins while the gel and filter papers were discarded. The Blot was washed with distilled water to remove excess Ponceau S solution. Following transfer, the nitrocellulose membranes were transferred to clean baths and immersed in solution of phosphate buffered saline (PBS) mixed with Tween (PBST) containing 5% skimmed milk (Marvel) and gently agitated for at least 1 hr. This milk solution acts to bind and block non-specific proteins and improve resolution of antibody identification. After blocking, the blot was washed once every 5 mins for 25 mins in PBST.

2.6.2.3 Protein identification

Primary antibody was diluted 1:1000 by addition 10 μl of rabbit anti-iNOS antibody (BD Transduction Laboratories) into 10ml of 5% skimmed milk (dissolved in PBST). The blot was incubated with the primary antibody overnight at 4°C with

constant agitation. On completion of the overnight exposure to primary antibody, the blot was washed with 5 changes of PBST each for 5 mins.

The secondary antibody (peroxidase-conjugated goat anti-rabbit immunoglobulin; Dako Cytomation) was diluted 1:1000 by addition 10 μ l of secondary antibody into 10ml of 5% skimmed milk (dissolved in PBST) and incubated with the blot for 1 hr at room temperature. The secondary antibody was discarded and the blot was washed extensively with PBST at least 5 times, each for 5 mins. Development of the bound secondary antibody was achieved with the enhanced chemiluminescence (ECL) that is based on the enzymatic production of an acridinium ester, by horseradish peroxidase, which emits light. Each gel was covered with ECL for 2 mins. The blot was placed in autoradiography hypercassette and developed immediately using an automated developer (Compact X4, X-ograph). Finally, the developed films were scanned onto a computer with a flat-bed scanner. Localisation and identification of iNOS bands was achieved by comparison to a known iNOS-positive control.

2.7 Materials

The following compounds were obtained from Sigma; (1-[p-Chlorobenzoyl]-5-methoxy-2-methylindole-3-acetic acid; indomethacin), 9,11-Dideoxy-11 α ,9 α epoxymethano-prostaglandin (U46619), acetylcholine chloride, N-acetyl-D-penicillamine, N-acetyl-DL-penicillamine, 4-aminobenzoic hydrazide, ammonium sulphamate, atrial natriuretic peptide (from rat), bathocuproinedisulfonic acid, cantharidic acid, cupric sulfate anhydrous, D-cysteine hydrochloride monohydrate, L-cysteine hydrochloride anhydrous, histamine dihydrochloride, Krebs ringer solution (10x), lipopolysaccharide (*Salmonella typhosa*), mercuric chloride, milrinone, N-(1-naphthyl)ethylendiamine dihydrochloride, N^G-nitro-L-arginine methyl ester (L-NAME), phenylephrine hydrochloride, sodium nitrite, sodium nitroprusside, spermine-NONOate ([N-(2-Aminoethyl)-N-(2-hydroxy-2-nitrosohydrazono)-1,2 ethylene-diamine; SPER-NO), sulfanilamide, Cu/Zn superoxide dismutase (bovine)

and vinpocetine. C-type natriuretic peptide (human and porcine), okadaic acid and thymeleatoxin were purchased from Calbiochem. Acetonitrile, hydrochloric acid and potassium chloride were obtained from VWR LTD. 8-bromo- adenosine-3',5'-cyclic monophosphate (8-Br-cAMP), 8-bromoguanosine-3',5'-cyclic monophosphate (8-Br-cGMP), N-(3-(aminomethyl)benzyl) acetamidine (1400W), forskolin and phorbol 12-myristate 13-acetate were obtained from Alexis Corporation. Glyceryl trinitrate was obtained from Faulding Pharmaceuticals plc. BAY 58-2667 was obtained from Bayer AG, Germany. 1*H*-[1,2,4]-oxadiazolol-[4,3-*a*]quinoxalin-1-one (ODQ), L- and D-glutathione and sildenafil were synthesised at the Wolfson Institute for Biomedical Research, University College London.

2.8 Data analysis

Data was expressed as mean (\pm standard error of the mean (SEM)) for multiple replicates of each experiment. In organ bath studies, active tension was expressed as a percentage of that generated by potassium chloride. Relaxation was expressed as a percentage reversal of pre-contraction tension.

Concentration-response curves were fitted to all the data by non-linear regression using Prism (Graph Pad Software, San Diego, CA, USA) to calculate pEC₅₀ values (-log of the EC₅₀ values). pEC₅₀ values were used to compare the relaxant effects of drugs. All results were compared by two-way analysis of variance (TW-ANOVA) for repeated measures and where appropriate (as described in the text) adjusted with Bonferroni's correction (BC), with $P < 0.05$ was considered statistically significant.

It should be noted that in the organ bath experimentation, changes in the responsiveness of aortic rings to different agonists/antagonists was assessed by measuring changes in pEC₅₀. Although variability between experiments was small and the magnitude of desensitisation large, there are clear limitations of using this index alone that might arise from a small n number in certain experiments as well as its inability to detect changes in the maximum response. The small n number of some studies reported in this thesis may also limit the value of parametric statistics.

CHAPTER THREE

BIOTRANSFORMATION OF

***S*-NITROSOTHIOLS**

3.1 INTRODUCTION

The biological, physiological (section 1.4.4 and 1.4.5), pathophysiological (section 1.4.6) and therapeutic (section 1.4.7) importance of *S*-nitrosothiols has been discussed previously. Exploring their roles in biological systems remains limited by a lack of full understanding of the mechanisms whereby they are synthesised or degraded in biological systems. Therefore it is important to investigate the mechanisms by which these NO-donor are bio-transformed.

Evidence that endogenous *S*-nitrosothiols require metabolism to release NO comes from studies demonstrating that the rate of spontaneous release of NO from *S*-nitrosothiols correlates poorly with their potency in biological systems (Kowaluk & Fung 1990; Mathews & Kerr, 1993). Non-enzymatic catalysis of *S*-nitrosothiols by metal ions, (particularly iron and copper) (Williams, 1996), glutathione and ascorbic acid, has been implicated in the decomposition of *S*-nitrosothiols (Kashiba-Iwatsuki *et al.*, 1997).

One approach to define the possible existence of the enzyme-dependent mechanisms is to compare the relative biological potencies of stereoisomers of specific substrate by specific cell type or enzyme. Differences in the biological potencies suggest the presence of stereoselectivity toward *S*-nitrosothiols, given that stereoisomers decompose equally to NO (at least chemically). Several studies have been reported using this approach to examine the relative contribution of enzyme-dependent biotransformation of *S*-nitrosothiols (section 1.4.4.3).

The relative contribution of enzymatic mechanisms of NO release from certain *S*-nitrosothiols in vascular tissue is controversial (Davisson *et al.*, 1996; Cavero *et al.*, 2000). The aim of this study was to determine whether the biotransformation of *S*-nitrosothiols by isolated blood vessels is enzymatic or non-enzymatic. To achieve this, stereoisomers of endogenous (GSNO and CYSNO) and exogenous (SNAP) *S*-nitrosothiols were synthesised and their decomposition and relaxant effects characterised. In particular I chose to examine the effects of free copper in solution (as a non-stereospecific control), with the effects of a vascular copper containing enzyme

(Cu/Zn SOD) and whole aorta on the stability of *S*-nitrosothiols. In addition I examined whether there was evidence for stereospecific functional effects of these *S*-nitrosothiols.

3.2 EXPERIMENTAL PROTOCOLS AND STATISTICS

3.2.1 Decomposition of *S*-nitrosothiols; effects of Cu(I), Cu(II) and copper chelation

Stock solutions of Cu(I) (10 μ M and 1mM), Cu(II) (10 μ M and 1mM), BCS (2mM) and various stereoisomers of *S*-nitrosothiols (GSNO, SNAP and CYSNO; 222 μ M each) were made in deionised water. These solutions were kept on ice and protected from light. The effect of copper ions (1 μ M or 100 μ M final concentration) on *S*-nitrosothiol concentration (100 μ M final concentration) was determined over 60 mins at room temperature. This protocol was repeated in the presence of BCS (100 μ M-1mM). The Saville assay was used to determine the concentration of L-or D-isomers of GSNO, SNAP and CYSNO following these treatments (as described in 2.1.2).

3.2.2 Decomposition of L-and D-GSNO and DL-and D-SNAP by Cu/Zn SOD

Cu/Zn SOD (20 μ M final concentration) was incubated with *S*-nitrosothiols (100 μ M final concentration) for up to 60 min at 37°C. This protocol was repeated in the presence of GSH (100 μ M final concentration) and BCS (100 μ M final concentration). The Saville assay was used to determine *S*-nitrosothiol concentration following these treatments.

3.2.3 Decomposition of L-and D-GSNO by rat aorta in the presence of BCS

Stock solutions of L-and D-GSNO (1mM) and BCS (10mM), and subsequent dilutions, were prepared in Krebs' solution as described in section 2.2.2. Thoracic aorta was obtained from male Sprague Dawley rats (200-250g) as described in section 2.3.2. Aortic rings (2-3mm) were cut into half and incubated with L-or D-GSNO

(100 μ M final concentration) for up to 60 min at 37°C. To examine the effect of endogenous copper ions on the decomposition rate of L-or D-GSNO, the protocol was repeated in the presence of BCS (100 μ M). The Saville assay was used to determine the concentration of L-and D-GSNO.

3.2.4 Effects of the stereoisomers of *S*-nitrosothiols on rat aorta

Organ bath studies were performed on rings of rat thoracic aorta from male Sprague Dawley rats (200-250 g) killed by cervical dislocation and prepared as mentioned in section 2.3.2. Concentration-response curves to L-and D-GSNO (1nM-1 μ M), DL-and D-SNAP (1nM-10 μ M) and L-and D-CYSNO (1nM-10 μ M) were constructed in rings precontracted to an approximately EC₈₀ with PE. Studies were repeated in the presence of BCS (10-100 μ M; pre-incubated for 30 mins). The effect of BCS on the response to ACh (1nM-10 μ M) and SPER-NO (1nM-10 μ M) was also determined.

3.2.5 Effect Cu(I) ions on the intracellular content of *S*-nitrosothiols

Concentration-response curves were constructed to Cu(I) (100nM-300 μ M) in rat aortic rings precontracted to an EC₈₀ with PE in the presence and absence of endothelium, the sGC inhibitor ODQ (5 μ M; preincubated for 30 mins) and NOS inhibitor, L-NAME (300 μ M; preincubated for 30 mins). Concentration-response curves to acetonitrile (100nM-300 μ M) were also constructed in rat aortic rings precontracted to an EC₈₀ with PE as a control.

3.2.6 Calculations and statistics

S-nitrosothiol concentration was calculated using a standard curve constructed with 0-200 μ M of sodium nitrite by using SoftMax Pro Software. The effect of different treatments on the stability *S*-nitrosothiols was expressed as a percentage of initial concentration of *S*-nitrosothiols, and expressed as mean \pm SEM. All the data were analysed by TW-ANOVA and where appropriate Bonferroni's correction (BC) was applied. Organ bath studies were expressed as described in section 2.8.

3.3 RESULTS

3.3.1 Decomposition of *S*-nitrosothiols by copper ions

3.3.1.1 Decomposition of DL-SNAP by copper ions

DL-SNAP was relatively stable in the absence of copper ions. Cu(I) (1 μ M) caused a time-dependent decomposition of DL-SNAP ($P < 0.05$ versus control; $n = 4$; Figure 3.1; Table 3.1). At 60 minutes, 1 μ M Cu(I) caused 52.5% decomposition of the initial concentration of DL-SNAP. Similarly, 1 μ M Cu(II) caused a time-dependent decomposition of DL-SNAP ($P < 0.05$ versus control; $n = 4$; Figure 3.1). At 60 mins, 1 μ M Cu(II) caused 73% decomposition of the initial concentration of DL-SNAP. The Cu(I) chelator BCS (100 μ M) completely blocked the decomposition of DL-SNAP by both Cu(I) and Cu(II) ($P < 0.05$ versus the presence of Cu(I) or Cu(II) alone; $n = 4$; Figure 3.1).

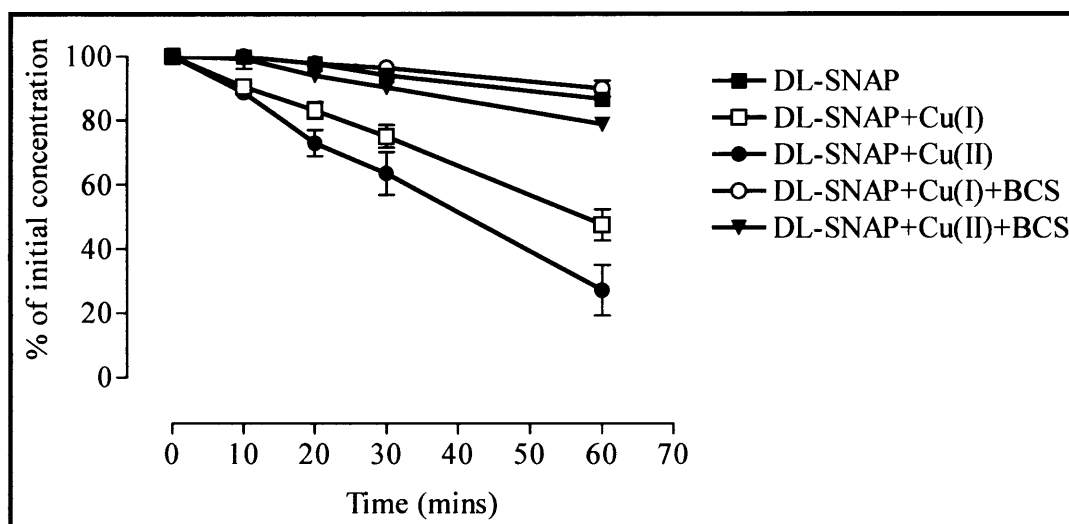


Figure 3.1 Time-dependent decomposition of DL-SNAP in the presence or absence of Cu(I) (1 μ M), Cu(II) (1 μ M) and BCS (100 μ M). Each point represents the mean \pm SEM ($n = 4$).

3.3.1.2 Decomposition of D-SNAP by copper ions

D-SNAP was relatively stable in the absence of copper ions. However, Cu(I) (1 μ M) caused a time-dependent decomposition of D-SNAP ($P<0.05$ versus control; $n=4$; Figure 3.2; Table 3.1). At 60 mins, 1 μ M Cu(I) caused approximately 54.7% decomposition of the initial concentration of D-SNAP. Similarly, Cu(II) (1 μ M) also caused a time-dependent decomposition of D-SNAP ($P<0.05$ versus control; $n=4$; Figure 3.2). At 60 mins, Cu(II) (1 μ M) caused approximately 65.6% decomposition of the initial concentration of D-SNAP. The Cu(I) chelator BCS (100 μ M) completely blocked the decomposition of D-SNAP by both Cu(I) and Cu(II) ($P<0.05$ versus the presence of Cu(I) or Cu(II) alone; $n=4$; Figure 3.2). DL-SNAP and D-SNAP decomposed at an equivalent rate in the presence of copper ions ($P>0.05$; $n=4$; Table 3.1).

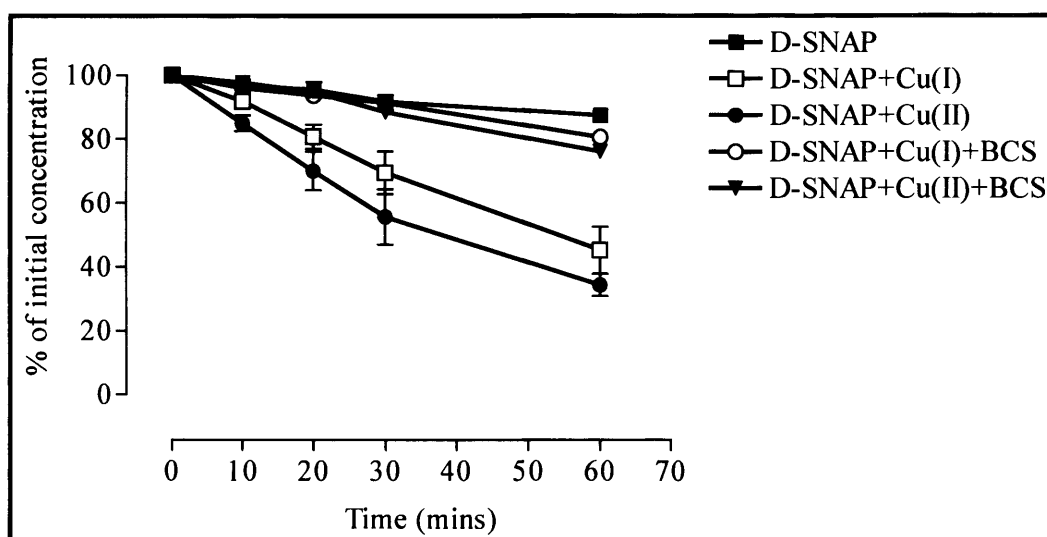


Figure 3.2 Time-dependent decomposition of D-SNAP in the presence or absence of Cu(I) (1 μ M), Cu(II) (1 μ M) and BCS (100 μ M). Each point represents the mean \pm SEM ($n=4$).

Treatments	P values
DL-SNAP vs. DL-SNAP + Cu(I)	* $P < 0.05$
DL-SNAP vs. DL-SNAP + Cu(II)	* $P < 0.05$
DL-SNAP + Cu(I) vs. DL-SNAP + Cu(I) + BCS	* $P < 0.05$
DL-SNAP + Cu(II) vs. DL-SNAP + Cu(II) + BCS	* $P < 0.05$
D-SNAP vs. D-SNAP + Cu(I)	* $P < 0.05$
D-SNAP vs. D-SNAP + Cu(II)	* $P < 0.05$
D-SNAP + Cu(I) vs. D-SNAP + Cu(I) + BCS	* $P < 0.05$
D-SNAP + Cu(II) vs. D-SNAP + Cu(II) + BCS	* $P < 0.05$
DL-SNAP vs. D-SNAP	$P > 0.05$
DL-SNAP + Cu(I) vs. D-SNAP + Cu(I)	$P > 0.05$
DL-SNAP + Cu(II) vs. D-SNAP + Cu(II)	$P > 0.05$

Table 3.1 Comparison of the decomposition of DL- and D-SNAP in the absence and presence of copper ions ($n=4$); TW-ANOVA with BC.

3.3.1.3 Decomposition of L-GSNO by copper ions

L-GSNO was stable in the absence of copper ions. Cu(I) ($1\mu\text{M}$) had no effect on the stability of L-GSNO ($P > 0.05$ versus control; $n=4$; Figure 3.3; Table 3.2). Similarly, Cu(II) ($1\mu\text{M}$) had no effect on the stability of L-GSNO ($P > 0.05$ versus control; $n=4$; Figure 3.3). At $100\mu\text{M}$ Cu(I), there was a time-dependent decomposition of L-GSNO ($P < 0.05$ versus control; $n=6$; Figure 3.3; Table 3.2). At 60 mins, Cu(I) ($100\mu\text{M}$) caused 36.7% decomposition of the initial concentration of L-GSNO. Cu(II) ($100\mu\text{M}$) caused a small but significant time-dependent decomposition of L-GSNO ($P < 0.05$ versus control; $n=6$; Figure 3.3). At 60 mins, Cu(II) ($100\mu\text{M}$) caused 17.2% decomposition of L-GSNO. The Cu(I) chelator BCS (1mM) completely blocked the decomposition of L-GSNO by both Cu(I) and Cu(II) ($P < 0.05$ versus the presence of Cu(I) or Cu(II) alone; $n=6$; Figure 3.3).

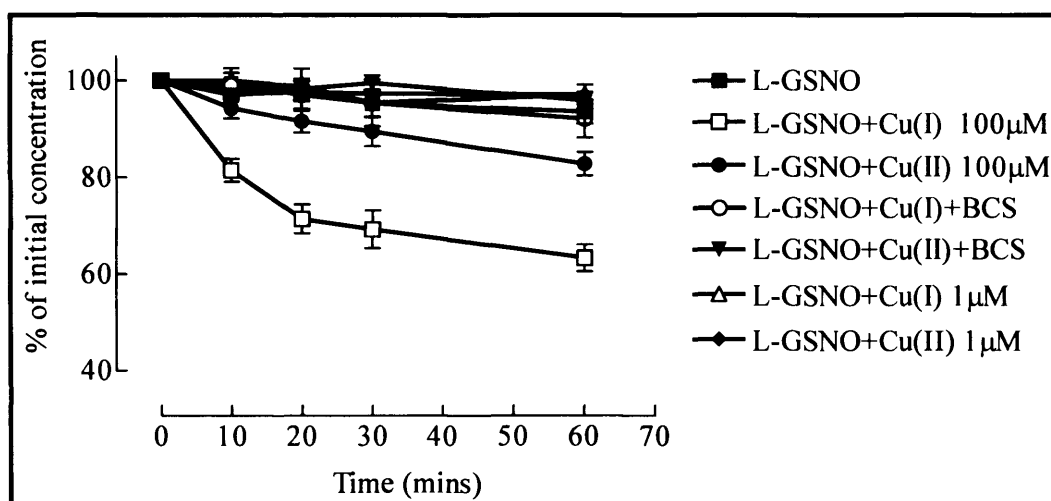


Figure 3.3 Time-dependent decomposition of L-GSNO in the presence or absence of Cu(I) (1-100µM), Cu(II) (1-100µM) and BCS (1mM) . Each point represents the mean \pm SEM ($n \geq 4$).

3.3.1.4 Decomposition of D-GSNO by copper ions

D-GSNO was stable in the absence of copper ions. However, Cu(I) (100µM) caused a time-dependent decomposition of D-GSNO ($P < 0.05$ versus control; $n = 6$; Figure 3.4; Table 3.2). At 60 mins, Cu(I) (100µM) and Cu(II) (100µM) caused approximately 33.5% and 22.3% decomposition of the initial concentration of D-GSNO, respectively. The Cu(I) chelator BCS (1mM) completely blocked the decomposition of D-GSNO by both Cu(I) and Cu(II) ($P < 0.05$ versus the presence of Cu(I) or Cu(II) alone; $n = 6$; Figure 3.4). L-GSNO and D-GSNO decomposed at an equivalent rate in the presence of copper ions ($P > 0.05$; $n = 5$; Table 3.2).

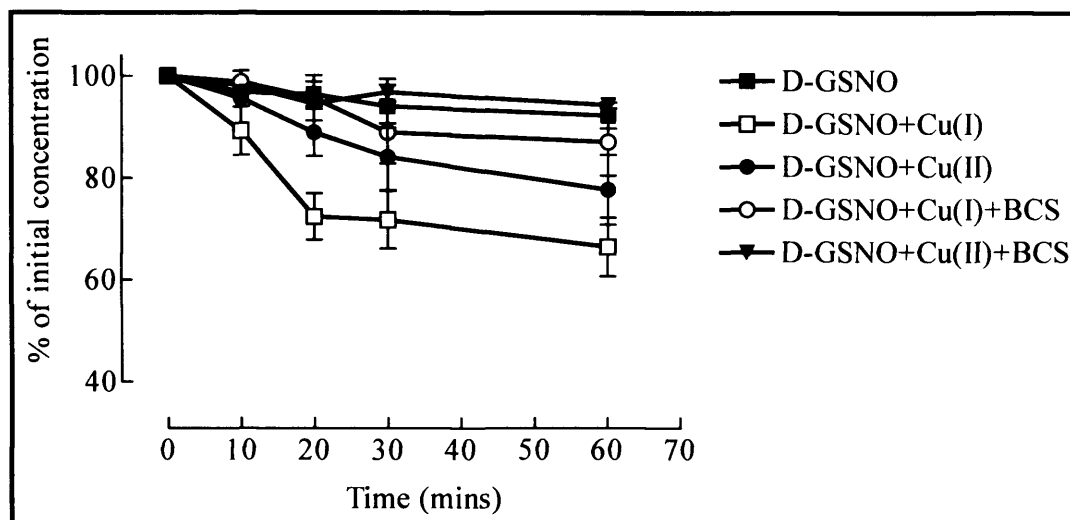


Figure 3.4 Time-dependent decomposition of D-GSNO in the presence or absence of Cu(I) (100 μ M), Cu(II) (100 μ M) and BCS (1mM) . Each point represents the mean \pm SEM (n=6).

Treatments	P values
L-GSNO vs. L- GSNO + Cu(I) 1 μ M	$P>0.05$
L-GSNO vs. L- GSNO + Cu(II) 1 μ M	$P>0.05$
L-GSNO vs. L- GSNO + Cu(I) 100 μ M	$*P<0.05$
L- GSNO vs. L- GSNO + Cu(II) 100 μ M	$*P<0.05$
L-GSNO + Cu(I) vs. L-GSNO + Cu(I) 100 μ M + BCS	$*P<0.05$
L-GSNO + Cu(II) vs. L-GSNO + Cu(II) 100 μ M + BCS	$*P<0.05$
D-GSNO vs. D-GSNO + Cu(I) 100 μ M	$*P<0.05$
D-GSNO vs. D-GSNO + Cu(II) 100 μ M	$*P<0.05$
D-GSNO + Cu(I) vs. D-GSNO + Cu(I) + BCS	$*P<0.05$
D-GSNO + Cu(II) vs. D-GSNO + Cu(II) + BCS	$*P<0.05$
L-GSNO vs. D-GSNO	$P>0.05$
L-GSNO + Cu(I) vs. D-GSNO + Cu(I)	$P>0.05$
L-GSNO + Cu(II) vs. D-GSNO + Cu(II)	$P>0.05$

Table 3.2 Comparison of the decomposition of L- and D- GSNO in the absence and presence of copper ions (n=6); TW-ANOVA with BC.

3.3.1.5 Decomposition of L-CYSNO by copper ions

L-CYSNO was unstable in the absence of added copper ions. After 60 mins there was 44% decomposition of L-CYSNO under control condition. BCS protected L-CYSNO from spontaneous decomposition ($P<0.05$ versus control; $n=5$; Figure 3.5 Table 3.3). Cu(I) ($1\mu\text{M}$) caused a rapid, time-dependent decomposition of L-CYSNO ($P<0.05$ versus control; $n=5$; Figure 3.5). As early as 10 mins, Cu(I) ($1\mu\text{M}$) caused 91.6% decomposition of the initial concentration of L-CYSNO, and at 30 mins, Cu(I) ($1\mu\text{M}$) caused complete decomposition of L-CYSNO. The Cu(I) chelator BCS ($100\mu\text{M}$) completely blocked the decomposition of L-CYSNO by Cu(I) ($P<0.05$ versus the presence of Cu(I) alone; $n=5$). Similarly, Cu(II) ($1\mu\text{M}$) caused a time-dependent decomposition of L-CYSNO ($P<0.05$ versus control; $n=5$; Figure 3.5). At 10 minutes, Cu(II) ($1\mu\text{M}$) caused almost complete decomposition of L-CYSNO. BCS ($100\mu\text{M}$) completely blocked the decomposition of L-CYSNO by Cu(II) ($P<0.05$ versus the presence of Cu(II) alone; $n=5$; Figure 3.5).

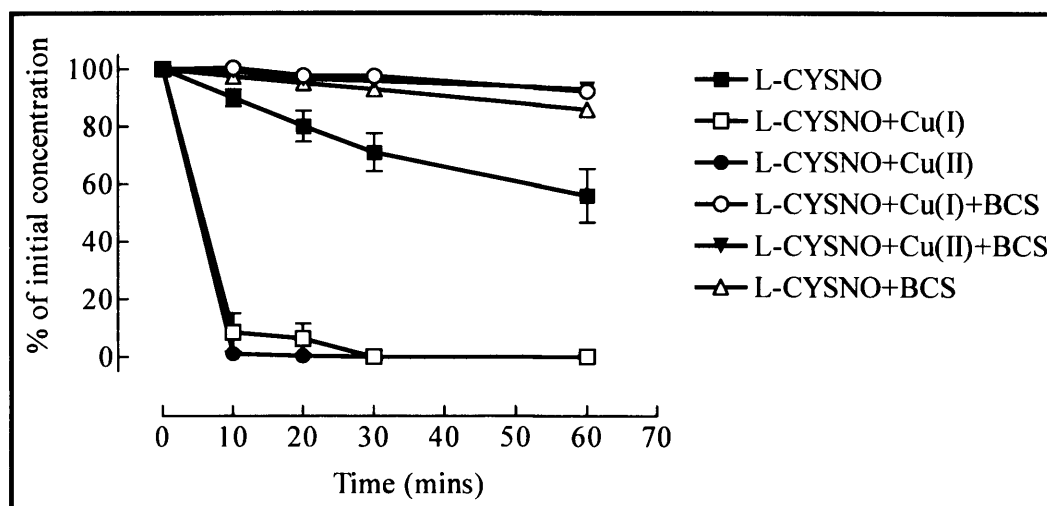


Figure 3.5 Time-dependent decomposition of L-CYSNO in the presence or absence of Cu(I) ($1\mu\text{M}$), Cu(II) ($1\mu\text{M}$) and BCS ($100\mu\text{M}$). Each point represents the mean \pm SEM ($n=5$).

3.3.1.6 Decomposition of D-CYSNO by copper ions

In a similar fashion, D-CYSNO was unstable over a period of 60 mins under control condition. At 60 mins, approximately 43.2% of the initial concentration of D-CYSNO was decomposed. BCS (100 μ M) protected D-CYSNO from this decomposition ($P<0.05$ versus control; $n=5$; Figure 3.6; Table 3.3). Cu(I) (1 μ M) caused a fast, time-dependent decomposition of D-CYSNO ($P<0.05$ versus control; $n=5$; Figure 3.6). At 10 mins, Cu(I) (1 μ M) caused approximately 89% decomposition of D-CYSNO, and at 30 mins, Cu(I) (1 μ M) caused complete decomposition of D-CYSNO. Chelation of Cu(I) with BCS (100 μ M) completely blocked the decomposition of D-CYSNO by Cu(I) ($P<0.05$ versus the presence of Cu(I) alone; $n=5$). Similarly, Cu(II) (1 μ M) caused a time-dependent decomposition of D-CYSNO ($P<0.05$ versus control; $n=5$; Figure 3.6). At 10 mins, 1 μ M Cu(II) caused 93.7% decomposition of D-CYSNO. BCS (100 μ M) completely blocked the decomposition of D-CYSNO by Cu(II) ($P<0.05$ versus the presence of Cu(II) alone; $n=5$; Figure 3.6). L-CYSNO and D-CYSNO decomposed at an equivalent rate in the absence or presence of copper ions ($P>0.05$; $n=5$; Table 3.3).

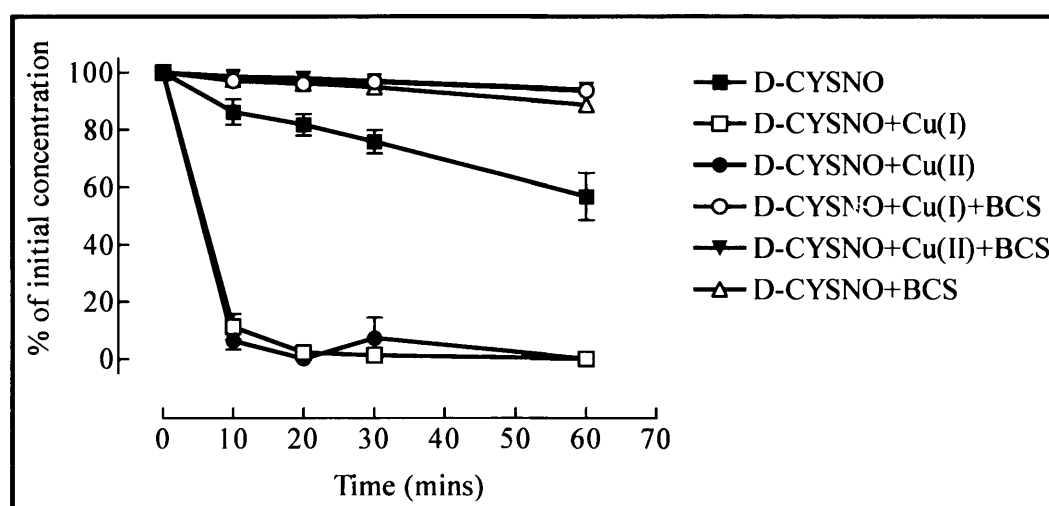


Figure 3.6 Time-dependent decomposition of D-CYSNO in the presence or absence of Cu(I) (1 μ M), Cu(II) (1 μ M) and BCS (100 μ M) . Each point represents the mean \pm SEM ($n=5$).

Treatments	P values
L- CYSNO vs. L- CYSNO + Cu(I)	* $P<0.05$
L- CYSNO vs. L- CYSNO + Cu(II)	* $P<0.05$
L-CYSNO + Cu(I) vs. L-CYSNO + Cu(I) + BCS	* $P<0.05$
L-CYSNO + Cu(II) vs. L-CYSNO + Cu(II) + BCS	* $P<0.05$
D-CYSNO vs. D-CYSNO + Cu(I)	* $P<0.05$
D-CYSNO vs. D-CYSNO + Cu(II)	* $P<0.05$
D-CYSNO + Cu(I) vs. D-CYSNO + Cu(I) + BCS	* $P<0.05$
D-CYSNO + Cu(II) vs. D-CYSNO + Cu(II) + BCS	* $P<0.05$
L-CYSNO vs. D-CYSNO	$P>0.05$
L-CYSNO + Cu(I) vs. D-CYSNO + Cu(I)	$P>0.05$
L-CYSNO + Cu(II) vs. D-CYSNO + Cu(II)	$P>0.05$

Table 3.3 Comparison of the decomposition of L- and D- CYSNO in the absence and presence of copper ions ($n=5$); TW-ANOVA with BC.

3.3.2 Effect of Cu/Zn SOD on the stability of S-nitrosothiols

3.3.2.1 Decomposition of L-GSNO by Cu/Zn SOD

Cu/Zn SOD (20 μ M) alone had no effect on the stability of L-GSNO ($P>0.05$ versus control; $n=4$; Figure 3.7; Table 3.4). GSH (100 μ M) alone caused a small but significant, time-dependent decomposition of L-GSNO ($P<0.05$ versus control; $n=3$). At 60 mins, GSH (100 μ M) caused 14.6% decomposition of the initial concentration of L-GSNO. However, both Cu/Zn SOD (20 μ M) and GSH (100 μ M) caused greater decomposition of L-GSNO ($P<0.05$ versus control; $n=4$) than that of GSH or Cu/Zn SOD alone. At 60 mins, both Cu/Zn SOD and GSH caused 47.5% decomposition of L-GSNO. BCS (100 μ M) significantly blocked the decomposition of L-GSNO by both Cu/Zn SOD and GSH ($P<0.05$ versus the presence of both Cu/Zn SOD with GSH alone; $n=4$; Figure 3.7).

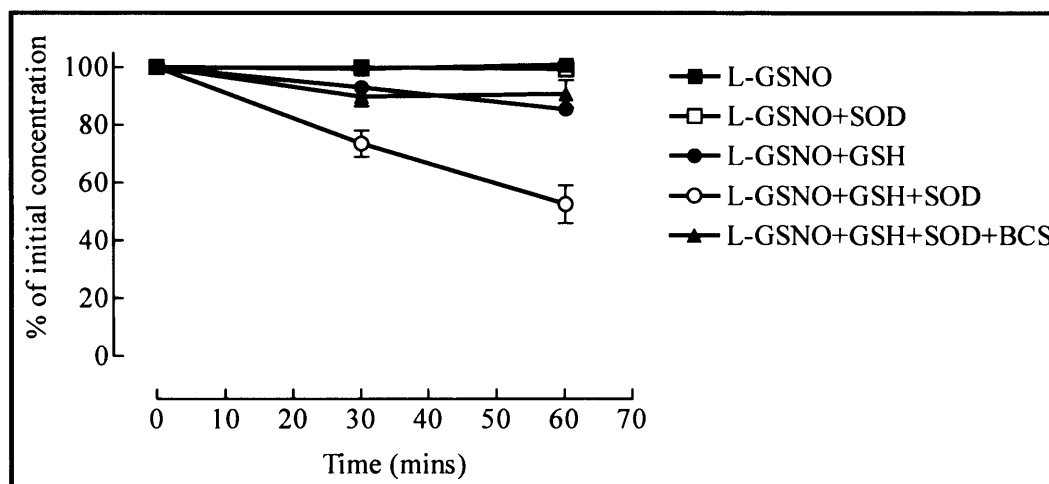


Figure 3.7 Time-dependent decomposition of L-GSNO in the presence or absence of Cu/Zn SOD (20 μ M), GSH (100 μ M), Cu/Zn SOD plus GSH or a combination of Cu/Zn SOD, GSH and BCS (100 μ M). Each point represents the mean \pm SEM ($n=4$).

3.3.2.2 Decomposition of D-GSNO by Cu/Zn SOD

Cu/Zn SOD (20 μ M) alone had no effect on the stability of D-GSNO ($P>0.05$ versus control; $n=4$; Figure 3.8; Table 3.4). GSH (100 μ M) alone caused a significant time-dependent decomposition of D-GSNO ($P<0.05$ versus control; $n=3$). At 60 mins, GSH (100 μ M) caused 17.1% decomposition of D-GSNO. However, both Cu/Zn SOD (20 μ M) and GSH (100 μ M) caused greater time-dependent decomposition of D-GSNO compared with that of GSH or Cu/Zn SOD alone ($P<0.05$ versus GSH alone; $n=4$). At 60 mins, both Cu/Zn SOD and GSH caused 54.1% decomposition of the initial concentration of D-GSNO. BCS (100 μ M) significantly blocked the decomposition of D-GSNO by both Cu/Zn SOD and GSH ($P<0.05$ versus the presence of both Cu/Zn SOD with GSH alone; $n=4$; Figure 3.8). Cu/Zn SOD (20 μ M) and GSH (100 μ M) caused similar decomposition of D-GSNO and L-GSNO ($P>0.05$; $n=4$).

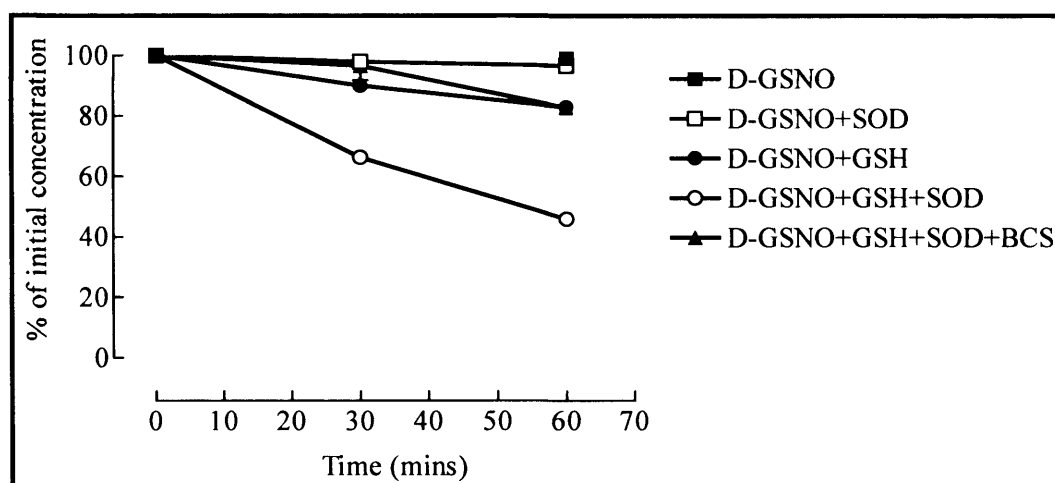


Figure 3.8 Time-dependent decomposition of D-GSNO in the presence or absence of Cu/Zn SOD (20 μ M), GSH (100 μ M), Cu/Zn SOD plus GSH or a combination of Cu/Zn SOD, GSH and BCS (100 μ M). Each point represents the mean \pm SEM ($n=4$).

Treatments	<i>P</i> values
L-GSNO vs. L-GSNO + SOD	$P>0.05$
L-GSNO vs. L-GSNO + GSH	$*P<0.05$
L-GSNO vs. L-GSNO + SOD + GSH	$*P<0.05$
L-GSNO + GSH vs. L-GSNO + SOD + GSH	$*P<0.05$
L-GSNO + SOD + GSH vs. L-GSNO + SOD + GSH + BCS	$*P<0.05$
L-GSNO + SOD + GSH vs. D-GSNO + SOD + GSH	$P>0.05$
D-GSNO vs. D-GSNO + SOD	$P>0.05$
D-GSNO vs. D-GSNO + GSH	$*P<0.05$
D-GSNO vs. D-GSNO + SOD + GSH	$*P<0.05$
D-GSNO + GSH vs. D-GSNO + SOD + GSH	$*P<0.05$
D-GSNO + SOD + GSH vs. D-GSNO + SOD + GSH + BCS	$*P<0.05$

Table 3.4 Comparison of the decomposition of L-and D-GSNO in the absence and presence of Cu/Zn SOD, GSH and BCS ($n=4$); TW-ANOVA with BC.

3.3.2.3 Decomposition of DL-SNAP by Cu/Zn SOD

Cu/Zn SOD (20 μ M) had no effect on the stability of DL-SNAP ($P>0.05$ versus control; $n=6$; Figure 3.9; Table 3.5). GSH (100 μ M) also had no effect on the stability of DL-SNAP ($P>0.05$ versus control; $n=6$). However, the presence of both Cu/Zn SOD (20 μ M) and GSH (100 μ M) caused a significant time-dependent decomposition of DL-SNAP ($P<0.05$ versus control; $n=6$; Figure 3.9). At 60 mins, both Cu/Zn SOD and GSH caused 59.3% decomposition of the initial concentration of DL-SNAP. BCS (100 μ M) completely blocked the decomposition of DL-SNAP by both Cu/Zn SOD and GSH ($P<0.05$ versus the presence of Cu/Zn SOD with GSH alone; $n=6$; Figure 3.9).

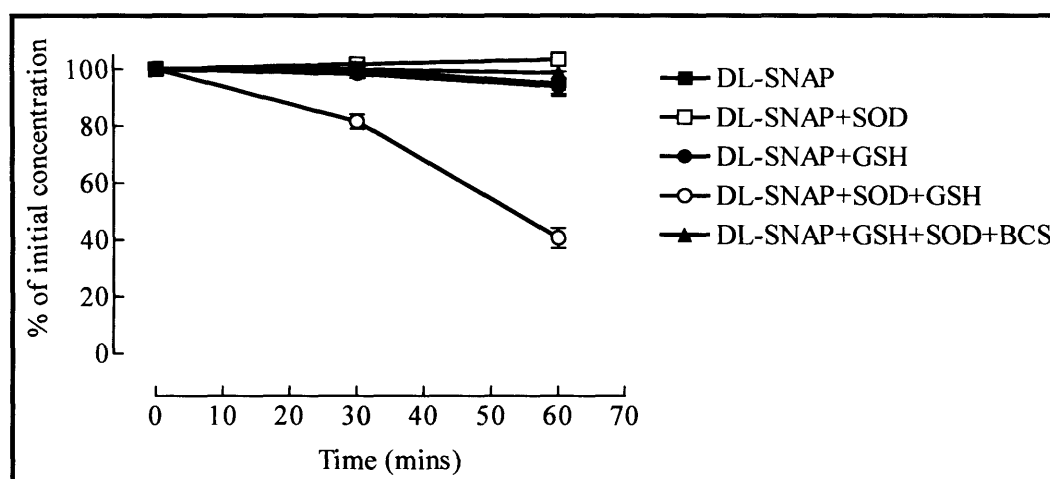


Figure 3.9 Time-dependent decomposition of DL-SNAP in the presence or absence of Cu/Zn SOD (20 μ M), GSH (100 μ M), Cu/Zn SOD plus GSH or a combination of Cu/Zn SOD, GSH and BCS (100 μ M). Each point represents the mean \pm SEM ($n=6$).

3.3.2.4 Decomposition of D-SNAP by Cu/Zn SOD

Cu/Zn SOD (20 μ M) alone had no effect on the stability of D-SNAP ($P>0.05$ versus control; $n=6$; Figure 3.10; Table 3.5). GSH (100 μ M) alone also had no effect on the stability of D-SNAP ($P>0.05$ versus control; $n=6$). However, both Cu/Zn SOD (20 μ M) and GSH (100 μ M) caused a significant time-dependent decomposition of D-SNAP ($P<0.05$ versus control; $n=6$). At 60 mins, both Cu/Zn SOD and GSH

caused 61% decomposition of the initial concentration of D-SNAP. BCS (100 μ M) completely blocked the decomposition of D-SNAP by both Cu/Zn SOD and GSH ($P<0.05$ versus the presence of Cu/Zn SOD with GSH alone; $n=6$; Figure 3.10). Cu/Zn SOD (20 μ M) and GSH (100 μ M) caused similar decomposition of D-SNAP and L-SNAP ($P>0.05$; $n=6$).

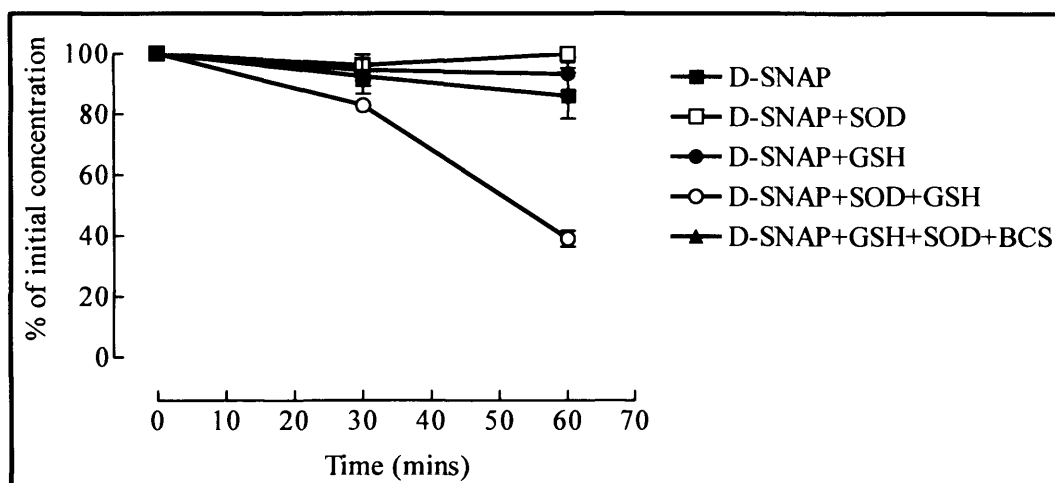


Figure 3.10 Time-dependent decomposition of D-SNAP in the presence or absence of Cu/Zn SOD (20 μ M), GSH (100 μ M), Cu/Zn SOD plus GSH or a combination of Cu/Zn SOD, GSH and BCS (100 μ M). Each point represents the mean \pm SEM ($n=6$).

Treatments	P values
DL-SNAP vs. DL-SNAP + SOD	$P>0.05$
DL-SNAP vs. DL-SNAP + GSH	$P>0.05$
DL-SNAP vs. DL-SNAP + SOD + GSH	$*P<0.05$
DL-SNAP + SOD + GSH vs. DL-SNAP + SOD + GSH + BCS	$*P<0.05$
DL-SNAP + SOD + GSH vs. D-SNAP + SOD + GSH	$P>0.05$
D-SNAP vs. D-SNAP + SOD	$P>0.05$
D-SNAP vs. D-SNAP + GSH	$P>0.05$
D-SNAP vs. D-SNAP + SOD + GSH	$*P<0.05$
D-SNAP + SOD + GSH vs. D-SNAP + SOD + GSH + BCS	$*P<0.05$

Table 3.5 Comparison of the decomposition of DL-and D-SNAP in the absence and presence of Cu/Zn SOD, GSH and BCS ($n=4$); TW-ANOVA with BC.

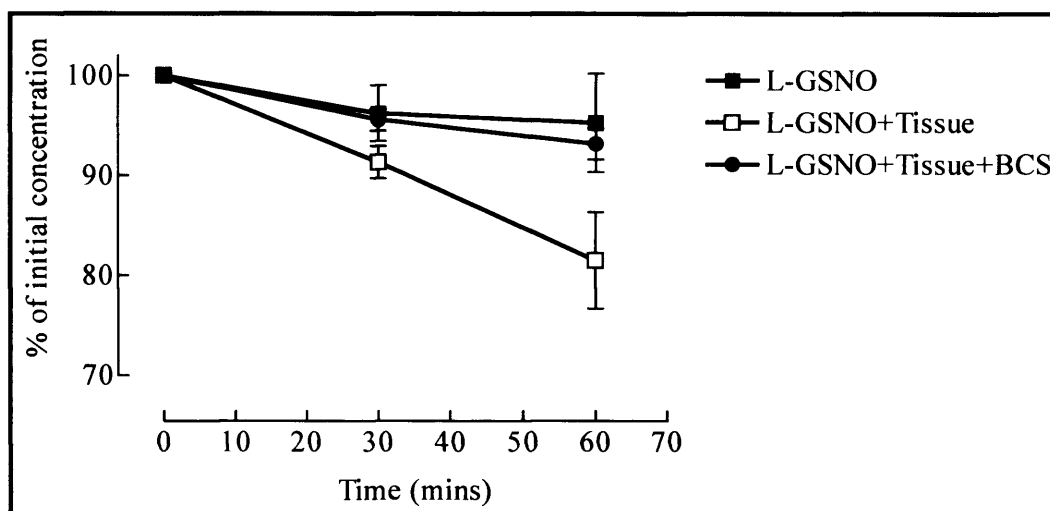
3.3.3 Decomposition of L-and D-GSNO by rat aorta

Rat aortic tissue caused a time-dependent decomposition of L-GSNO ($P<0.05$ versus control; $n=4$; Figure 3.11A; Table 3.6). At 60 mins, rat aorta caused 18.5% decomposition of the initial concentration of L-GSNO. BCS (100 μ M) completely blocked the decomposition of L-GSNO by rat aorta ($P<0.05$ versus the presence of tissue; $n=4$; Figure 3.11A). In a similar fashion, rat aortic tissue caused a time-dependent ($P<0.05$ versus control; $n=4$; Figure 3.11B) decomposition of D-GSNO. At 60 mins, rat aorta caused 20.5% decomposition of the initial concentration of D-GSNO. BCS (100 μ M) completely blocked the decomposition of D-GSNO by rat aorta ($P<0.05$ versus the presence of tissue; $n=4$; Figure 3.11B). Thus, the effect of rat aorta on the decomposition of L- and D-GSNO was equivalent ($P>0.05$ versus control; $n=4$).

Treatments	<i>P</i> values
L-GSNO vs. L-GSNO + Tissue	* $P<0.05$
L-GSNO+ Tissue vs. L-GSNO + Tissue + BCS	* $P<0.05$
D-GSNO vs. D-GSNO + Tissue	* $P<0.05$
D-GSNO+ Tissue vs. D-GSNO + Tissue + BCS	* $P<0.05$
L-GSNO+ Tissue vs. D-GSNO+ Tissue	$P>0.05$

Table 3.6 Comparison of the decomposition of L- and D- GSNO in the absence and presence of aortic tissue and BCS ($n=4$); TW-ANOVA with BC.

A



B

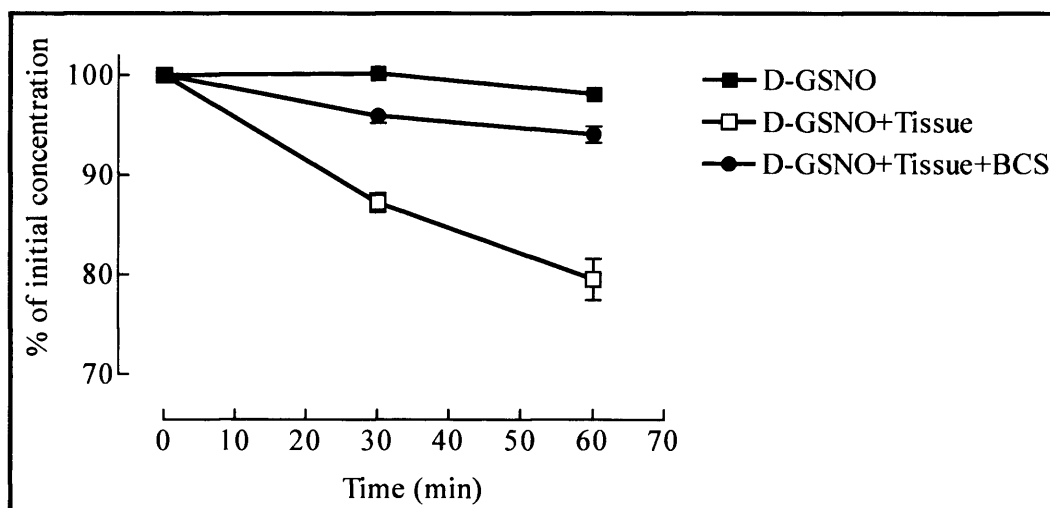


Figure 3.11 Time-dependent decomposition of (A) L-GSNO and (B) D-GSNO in the absence and presence of aortic tissue and BCS (100 μ M). Each point represents the mean \pm SEM ($n=4$).

3.3.4 Responses of rat aorta to L-and D-isomers of S-nitrosothiols

3.3.4.1 Responses of rat aorta to DL-and D-SNAP

DL- and D-isomers of SNAP caused equipotent concentration-dependent relaxation of PE-precontracted (EC₈₀) rat aorta. The pEC₅₀ values for DL-and D-SNAP (7.7 ± 0.17 and 7.6 ± 0.17 respectively; $n=9$; $P>0.05$; Figure 3.12) were not significantly different. Pre-incubation of rat aortic rings with BCS (10 μ M) for 30 mins significantly reduced the potency of both DL-SNAP and D-SNAP. The pEC₅₀ values for DL-and D-SNAP in the presence of BCS (6.47 ± 0.18 and 6.39 ± 0.12 respectively; $n=9$; $P<0.05$ versus control; BC; Figure 3.12) were approximately one order of magnitude less as compared to control, but were not significantly different from each other ($n=9$; $P>0.05$). Curves were compared by TW-ANOVA.

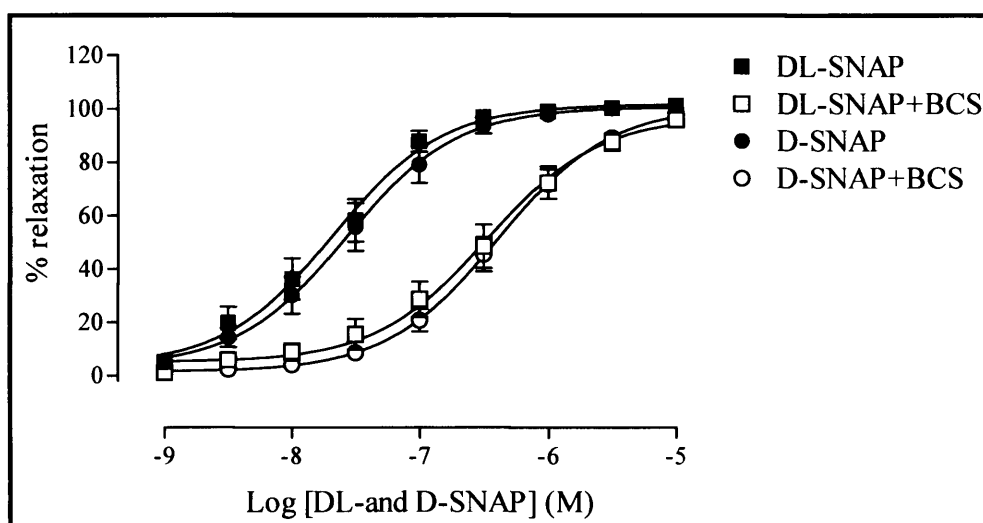


Figure 3.12 Concentration-response curves to DL-SNAP and D-SNAP (1nM-10 μ M) following 30 mins incubation with vehicle or BCS (10 μ M). Relaxation is expressed as the percentage reversal of the PE-induced tone. Each point represents mean \pm SEM $n=9$.

3.3.4.2 Responses of rat aorta to L-and D-GSNO

L-and D-isomers of GSNO also caused equipotent concentration-dependent relaxation of PE-precontracted (EC₈₀) rat aorta. The pEC₅₀ values for L-and D-GSNO

(7.37 ± 0.15 and 7.12 ± 0.19 respectively; $n=5$; $P>0.05$ ($P=0.13$); Figure 3.13) were similar. Incubation of rat aortic rings with BCS ($10\mu\text{M}$), for 30 mins significantly reduced the potency of both L- and D-GSNO. The pEC_{50} values for L-GSNO and D-GSNO in the presence of BCS (6.52 ± 0.27 and 6.67 ± 0.21 respectively; $n=5$; $P<0.05$ versus control; BC; Figure 3.13) were significantly less compared to control, but not significantly different from each other ($n=5$; $P>0.05$). Curves were compared by TW-ANOVA.

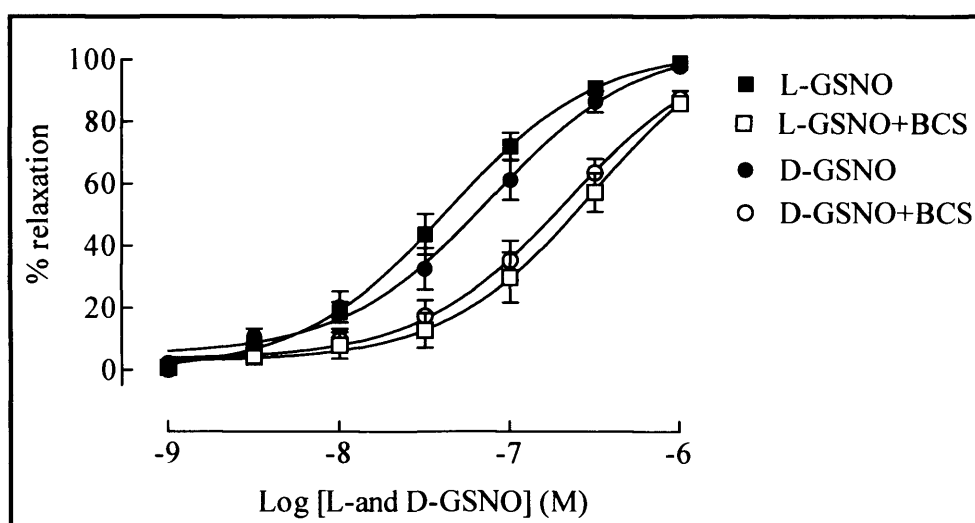


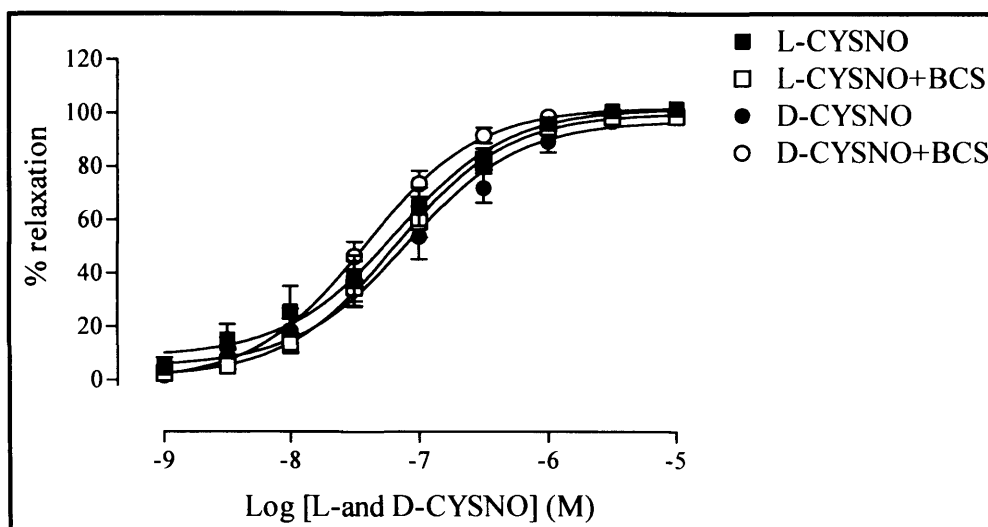
Figure 3.13 Concentration-response curves to L- and D-GSNO (1nM – $1\mu\text{M}$) following 30 mins incubation with vehicle or BCS ($10\mu\text{M}$). Relaxation is expressed as the percentage reversal of the PE-induced tone. Each point represents mean \pm SEM ($n=5$).

3.3.4.3 Responses of rat aorta to L- and D-CYSNO

L- and D-isomers of CYSNO caused concentration-dependent relaxation of PE-precontracted (EC_{80}) rat aorta. The pEC_{50} values for L- and D-CYSNO (7.17 ± 0.21 and 7.09 ± 0.2 respectively; $n=4$; $P>0.05$; Figure 3.14A) were not significantly different. Incubation of rat aortic rings with BCS ($10\mu\text{M}$), for 30 mins had no effect on the potency of L- and D-CYSNO. The pEC_{50} values for L- and D-CYSNO in the presence of $10\mu\text{M}$ BCS (7.18 ± 0.12 and 7.41 ± 0.12 respectively; $n=4$; $P>0.05$ versus control; Figure 3.14A) were not significantly different from control. However, incubation of rat aortic

rings with 100 μ M BCS for 30 mins significantly reduced the potency of both L- and D-CYSNO (pEC_{50} : 6.14 ± 0.15 and 6.33 ± 0.13 respectively; $n=5$; $P < 0.05$ versus control; BC; Figure 3.14B). Curves were compared by TW-ANOVA.

A



B

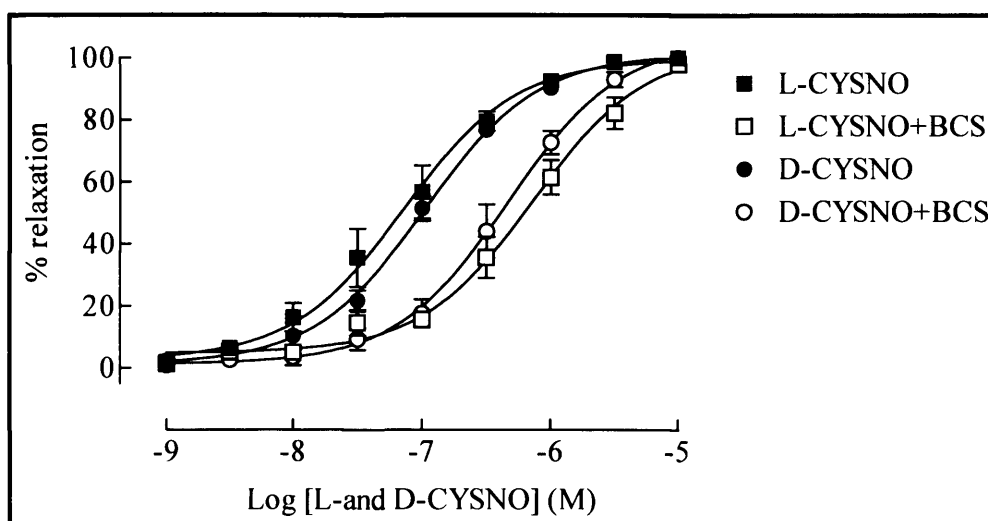


Figure 3.14 Concentration-response curves to L- and D-CYSNO (1nM-10 μ M) following 30 mins incubation with vehicle or BCS (A) 10 μ M (B) 100 μ M. Relaxation is expressed as the percentage reversal of the PE-induced tone. Each point represents mean \pm SEM ($n=4$).

3.3.4.4 Effects of BCS on the responses of rat aorta to SPER-NO

To control for non-specific effects of BCS, the effect of Cu(I) chelation on the vasorelaxant activity of SPER-NO was examined. SPER-NO caused concentration-dependent relaxation of PE-precontracted rat aorta (EC_{80}) with a pEC_{50} value of 6.57 ± 0.2 in the absence and 6.76 ± 0.14 in the presence of BCS ($10 \mu M$ for 30 minutes; $n=5$; $P>0.05$ versus control; TW-ANOVA; Figure 3.15).

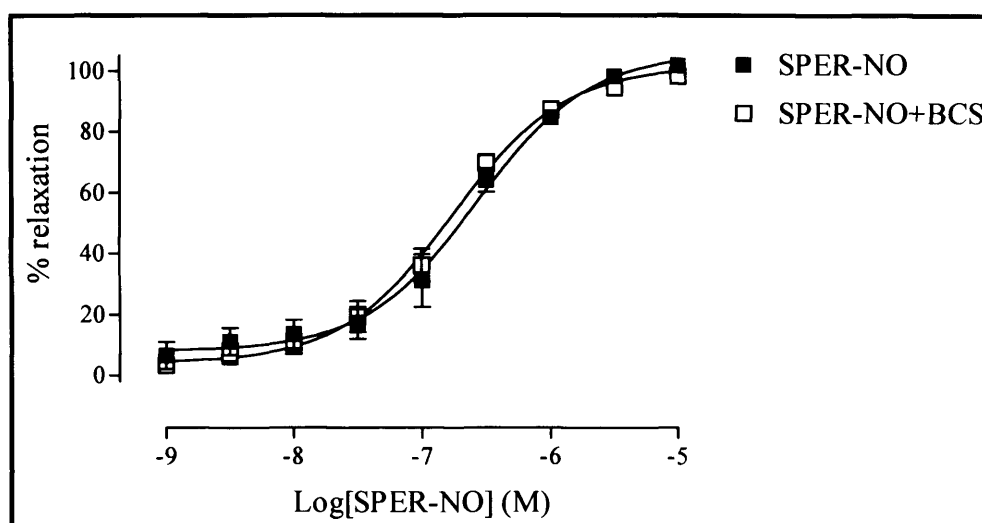


Figure 3.15 Concentration-response curves to SPER-NO ($1nM$ - $10 \mu M$) following 30 mins incubation with vehicle or BCS ($10 \mu M$); Relaxation is expressed as the percentage reversal of the PE-induced tone. Each point represents mean \pm SEM ($n=5$).

3.3.5 Effects of BCS and Cu(I) on endogenous NO-mediated responses of rat aorta

ACh caused concentration-dependent relaxation of PE-precontracted (EC_{80}) rat aorta that was unaffected by BCS ($10 \mu M$; 30 mins). The pEC_{50} value for ACh in the presence and absence of BCS is 7.73 ± 0.19 and 7.81 ± 0.25 respectively $n=5$; $P>0.05$; TW-ANOVA; Figure 3.16. Addition of Cu(I) ($100nM$ - $300 \mu M$) caused concentration-

dependent relaxation of PE-precontracted (EC_{80}) rat aortic rings that was endothelium-dependent (The pEC_{50} values is 5.84 ± 0.34 ; $n=3$; $P<0.05$ versus acetonitrile, ODQ, L-NAME or denuded tissue; TW-ANOVA with BC; Figure 3.17). In endothelium-intact vessels relaxation to Cu(I) was inhibited by the sGC inhibitor, ODQ ($5\mu M$; 30 mins) and L-NAME ($300\mu M$; 30 mins). Endothelial denudation also abolished relaxations to Cu(I)-acetonitrile alone had no effect on the precontracted vessels (Figure 3.17).

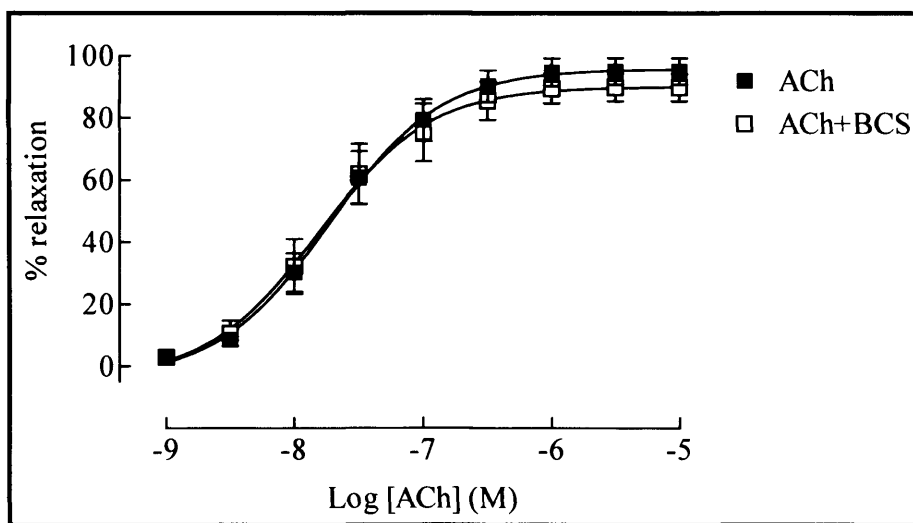


Figure 3.16 Concentration-response curves to ACh ($1nM$ - $10\mu M$) following 30 mins incubation with vehicle or BCS ($10\mu M$); Relaxation is expressed as the percentage reversal of the PE-induced tone. Each point represents mean \pm SEM ($n=5$).

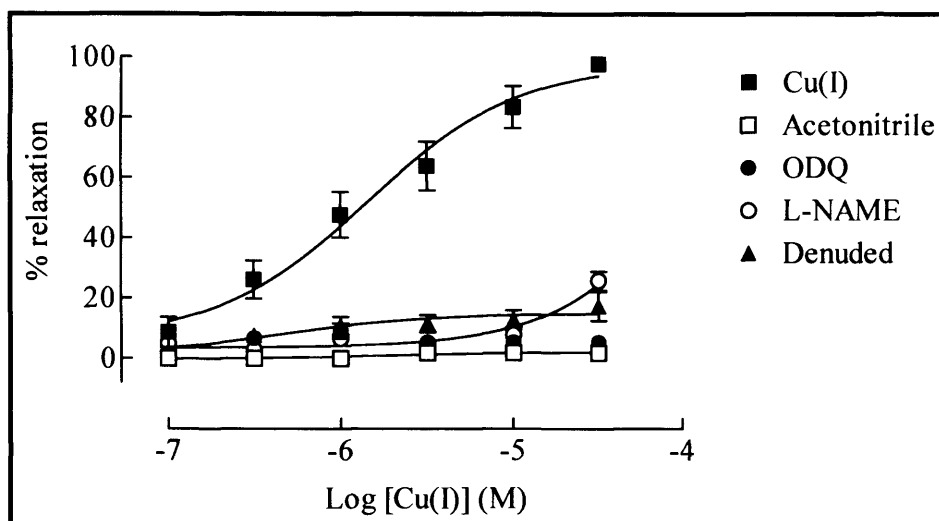


Figure 3.17 Concentration-response curves to Cu(I)-acetonitrile (100nM-300μM) and acetonitrile (100nM-300μM) in the presence and absence of endothelium, ODQ (5μM; 30 mins) and L-NAME (300μM; 30 mins). Relaxation is expressed as the percentage reversal of the PE-induced tone. Each point represents mean ± SEM (n=3).

3.4 DISCUSSION

In the present study, I investigated the effect of free copper ions, the copper-containing enzyme, Cu/Zn SOD, and rat aorta on the stability of stereoisomers of *S*-nitrosothiols. I also investigated the responsiveness of rat isolated aorta to stereoisomers of the endogenous *S*-nitrosothiols, GSNO and CYSNO, and the exogenous *S*-nitrosothiol, SNAP. These studies demonstrated that biotransformation of *S*-nitrosothiols was in part dependent on the chemical effect of Cu(I) ions. There was no evidence of a stereospecific effect of a copper containing enzyme or tissue. In rat isolated aorta, there were no stereospecific vasorelaxant effects of *S*-nitrosothiols, consistent with non-enzymatic Cu (I)-dependent release of NO.

3.4.1 Decomposition of *S*-nitrosothiols by copper ions

The effect of Cu(I) and Cu(II) on the decomposition of stereoisomers of GSNO, CYSNO and SNAP was examined in a protein free system *in vitro*. Previous studies had identified a role for Cu(I) rather than Cu(II) because of the action of the Cu(I) chelator, neocuproine. In this chapter I used a novel Cu(I)-releasing complex copper (I)-acetonitrile that was soluble in aqueous solution to get a more direct insight into the role of this copper species on *S*-nitrosothiol breakdown. L- and D-isomers of *S*-nitrosothiols decomposed on exposure to Cu(I), and as expected there was no difference between stereoisomers. The decomposition of *S*-nitrosothiols by Cu(I) and Cu(II) was completely blocked by the specific Cu(I) chelator, BCS, suggesting that the effective catalyst in the decomposition is Cu(I) not the oxidised form, Cu(II), supporting previous findings (Dicks *et al.*, 1996; Gorren *et al.*, 1996).

There were clear differences in the stability of the different *S*-nitrosothiols in the presence of copper ions. The presence of as little as 1 μ M Cu(I) has a profound effect on CYSNO, which showed complete decomposition within a few minutes. The effect of Cu(I) on SNAP is also significant but considerably less than that of CYSNO. However, GSNO required comparatively large concentrations of Cu(I) to greatly affect its stability. These observations suggest that the rank order of stability in the

requires other factors. The presence of GSH caused a dramatic acceleration of the decomposition rate by Cu/Zn SOD; GSH alone had a minimal direct effect. This indicates the requirement of GSH to enhance the decomposition of GSNO and SNAP by Cu/Zn SOD. Chelation of Cu(I) by BCS completely blocked the decomposition of GSNO and SNAP by Cu/Zn SOD, indicating that decomposition occurs by reaction with Cu(I) rather than other components of the enzyme. GSH may act to reduce Cu(II) to Cu (I) that is either bound to the enzyme or which has dissociated in solution. Alternatively GSH could cause conformational changes in Cu/Zn SOD leading to exposure of copper ions to react with GSNO and SNAP. The effect of GSH on GSNO, although small, suggests that a transnitrosation reaction might have occurred. This effect seems to be specific to GSNO as GSH had no effect on SNAP.

The plasma membrane of many cell types including endothelial and VSMC, contains a variety of enzymes that contain copper ions such as, vascular adhesion protein 1, lysyl oxidase, benzylamine oxidase, methylamine oxidase (Buffoni & Ignesti, 2000; Jalkanen & Salmi, 2001), Cu-ATPase and Cu/Zn SOD (Harris, 2000). In the plasma there are also copper-containing proteins such as ceruloplasmin and albumin (Harris, 2000). These copper-containing molecules might determine the biotransformation of *S*-nitrosothiols *in vivo* (Figure 3.18).

3.4.3 Decomposition of stereoisomers of *S*-nitrosothiols by rat aorta

Consistent with the results obtained with Cu/Zn SOD, the decomposition of L-GSNO by rat aorta was similar to that of D-GSNO. Moreover, decomposition of L- and D-GSNO by rat aorta was prevented by Cu(I) chelation. Therefore, whole tissue metabolism of GSNO is non-stereospecific and consistent with a direct effect of Cu(I). It is not possible to say which of the Cu containing proteins described in section 3.4.2 might contribute to the metabolism of GSNO by rat aorta.

3.4.4 Non-stereospecific relaxation of rat aorta by *S*-nitrosothiols

The vasorelaxant response of rat aorta to L- and D-isomers of GSNO, SNAP and CYSNO were similar with no evidence of a stereospecific effect and consistent with non-enzymatic release of NO from these *S*-nitrosothiols. Cavero *et al* made similar observations with CYSNO and SNAP, but reported L-GSNO to be more potent in this vessel than D-GSNO (Cavero *et al.*, 2000). One explanation for the difference between the results presented in this chapter and those previously reported, is that both stereoisomers of GSH were synthesised in house in order to minimise any differences arising from different methods of synthesis (that might, for instance, contain different impurities). In addition, in this study spectroscopy was used to ensure that the concentrations of L- and D-GSNO in stock solutions were similar. The effect of Cu(I) chelation on the stereoisomers was also similar. Stereospecific effects of *S*-nitrosothiols have been reported in animals *in vitro* and *in vivo*, so it remains possible that enzymatic release of NO might occur in other systems. However, I could find no evidence of this in the systems used in this thesis.

Discrepancy between my observations and previous reports that have demonstrated stereospecific and/or enzymatic bioactivation of *S*-nitrosothiols might be due to differences in the model (Davisson *et al.*, 1996), type of tissue (Davisson *et al.*, 1997; Zai *et al.*, 1999; Root *et al.*, 2004), source of GSH (Cavero *et al.*, 2000) and the *S*-nitrosothiol studied (Travis *et al.*, 1996). As mentioned above, enzymes such as xanthine oxidase (Trujillo *et al.*, 1998) and DPI (Zai *et al.*, 1999; Root *et al.*, 2004) have also been reported to cause decomposition of *S*-nitrosothiols. However, in the systems that I studied, there was no evidence to support any endogenous enzymatic decomposition of *S*-nitrosothiols; this observation suggests that these enzymes, may not contribute to the biological activity of *S*-nitrosothiols in vascular tissue. Moreover, since xanthine oxidase and DPI have been reported to contain copper ions (Roussos & Morrow, 1966; Narindrasorasak *et al.*, 2003), the inhibitory effects of copper chelators on the bioactivation of *S*-nitrosothiols should be interpreted with caution.

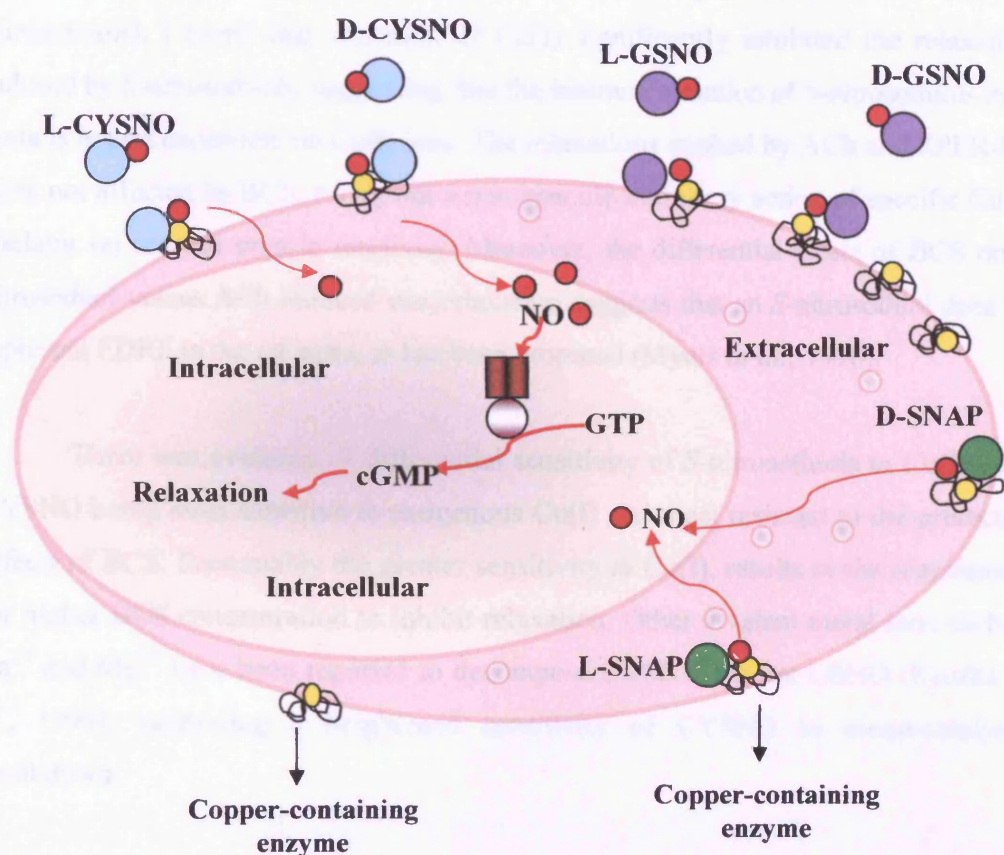


Figure 3.18 Schematic representation showing the stereoisomers of *S*-nitrosothiols bind in a non-stereospecific manner to copper-containing enzymes on the cell membrane leading to decomposition and release of NO.

3.4.5 Effect of metal chelation on the response of rat aorta to *S*-nitrosothiols

Previous reports indicate that the biological activity of *S*-nitrosothiols can be modulated by Cu(I) in platelets (Askew *et al.*, 1995; Gordge *et al.*, 1995), the rat isolated perfused tail artery (Al-Sa'doni *et al.*, 1997) and murine cavernosum (Gocmen *et al.*, 2000). Similarly, experiments with neocuproine and cuprizone, selective chelators of Cu(I) and Cu(II), respectively, in rat and mouse gastric smooth muscle provide evidence that Cu(I), and not Cu(II), modulate the biological activity of *S*-nitrosothiols (De Man *et al.*, 1999). In keeping with the conclusions from these

studies (that endogenous Cu(I) plays a role in the generation of NO from *S*-nitrosothiols), I found that chelation of Cu(I) significantly inhibited the relaxations induced by *S*-nitrosothiols, suggesting that the biotransformation of *S*-nitrosothiols in rat aorta is in part dependent on Cu(I) ions. The relaxations evoked by ACh and SPER-NO were not affected by BCS, ruling out a non-specific inhibitory action of specific Cu(I)-chelator on smooth muscle reactivity. Moreover, the differential effect of BCS on *S*-nitrosothiol-versus ACh-induced vasorelaxation suggests that an *S*-nitrosothiol does not represent EDRF in the rat aorta, as has been proposed (Myers *et al.*, 1990).

There was evidence of differential sensitivity of *S*-nitrosothiols to Cu(I), with CYSNO being most sensitive to exogenous Cu(I) and most resistant to the protective effects of BCS. Presumably the greater sensitivity to Cu(I), results in the requirement for higher BCS concentration to inhibit relaxation. Other divalent metal ions such as Ca^{2+} and Mg^{2+} have been reported to decompose CYSNO but not GSNO (Kostka *et al.*, 1999), supporting a heightened sensitivity of CYSNO to metal-catalysed breakdown.

3.4.6 Endogenous *S*-nitrosothiols

The relaxant effect of Cu(I) was blocked by ODQ and denudation of the endothelium indicating that the effect is endothelium-dependent NO relaxation. However, the blocking effect of L-NAME indicates that the relaxant effect of Cu(I) is eNOS dependent rather than mediated by endogenous *S*-nitrosothiols. Further studies would be required to investigate this further.

3.4.7 Summary and conclusions

This chapter suggests that the biotransformation of *S*-nitrosothiols by rat aorta does not involve stereospecific decomposition, consistent with non-enzymatic release of NO. Biotransformation of *S*-nitrosothiols is in part dependent on Cu(I) ions.

CHAPTER FOUR

DESENSITISATION OF SOLUBLE AND PARTICULATE GUANYLATE CYCLASES BY LIPOPOLYSACCHARIDE

4.1 INTRODUCTION

Previous reports demonstrated that the sGC–cGMP system is influenced by the ambient concentration of NO (Hussain *et al.*, 1999). Moreover, through a cGMP-dependent process, cross-talk between the sGC–cGMP and the pGC–cGMP systems might occur, such that the changes in the sensitivity of one pathway are mirrored by the other cGMP-generating system (Hussain *et al.*, 2001; Madhani *et al.*, 2003). Further evidence for desensitisation of sGC and pGC pathways by the ambient concentration of NO are described in more details in section 1.5.1. These observations support the hypothesis that the sGC–cGMP and pGC–cGMP pathways play a complementary role in regulating cardiovascular homeostasis. The physiological, pathophysiological and therapeutic significance of the interaction between sGC–cGMP and pGC–cGMP pathways is described in detail in section 1.5.3.

Inflammatory cardiovascular diseases are commonly associated with iNOS expression and ‘high-output’ (i.e. excessive) NO production (Julou-Schaeffer *et al.*, 1990; Fleming *et al.*, 1991; Shah, 2000). Bacterial sepsis is a systemic inflammatory state characterised by vascular smooth muscle dysfunction, leading to hypotension, inadequate tissue perfusion, and organ failure. The disease is also associated with endothelial dysfunction, predominantly reduced vasodilator influence of eNOS-derived NO (Chauhan *et al.*, 2003c). In animal models, sepsis has been mimicked by administration of LPS; such a protocol can also be used to induce iNOS expression *in vitro* and thereby permit study of isolated vascular rings. In this chapter, I examined whether the endothelial and smooth muscle dysfunction following exposure of vascular tissue to LPS alters responsiveness to both sGC and pGC pathways (i.e. NO and ANP) and if this dysfunction is specific to cGMP-dependent signalling.

4.2 EXPERIMENTAL PROTOCOLS AND STATISTICS

4.2.1 Organ bath studies

Organ bath studies were performed on rings from rat (male; Sprague-Dawley; 200-250 g) thoracic aorta. Vessel harvesting and preparation are as described in Chapter Two section 2.3.2.

4.2.1.1 Characterisation of the effect of LPS on contraction

Responses to PE (0.001-10 μ M; *n*=6) and U46619 (0.001-1 μ M; *n*=10) were examined in vessels incubated with LPS (0.01-1 μ g/ml), or vehicle (saline) for 4hr. Constrictor responses to U46619 (0.001-1 μ M) were also determined after co-incubation of vessels with LPS and the iNOS inhibitor, 1400W (10 μ M; *n*=10), or the cyclooxygenase inhibitor, indomethacin (10 μ M; *n*=10). Details of the IC₅₀ of these inhibitors are described in Table 2.1.

4.2.1.2 Effect of LPS on sGC-mediated relaxation

Vessels were incubated with vehicle or LPS (0.3 μ g/ml) for 4hr and pre-contracted with U46619 to an approximate EC₈₀. Concentration-response curves were constructed to ACh (*n*=6), histamine (*n*=5), SPER-NO (*n*=12), BAY 58-2667 (*n*=7), GSNO (*n*=7) and SNP (*n*=7). The effect of co-incubation of LPS with 1400W (10 μ M; 4hr; *n*=7), and indomethacin (10 μ M; 4hr; *n*=5) on the response to ACh and SPER-NO was also determined.

4.2.1.3 Effect of LPS on pGC-mediated relaxation

Vessels were incubated with vehicle or LPS (0.3 μ g/ml) for 4hr and pre-contracted with U46619 to an approximate EC₈₀. Concentration-response curves were constructed to CNP (0.1nM-1 μ M; *n*=4) and ANP (0.01nM-0.1 μ M; *n*=10). The effect

of co-incubation of LPS with 1400W (10 μ M; $n=6$), ODQ (5 μ M; $n=7$), or both ODQ and 1400W ($n=5$), on the response to ANP was determined.

4.2.1.4 Effect of LPS on the sensitivity of vessels to cGMP

Vessels were incubated with vehicle or LPS (0.3 μ g/ml) for 4hr and pre-contracted with U46619 to an approximate EC₈₀. Concentration-response curves were constructed to 8-bromoguanosine-3',5'-cyclic monophosphate (8-Br-cGMP; 1-300 μ M; $n=5$). In further studies, LPS-treated vessels were co-incubated with both ODQ (5 μ M) and 1400W (10 μ M; $n=5$) for 4hr, after which the response to 8-Br-cGMP was determined ($n=5$). To assess the effects of prolonged exposure of vessels to an NO donor on cGMP-mediated dilatation, vessels were incubated with glyceryl trinitrate (GTN) alone (30 μ M; $n=4$) or GTN (30 μ M) and ODQ (5 μ M; $n=4$) for 4hr. Vessels were pre-contracted with U46619 to an approximate EC₈₀ and concentration-response curves were constructed to 8-Br-cGMP (1-300 μ M).

4.2.1.5 Effect of LPS on cAMP-mediated relaxation

Vessels were incubated with vehicle or LPS (0.3 μ g/ml) for 4hr and pre-contracted with U46619 to an approximate EC₈₀. Concentration-response curves to forskolin (0.001-1 μ M; $n=7$) or 8-Bromoadenosine-3',5'-cyclic monophosphate (8-Br-cAMP; 1-300 μ M; $n=4$) were constructed.

4.2.1.6 Reversibility of desensitisation of cGMP-mediated relaxation

To determine whether LPS-induced changes in cGMP-mediated relaxation were reversible, vessels were incubated with LPS (0.3 μ g/ml) for 4hr, after which ODQ (5 μ M; $n=7$), 1400W (10 μ M; $n=7$) or both ($n=5$) were added to the LPS-treated rings. Tissues were pre-contracted with U46619 to an approximate EC₈₀ and

concentration-response curves to ANP (0.01nM-0.1µM) or 8-Br-cGMP (1-300µM) were constructed.

4.2.2 Western blotting

Western blotting was used to detect iNOS protein following incubation of the tissues with LPS (0.3µg/ml; 4hr) *in vitro*. Aortic rings were removed from the organ bath, wrapped in aluminium foil, immediately snap frozen in liquid nitrogen and then stored at -80°C. Details of sample preparation, protein separation and identification by western blotting are described in section 2.6

4.2.3 Statistics

Organ bath studies are expressed as described in section 2.8. All curves were analysed by TW-ANOVA and where appropriate Bonferroni's correction (BC) was applied.

4.3 RESULTS

4.3.1 Effect of LPS on contraction

Incubation of rat aorta rings with LPS (0.01-1 μ g/ml) for 4hr significantly reduced the response to PE (Figure 4.1A). It was not possible to achieve stable pre-contractions to PE after LPS treatment. Incubation of vessels with LPS (0.3 μ g/ml; 4hr) also reduced the sensitivity to U46619 (pEC_{50} : 7.27 ± 0.17 versus 6.63 ± 0.17 in the absence and presence of LPS, respectively; $n=10$; $P<0.05$; Figure 4.1B). Co-incubation with 1400W (10 μ M) significantly reversed the LPS-induced hyporeactivity to U46619 (pEC_{50} : 7.44 ± 0.17 ; $n=10$; $P<0.05$ versus LPS alone), whereas co-incubation with indomethacin (10 μ M) had no effect (pEC_{50} : 6.34 ± 0.27 ; $n=10$; $P>0.05$ versus LPS alone; Figure 4.1B). U46619 caused stable contractions in vessels incubated with LPS and was therefore used in all subsequent experiments to pre-contract tissues similarly (approximate EC_{80} : $\sim 0.1 \mu$ M in control tissues and $\sim 0.3 \mu$ M in LPS-treated tissues). Curves were compared by TW-ANOVA with BC.

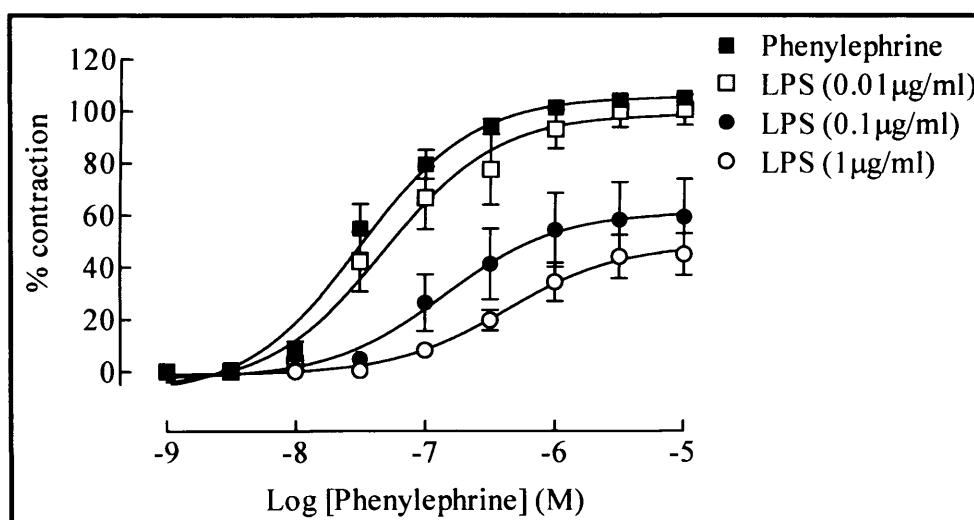
4.3.2 Effect of LPS on relaxation

4.3.2.1 Effect of LPS on sGC-mediated relaxation

Incubation of rat aortic rings with LPS (0.3 μ g/ml, 4hr) significantly reduced the potency of ACh (pEC_{50} : 7.77 ± 0.27 versus 6.99 ± 0.39 in the absence and presence of LPS, respectively; $n=6$; $P<0.05$; Figure 4.2A), histamine (pEC_{50} : 6.22 ± 0.33 versus 5.96 ± 0.25 ; $n=5$; $P<0.05$; Figure 4.2B), SPER-NO (pEC_{50} : 7.08 ± 0.35 versus 6.34 ± 0.63 ; $n=12$; $P<0.05$; Figure 4.3A), BAY 58-2667 (pEC_{50} : 8.13 ± 0.26 versus 6.31 ± 0.39 ; $n=7$; $P<0.05$; Figure 4.3B) GSNO (pEC_{50} : 7.14 ± 0.37 versus 6.87 ± 0.17 ; $n=7$; $P<0.05$; Figure 4.3C) and SNP (pEC_{50} : 8.96 ± 0.28 versus 7.49 ± 0.41 ; $n=7$; $P<0.05$; Figure 4.3D). Incubation of vessels with 1400W (10 μ M) preserved relaxation to ACh after administration of LPS (pEC_{50} : 7.18 ± 0.23 versus 7.80 ± 0.357 in the absence and presence of 1400W, respectively; $n=7$; $P<0.05$; Figure 4.4A). Incubation with indomethacin (IM; 10 μ M) had no effect on responses to ACh (pEC_{50} : 7.35 ± 0.39 ; $n=5$; $P>0.05$; Figure 4.4A). 1400W (10 μ M) alone had no effect on responses to ACh (pEC_{50} : 7.77 ± 0.27 versus 7.92 ± 0.32 in the absence and presence of 1400W, respectively; $n=3$; $P>0.05$; Figure 4.4A). Responses to SPER-NO were also restored

by 1400W (pEC_{50} : 6.47 ± 0.68 versus 6.94 ± 0.17 in the absence and presence of 1400W, respectively; $n=5$; $P<0.05$) but not by indomethacin (pEC_{50} : 6.13 ± 1.2 ; $n=4$; $P>0.05$; Figure 4.4B). All curves were compared by TW-ANOVA with BC.

4.1A



4.1B

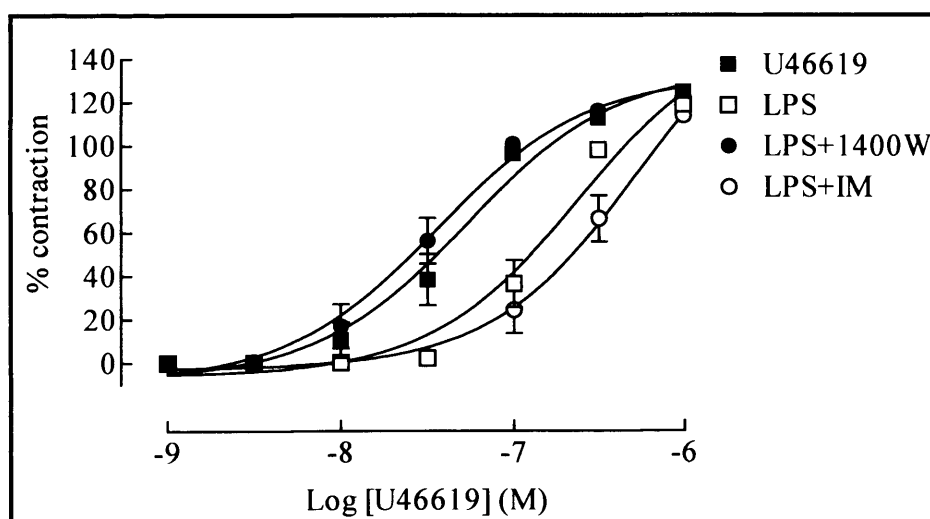
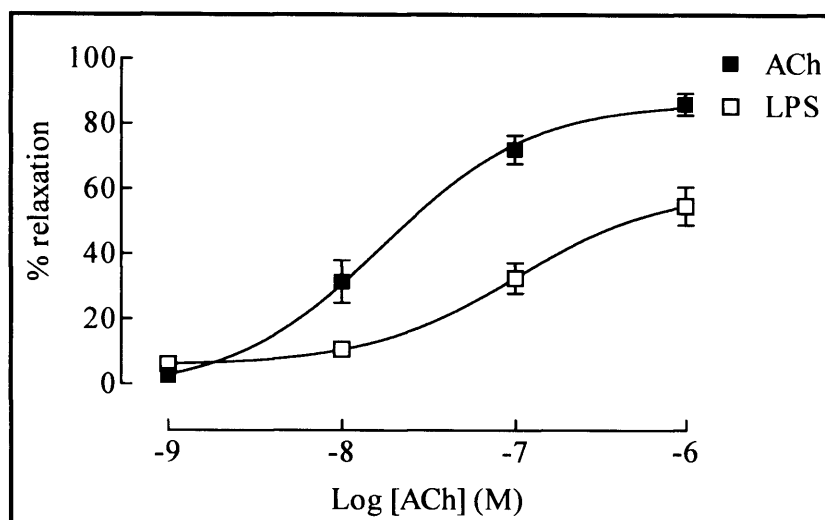


Figure 4.1 Concentration-response curves to (A) PE (1nM-10µM) following 4hr incubation with vehicle or LPS (0.01-1µg/ml; $n=6$) and (B) U46619 (1nM-1µM) following 4hr incubation with vehicle, LPS (0.3µg/ml), LPS plus 1400W (10µM) or LPS plus indomethacin (IM; 10µM; $n=10$). Contraction is expressed as the percentage of the contraction to KCl (48mM). Each point represents mean \pm SEM.

4.2A



4.2B

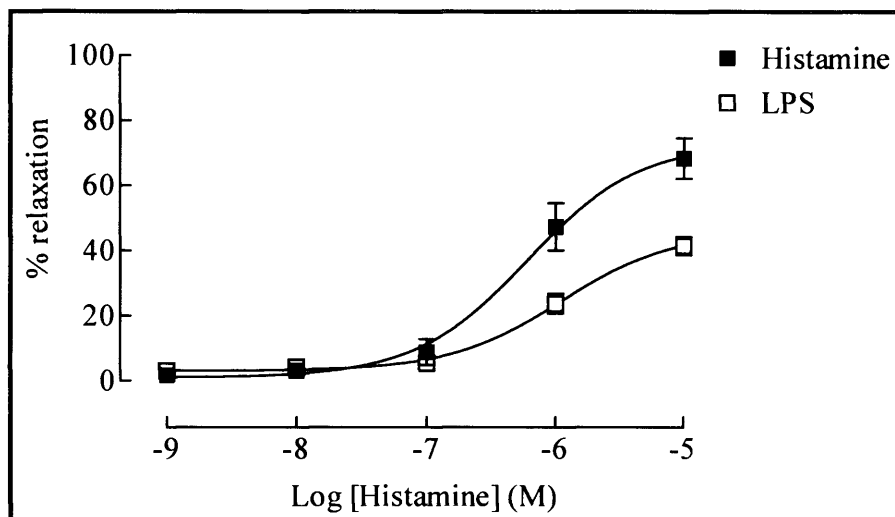
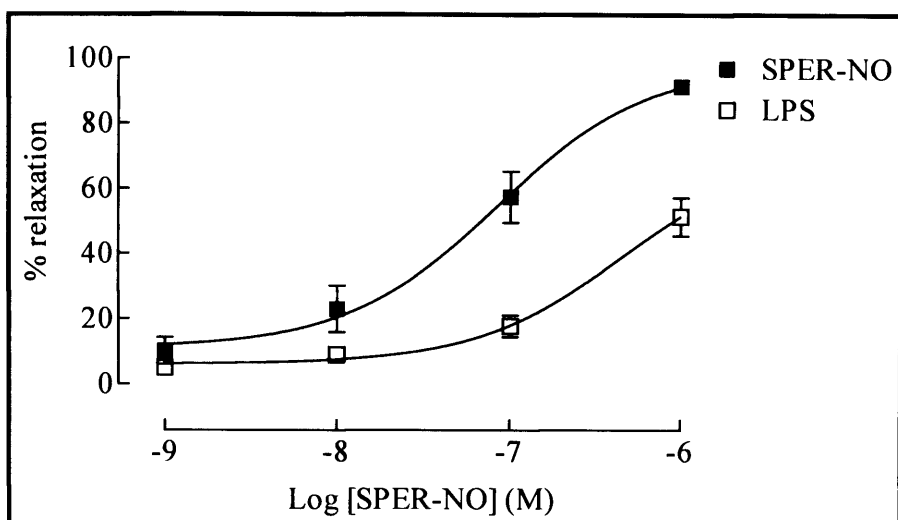
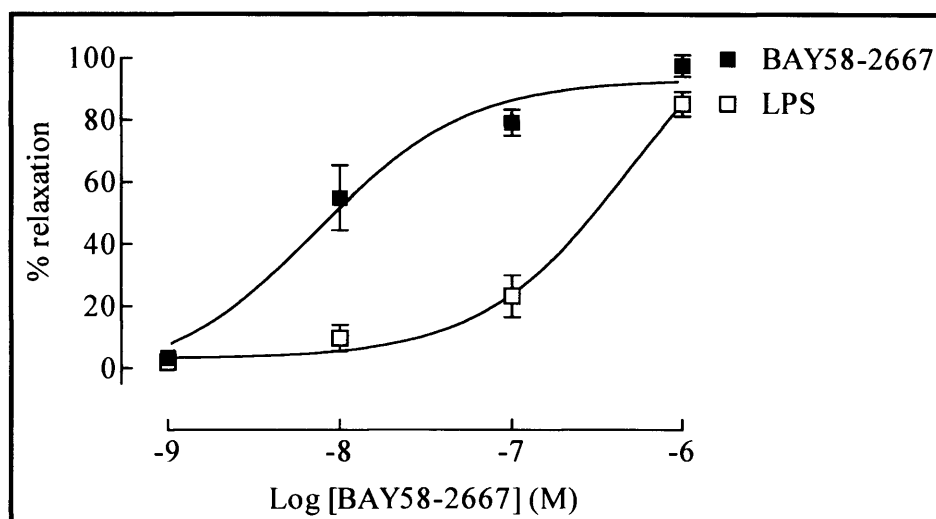


Figure 4.2 Concentration-response curves to (A) ACh (1nM-1 μ M) and (B) histamine (1nM-10 μ M) following 4hr incubation with vehicle or LPS (0.3 μ g/ml); $n=5$. Relaxation is expressed as the percentage reversal of the U46619-induced tone. Each point represents mean \pm SEM.

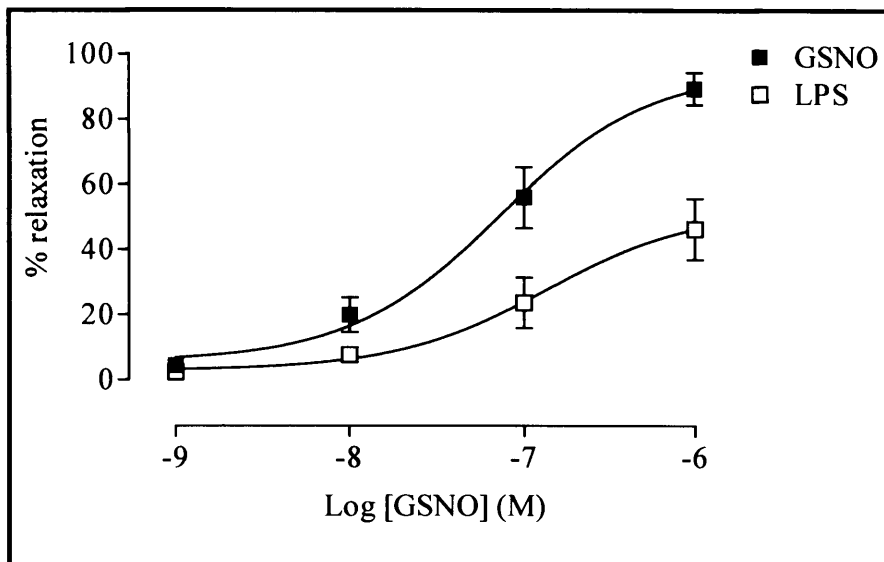
4.3A



4.3B



4.3C



4.3D

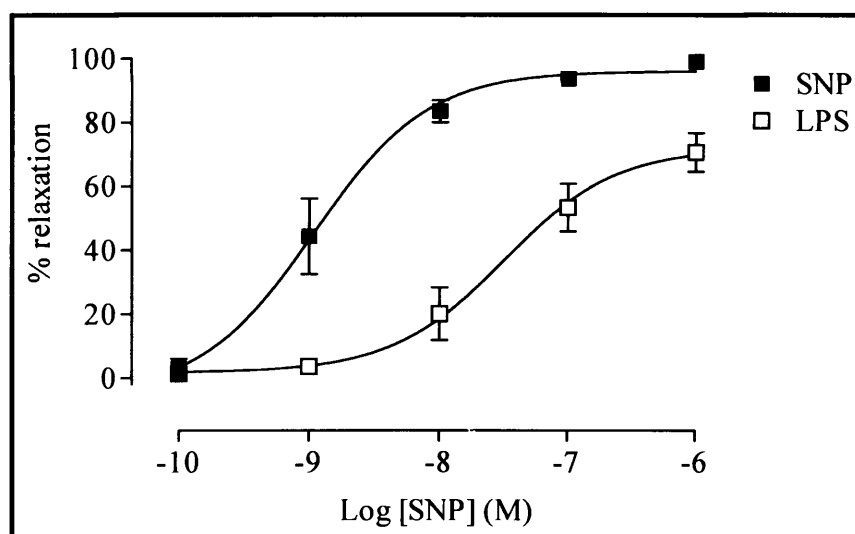
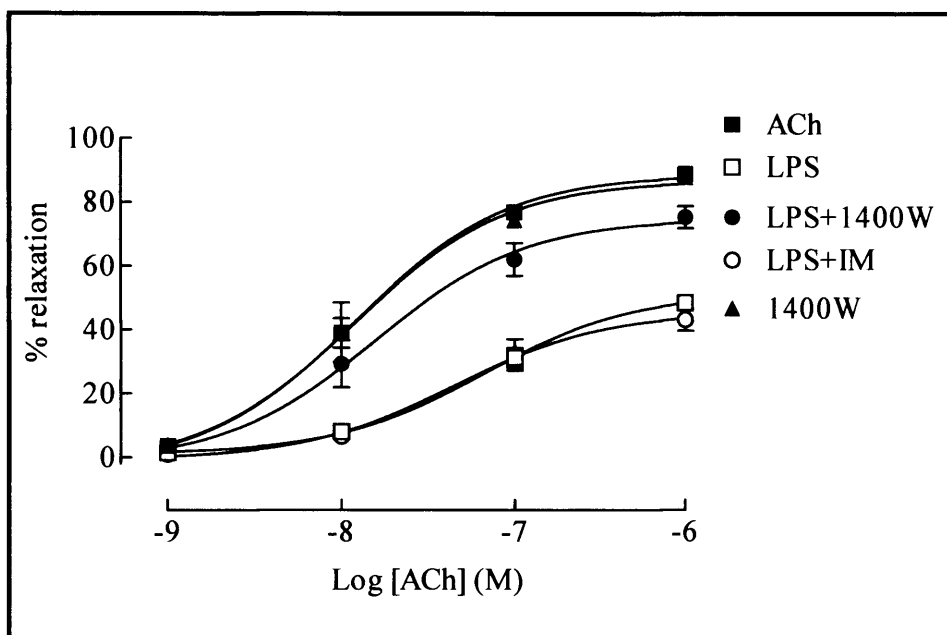


Figure 4.3 Concentration-response curves to (A) SPER-NO (1nM-1 μ M), (B) BAY 58-2667 (1nM-1 μ M), (C) GSNO (1nM-1 μ M) and (D) SNP (0.1nM-1 μ M) following 4hr incubation with vehicle or LPS (0.3 μ g/ml); n=5. Relaxation is expressed as the percentage reversal of the U46619-induced tone. Each point represents mean \pm SEM

4.4A



4.4B

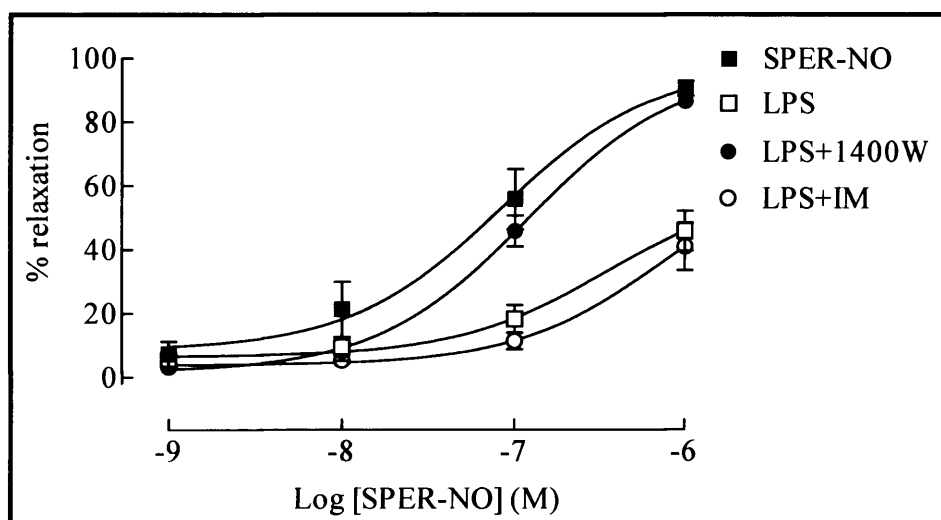


Figure 4.4 Concentration-response curves to (A) ACh (1nM-1μM) and (B) SPER-NO (1nM-1μM) following 4hr incubation with vehicle, LPS (0.3μg/ml), 1400W (10μM), LPS plus 1400W or LPS plus indomethacin (IM; 10μM); $n \geq 3$. Relaxation is expressed as the percentage reversal of the U46619-induced tone. Each point represents mean \pm SEM.

4.3.2.2 Effect of LPS on pGC-mediated relaxation

LPS (0.3 μ g/ml; 4hr) significantly reduced the potency of CNP (pEC₅₀: 7.38 \pm 0.41 versus 6.54 \pm 0.44 in the absence and presence of LPS, respectively; $n=4$; $P<0.05$; Figure 4.5). Similarly, LPS (0.3 μ g/ml; 4hr) significantly reduced the potency of ANP (pEC₅₀: 8.95 \pm 0.17 versus 8.05 \pm 0.26 in the absence and presence of LPS, respectively; $n=10$; $P<0.05$; Figure 4.6). Co-incubation with 1400W (10 μ M) with LPS preserved responses to ANP (pEC₅₀: 8.44 \pm 0.29; $n=6$; $P<0.05$ versus LPS alone). Similarly, co-incubation with ODQ (5 μ M), preserved relaxation to ANP (pEC₅₀: 8.59 \pm 0.37; $n=7$; $P<0.05$ versus LPS alone). In the presence of both ODQ and 1400W, relaxation to ANP was fully restored (pEC₅₀: 8.89 \pm 0.38, $n=5$; $P<0.05$ versus LPS alone; Figure 4.6). However, 1400W (10 μ M) alone had no effect on responses to ANP in control tissues (pEC₅₀: 8.68 \pm 0.53 versus; $n=3$; $P>0.05$ versus control; Figure 4.6). Comparisons were done by TW-ANOVA with BC.

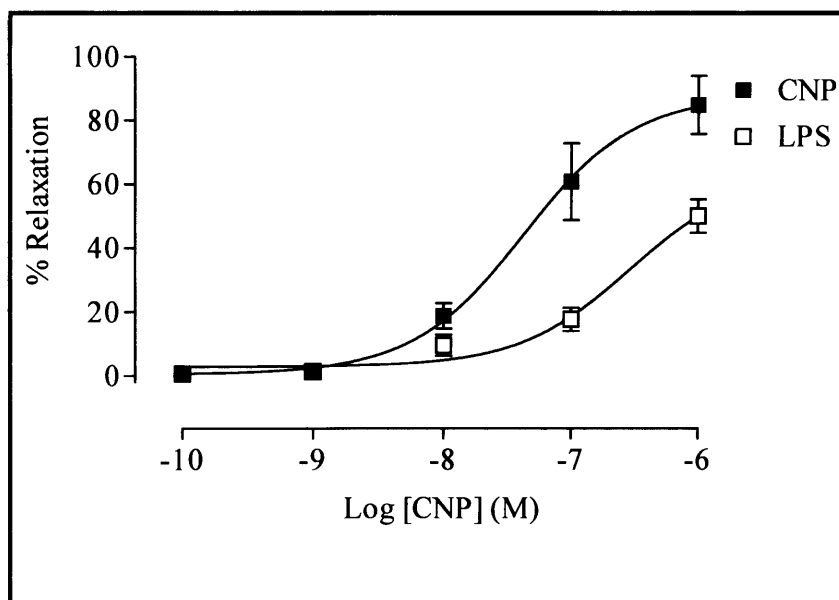


Figure 4.5 Concentration-response curves to CNP (0.1nM-1 μ M) following 4hr incubation with vehicle or LPS (0.3 μ g/ml); $n=4$. Relaxation is expressed as the percentage reversal of the U46619-induced tone. Each point represents mean \pm SEM.

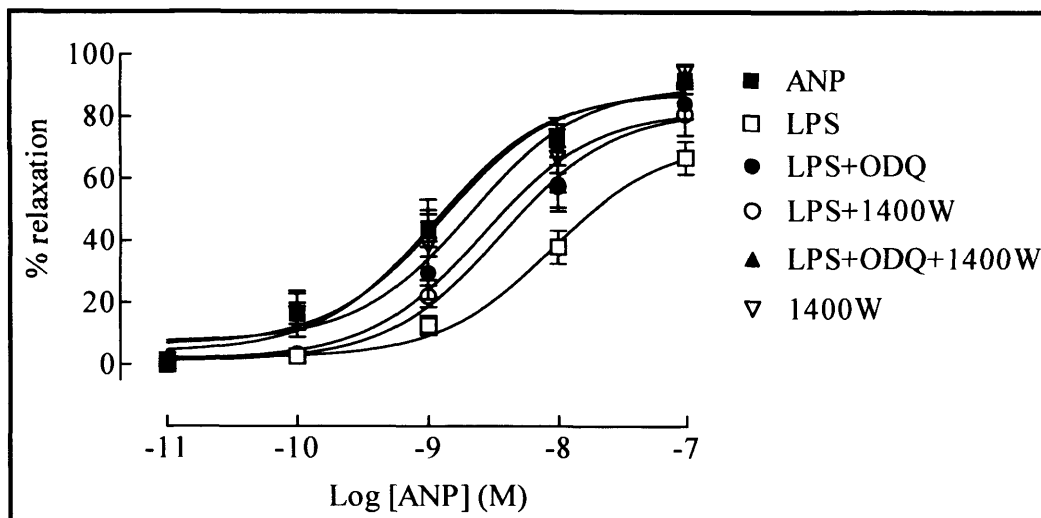


Figure 4.6 Concentration-response curves to ANP (0.01nM - $0.1\mu\text{M}$) following 4hr incubation with vehicle, LPS ($0.3\mu\text{g/ml}$), LPS plus 1400W ($10\mu\text{M}$), LPS plus ODQ ($5\mu\text{M}$) or LPS plus both ODQ and 1400W; $n=5$. Relaxation is expressed as the percentage reversal of the U46619-induced tone. Each point represents mean \pm SEM.

4.3.2.2.1 Reversibility of desensitisation of ANP-mediated relaxation

Incubation with LPS ($0.3\mu\text{g/ml}$) for 4 hrs significantly reduced the potency of ANP (pEC_{50} : 9.29 ± 0.41 versus $7.91\pm.36$ in the absence and presence of LPS, respectively; $n=5$; $P<0.05$). The responsiveness to ANP was restored immediately by addition of 1400W ($10\mu\text{M}$; pEC_{50} 8.26 ± 0.25 ; $n=7$; $P<0.05$ versus LPS alone), ODQ ($5\mu\text{M}$; pEC_{50} : 8.83 ± 0.18 ; $n=7$; $P<0.05$ versus LPS alone) or both (pEC_{50} : 9.02 ± 0.38 ; $n=5$; $P<0.05$ versus LPS alone; Figure 4.7). Curves were compared by TW-ANOVA with BC.

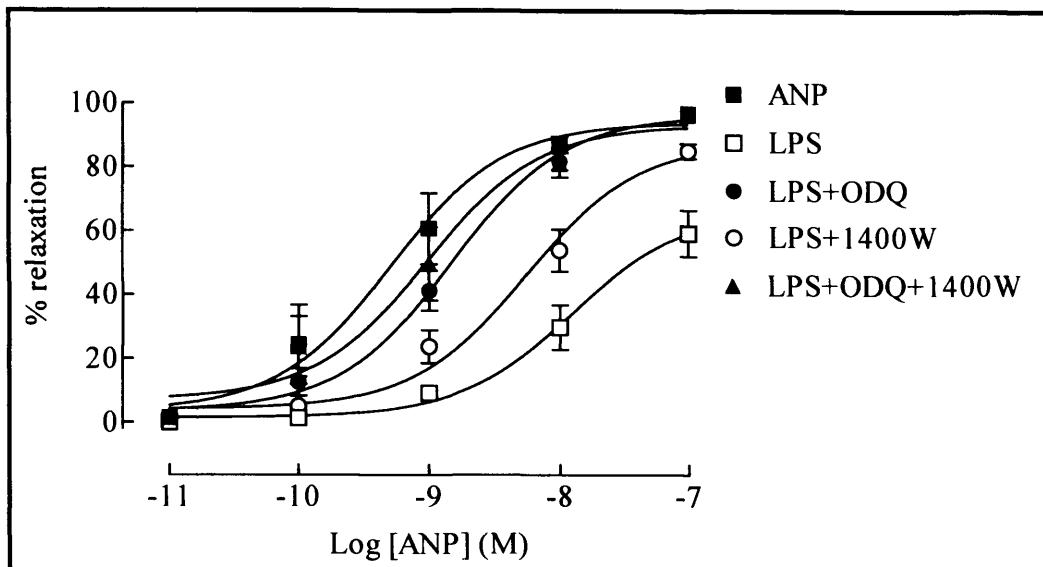
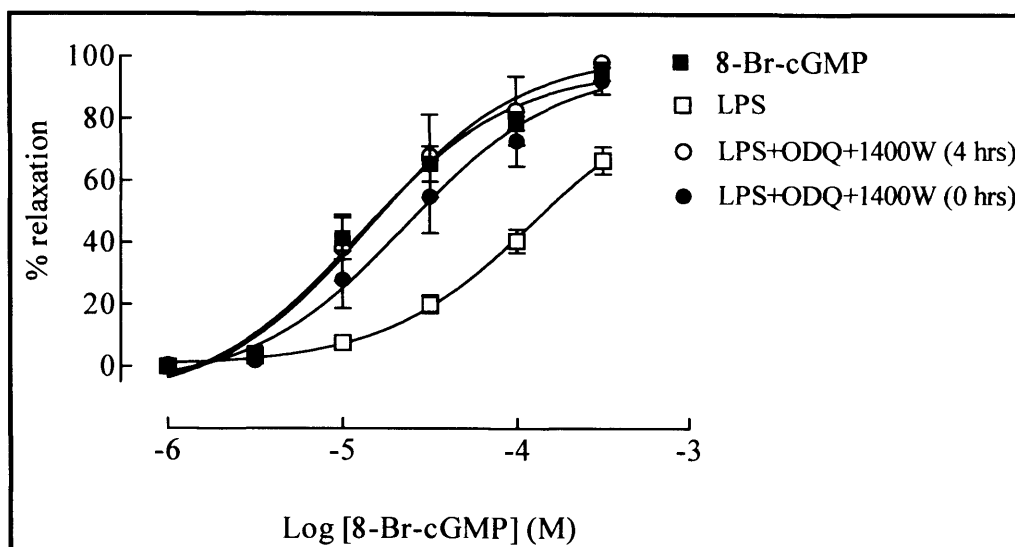


Figure 4.7 Concentration-response curves to ANP (0.01nM-0.1μM) following 4hr incubation with vehicle or LPS (0.3μg/ml). At 4hr, 1400W (10μM), ODQ (5μM) or both ODQ plus 1400W were added to LPS-treated vessels; $n=5$. Relaxation is expressed as the percentage reversal of the U46619-induced tone. Each point represents mean \pm SEM.

4.3.2.3 Effect of LPS on the sensitivity of vessels to cGMP

LPS (0.3μg/ml; 4hr) significantly reduced the potency of 8-Br-cGMP (pEC_{50} : 4.9 ± 0.2 versus 3.91 ± 0.22 in the absence and presence of LPS, respectively; $n=5$; $P<0.05$; figure 4.8A). Co-incubation with both 1400W (10μM) and ODQ (5μM) with LPS preserved the relaxations to 8-Br-cGMP (pEC_{50} : 4.64 ± 0.34 ; $n=5$; $P<0.05$ versus LPS alone; Figure 4.8A). Similarly, ODQ and 1400W immediately restored responsiveness to 8-Br-cGMP following 4hr incubation with LPS (pEC_{50} : 3.91 ± 0.22 versus 4.95 ± 0.36 in the absence and presence of ODQ and 1400W; $n=5$; $P<0.05$; Figure 4.8A). Incubation with GTN (30μM) for 4 hrs also reduced the potency of 8-Br-cGMP (pEC_{50} : 4.48 ± 0.15 versus 4.98 ± 0.26 in the presence and absence of GTN respectively; $n=4$; $P<0.05$ Figure 4.8B). Co-incubation of ODQ (5μM) with GTN preserved the relaxations to 8-Br-cGMP (pEC_{50} : 4.74 ± 0.15 ; $n=4$; $P<0.05$ versus GTN alone; Figure 4.8B). Curves were compared by TW-ANOVA with BC.

4.8A



4.8B

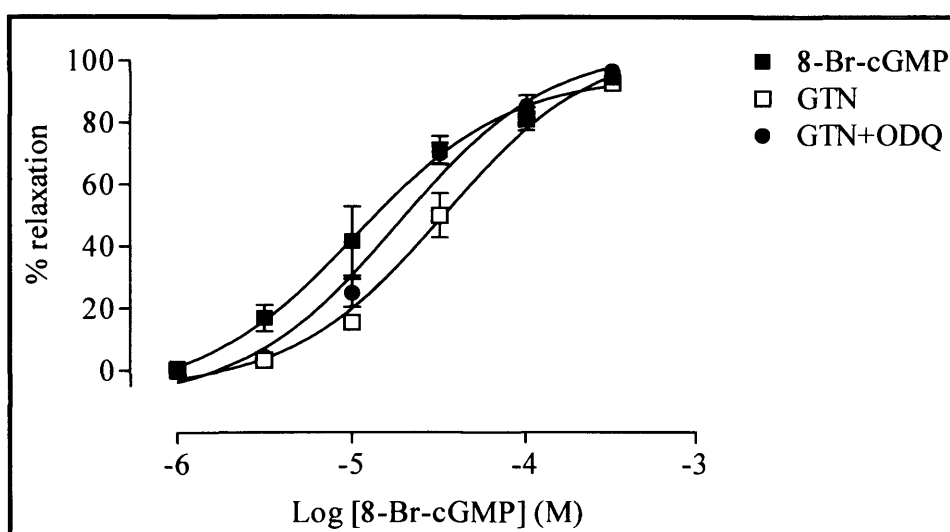
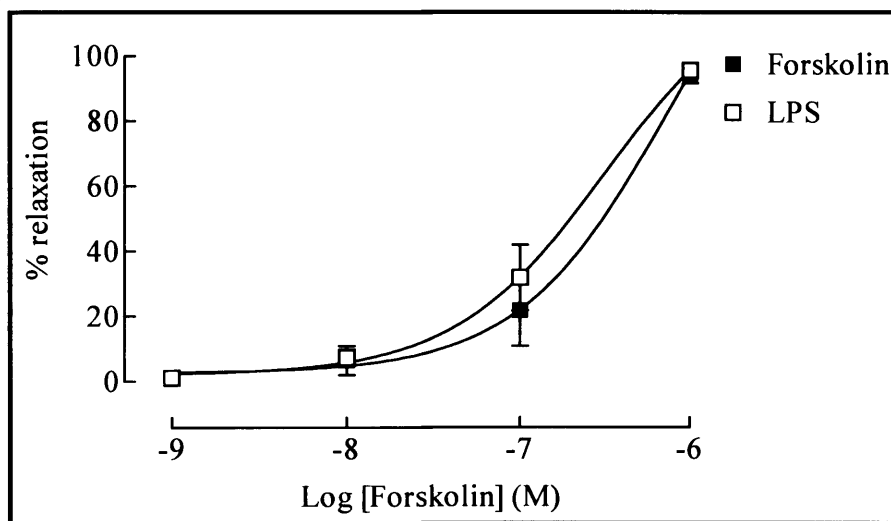


Figure 4.8 Concentration-response curves to (A) 8-Br-cGMP (1-300 μ M) following 4hr incubation with vehicle, LPS (0.3 μ g/ml), or LPS plus both 1400W (10 μ M) and ODQ (5 μ M), or 4 hrs incubation with LPS (0.3 μ g/ml) and addition of 1400W plus ODQ at the 4hr timepoint ($n=5$) and (B) 8-Br-cGMP (1-300 μ M) following 4hr incubation with vehicle, GTN (30 μ M), or GTN plus ODQ (5 μ M); $n=4$. Relaxation is expressed as the percentage reversal of the U46619-induced tone. Each point represents mean \pm SEM.

4.3.2.4 Effect of LPS on cAMP-mediated relaxation

LPS (0.3 μ g/ml; 4hr) had no effect on the potency of the adenylate cyclase activator, forskolin, (pEC₅₀: 6.15 \pm 0.74 versus 6.52 \pm 0.36 in the absence and presence of LPS, respectively; $n=6$; $P>0.05$; Figure 4.9A) or 8-Br-cAMP (pEC₅₀: 3.43 \pm 0.26 versus 3.58 \pm 0.21 in the absence and presence of LPS, respectively; $n=4$; $P>0.05$; Figure 4.9B). Curves were compared by TW-ANOVA.

4.9A



4.9B

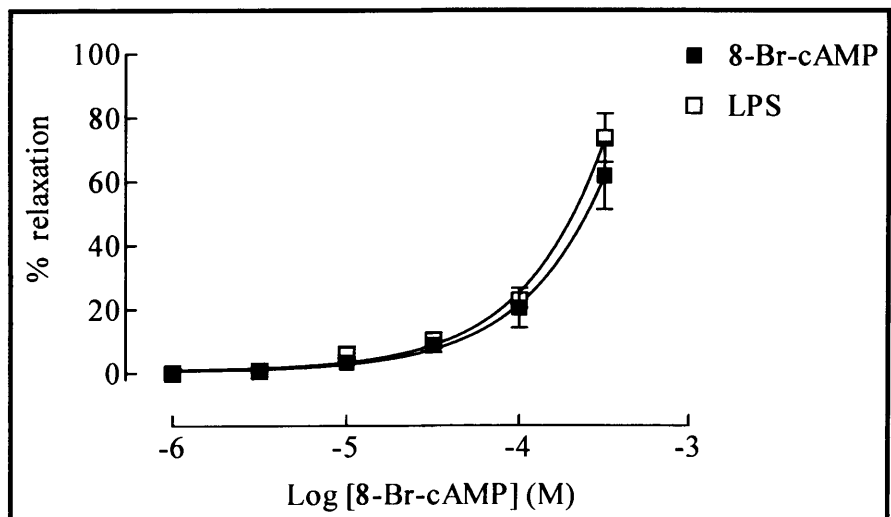
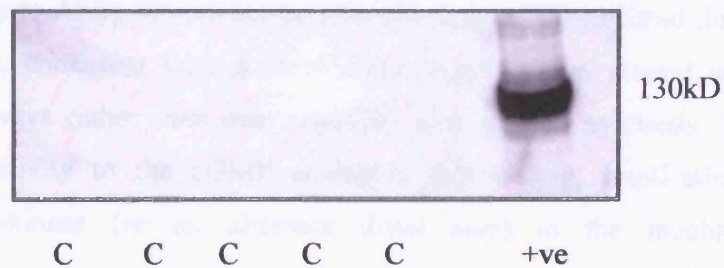


Figure 4.9 Concentration-response curves to (A) forskolin (1nM-1 μ M; $n=6$) and (B) 8-Br-cAMP (1-300 μ M; $n=4$) following 4hr incubation with vehicle or LPS (0.3 μ g/ml). Relaxation is expressed as the percentage reversal of the U46619-induced tone. Each point represents mean \pm SEM.

4.3.3 Detection of iNOS protein in LPS treated vessels

In the absence of LPS treatment, there was no detectable iNOS expression (Figure 4.10A). However, iNOS was detected in aortic rings treated with LPS (0.3 μ g/ml; 4hr) Figure 4.10B.

(A) Control



(B) LPS treatment

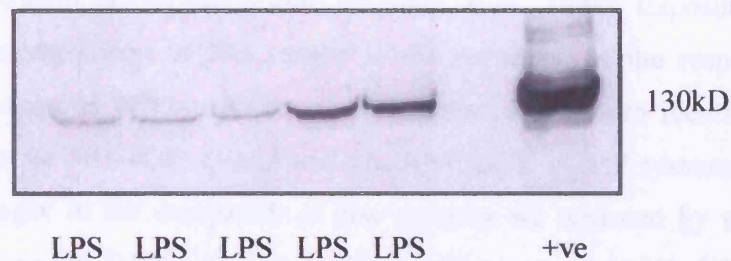


Figure 4.10 Detection of iNOS protein by western blotting following incubation of vessels with (A) vehicle (B) LPS (0.3 μ g/ml; 4hr); n=5.

4.4 DISCUSSION

This chapter demonstrates that exposure of rat aorta to LPS reduces the sensitivity of both sGC- and pGC-mediated relaxation. Desensitisation can be prevented by iNOS inhibition, consistent with iNOS-derived NO down-regulates both pathways. The effect is specific for cGMP signalling, since cAMP-mediated relaxation is unaffected. Desensitisation is mediated, at least in part, by cGMP generation, because inhibition of NO-mediated cGMP synthesis with ODQ partially restores sensitivity to ANP. Moreover, desensitisation of ANP-mediated dilatation is rapidly reversible, consistent with a mechanism dependent on altered activity of constitutive pathways rather than one requiring new protein synthesis. LPS also reduced the sensitivity to the cGMP analogue, 8-Br-cGMP, implicating down-regulation of G-kinase (or an alternate distal step) in the mechanism of desensitisation.

Previous reports have shown that the NO–cGMP system is influenced by the prevailing concentration of NO and cGMP (Hussain *et al.*, 1999). Exposure of the tissue to high concentrations of NO results in the reduction of the responses to subsequent application of NO or NO donors. Moreover, it has been identified that cross-talk between the NO–sGC–cGMP and the ANP–pGC–cGMP systems occurs, such that the changes in the sensitivity of one pathway are mirrored by the other cGMP-generating system (Hussain *et al.*, 2001; Madhani *et al.*, 2003). NO-donors reduce the sensitivity of murine aorta to ANP, an effect that is reduced by prevention of cGMP production with ODQ; conversely ANP reduces responsiveness to NO (Madhani *et al.*, 2003). These observations directly implicate cGMP as a mediator of desensitisation of the cyclase pathways in response to GC activation.

It has been shown that iNOS-derived NO also desensitises blood vessels to NO donors, but the mechanism has not been described in detail (Chauhan *et al.*, 2003c; Bogle *et al.*, 2000). In the present study, incubation with LPS was used to elicit iNOS induction (as confirmed by western blotting) and exposure of vessels to

'high-output' NO. LPS treatment reduced constrictor responses to PE and U46619, and hyporeactivity to U46619 was reversed by specific iNOS inhibition with 1400W, consistent with previous findings that hyporeactivity to vasoconstrictors in septic shock is in part a result of production of high output iNOS-derived NO (O'Brien *et al.*, 2001 ;Miyamoto *et al.*, 2004). Despite the reduction in response, contractions to U46619 (unlike PE) were sufficiently stable to investigate whether LPS-treatment induced vasodilator dysfunction. LPS-treatment reduced responses to the endothelium-dependent agonists (ACh and histamine) and SPER-NO, effects that were prevented by 1400W but not indomethacin. These data suggest that the principal cause of dilator dysfunction is iNOS-derived NO leading to reduced sensitivity of the vascular smooth muscle. The observed reduction in the sensitivity of sGC-cGMP pathway also extended to NO-independent activation of sGC, as responses to the direct sGC activator, BAY 58-2667, were also diminished in a similar fashion.

To investigate whether there was a generalised reduction in responses to GC activation, the response to CNP and ANP was used to determine the sensitivity of pGC in control and LPS-treated vessels. CNP and ANP-mediated relaxation was impaired, with restoration of the responses to ANP achieved by iNOS or sGC inhibition; indeed the combination of both 1400W and ODQ normalised responses to ANP. These data demonstrate that LPS causes an NO- and cGMP- dependent reduction in the responsiveness of vascular smooth muscle to activation of sGC and pGC. The reduction in sensitivity was specific to the sGC and pGC pathways because the direct adenylate cyclase activator forskolin and the cell permeable cAMP analogue, 8-Br-cAMP, were equipotent in control and LPS-treated vessels. It is possible that different pre-contracting concentrations of U46619 in the presence and absence of LPS might affect the magnitude of relaxation. However, since the desensitisation is specific to the cGMP pathway (i.e. not cAMP), a potential confounding influence of different U46619 concentrations is unlikely.

The mechanism of desensitisation of pGC is at least in part dependent on cGMP generation, evidenced by the effect of ODQ. Desensitisation to ANP was also rapidly reversible, because addition of ODQ and/or 1400W restored responsiveness within minutes, suggesting that desensitisation of pGC pathway is a consequence of biochemical rather than expressional changes in enzyme activity.

These observations are consistent with other previous findings using NO donors to induce GC desensitisation in murine aorta (Hussain *et al.*, 1999). However, these studies indicated that the response to cGMP itself was unaffected by NO-induced desensitisation of the cyclase pathways. In the present study, I used 8-Br-cGMP to determine the sensitivity of G-kinase and down-stream effector pathways in LPS-treated tissues. Responses to 8-Br-cGMP were reduced in LPS-treated vessels suggesting that G-kinase activity might be reduced. Prolonged exposure of vessels to high concentrations of GTN also reduced the response to 8-Br-cGMP, raising the possibility that with longer exposure of tissues to excess NO/cGMP, desensitisation occurs in distal parts of the cGMP signalling pathway. In both cases, inhibition of cGMP synthesis by ODQ partially restored the response to 8-Br-cGMP, indicating that under these conditions, the response to cGMP is regulated by a classical negative feedback mechanism. Further studies will be necessary to delineate the components of this feedback loop.

These results extend the prior observations of the reciprocal regulation of ANP/NO signalling (Hussain *et al.*, 2001; Madhani *et al.*, 2003). This phenomenon has now been identified in murine, human and rat tissues, occurs *in vivo* (Sabrane *et al.*, 2003), and largely accounts for vasodilator dysfunction in pathological states associated with iNOS induction (Chauhan *et al.*, 2003c). It might also provide a mechanism to explain the link between the sustained increases in endogenous BNP and cardiovascular risk that has been reported recently in a variety of patient groups (Wang *et al.*, 2004). Relaxation to GSNO was also desensitised by LPS implying that the responses to *S*-nitrosothiols are affected by similar desensitisation mechanisms as other NO-donors. There is no evidence that LPS induces a bioactivation mechanism of GSNO to modify the response to this NO-donor.

Thus, altered vascular smooth muscle responsiveness to endogenous NO and ANP is a fundamental physiological mechanism within the blood vessel that is likely to play an important role in vascular tone and blood flow. It is possible that in vascular inflammation associated with bacterial sepsis, desensitisation of smooth muscle and platelet cGMP pathways contributes to microvascular constriction, thrombosis and tissue hypoxia (Vallet, 2003). Moreover, this mechanism has implications for the development of tolerance to NO or GC activators administered as therapy for angina and heart failure and the fluid retention in patients receiving nitrates. In particular, these data suggest that tolerance is a likely consequence of any vasodilator that is cGMP-mediated.

CHAPTER FIVE

**MECHANISMS OF DESENSITISATION
BY LIPOPOLYSACCHARIDE**

5.1 INTRODUCTION

I have shown in chapter 4 that incubation of LPS with rat aorta resulted in the induction of iNOS. This in turn resulted in desensitisation of both the sGC and pGC signalling pathways. However, the mechanism(s) by which high output NO desensitises both sGC and pGC are unknown. The aim of this chapter was to explore mechanisms of the desensitisation using a pharmacological approach. A variety of mechanisms have been implicated in regulation of the sensitivity of GC signalling. These have been discussed in detail in Chapter 1 but are briefly discussed below.

Certain PDEs play an important role in the regulation of cGMP-signalling pathways (Rybalkin *et al.*, 2003). In the rat, following induction of GTN tolerance *in vivo*, desensitisation of rat aortic rings *in vitro* to GTN was reversed by treatment with a selective cGMP phosphodiesterase (PDE5) inhibitor (De Garavilla *et al.*, 1996). In addition, in this model of reduced responsiveness to sGC activation, there is also evidence of increased activity and expression of other PDE isoenzymes, specifically PDE1A1 (Kim *et al.*, 2001). PDE3 may be involved in inflammatory vascular disease (Kondo *et al.*, 1999). Protein kinase C (PKC) activation has also been shown to play a role in the regulation of guanylate cyclases, since it desensitises both sGC (Morrison *et al.*, 1990; Murphy *et al.*, 1994) and pGC (Potter & Garbers, 1994). However, the PKC-isozymes(s) causing this desensitisation is uncertain. Pathways that specifically regulate the sensitivity of sGC or pGC also appear to exist. For instance, desensitisation of pGC by protein phosphatase 2 A (PP2A) is well established (Potter & Garbers, 1992), possibly via activation by PKG (Zhou *et al.*, 1996). In contrast, generation of oxygen free radicals (e.g. superoxide) is associated with impairment of NO-sGC signalling via scavenging of NO (Xia & Zweier, 1997; Stoclet *et al.*, 1999) and by direct oxidation of sGC protein thiols (Mingone *et al.*, 2006). Similarly, neutrophil-derived myeloperoxidase (MPO) modulates NO-mediated vasodilator responses during acute inflammation through its ability to generate free radicals (Eiserich *et al.*, 2002).

One approach to assess the roles of various signalling pathways in biological systems is to inhibit or activate certain components in the pathway of interest and observe the changes that occur. To investigate the mechanism(s) of NO-induced desensitisation of sGC and pGC, pharmacological tools (specific inhibitors or activators) were used to probe the putative roles of PDEs (types 1A1, 3 and 5), PKC, PP2A, SOD and MPO.

5.2 EXPERIMENTAL PROTOCOLS AND STATISTICS

5.2.1 Effect of LPS on the sensitivity of GC in the presence of sildenafil

Vessels were incubated with vehicle (DMSO; 0.03%), the PDE-5 inhibitor sildenafil (3 μ M), LPS (0.3 μ g/ml) or both LPS and sildenafil for 4 hrs. Vessels were pre-contracted with U46619 to an approximate EC₈₀ and concentration-response curves to SPER-NO (1nM-10 μ M; $n=4$) and ANP (0.01nM-0.1 μ M; $n=4$) were constructed. Details of the IC₅₀ of sildenafil and the other inhibitors used in this Chapter are described in Table 2.1.

5.2.2 Effect of LPS on the sensitivity of GC in the presence of vinpocetine

Vessels were incubated with vehicle (DMSO; 1%), the PDE-1A1 inhibitor vinpocetine (100 μ M; 30 mins pre-incubation), LPS (0.3 μ g/ml; 4hr) or both LPS and vinpocetine. Unlike other inhibitors, which inhibit PDE1 indirectly by binding to calmodulin, vinpocetine causes its effect by direct interaction with PDE1A1. The IC₅₀ of vinpocetine was reported previously as 20 μ M (Hagiwara *et al.*, 1984), but recent studies in rat aortic rings showed significant effects at 100 μ M when incubated for 30 mins (Kim *et al.*, 2001). Vinpocetine was added 30 mins before pre-contraction and at 4 hrs, vessels were pre-contracted with U46619 to an approximate EC₈₀ and concentration-response curves to SPER-NO (1nM-10 μ M; $n=5$) and ANP (0.01nM-0.1 μ M; $n=6$) were constructed.

5.2.3 Effect of LPS on the sensitivity of GC in the presence of milrinone

Vessels were incubated with vehicle (DMSO; 0.1%), the PDE-3 inhibitor milrinone (10 μ M; 30 mins pre-incubation), LPS (0.3 μ g/ml; 4hr) or both LPS and milrinone. Milrinone was added 30 mins before pre-contraction and at 4 hrs vessels were pre-contracted with U46619 to an approximate EC₈₀ and concentration-response curves to SPER-NO (1nM-10 μ M; $n=4$) and ANP (0.01nM-0.1 μ M; $n=4$) were constructed.

5.2.4 Effect of LPS on the sensitivity of sGC in the presence of SOD

Vessels were incubated with vehicle, SOD (2000units/ml; 4hr), LPS (0.3 μ g/ml; 4hr) or both LPS and SOD for 4hr. Vessels were pre-contracted with U46619 to an approximate EC₈₀ and concentration-response curves were constructed to SPER-NO (1nM-1 μ M; $n=4$) and ACh (1nM-1 μ M; $n=3$).

5.2.5 Effect of LPS on the sensitivity of sGC in the presence of 4-aminobenzoic hydrazide

Vessels were incubated with vehicle (DMSO; 0.01%), the MPO inhibitor 4-aminobenzoic hydrazide (ABAH; 10 μ M; 30 mins), LPS (0.3 μ g/ml; 4hr) or both LPS and ABAH. ABAH is a suicide substrate that promotes inactivation of MPO through modulation of its haem group leading to the formation of the inactive ferrous enzyme (Kettle *et al.*, 1995). ABAH was added 30 mins before pre-contraction and at 4 hrs vessels were pre-contracted with U46619 to an approximate EC₈₀ and concentration-response curves to SPER-NO (1nM-10 μ M; $n=4$) were constructed.

5.2.6 Effect of the PKC activators on the sensitivity of GC and AC

Concentration-response curves to phorbol 12-myristate 13-acetate (PMA; 1nM-10 μ M), and potassium chloride (KCl; 1-100mM) were constructed to determine their EC₈₀. PMA causes contraction via direct activation of PKC (it non-selectively activates both the conventional PKC isoforms α , β , and γ and the novel PKC isoforms ϵ , η , θ , δ and μ ; Tsao & Wang, 1997; Kim *et al.*, 1997; Krotova *et al.*, 2003) while KCl causes contraction in a PKC-independent manner by opening dihydropyridine-

sensitive voltage-gated Ca^{2+} channels (Ratz *et al.*, 2005). Vessels were pre-contracted with PMA, U46619 and KCl to an approximate EC_{80} of their maximum contraction and concentration-response curves to ACh (1nM-10 μ M; $n=4$), SPER-NO (1nM-10 μ M; $n=4$), ANP (0.01nM-0.1 μ M; $n=4$), 8-Br-cGMP (1-300 μ M; $n=4$) and forskolin (1nM-1 μ M; $n=4$) were constructed.

To determine roles for specific PKC isoforms in the desensitisation of GC and AC, vessels were equipotently pre-contracted with the selective PKC activator thymeleatoxin (a phorbol ester that selectively activates the conventional-PKC isoforms α , β and γ ; Ryves *et al.*, 1991; Armstrong & Ganote, 1994; Llosas *et al.*, 1996; Krotova *et al.*, 2003) and U46619 and concentration-response curves to ACh (1nM-10 μ M; $n=4$), SPER-NO (1nM-10 μ M; $n=4$), ANP (0.01nM-0.1 μ M; $n=4$) and forskolin (1nM-1 μ M; $n=4$) were constructed.

5.2.7 Effect of LPS on the sensitivity of GC and AC in the presence of protein phosphatase 2A inhibitors

Vessels were incubated with vehicle (DMSO; 0.03%), okadaic acid (300nM; 30 mins) or cantharidic acid (500nM; 30 mins; both are PP2A inhibitors; Bialojan & Takai, 1988; Li & Casida, 1992), LPS (0.3 μ g/ml; 4hr) or both LPS plus okadaic acid or cantharidic acid. Okadaic acid or cantharidic acid was added 30 mins before pre-contraction and at 4 hrs vessels were pre-contracted with U46619 to an approximate EC_{80} and concentration-response curves to ANP (0.01nM-0.1 μ M; $n=5$) were constructed. In some experiments, concentration-response curves were also constructed to SPER-NO (1nM-10 μ M; $n=4$) and forskolin (1nM-1 μ M; $n=4$) in the presence of okadaic acid.

5.2.8 Statistics

Organ bath studies are expressed as described in section 2.8. All curves were analysed by TW-ANOVA and where appropriate Bonferroni's correction (BC) was applied.

5.3 RESULTS

5.3.1 Effect of LPS on sGC-mediated relaxation in the presence of sildenafil

Incubation of aortic rings with LPS (0.3 μ g/ml) for 4 hrs significantly reduced the potency of SPER-NO (pEC₅₀: 6.89 \pm 0.26 versus 6.15 \pm 0.38 in the absence and presence of LPS, respectively; $n=4$; $P<0.05$). The PDE5 inhibitor sildenafil (3 μ M) had no effect on the relaxations to SPER-NO in the presence of LPS (pEC₅₀: 5.89 \pm 0.43 in the presence of sildenafil; $n=4$; $P>0.05$ versus LPS alone; Figure 5.1). Sildenafil significantly reduced responses to U46619 and enhanced the relaxation to SPER-NO (pEC₅₀: 7.54 \pm 0.24 in the presence of sildenafil; $n=4$; $P<0.05$ versus control; Figure 5.1). Curves were compared by TW-ANOVA with BC.

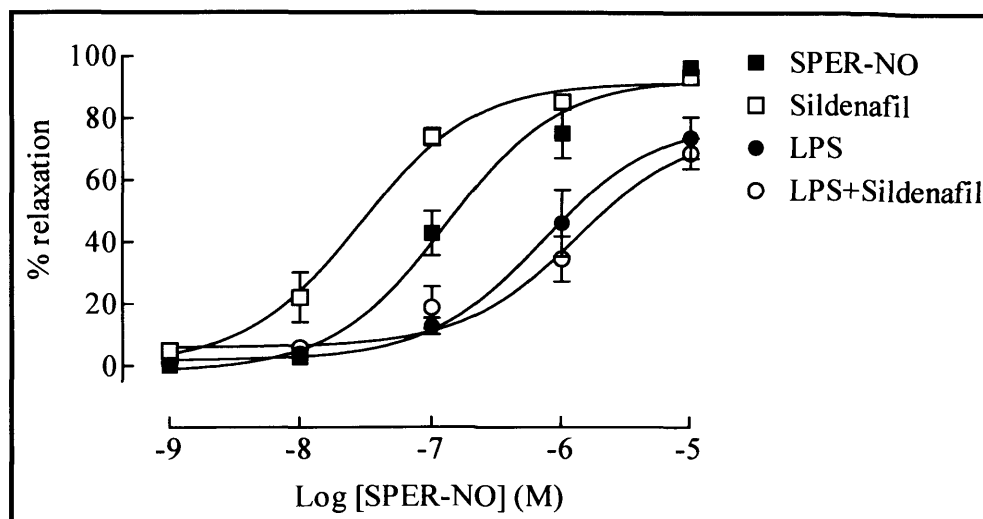


Figure 5.1 Concentration-response curves to SPER-NO (1nM-10 μ M) following 4hr incubation with vehicle, LPS (0.3 μ g/ml), sildenafil (3 μ M) or LPS plus sildenafil; $n=4$. Relaxation is expressed as the percentage reversal of the U46619-induced tone. Each point represents mean \pm SEM.

5.3.2 Effect of LPS on pGC-mediated relaxation in the presence of sildenafil

Incubation of aortic rings with LPS (0.3 μ g/ml) for 4 hrs significantly reduced the potency of ANP (pEC₅₀: 8.97 \pm 0.26 versus 8.27 \pm 0.65 in the absence and presence of

LPS, respectively; $n=4$; $P<0.05$; BC). Sildenafil ($3\mu\text{M}$) had no effect on relaxations to ANP in the presence of LPS (pEC_{50} : 8.38 ± 0.39 in the presence of sildenafil; $n=4$; $P>0.05$ versus LPS alone; Figure 5.2). Sildenafil significantly reduced responses to U46619, but had no effect on the relaxation to ANP (pEC_{50} : 9.23 ± 0.2 in the presence of sildenafil; $n=4$; $P>0.05$ versus control). Curves were compared by TW-ANOVA.

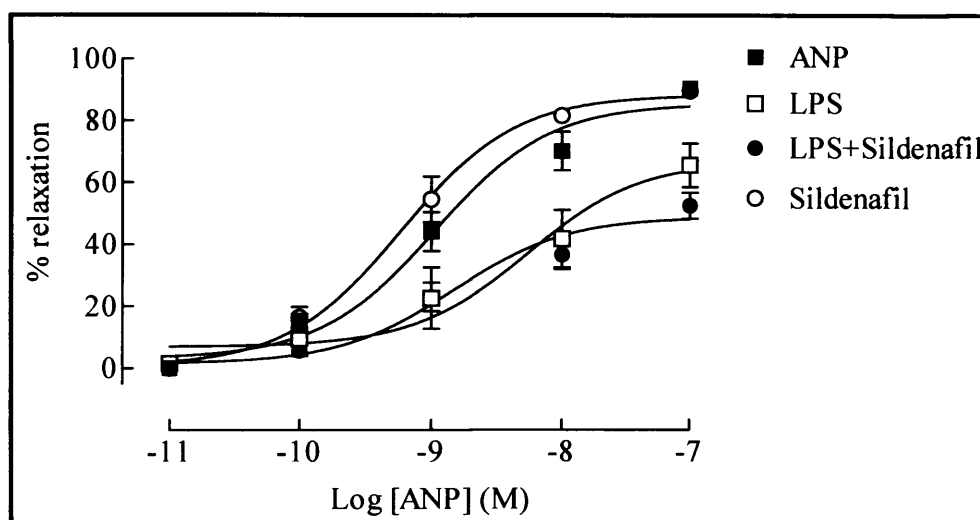


Figure 5.2 Concentration-response curves to ANP (0.01nM - $0.1\mu\text{M}$) following 4hr incubation with vehicle, LPS ($0.3\mu\text{g/ml}$), sildenafil ($3\mu\text{M}$) or LPS plus sildenafil; $n=4$. Relaxation is expressed as the percentage reversal of the U46619-induced tone. Each point represents mean \pm SEM.

5.3.3 Effect of LPS on sGC-mediated relaxation in the presence of vinpocetine

As expected, incubation of rat aortic rings with LPS ($0.3\mu\text{g/ml}$) for 4 hrs significantly reduced the potency of SPER-NO (pEC_{50} : 6.31 ± 0.22 versus 5.72 ± 0.28 in the absence and presence of LPS, respectively; $n=5$; $P<0.05$; BC). The PDE1A1 inhibitor, vinpocetine ($100\mu\text{M}$), had no effect on the relaxations to SPER-NO in the presence of LPS (pEC_{50} : 5.75 ± 0.24 in the presence of vinpocetine; $n=5$; $P>0.05$ versus LPS alone; Figure 5.3). Vinpocetine significantly reduced responses to U46619, but had no effect on the relaxation to SPER-NO (pEC_{50} : 6.30 ± 0.15 in the

presence of vinpocetine; $n=5$; $P>0.05$; versus control). Curves were compared by TW-ANOVA.

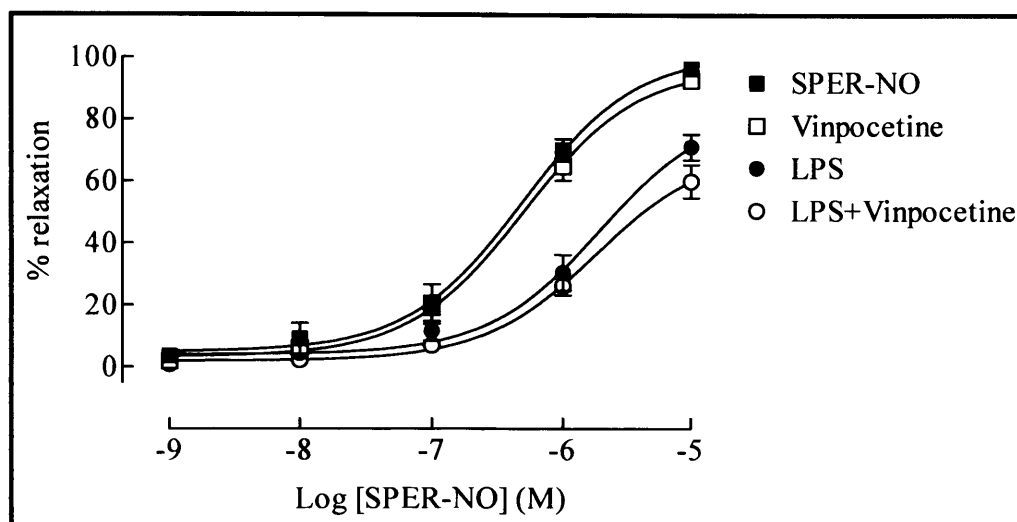


Figure 5.3 Concentration-response curves to SPER-NO (1nM-10 μ M) following incubation with vehicle, LPS (0.3 μ g/ml; 4 hrs), vinpocetine (100 μ M; 30 mins) or LPS plus vinpocetine; $n=5$. Relaxation is expressed as the percentage reversal of the U46619-induced tone. Each point represents mean \pm SEM.

5.3.4 Effect of LPS on pGC-mediated relaxation in the presence of vinpocetine

Similarly, incubation of rat aortic rings with LPS (0.3 μ g/ml) for 4 hrs significantly reduced the potency of ANP (pEC_{50} : 8.76 ± 0.13 versus 7.92 ± 0.24 in the absence and presence of LPS, respectively; $n=6$; $P<0.05$; BC). Co-incubation with vinpocetine (100 μ M) had no effect on the relaxations to ANP in the presence of LPS (pEC_{50} : 8.98 ± 0.26 in the presence of vinpocetine; $n=6$; $P>0.05$; versus LPS alone; Figure 5.4). Vinpocetine significantly reduced responses to U46619, but had no effect on the relaxation to ANP (pEC_{50} : 8.98 ± 0.16 in the presence of vinpocetine; $n=6$; $P>0.05$ versus control). Curves were compared by TW-ANOVA.

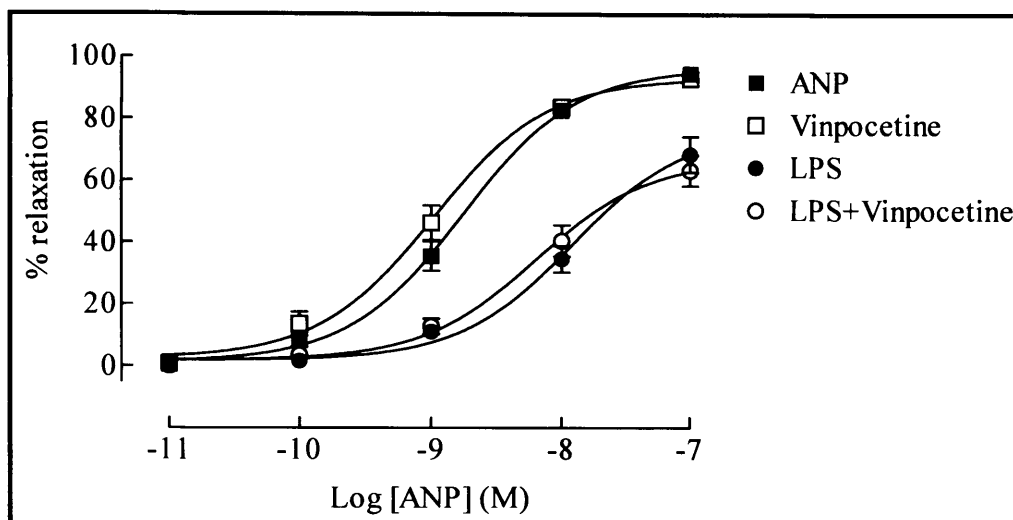


Figure 5.4 Concentration-response curves to ANP (0.01nM-0.1 μ M) following incubation with vehicle, LPS (0.3 μ g/ml; 4 hrs), vinpocetine (100 μ M; 30 mins) or LPS plus vinpocetine; $n=6$. Relaxation is expressed as the percentage reversal of the U46619-induced tone. Each point represents mean \pm SEM.

5.3.5 Effect of LPS on sGC-mediated relaxation in the presence of milrinone

Treatment of rat aortic rings with LPS (0.3 μ g/ml) for 4 hrs significantly reduced the potency of SPER-NO (pEC_{50} : 6.79 ± 0.38 versus 5.63 ± 0.29 in the absence and presence of LPS, respectively; $n=4$; $P < 0.05$; BC). The PDE 3 inhibitor, milrinone (10 μ M) had no effect on the relaxations to SPER-NO in the presence of LPS (pEC_{50} : 5.86 ± 0.38 in the presence of milrinone; $n=4$; $P > 0.05$; versus LPS alone; Figure 5.5). Milrinone significantly reduced responses to U46619, but had no effect on the relaxation to SPER-NO (pEC_{50} : 6.55 ± 0.18 in the presence of milrinone; $n=4$; $P > 0.05$ versus control). Curves were compared by TW-ANOVA.

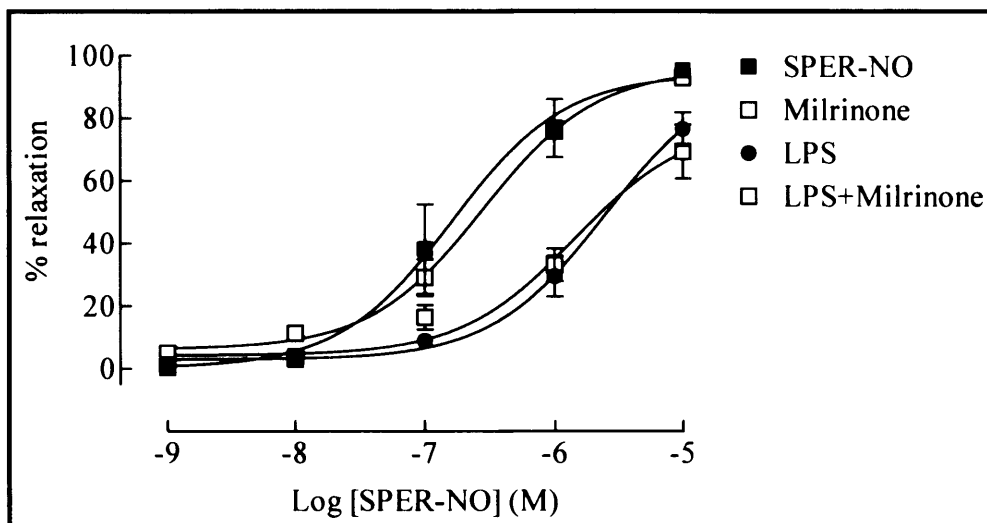


Figure 5.5 Concentration-response curves to SPER-NO (1nM-10 μ M) following incubation with vehicle, LPS (0.3 μ g/ml; 4 hrs), milrinone (10 μ M; 30 mins) or LPS plus milrinone; $n=4$. Relaxation is expressed as the percentage reversal of the U46619-induced tone. Each point represents mean \pm SEM.

5.3.6 Effect of LPS on pGC-mediated relaxation in the presence of milrinone

Treatment of rat aortic rings with LPS (0.3 μ g/ml) for 4 hrs significantly reduced the potency of ANP (pEC_{50} : 8.74 ± 0.32 versus 8.20 ± 0.58 in the absence and presence of LPS, respectively; $n=4$; $P < 0.05$; BC). Milrinone (10 μ M) had no effect on the relaxations to ANP in the presence of LPS (pEC_{50} : 7.99 ± 0.34 in the presence of milrinone; $n=4$; $P > 0.05$ versus LPS alone; Figure 5.6). Milrinone significantly reduced responses to U46619, but had no effect on the relaxation to ANP (pEC_{50} : 8.55 ± 0.19 in the presence of milrinone; $n=4$; $P > 0.05$ versus control). Curves were compared by TW-ANOVA.

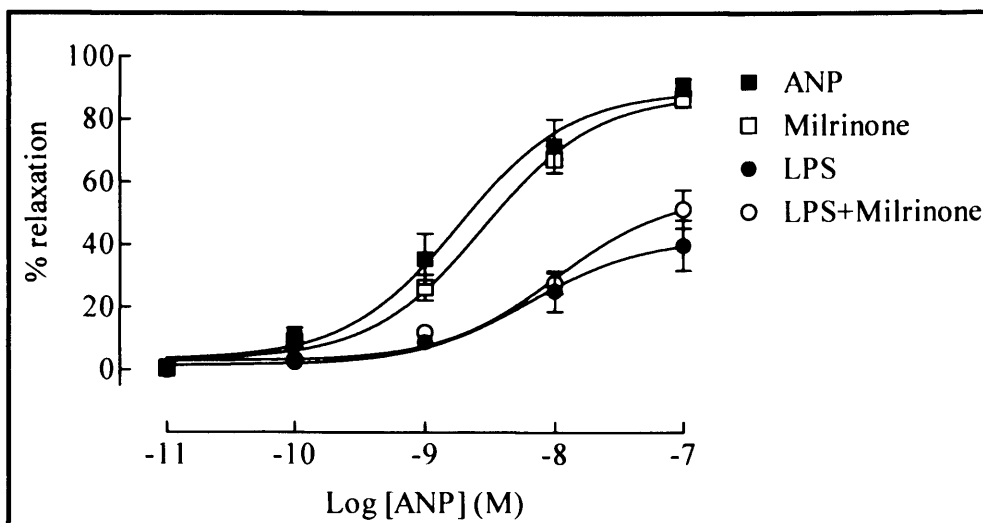
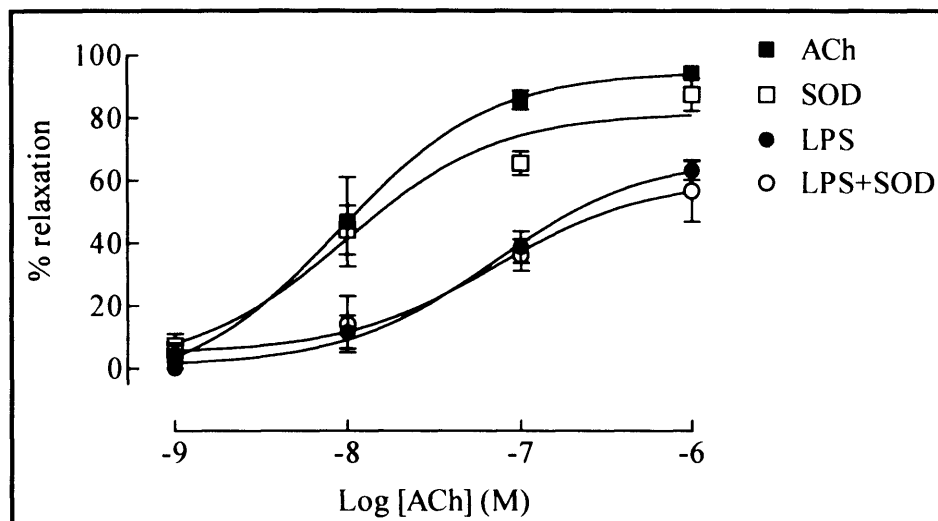


Figure 5.6 Concentration-response curves to ANP (0.01nM-0.1μM) following incubation with vehicle, LPS (0.3μg/ml; 4 hrs), milrinone (10μM; 30 mins) or LPS plus milrinone; *n*=4. Relaxation is expressed as the percentage reversal of the U46619-induced tone. Each point represents mean ± SEM.

5.3.7 Effect of LPS on sGC-mediated relaxation in the presence of superoxide dismutase

Incubation of rat aortic rings with LPS (0.3μg/ml) for 4 hrs significantly reduced the potency of ACh (pEC_{50} : 8.04 ± 0.43 versus 7.16 ± 0.35 in the absence and presence of LPS, respectively; *n*=3; *P*<0.05; BC). SOD (2000U/ml) had no effect on the relaxations to ACh in the presence of LPS (pEC_{50} : 7.15 ± 0.77 in the presence of SOD; *n*=3; *P*>0.05 versus LPS alone; Figure 5.7A). SOD alone had no effect on the relaxation to ACh (pEC_{50} : 8.0 ± 0.47 in the presence of SOD; *n*=3; *P*>0.05 versus control). Similarly, LPS significantly reduced the potency of SPER-NO (pEC_{50} : 7.12 ± 0.35 versus 6.51 ± 0.73 in the absence and presence of LPS, respectively; *n*=4; *P*<0.05; BC). SOD (2000U/ml) had no effect on the relaxations to SPER-NO in the presence of LPS (pEC_{50} : 6.13 ± 0.38 in the presence of SOD; *n*=4; *P*>0.05 versus LPS alone; Figure 5.7B). SOD alone had no effect on the relaxation to SPER-NO (pEC_{50} : 7.01 ± 0.52 in the presence of SOD; *n*=4; *P*>0.05 versus control). Curves were compared by TW-ANOVA.

A



B

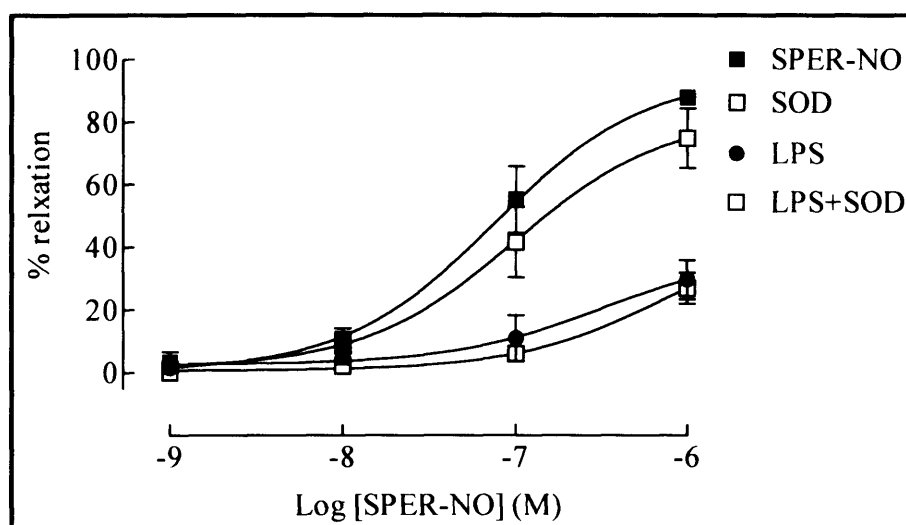


Figure 5.7 Concentration-response curves to (A) ACh (1nM-1μM) and (B) SPER-NO (1nM-1μM) following 4hr incubation with vehicle, LPS (0.3μg/ml), SOD (2000u/ml) or LPS plus SOD; $n \geq 3$. Relaxation is expressed as the percentage reversal of the U46619-induced tone. Each point represents mean \pm SEM.

5.3.8 Effect of LPS on sGC-mediated relaxation in the presence of aminobenzoic hydrazide

Rat aortic rings treated with LPS (0.3µg/ml) for 4 hrs showed significant reduction in the potency of SPER-NO (pEC₅₀: 6.36±0.22 versus 5.66±0.27 in the absence and presence of LPS, respectively; *n*=4; *P*<0.05; BC). Co-incubation with the MPO inhibitor, 4-aminobenzoic hydrazide (ABAH; 10µM) had no effect on the relaxations to SPER-NO in the presence of LPS (pEC₅₀: 5.58±0.27 in the presence of ABAH; *n*=4; *P*>0.05 versus LPS alone; Figure 5.8). ABAH alone had no effect on the relaxation to SPER-NO (pEC₅₀: 6.45±0.31 in the presence of ABAH; *n*=4; *P*>0.05 versus control). Curves were compared by TW-ANOVA.

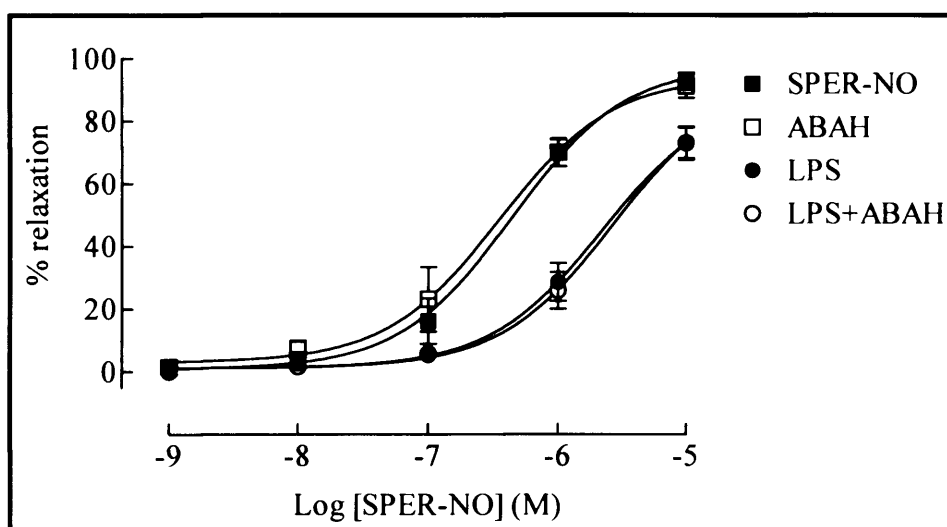
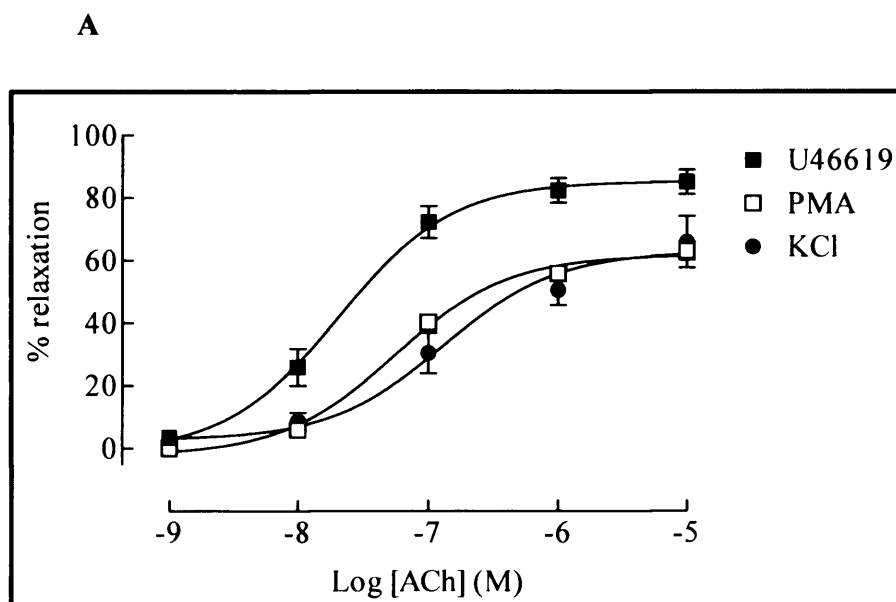


Figure 5.8 Concentration-response curves to SPER-NO (1nM-10µM) following incubation with vehicle, LPS (0.3µg/ml; 4 hrs), ABAH (10µM; 30 mins) or LPS plus ABAH; *n*=4. Relaxation is expressed as the percentage reversal of the U46619-induced tone. Each point represents mean ± SEM.

5.3.9 Responses to sGC-mediated vasorelaxation in tissue precontracted with phorbol myristate acetate (PMA)

The effect of activation of protein kinase C on the sensitivity of sGC-cGMP pathway was studied by examining the response of rat aortic rings precontracted with the PKC activator, PMA, to ACh and SPER-NO and compared with aortic rings precontracted with U46619 and potassium chloride (KCl). The responsiveness of vessels precontracted with PMA, U46619 and KCl to ACh was as follows: (pEC_{50}) 7.26 ± 0.13 , 7.69 ± 0.26 and 6.89 ± 0.42 , respectively. Relaxations to ACh were reduced in vessels precontracted with both PMA and KCl versus U46619 ($n=4$; $P<0.05$; Figure 5.9A). The pEC_{50} values for SPER-NO-induced relaxation in vessels precontracted with PMA, U46619 and KCl were 6.17 ± 0.14 , 6.65 ± 0.18 and 6.55 ± 0.33 , respectively ($n=4$). The pEC_{50} value for SPER-NO in vessels precontracted with PMA was significantly less than that of U46619 and KCl ($P<0.05$; $n=4$; Figure 5.9B). Curves were compared by TW-ANOVA with BC.



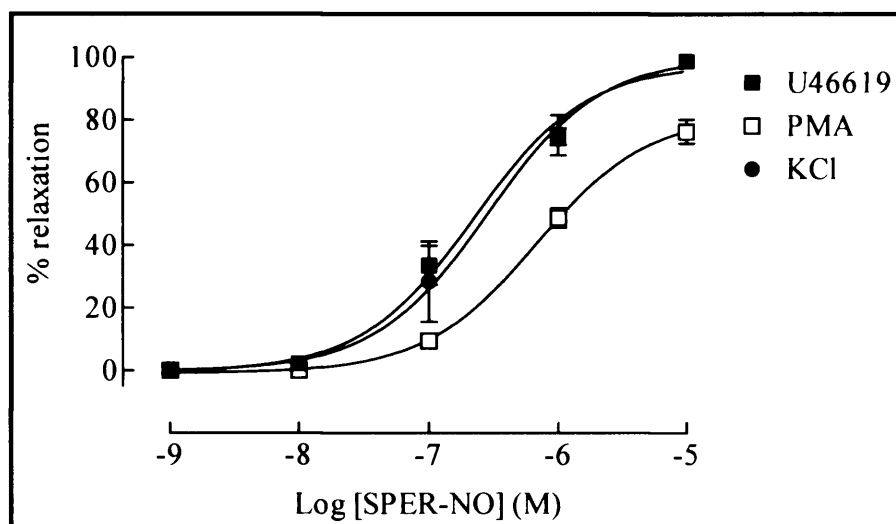
B

Figure 5.9 Concentration-response curves to (A) ACh (1nM-10μM) and (B) SPER-NO (1nM-10μM) in vessels precontracted to an EC_{80} with PMA, U46619 and KCl; $n \geq 4$. Relaxation is expressed as the percentage reversal of the PMA, U46619 or KCl-induced tone. Each point represents mean \pm SEM.

5.3.10 Responses to pGC-mediated vasorelaxation in tissue precontracted with PMA

The effect of activation of PKC on the sensitivity of the pGC-cGMP pathway was also examined by stimulating pGC with ANP in aortic rings precontracted with PMA, U46619 and KCl. The responsiveness of vessels precontracted with PMA, U46619 and KCl to ANP was as follows: (pEC_{50}) 8.26 ± 0.26 , 8.94 ± 0.28 and 9.01 ± 0.29 , respectively ($n=4$). The pEC_{50} for ANP-induced relaxations in vessels precontracted with PMA was significantly less than that of U46619 and KCl ($P < 0.05$; $n=4$; Figure 5.10). Curves were compared by TW-ANOVA with BC.

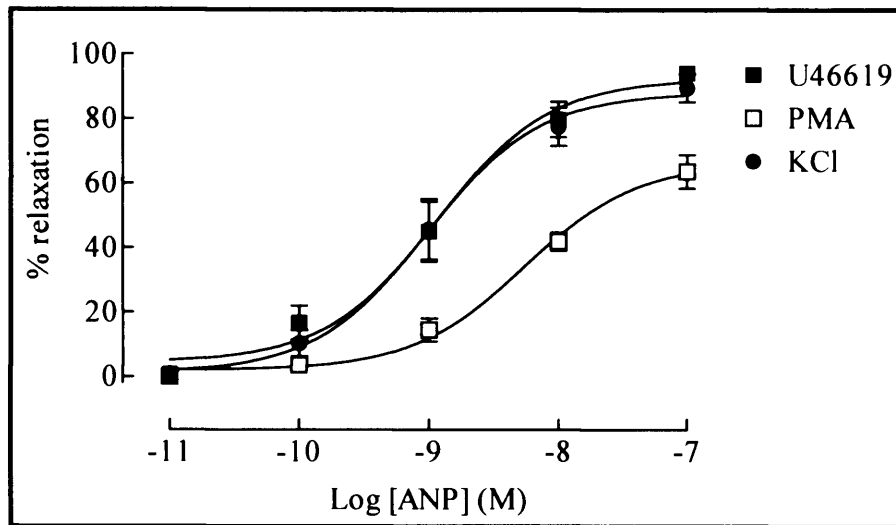


Figure 5.10 Concentration-response curves to ANP (0.01nM-0.1 μ M) in vessels precontracted to an EC_{80} with PMA, U46619 and KCl; $n=4$. Relaxation is expressed as the percentage reversal of the PMA, U46619 and KCl-induced tone. Each point represents mean \pm SEM.

5.3.11 Responses to cGMP-mediated vasorelaxation in tissue precontracted with PMA

The effect of activation of PKC on the sensitivity of the downstream cGMP-pathway was examined by direct stimulation of protein kinase G with 8-Br-cGMP, in aortic rings precontracted with PMA or U46619. The potency of 8-Br-cGMP in vessels precontracted with PMA was significantly reduced (pEC_{50} : 3.68 ± 0.22 and 4.57 ± 0.23 in tissues contracted with PMA or U46619, respectively; $n \geq 4$; $P < 0.05$; Figure 5.11). Curves were compared by TW-ANOVA with BC.

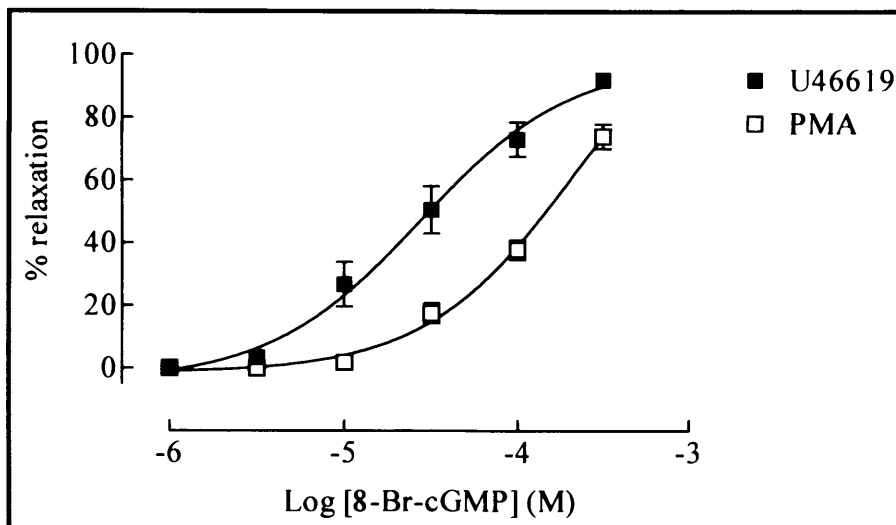


Figure 5.11 Concentration-response curves to 8-Br-cGMP (1-300 μ M) in vessels precontracted to an EC_{80} with PMA and U46619; $n \geq 4$. Relaxation is expressed as the percentage reversal of the PMA and U46619. Each point represents mean \pm SEM.

5.3.12 Responses to AC-mediated vasorelaxation in tissue precontracted with PMA

The effect of activation of PKC on the sensitivity of adenylate cyclase (AC) was also studied by examining the vasorelaxant potency of forskolin in rat aortic rings precontracted with PMA, U46619 or KCl. The responsiveness of vessels precontracted with PMA, U46619 and KCl to forskolin was as follows: (pEC_{50}) 6.11 ± 0.36 , 6.77 ± 0.34 and 6.68 ± 0.43 , respectively ($n=4$). The pEC_{50} for forskolin in vessels precontracted with PMA was significantly less than that of U46619 and KCl ($P < 0.05$; $n=4$; Figure 5.12). Curves were compared by TW-ANOVA with BC.

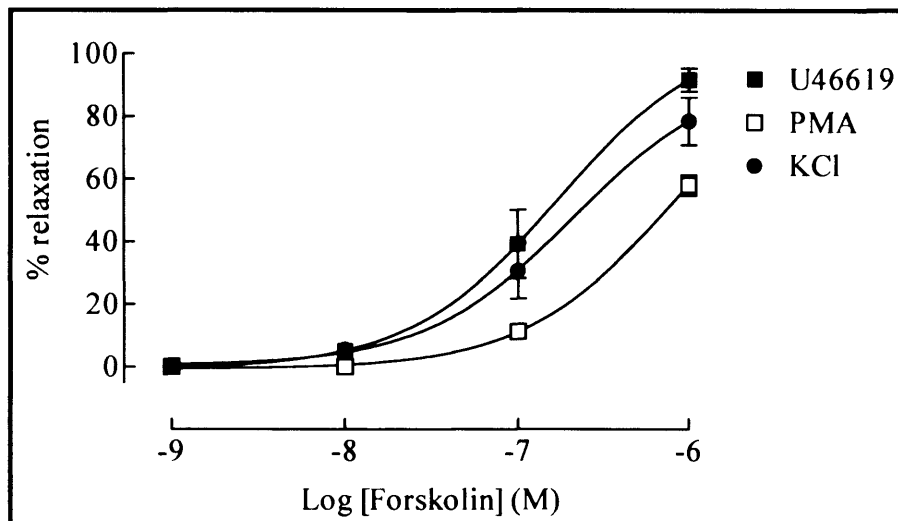


Figure 5.12 Concentration-response curves to forskolin (1nM-1μM) in vessels precontracted to an EC_{80} with PMA, U46619 and KCl; $n=4$. Relaxation is expressed as the percentage reversal of the PMA, U46619 and KCl-induced tone. Each point represents mean \pm SEM.

5.3.13 Responses to sGC-mediated vasorelaxation in tissue precontracted with thymeatoxin

The effect of activation of PKC on the sensitivity of sGC was confirmed by using a more selective PKC activator, thymeatoxin (which only activates the conventional PKC isoforms α , β and γ). The responsiveness of vessels precontracted with thymeatoxin to ACh was significantly reduced compared to U46619 (pEC_{50} : 8.04 ± 0.39 and 6.87 ± 0.42 in vessels contracted with U46619 or thymeatoxin, respectively; $n=3$; $P<0.05$; Figure 5.13A). The responsiveness of vessels precontracted with thymeatoxin to SPER-NO was also significantly reduced compared to U46619 (pEC_{50} : 6.84 ± 0.33 and 5.58 ± 0.26 in vessels contracted with U46619 or thymeatoxin, respectively; $n=3$; $P<0.05$; Figure 5.13B). All curves were compared by TW-ANOVA with BC.

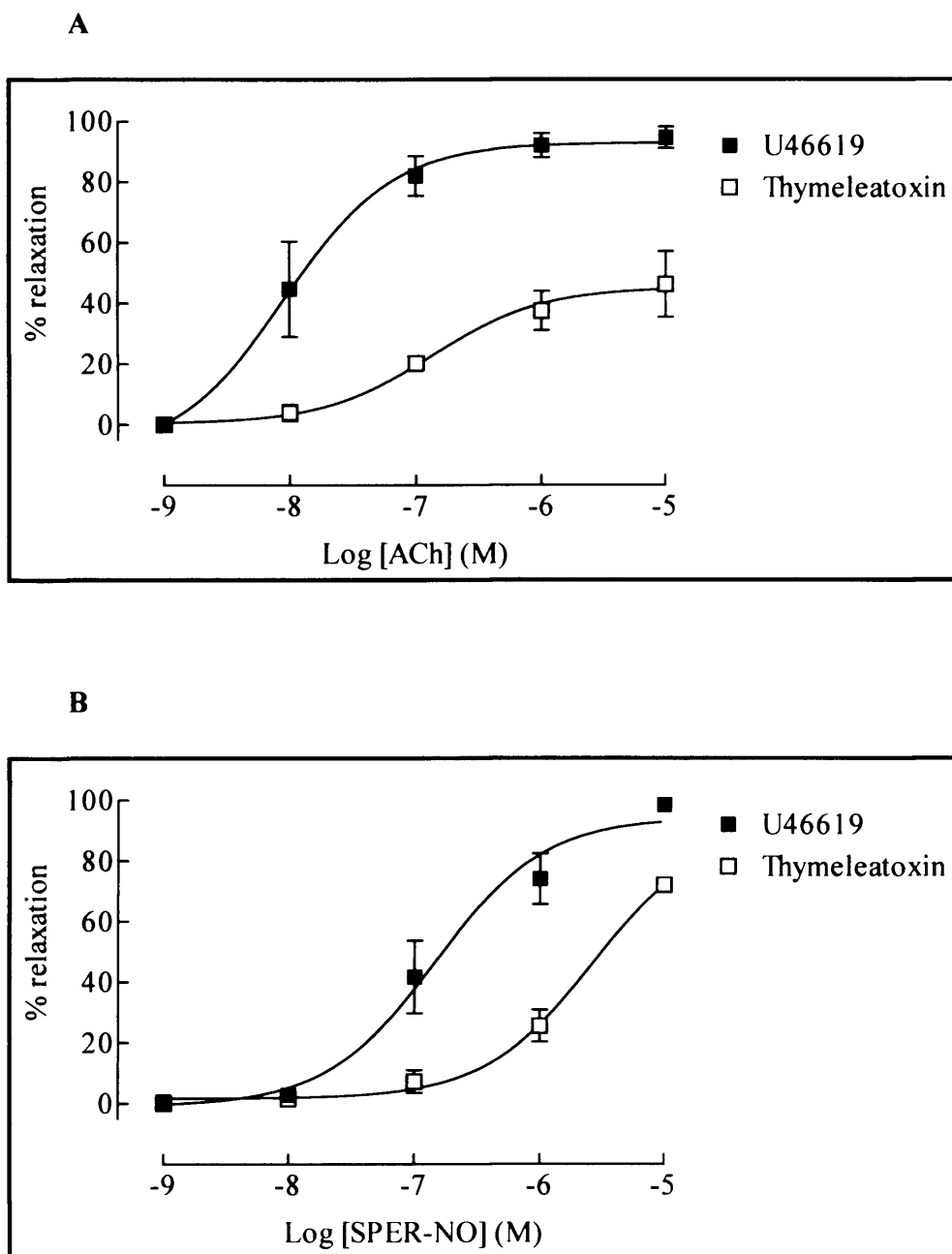


Figure 5.13 Concentration-response curves to (A) ACh (1nM-10 μ M) and (B) SPER-NO (1nM-10 μ M) in vessels equipotently precontracted with thymeleatoxin and U46619; $n=3$. Relaxation is expressed as the percentage reversal of the thymeleatoxin or U46619-induced tone. Each point represents mean \pm SEM.

5.3.14 Responses to pGC -mediated vasorelaxation in tissue precontracted with thymeleatoxin

The effect of activation of PKC on the sensitivity of pGC was also examined by pre-contracting vessels with thymeleatoxin or U46619. The responsiveness of vessels precontracted with thymeleatoxin to ANP was significantly reduced (pEC_{50} : 8.59 ± 0.38 and 7.65 ± 0.36 in vessels contracted with U46619 or thymeleatoxin, respectively; $P < 0.05$; TW-ANOVA with BC; $n=3$; Figure 5.14).

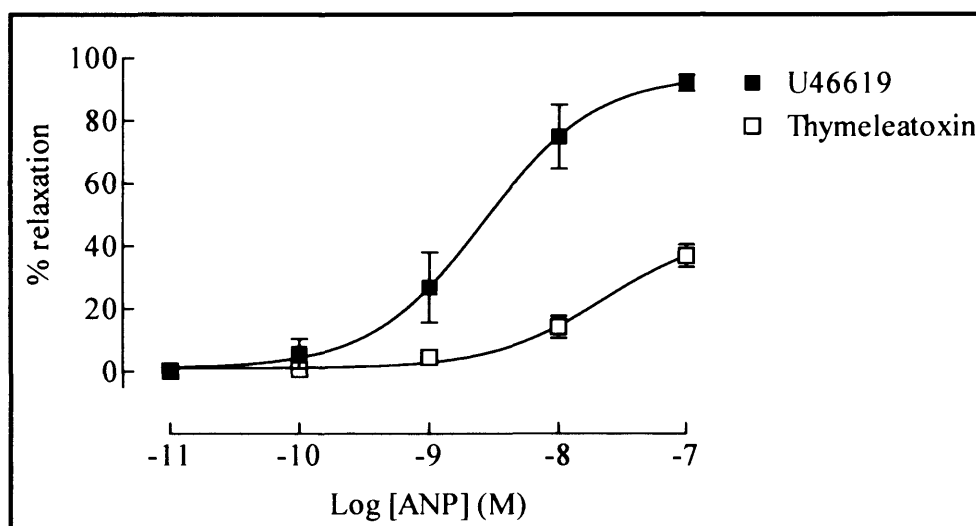


Figure 5.14 Concentration-response curves to ANP (0.01nM-0.1 μ M) in vessels equipotently precontracted with thymeleatoxin and U46619; $n=3$. Relaxation is expressed as the percentage reversal of the thymeleatoxin or U46619-induced tone. Each point represents mean \pm SEM.

5.3.15 Responses to AC-mediated vasorelaxation in tissue precontracted with thymeleatoxin

The response of rat aortic rings to forskolin was also studied in tissues precontracted with thymeleatoxin or U46619. The response of vessels precontracted with thymeleatoxin to forskolin was significantly reduced (pEC_{50} : 7.05 ± 0.47 and

5.64±0.36 in vessels contracted with U46619 or thymeleatoxin, respectively; $n=3$; $P<0.05$; TW-ANOVA with BC; Figure 5.15).

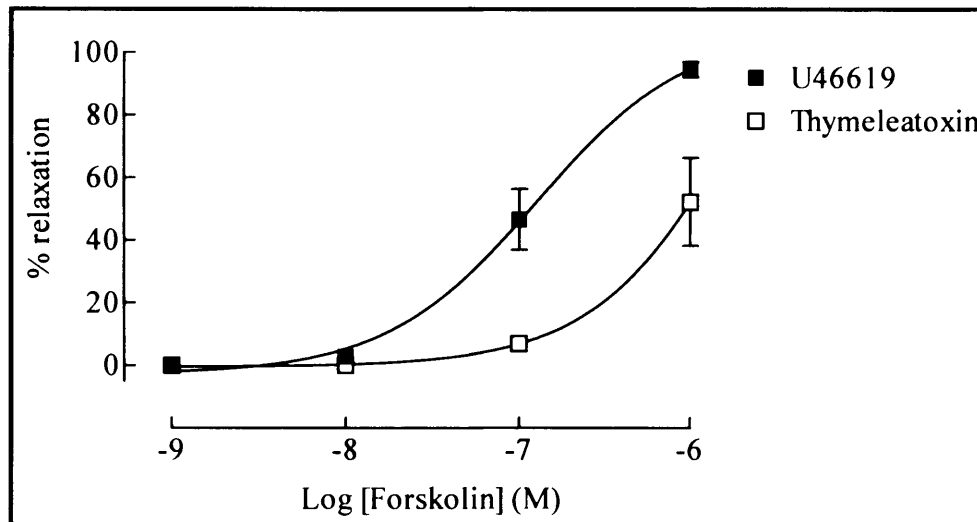


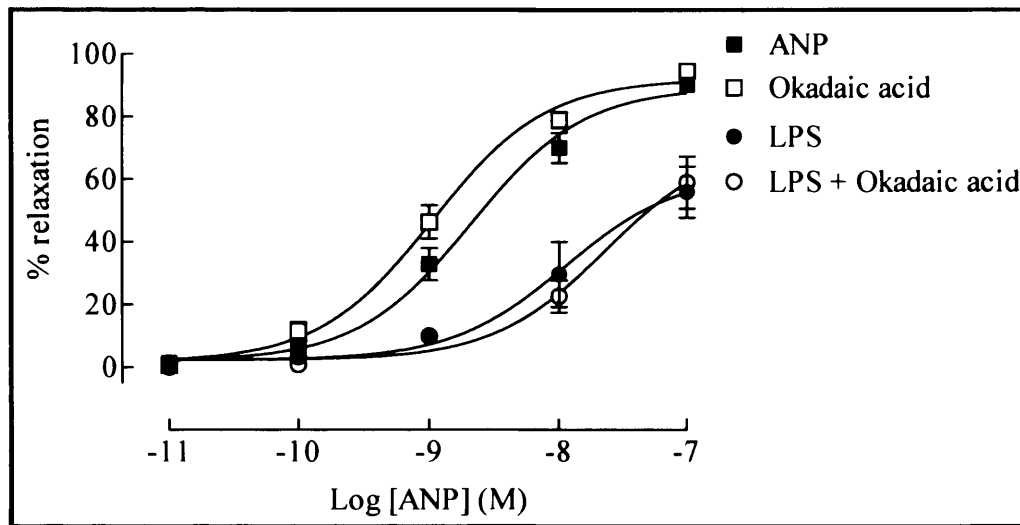
Figure 5.15 Concentration-response curves to forskolin (1nM-1μM) in vessels equipotently precontracted with thymeleatoxin and U46619; $n=3$. Relaxation is expressed as the percentage reversal of the thymeleatoxin or U46619-induced tone. Each point represents mean ± SEM.

5.3.16 Effect of okadaic acid on the sensitivity of GC and AC-mediated relaxation

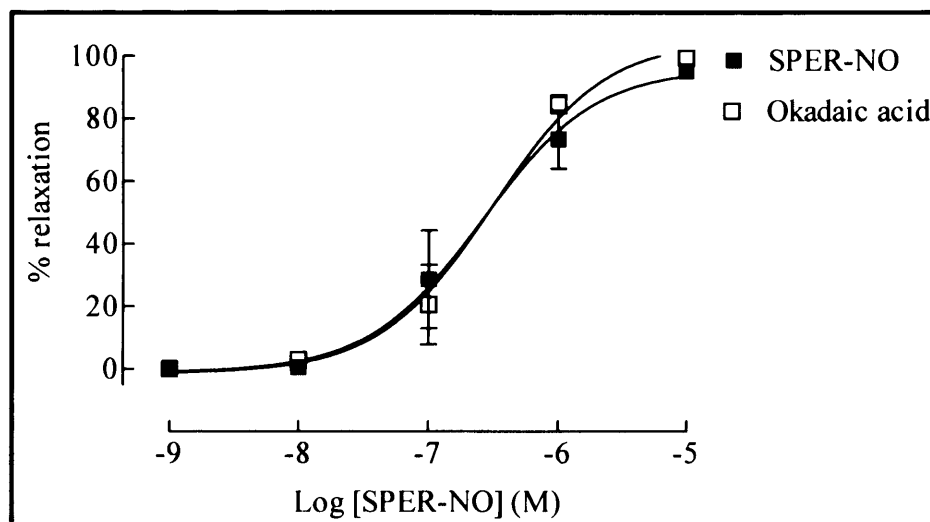
Rat aortic rings treated with LPS (0.3μg/ml) for 4 hrs showed significant reduction in the potency of ANP (pEC₅₀: 8.68±0.19 versus 7.96±0.51 in the absence and presence of LPS, respectively; $n=4$; $P<0.05$; BC). Co-incubation with the PP2A inhibitor, okadaic acid (300nM; 30min) had no effect on the relaxations to ANP in the presence of LPS (pEC₅₀: 7.89±0.26 in the presence of okadaic acid; $n=4$; $P>0.05$ versus LPS alone; Figure 5.16A). Okadaic acid alone had a small but significant effect on the relaxation to ANP (pEC₅₀: 8.98±0.15 in the presence of okadaic acid; $n=4$; $P<0.05$ versus control; BC), without affecting the sensitivity of SPER-NO (pEC₅₀: 6.59±0.41 versus 6.51±0.29 in the absence and presence of okadaic acid,

respectively; $n=4$; $P>0.05$; Figure 5.16B) or forskolin (pEC_{50} : 6.69 ± 0.57 versus 6.77 ± 0.34 in the absence and presence of okadaic acid, respectively; $n=4$; $P>0.05$; Figure 5.16C). All curves were compared by TW-ANOVA.

A



B



C

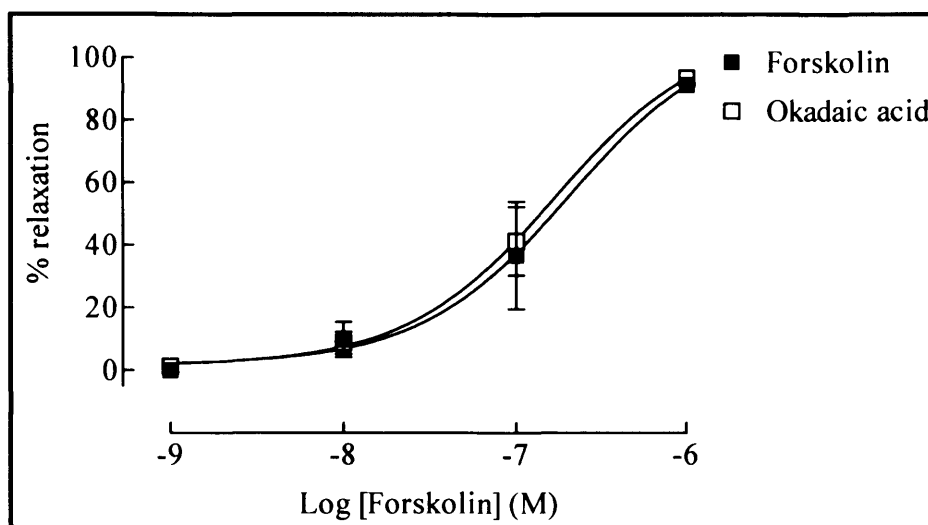


Figure 5.16 Concentration-response curves to (A) ANP (0.01nM-0.1 μ M) following incubation with vehicle, LPS (0.3 μ g/ml; 4hr), okadaic acid (300nM; 30 mins) or LPS plus okadaic acid ($n=4$); (B) SPER-NO (1nM-10 μ M; $n=4$) and (C) forskolin (1nM-1 μ M; $n=4$) following 30 mins incubation with vehicle or okadaic acid (300nM). Relaxation is expressed as the percentage reversal of the U46619-induced tone. Each point represents mean \pm SEM.

5.3.17 Effect of LPS on pGC-mediated relaxation in the presence of cantharidic acid

Rat aortic rings treated with LPS (0.3 μ g/ml) for 4 hrs showed significant reduction in the potency of ANP (pEC₅₀: 8.87 \pm 0.22 versus 8.01 \pm 0.41 in the absence and presence of LPS, respectively; $n=5$; $P<0.05$; BC). Co-incubation with the PP2A inhibitor, cantharidic acid (500nM; 30min) had no effect on the relaxations to ANP in the presence of LPS (pEC₅₀: 7.89 \pm 0.26 in the presence of cantharidic acid; $n=4$; $P>0.05$ versus LPS alone; Figure 5.17). Cantharidic acid alone had no effect on the

relaxation to ANP (pEC_{50} : 8.72 ± 0.41 in the presence of cantharidic acid; $n=4$; $P>0.05$ versus control). Curves were compared by TW-ANOVA.

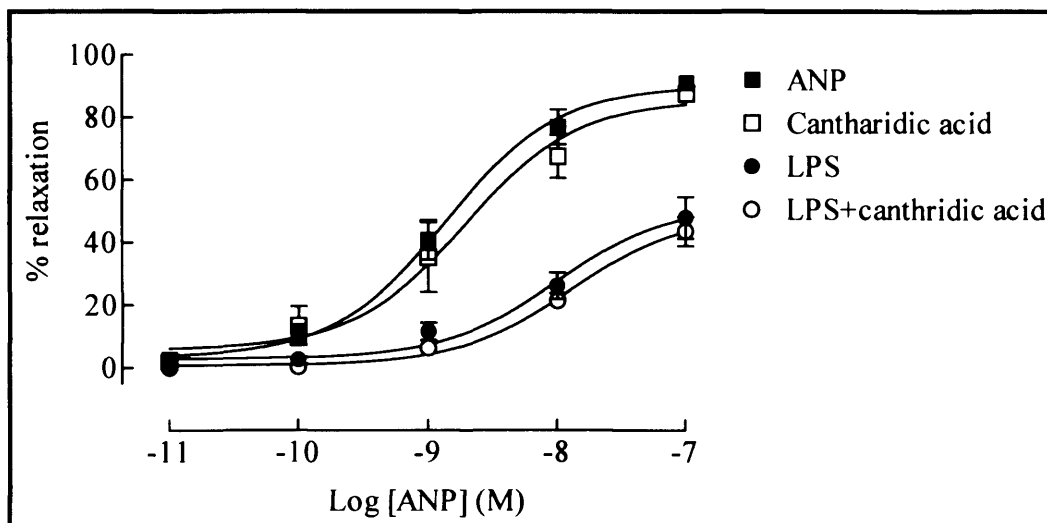


Figure 5.17 Concentration-response curves to ANP ($0.01nM$ - $0.1\mu M$) following incubation with vehicle, LPS ($0.3\mu g/ml$; 4 hrs), cantharidic acid ($500nM$; 30 mins) or LPS plus cantharidic acid; $n=4$. Relaxation is expressed as the percentage reversal of the U46619-induced tone. Each point represents mean \pm SEM.

5.4 DISCUSSION

In this chapter, I have investigated mechanisms that might be involved in the desensitisation of the GC-cGMP pathway in LPS-treated vessels. The results obtained from this study demonstrate that the mechanism of iNOS-induced desensitisation of the GC-cGMP pathway does not involve activation of the phosphodiesterases PDE5, PDE1A1 and PDE3. It also suggests that the desensitisation is not explained solely by increased activity of PKC or PP2A. Moreover, it demonstrates that the reduced response to NO-donors is not mediated by the production of free radicals leading to a reduction in NO bioavailability.

5.4.1 Phosphodiesterases

Degradation of cGMP is tightly controlled by PDEs. These enzymes are abundant in various tissues including vascular smooth muscle. PDE5 is the most highly expressed cGMP-hydrolyzing isoform in VSMC with high specificity for cGMP (Rybalkin *et al.*, 2003). The physiological importance of PDE5 in the regulation of vascular tone in human and animal has been demonstrated most clearly by the use of the selective inhibitor, sildenafil (Wallis *et al.*, 1999; Sharabi *et al.*, 2005). The finding that inhibition of PDE activities restored GTN-induced reduction in the response of rat model of tolerance to further treatment of GTN (Pagani *et al.*, 1993; De Garavilla *et al.*, 1996) prompted me to investigate whether PDE5 is involved in the mechanism of desensitisation of sGC and pGC, as upregulation of PDE5 would lead to reduction in the activity of both GC signalling pathways. However, there does not seem to be a role for increased activity of PDE5 in the desensitisation, because sildenafil (at a concentration that reduced contraction to U46619 and shifted concentration-response curves for at least SPER-NO to the left suggesting efficient inhibition of PDE5) had no effect on the response to SPER-NO and ANP in LPS-treated tissues. Sildenafil enhanced relaxations to SPER-NO but not ANP; this raises the possibility of a specific subcellular localisation of PDE5 that enables the enzyme to metabolise sGC-, but not pGC-, generated cGMP.

In the vasculature, PDE1A1 is present in VSMC (Sonnenburg *et al.*, 1998). Moreover, it appeared that PDE1A1 activity is important for the regulation of vascular smooth muscle cGMP levels and reactivity because PDE1A1 activity, mRNA and protein levels are selectively upregulated following nitrate tolerance in the rat (Kim *et al.*, 2001). These observations encouraged me to examine the possible involvement of PDE1A1 in the mechanism of desensitisation induced by LPS. However, vinpocetine (Hagiwara *et al.*, 1984) did not restore LPS-induced desensitisation of SPER-NO and ANP suggesting that upregulation of PDE1A1 activity is not involved in the mechanism of desensitisation of the sGC-cGMP and pGC-cGMP pathways.

PDE3 is one of the major PDEs that is present in VSMC. Although PDE3 is considered to hydrolyse cAMP preferentially, it is also able to breakdown cGMP (Beavo, 1995). In order to examine whether upregulation of PDE3 might underlie the mechanism of desensitisation of the sGC-cGMP and pGC-cGMP pathways, LPS-treated tissues were incubated with milrinone. However, PDE3 does not seem to play a role in the desensitisation mediated by LPS because milrinone (at a concentration that reduced contraction to U46619- suggesting efficient increased production of cGMP and/or cAMP and inhibition of PDE3) did not restore relaxation to SPER-NO and ANP. The inability of milrinone to enhance relaxation to SPER-NO and ANP may suggest that PDE3 is less effective in metabolizing cGMP compared to cAMP. In summary, these observations suggest that PDE5, PDE1A1 and PDE3 are unlikely responsible for the desensitisation of GC-cGMP induced by LPS.

5.4.2 Protein kinase C

Several PKC isoforms have been reported to exist in VSMC including the conventional-PKC isoforms (α and β), the novel-PKC isoforms (ϵ , η , θ , δ and μ) and the atypical (ζ and λ) (Yano *et al.*, 1999; Itoh *et al.*, 2001; Salamanca & Khalil, 2005). Precontraction of rat aortic rings with the PKC activators, PMA (which activates both the conventional and the novel-PKC isoforms) or the more selective

5.4 DISCUSSION

In this chapter, I have investigated mechanisms that might be involved in the desensitisation of the GC-cGMP pathway in LPS-treated vessels. The results obtained from this study demonstrate that the mechanism of iNOS-induced desensitisation of the GC-cGMP pathway does not involve activation of the phosphodiesterases PDE5, PDE1A1 and PDE3. It also suggests that the desensitisation is not explained solely by increased activity of PKC or PP2A. Moreover, it demonstrates that the reduced response to NO-donors is not mediated by the production of free radicals leading to a reduction in NO bioavailability.

5.4.1 Phosphodiesterases

Degradation of cGMP is tightly controlled by PDEs. These enzymes are abundant in various tissues including vascular smooth muscle. PDE5 is the most highly expressed cGMP-hydrolyzing isoform in VSMC with high specificity for cGMP (Rybalkin *et al.*, 2003). The physiological importance of PDE5 in the regulation of vascular tone in human and animal has been demonstrated most clearly by the use of the selective inhibitor, sildenafil (Wallis *et al.*, 1999; Sharabi *et al.*, 2005). The finding that inhibition of PDE activities restored GTN-induced reduction in the response of rat model of tolerance to further treatment of GTN (Pagani *et al.*, 1993; De Garavilla *et al.*, 1996) prompted me to investigate whether PDE5 is involved in the mechanism of desensitisation of sGC and pGC, as upregulation of PDE5 would lead to reduction in the activity of both GC signalling pathways. However, there does not seem to be a role for increased activity of PDE5 in the desensitisation, because sildenafil (at a concentration that reduced contraction to U46619 and shifted concentration-response curves for at least SPER-NO to the left suggesting efficient inhibition of PDE5) had no effect on the response to SPER-NO and ANP in LPS-treated tissues. Sildenafil enhanced relaxations to SPER-NO but not ANP; this raises the possibility of a specific subcellular localisation of PDE5 that enables the enzyme to metabolise sGC-, but not pGC-, generated cGMP.

In the vasculature, PDE1A1 is present in VSMC (Sonnenburg *et al.*, 1998). Moreover, it appeared that PDE1A1 activity is important for the regulation of vascular smooth muscle cGMP levels and reactivity because PDE1A1 activity, mRNA and protein levels are selectively upregulated following nitrate tolerance in the rat (Kim *et al.*, 2001). These observations encouraged me to examine the possible involvement of PDE1A1 in the mechanism of desensitisation induced by LPS. However, vinpocetine (Hagiwara *et al.*, 1984) did not restore LPS-induced desensitisation of SPER-NO and ANP suggesting that upregulation of PDE1A1 activity is not involved in the mechanism of desensitisation of the sGC-cGMP and pGC-cGMP pathways.

PDE3 is one of the major PDEs that is present in VSMC. Although PDE3 is considered to hydrolyse cAMP preferentially, it is also able to breakdown cGMP (Beavo, 1995). In order to examine whether upregulation of PDE3 might underlie the mechanism of desensitisation of the sGC-cGMP and pGC-cGMP pathways, LPS-treated tissues were incubated with milrinone. However, PDE3 does not seem to play a role in the desensitisation mediated by LPS because milrinone (at a concentration that reduced contraction to U46619- suggesting efficient increased production of cGMP and/or cAMP and inhibition of PDE3) did not restore relaxation to SPER-NO and ANP. The inability of milrinone to enhance relaxation to SPER-NO and ANP may suggest that PDE3 is less effective in metabolizing cGMP compared to cAMP. In summary, these observations suggest that PDE5, PDE1A1 and PDE3 are unlikely responsible for the desensitisation of GC-cGMP induced by LPS.

5.4.2 Protein kinase C

Several PKC isoforms have been reported to exist in VSMC including the conventional-PKC isoforms (α and β), the novel-PKC isoforms (ϵ , η , θ , δ and μ) and the atypical (ζ and λ) (Yano *et al.*, 1999; Itoh *et al.*, 2001; Salamanca & Khalil, 2005). Precontraction of rat aortic rings with the PKC activators, PMA (which activates both the conventional and the novel-PKC isoforms) or the more selective

PKC activator, thymeleatoxin (which activates only the conventional-PKC isoforms) reduced the responsiveness of rat aorta to sGC (ACh and SPER-NO), pGC (ANP) and AC (forskolin) activators, suggesting that PKC activity desensitises both GC and AC signalling pathways. Since the observation that iNOS-induced desensitisation is specific to the cGMP pathway, and that PKC activators desensitised both GC and AC-dependent signalling, it is unlikely that the mechanism of desensitisation is mediated solely by up-regulation of PKC in the LPS-treated vessels (as if it was mediated by PKC, then the responsiveness to forskolin in LPS-treated vessels would have been also reduced).

It is not clear which PKC isozymes cause desensitisation of GC and AC signalling pathways in the vasculature. The specific effect of thymeleatoxin suggests that one or both of the thymeleatoxin-activated PKC isozymes (α and β ; both are expressed in VSMC) are more likely to underlie the desensitisation of GC and AC. The effect of PMA on sGC and AC is consistent with Kamata *et al.*, who showed that in PMA-precontracted mesenteric vessels, responses to both SNP and forskolin were reduced (Kamata *et al.*, 1995). The effect of PMA on the cell permeable cGMP analogue, 8-Br-cGMP, suggests that the cGMP down-stream pathway is also desensitised. This study also provides functional data on the role of PKC on responses to ANP, which is in accord with the observed role of PKC on the phosphorylation status of the ANP receptor in cultured VSMC (Yasunari *et al.*, 1992). The mechanism by which PKC attenuates ANP responses is thought to occur as a result of dephosphorylation of ANP receptor (Potter & Garbers., 1994). Whether PKC causes phosphorylation-mediated inhibition of (so far unknown) a protein kinase that (normally) phosphorylates ANP receptor, or causes phosphorylation-mediated activation of a protein phosphatase (possibly PP2A) that ultimately dephosphorylates the receptor, is unknown.

Unlike PKC-mediated contraction, K^+ at higher concentrations causes depolarisation of VSMC leading to influx of Ca^{2+} through voltage-gated channels (Ratz *et al.*, 2005). Thus, the reduced vasorelaxant potency of GC and

5.4.4 Role of superoxide

It has been reported that endotoxin treatment may be associated with O_2^- production in the vasculature (Javesghani *et al.*, 2003). Moreover, tolerance and cross-tolerance to NO-donors may result from increased O_2^- production (Munzel *et al.*, 1995) since O_2^- is known to inactivate NO (Gryglewski *et al.*, 1986). SOD is an important determinant of NO bioavailability in blood vessels through its ability to dismutate O_2^- (Munzel *et al.*, 1995; Fukai *et al.*, 2002). To examine the role of O_2^- in the reduced responsiveness to ACh and SPER-NO in LPS-treated tissues, vessels were incubated with SOD. The results demonstrate that SOD does not restore the relaxation to ACh or SPER-NO, suggesting that the reduced responsiveness to these agents is not mediated by reduced bioactivity of NO as a result of increased production of O_2^- . However, although SOD was added in excess (2000U/ml), it is possible that SOD did not cause an effect due to difficulty in penetrating cell membranes.

5.4.5 Myeloperoxidase

Acute inflammation has been associated with an increase in the activity of MPO, which itself has been reported to modulate vascular signalling and vasodilatory functions of NO, either by direct consumption of NO or via MPO-derived substrate radicals (Eiserich *et al.*, 2002) leading to a reduction in NO bioavailability. Moreover, the effect of MPO could result from its ability to up-regulate the catalytic activity of iNOS by preventing NO feedback inhibition (Galijasevic *et al.*, 2003), thereby increasing iNOS-dependent desensitisation of GC. In order to examine whether MPO is involved in the reduced responsiveness of vascular tissue to SPER-NO, LPS-treated tissues were co-incubated with the MPO inhibitor, ABAH. ABAH did not restore relaxation to SPER-NO suggesting that reduced responses to the NO-donor are not mediated by consumption of NO by MPO or by MPO-generated free radicals. However, it is possible that MPO expression by vascular cells is not occurring and its availability is entirely dependent on expression by immune cells which are not present in this *in vitro* model.

5.4.6 Summary

In summary, this chapter attempted to investigate mechanisms that might be involved in the iNOS-induced desensitisation of sGC and pGC, by using pharmacological tools to probe the roles of PDEs (type 1A1, 3 and 5), PP2A, SOD and MPO, each of which has been shown to modulate cGMP activity. However, none of these pathways appears to be involved in desensitisation of the sGC and pGC-cGMP signalling pathways by iNOS-derived NO. PKC activation mimics to a degree the effect of LPS, but the vascular phenotype also include cAMP dilator dysfunction, which is not a component of that induced by LPS.

6. Summary

This thesis describes studies to investigate the regulation of guanylate cyclases pathways in blood vessels. This thesis attempted to answer three main questions:

1. What is the relative contribution of enzymatic and non-enzymatic mechanisms in the biotransformation of *S*-nitrosothiols in blood vessels?
2. What is the effect of LPS on the sensitivity of sGC and pGC-cGMP pathway?
3. What is the mechanism(s) that mediate the desensitisation of sGC and pGC by LPS?

6.1 Enzymatic or non-enzymatic?

In this study, I investigated the responsiveness of isolated rat aorta to stereoisomers of the endogenous, GSNO and CYSNO, and the exogenous *S*-nitrosothiols, SNAP to determine whether the biotransformation of *S*-nitrosothiols involves enzyme-dependent mechanism. I have also investigated the effect of free copper ions as a control for non-stereospecific effect, and the copper-containing enzyme, Cu/Zn SOD, on the stereoisomers of GSNO and SNAP. By using the colorimetric assay of Saville and the organ bath pharmacology, I demonstrated that in isolated rat aorta, there were no stereospecific vasorelaxant effects of *S*-nitrosothiols, consistent with non-enzymatic release of NO. Cu(I)-dependent mechanisms play an important role in the biotransformation of *S*-nitrosothiols by blood vessels.

The use of a novel water soluble derivative of Cu(I) complex, Cu(I)-acetonitrile and the selective Cu(I) chelator, BCS, gave a direct insight into the role of Cu(I) in the decomposition of *S*-nitrosothiols. This supported previous findings, in which Cu(I) but not Cu(II) is the active catalyst that cause the decomposition. *S*-nitrosothiols decomposed differently to copper ions with a ranking order of stability: GSNO > SNAP > CYSNO.

Data from individual enzyme, Cu/Zn SOD to whole tissue, rat aorta, suggest that *S*-nitrosothiols are metabolised non-stereospecifically. This non-stereospecificity

to *S*-nitrosothiols may be important physiologically. It suggests that access to endogenously stored or exogenously applied NO is easy due to the availability of various intracellular and extracellular copper-containing enzymes and any abnormality in the availability or functionality of one enzyme may be substituted by the many other copper-containing enzymes or proteins.

As discussed earlier, NO is an important vasodilator, anti-atherogenic, anti-proliferative, and anti-apoptotic agent. Therefore disturbance in NO bioavailability would lead to cardiovascular abnormalities. Indeed, a strong relationship between copper-deficiency and ischemic heart disease has been reported (Klevay, 2000). Increased aortic lesion areas and elevated serum cholesterol were found in animals fed with a copper-deficient diet, compared with the copper-adequate group (Hamilton *et al.*, 2000). Rats fed a copper-deficient diet developed a defect in NO-mediated dilatation an observation which supports the physiological relevance of this thesis (Schuschke *et al.*, 1992). Inhibition of Cu/Zn-SOD as a result of copper deficiency may increase the concentration of vascular superoxide. High level of superoxide is associated with various cardiovascular disorders such as hypertension, atherosclerosis, and diabetic vascular disease due to its ability to reduce NO bioavailability (Nedeljkovic *et al.*, 2003; Uriu-Adams *et al.*, 2005). In contrast, increased copper bioavailability that occurs in Wilson's disease, copper poisoning (Uriu-Adams *et al.*, 2005), and cystic fibrosis (Percival *et al.*, 1999) may lead to increased consumption of *S*-nitrosothiols and subsequently depletion of endogenous NO stores (Grasemann *et al.*, 1999). Therefore, the effect of copper ions on the bioavailability of NO from its endogenous stores might provide a link between copper ion bioavailability and cardiovascular diseases.

This thesis also demonstrates a possible role of Cu(I) ions in the regulation of vascular tone through its ability to activate eNOS. The exact mechanism by which eNOS is activated by Cu(I) is unknown. Previous reports demonstrated that Cu(II) activates eNOS (Demura *et al.*, 1998a), may be mediated by intracellular Ca^{2+} mobilisation (Demura *et al.*, 1998b). It is possible that Cu(II) is reduced by

endogenous thiols to Cu(I), which subsequently cause eNOS activation. However, further investigation is required to explore this mechanism. The role of Cu(I) on eNOS, further provides a strong link between copper ions and NO biology.

6.2 Feedback regulatory mechanism

The sensitivity of sGC to NO and pGC to ANP regulates vasodilatation in response to these mediators. To determine the role of endogenous NO as a feedback regulator of both sGC and pGC, rat aorta was incubated *in vitro* with LPS to stimulate production of high output NO as an *in vitro* model of sepsis. This thesis demonstrated that induction of iNOS by LPS (confirmed by western blotting) reduces the sensitivity of both sGC- and pGC-mediated relaxation. This desensitisation was blocked by specific iNOS inhibition, consistent with iNOS-derived NO down-regulating both pathways. The desensitisation is specific for cGMP signalling, and is mediated at least in part by cGMP generation, because inhibition of NO-mediated cGMP synthesis with ODQ partially restores sensitivity to ANP. Moreover, the observed desensitisation is rapidly reversible, consistent with a mechanism dependent on altered activity of constitutive pathways rather than expression of new protein. The reduced sensitivity to 8-Br-cGMP implicates down-regulation of one or more downstream pathways.

To conclude, alteration in the responsiveness to endogenous NO and ANP is an important negative feedback mechanism within the vasculature that is likely to play an important role in the regulation of vascular tone and blood flow. During inflammatory episodes such as in sepsis, this physiological mechanism might offset the systemic hypotension by causing vasoconstriction. Therapeutically, this desensitisation has implications for the development of tolerance to NO or GC activators administered as therapy for treatment for certain cardiovascular diseases emphasising that tolerance is a likely consequence of any vasodilator that is cGMP-mediated.

Extending this work to study the relationship between the two guanylate cyclase pathways *in vivo* particularly in human is now required. This *de novo* work will provide insight as to whether this regulatory mechanism is important in human health and disease.

6.3 What is causing the desensitisation?

In chapter five, I investigated possible mechanism(s) that might be involved in the desensitisation of GC-cGMP pathway in LPS-treated vessels. Pharmacological tools were used to investigate the roles of phosphodiesterases (type 1A1, 3 and 5), protein kinase C, protein phosphatase 2A, superoxide dismutase, and myeloperoxidase, each of which has been shown to modulate cGMP activity.

The results obtained from this study demonstrate that the mechanism of desensitisation of GC-cGMP pathway does not involve activation of the phosphodiesterases PDE5, since the selective inhibitor of PDE5, sildenafil did not restore the desensitisation to SPER-NO and ANP. Similarly, vinpocetine and milrinone, the inhibitors of PDE1A1 and PDE3 respectively, did not restore relaxation to SPER-NO and ANP in LPS treated tissues, ruling out the role of PDE1A1 and PDE3 in the mechanism of desensitisation.

The data obtained from this study reveal an important role for PKC in the desensitisation of both GC and AC signalling pathways. However, since the sensitivity of AC signalling pathway is intact in the LPS-treated tissue, but reduced under conditions of high PKC activity, this suggests that upregulation of PKC activity may not be responsible for the desensitisation of the GC-cGMP pathway following LPS treatment. Moreover, the data indicate that PKC- α and/or - β isoforms are likely responsible for the desensitisation. Since PKC normally phosphorylates enzymes while the mechanism of pGC desensitisation by PKC is thought to occur through dephosphorylation (Potter & Garbers, 1994), further work is required to explore the

signalling cascade involved in the PKC-mediated desensitisation leading to dephosphorylation of pGC.

Given the important role of sGC- and pGC-cGMP signalling pathways (as described in sections 1.1.7 and 1.2.3) in the regulation of cardiovascular physiology, their desensitisation by PKC might have important implications in the pathophysiology of cardiovascular disease. Indeed, increased PKC expression/activity has been suggested to play an important role in the elevation of blood pressure. PKC- α enhances Ca^{2+} -dependent VSMC contraction, and its overexpression has been implicated in the pathogenesis of hypertension (Salamanca & Khalil, 2005). Imbalance between NO-cGMP and PKC system has also been suggested to cause cerebral vasospasm (Laher & Zhang, 2001). Diabetes is commonly associated with abnormal vascular function. Increases in PKC specific activity in the membranous fraction induced by hyperglycemia have been reported in retina, aorta, heart, monocytes and glomeruli from animals and humans with diabetes (Way *et al.*, 2001). Preferential activation of the PKC- β isoform by elevated glucose is reported to occur in a variety of vascular tissues (Way *et al.*, 2001). In this thesis I demonstrated that PKC- α and/or - β cause desensitisation of GC and AC. If it was mediated by PKC- β , then this would be expected to cause abnormal GC and AC signalling in diabetic patients and causing further complications in this disease. Increased PKC activity is also associated with cardiac myocyte hypertrophy (Gu & Bishop, 1994) and heart failure (Bowling *et al.*, 1999).

This study also demonstrates that desensitisation of pGC by LPS is not mediated by increased activity of PP2A because the selective PP2A inhibitors, okadaic acid and cantharidic acid did not restore the sensitivity of ANP-mediated relaxation in LPS treated tissue. The reduced responses to NO donors is not mediated by scavenging of NO by superoxide or by free radicals generated by myeloperoxidase since superoxide dismutase or ABAH respectively did not restore relaxation to ACh and SPER-NO.

This thesis does not directly exclude the possibility of depletion of GC substrate (i.e GTP) that might occur through excessive utilisation as a result of continuous activation of GC by iNOS-induced NO in LPS treated tissues. However, since GTP is involved in so many cellular functions, one would expect that depletion of GTP would affect cellular function globally therefore making this potential mechanism unlikely.

To sum up, upregulation of PDE1A1, PDE3, PDE5, PKC and PP2A, or increased superoxide bioavailability or depletion of GTP are unlikely to be the mechanisms of desensitisation of sGC and pGC-cGMP by iNOS-derived NO. PKC desensitises both GC and AC signalling pathway, where PKC- α and/or - β isoforms are likely to mediate the desensitisation.

6.4 Future studies

In Chapter Three I showed that rat aorta decomposed *S*-nitrosothiols by a Cu(I)-dependent mechanism. However, whether the biotransformation of *S*-nitrosothiols occurred by the endothelial cells, VSMC or both remains uncertain. It is of interest to examine the relative contribution of endothelial versus VSMC in the Cu(I)-dependent decomposition of *S*-nitrosothiols. This study can be done by examining the decomposition of *S*-nitrosothiols by rat aorta in the presence and absence of endothelial cells. It is also of interest to examine the relative contribution of membranous versus cytosolic Cu(I) ions in the biotransformation of *S*-nitrosothiols. This study can be done by measuring the amount of NO release from *S*-nitrosothiols following exposure to membranes or cytosolic preparations.

In section 3.4.6 I showed that Cu(I) did not produce *S*-nitrosothiol-dependent relaxation. However, since *S*-nitrosothiols are light sensitive substances (Megson *et al.*, 2000a; Chauhan *et al.*, 2003b), it is possible that exposure of rat aorta in the organ bath to the ambient light for several hours before performing the concentration-

response curve to Cu(I) has depleted endogenously stored *S*-nitrosothiols. Further work in light protected preparations is required to confirm this study.

Another potential mechanism possibly causing the desensitisation of sGC and pGC-cGMP by iNOS-derived NO worth studying is the role of PKG. This study can be done either by pharmacological inhibition of PKG by using selective PKG inhibitor such as Rp-8-Br-PET-cGMPS, or by examining this mechanism in PKG knockout mice. However, it is important to note that such studies are likely to be complicated by the fact that PKG is responsible for mediating the relaxation to sGC and/or pGC activators. However, it is possible that a residual relaxation will remain to enable potential study of the mechanism of desensitisation.

It remains possible that an increase in the production of carbon monoxide (CO), which can activate sGC, by the inducible haem-oxygenase-1 (HO-1) could contribute to desensitisation of the GC-cGMP pathway. However, despite its poor purified-sGC activating ability (Stone & Marletta, 1994; Friebe *et al.*, 1996), one major problem of studying the effect of inhibition of HO-1, is that the most widely used inhibitors (zinc protoporphyrin IX, tin protoporphyrin IX and chromium mesoporphyrin) of this enzyme are known to produce HO-1-independent effects, by interfering with other pathways such as iNOS, sGC and ANP-mediated relaxation (Meffert *et al.*, 1994; Serfass & Burstyn *et al.*, 1998; Ny *et al.*, 1995; Jozkowicz & Dulak, 2003). Thus, the use of these inhibitors is not suitable. Therefore, synthesis of selective inhibitors for HO-1 is required for future work to explore the capacity of CO in causing desensitisation of GC-cGMP in sepsis. Alternatively, this study can be examined by stimulating sGC by CO-releasing molecules such as CORM-A1 and CORM-3 and observing their effects on the sensitivity of GC-cGMP pathway.

In contrast to septic shock, the physiological relationship between sGC- and pGC-cGMP pathways need to be further explored in disease states associated with reduced NO bioavailability. Diabetes mellitus, for instance, is commonly associated with endothelial dysfunction (Pieper & Peltier, 1995; Xiong *et al.*, 2003; Witte *et al.*,

2002; McNeill *et al.*, 2000). Further work is required to investigate the thesis that decreased production or activity of NO-sGC in diabetes might lead to an enhanced sensitivity of NPs-pGC to compensate for the reduced activity of the NO-cGMP pathway in this disease state. However, since PKC activity might be increased in diabetes mellitus (Way *et al.*, 2001), it is also important to investigate whether an increase in the activity of PKC might lead to a down-regulation of both pathways. This work can be done on vessels from animal model of type 1 diabetes mellitus such as streptozotocin-induced diabetes or on animal model of type 2 diabetes mellitus such as Goto-Kakizaki rat.

Contribution to this work

DL-, D-SNAP, L- and D-GSH was synthesised by Medicinal Chemistry Department, Wolfson Institute for Biomedical Research, University College London.

Reference List

Abassi ZA, Powell JR, Golomb E, & Keiser HR (1992). Renal and systemic effects of urodilatin in rats with high-output heart failure. *Am J Physiol* **262**, F615-F621.

Abu-Soud HM & Stuehr DJ (1993). Nitric oxide synthases reveal a role for calmodulin in controlling electron transfer. *Proc Natl Acad Sci U S A* **90**, 10769-10772.

Abu-Soud HM, Yoho LL, & Stuehr DJ (1994). Calmodulin controls neuronal nitric-oxide synthase by a dual mechanism. Activation of intra- and interdomain electron transfer. *J Biol Chem* **269**, 32047-32050.

Abu-Soud HM & Hazen SL (2000). Nitric oxide is a physiological substrate for mammalian peroxidases. *J Biol Chem* **275**, 37524-37532.

Ahluwalia A, MacAllister RJ, & Hobbs AJ (2004a). Vascular actions of natriuretic peptides. Cyclic GMP-dependent and -independent mechanisms. *Basic Res Cardiol* **99**, 83-89.

Ahluwalia A, Foster P, Scotland RS, McLean PG, Mathur A, Perretti M, Moncada S, & Hobbs AJ (2004b). Antiinflammatory activity of soluble guanylate cyclase: cGMP-dependent down-regulation of P-selectin expression and leukocyte recruitment. *Proc Natl Acad Sci U S A* **101**, 1386-1391.

Akhter S, Vignini A, Wen Z, English A, Wang PG, & Mutus B (2002). Evidence for S-nitrosothiol-dependent changes in fibrinogen that do not involve transnitrosation or thiolation. *Proc Natl Acad Sci U S A* **99**, 9172-9177.

Al-Sa'doni HH, Megson IL, Bisland S, Butler AR & Flitney FW (1997). Neocuproine, a selective Cu(I) chelator, and the relaxation of rat vascular smooth muscle by S-nitrosothiols. *Br J Pharmacol* **121**, 1047-1050.

Angus JA & Wright CE (2000). Techniques to study the pharmacodynamics of isolated large and small blood vessels. *J Pharmacol Toxicol Methods* **44**, 395-407.

Antos LK, Abbey-Hosch SE, Flora DR, & Potter LR (2005). ATP-independent activation of natriuretic peptide receptors. *J Biol Chem* **280**, 26928-26932.

Arakawa N, Nakamura M, Aoki H, & Hiramori K (1994). Relationship between plasma level of brain natriuretic peptide and myocardial infarct size. *Cardiology* **85**, 334-340.

Armstrong S & Ganote CE (1994). Preconditioning of isolated rabbit cardiomyocytes: effects of glycolytic blockade, phorbol esters, and ischaemia. *Cardiovasc Res* **28**, 1700-1706.

Askew SC, Barnett DJ, McAninly J & Williams DL (1995). Catalysis by nitric oxide release from S-nitrosothiols (RSNO) *J Chem. Soc. Perkin Trans 2*, 741-745.

Atlas SA, Kleinert HD, Camargo MJ, Januszewicz A, Sealey JE, Laragh JH, Schilling JW, Lewicki JA, Johnson LK, & Maack T (1984). Purification, sequencing and synthesis of natriuretic and vasoactive rat atrial peptide. *Nature* **309**, 717-719.

Ballard SA, Gingell CJ, Tang K, Turner LA, Price ME, & Naylor AM (1998). Effects of sildenafil on the relaxation of human corpus cavernosum tissue in vitro and on the activities of cyclic nucleotide phosphodiesterase isozymes. *J Urol* **159**, 2164-2171.

Batenburg WW, de Vries R, Saxena PR, & Danser AH (2004). L-S-nitrosothiols: endothelium-derived hyperpolarizing factors in porcine coronary arteries? *J Hypertens* **22**, 1927-1936.

Bauer JA & Fung HL (1991). Differential hemodynamic effects and tolerance properties of nitroglycerin and an S-nitrosothiol in experimental heart failure. *J Pharmacol Exp Ther* **256**, 249-254.

Bauer PM, Buga GM, Fukuto JM, Pegg AE, & Ignarro LJ (2001). Nitric oxide inhibits ornithine decarboxylase via S-nitrosylation of cysteine 360 in the active site of the enzyme. *J Biol Chem* **276**, 34458-34464.

Beavo JA (1995). Cyclic nucleotide phosphodiesterases: functional implications of multiple isoforms. *Physiol Rev* **75**, 725-748.

Bialojan C & Takai A (1988). Inhibitory effect of a marine-sponge toxin, okadaic acid, on protein phosphatases. Specificity and kinetics. *Biochem J* **256**, 283-290.

Bogle RG, McLean PG, Ahluwalia A, & Vallance P (2000). Impaired vascular sensitivity to nitric oxide in the coronary microvasculature after endotoxaemia. *Br J Pharmacol* **130**, 118-124.

Bolad I & Delafontaine P (2005). Endothelial dysfunction: its role in hypertensive coronary disease. *Curr Opin Cardiol* **20**, 270-274.

Bouchie JL, Hansen H, & Feener EP (1998). Natriuretic factors and nitric oxide suppress plasminogen activator inhibitor-1 expression in vascular smooth muscle cells. Role of cGMP in the regulation of the plasminogen system. *Arterioscler Thromb Vasc Biol* **18**, 1771-1779.

Bouloumie A, Bauersachs J, Linz W, Scholkens BA, Wiemer G, Fleming I, & Busse R (1997). Endothelial dysfunction coincides with an enhanced nitric oxide synthase expression and superoxide anion production. *Hypertension* **30**, 934-941.

Boutin JA (1997). Myristoylation. *Cell Signal* **9**, 15-35.

Bowling N, Walsh RA, Song G, Estridge T, Sandusky GE, Fouts RL, Mintze K, Pickard T, Roden R, Bristow MR, Sabbah HN, Mizrahi JL, Gromo G, King GL, & Vlahos CJ (1999). Increased protein kinase C activity and expression of Ca²⁺-sensitive isoforms in the failing human heart. *Circulation* **99**, 384-391.

Bredt DS & Snyder SH (1994). Transient nitric oxide synthase neurons in embryonic cerebral cortical plate, sensory ganglia, and olfactory epithelium. *Neuron* **13**, 301-313.

Brunner F (1997). Interaction of nitric oxide and endothelin-1 in ischemia/reperfusion injury of rat heart. *J Mol Cell Cardiol* **29**, 2363-2374.

Buechler WA, Nakane M, & Murad F (1991). Expression of soluble guanylate cyclase activity requires both enzyme subunits. *Biochem Biophys Res Commun* **174**, 351-357.

Buffoni F & Ignesti G (2000). The copper-containing amine oxidases: biochemical aspects and functional role. *Mol Genet Metab* **71**, 559-564.

Busse R & Mulsch A (1990). Induction of nitric oxide synthase by cytokines in vascular smooth muscle cells. *FEBS Lett* **275**, 87-90.

Busse R, Edwards G, Feletou M, Fleming I, Vanhoutte PM, & Weston AH (2002). EDHF: bringing the concepts together. *Trends Pharmacol Sci* **23**, 374-380.

Campbell DJ, Mitchelhill KI, Schlicht SM, & Booth RJ (2000). Plasma amino-terminal pro-brain natriuretic peptide: a novel approach to the diagnosis of cardiac dysfunction. *J Card Fail* **6**, 130-139.

Carvajal JA, Germain AM, Huidobro-Toro JP, & Weiner CP (2000). Molecular mechanism of cGMP-mediated smooth muscle relaxation. *J Cell Physiol* **184**, 409-420.

Catani MV, Bernassola F, Rossi A, & Melino G (1998). Inhibition of clotting factor XIII activity by nitric oxide. *Biochem Biophys Res Commun* **249**, 275-278.

Cavero M, Hobbs A, Madge D, Motherwell WB, Selwood D, & Potier P (2000). Synthesis and biological evaluation of enantiopure thionitrites: the solid-phase synthesis and nitrosation of D-glutathione as a molecular probe. *Bioorg Med Chem Lett* **10**, 641-644.

Charakida M, Deanfield JE, & Halcox JP (2006). The role of nitric oxide in early atherosclerosis. *Eur J Clin Pharmacol* **62 Suppl 13**, 69-78.

Chauhan SD, Nilsson H, Ahluwalia A, & Hobbs AJ (2003a). Release of C-type natriuretic peptide accounts for the biological activity of endothelium-derived hyperpolarizing factor. *Proc Natl Acad Sci U S A* **100**, 1426-1431.

Chauhan S, Rahman A, Nilsson H, Clapp L, MacAllister R, & Ahluwalia A (2003b). NO contributes to EDHF-like responses in rat small arteries: a role for NO stores. *Cardiovasc Res* **57**, 207-216.

Chauhan SD, Seggara G, Vo PA, MacAllister RJ, Hobbs AJ, & Ahluwalia A (2003c). Protection against lipopolysaccharide-induced endothelial dysfunction in resistance and conduit vasculature of iNOS knockout mice. *FASEB J* **17**, 773-775.

Chen HH & Burnett JC, Jr. (1998). C-type natriuretic peptide: the endothelial component of the natriuretic peptide system. *J Cardiovasc Pharmacol* **32 Suppl 3**, S22-S28.

Busse R, Edwards G, Feletou M, Fleming I, Vanhoutte PM, & Weston AH (2002). EDHF: bringing the concepts together. *Trends Pharmacol Sci* **23**, 374-380.

Campbell DJ, Mitchelhill KI, Schlicht SM, & Booth RJ (2000). Plasma amino-terminal pro-brain natriuretic peptide: a novel approach to the diagnosis of cardiac dysfunction. *J Card Fail* **6**, 130-139.

Carvajal JA, Germain AM, Huidobro-Toro JP, & Weiner CP (2000). Molecular mechanism of cGMP-mediated smooth muscle relaxation. *J Cell Physiol* **184**, 409-420.

Catani MV, Bernassola F, Rossi A, & Melino G (1998). Inhibition of clotting factor XIII activity by nitric oxide. *Biochem Biophys Res Commun* **249**, 275-278.

Cavero M, Hobbs A, Madge D, Motherwell WB, Selwood D, & Potier P (2000). Synthesis and biological evaluation of enantiopure thionitrites: the solid-phase synthesis and nitrosation of D-glutathione as a molecular probe. *Bioorg Med Chem Lett* **10**, 641-644.

Charakida M, Deanfield JE, & Halcox JP (2006). The role of nitric oxide in early atherosclerosis. *Eur J Clin Pharmacol* **62 Suppl 13**, 69-78.

Chauhan SD, Nilsson H, Ahluwalia A, & Hobbs AJ (2003a). Release of C-type natriuretic peptide accounts for the biological activity of endothelium-derived hyperpolarizing factor. *Proc Natl Acad Sci U S A* **100**, 1426-1431.

Chauhan S, Rahman A, Nilsson H, Clapp L, MacAllister R, & Ahluwalia A (2003b). NO contributes to EDHF-like responses in rat small arteries: a role for NO stores. *Cardiovasc Res* **57**, 207-216.

Chauhan SD, Seggara G, Vo PA, MacAllister RJ, Hobbs AJ, & Ahluwalia A (2003c). Protection against lipopolysaccharide-induced endothelial dysfunction in resistance and conduit vasculature of iNOS knockout mice. *FASEB J* **17**, 773-775.

Chen HH & Burnett JC, Jr. (1998). C-type natriuretic peptide: the endothelial component of the natriuretic peptide system. *J Cardiovasc Pharmacol* **32 Suppl 3**, S22-S28.

Chen PF, Tsai AL, & Wu KK (1995). Cysteine 99 of endothelial nitric oxide synthase (NOS-III) is critical for tetrahydrobiopterin-dependent NOS-III stability and activity. *Biochem Biophys Res Commun* **215**, 1119-1129.

Chen PF, Tsai AL, Berka V, & Wu KK (1997). Mutation of Glu-361 in human endothelial nitric-oxide synthase selectively abolishes L-arginine binding without perturbing the behavior of heme and other redox centers. *J Biol Chem* **272**, 6114-6118.

Cherry PD & Wolin MS (1989). Ascorbate activates soluble guanylate cyclase via H₂O₂-metabolism by catalase. *Free Radic Biol Med* **7**, 485-490.

Chinkers M & Garbers DL (1989). The protein kinase domain of the ANP receptor is required for signaling. *Science* **245**, 1392-1394.

Chinkers M, Singh S, & Garbers DL (1991). Adenine nucleotides are required for activation of rat atrial natriuretic peptide receptor/guanylyl cyclase expressed in a baculovirus system. *J Biol Chem* **266**, 4088-4093.

Choi HC & Lee KY (2004). CD14 glycoprotein expressed in vascular smooth muscle cells. *J Pharmacol Sci* **95**, 65-70.

Chowienczyk PJ, Watts GF, Cockcroft JR, & Ritter JM (1992). Impaired endothelium-dependent vasodilation of forearm resistance vessels in hypercholesterolaemia. *Lancet* **340**, 1430-1432.

Chung HT, Pae HO, Choi BM, Billiar TR, & Kim YM (2001). Nitric oxide as a bioregulator of apoptosis. *Biochem Biophys Res Commun* **282**, 1075-1079.

Clapp BR, Hingorani AD, Kharbanda RK, Mohamed-Ali V, Stephens JW, Vallance P, & MacAllister RJ (2004). Inflammation-induced endothelial dysfunction involves reduced nitric oxide bioavailability and increased oxidant stress. *Cardiovasc Res* **64**, 172-178.

Colucci WS, Elkayam U, Horton DP, Abraham WT, Bourge RC, Johnson AD, Wagoner LE, Givertz MM, Liang CS, Neibaur M, Haught WH, & LeJemtel TH (2000). Intravenous nesiritide, a natriuretic peptide, in the treatment of decompensated congestive heart failure. Nesiritide Study Group. *N Engl J Med* **343**, 246-253.

Connelly L, Madhani M, & Hobbs AJ (2005). Resistance to endotoxic shock in endothelial nitric-oxide synthase (eNOS) knock-out mice: a pro-inflammatory role for eNOS-derived NO in vivo. *J Biol Chem* **280**, 10040-10046.

Corradi M, Montuschi P, Donnelly LE, Pesci A, Kharitonov SA, & Barnes PJ (2001). Increased nitrosothiols in exhaled breath condensate in inflammatory airway diseases. *Am J Respir Crit Care Med* **163**, 854-858.

Crane MS, Rossi AG, & Megson IL (2005). A potential role for extracellular nitric oxide generation in cGMP-independent inhibition of human platelet aggregation: biochemical and pharmacological considerations. *Br J Pharmacol* **144**, 849-859.

Crozier IG, Nicholls MG, Ikram H, Espiner EA, Gomez HJ, & Warner NJ (1986). Haemodynamic effects of atrial peptide infusion in heart failure. *Lancet* **2**, 1242-1245.

Davisson RL, Travis MD, Bates JN, & Lewis SJ (1996). Hemodynamic effects of L- and D-S-nitrosocysteine in the rat. Stereoselective S-nitrosothiol recognition sites. *Circ Res* **79**, 256-262.

Davisson RL, Travis MD, Bates JN, Johnson AK, & Lewis SJ (1997). Stereoselective actions of S-nitrosocysteine in central nervous system of conscious rats. *Am J Physiol* **272**, H2361-H2368.

de Belder AJ, MacAllister R, Radomski MW, Moncada S, & Vallance PJ (1994). Effects of S-nitroso-glutathione in the human forearm circulation: evidence for selective inhibition of platelet activation. *Cardiovasc Res* **28**, 691-694.

De Garavilla L, Pagani ED, Buchholz RA, Dundore R, Bode DC, Volberg ML, Jackson KN, Pratt P, & Silver PJ (1996). Zaprinst, but not dipyridamole, reverses hemodynamic tolerance to nitroglycerin in vivo. *Eur J Pharmacol* **313**, 89-96.

De Man JG, Moreels TG, De Winter BY, Herman AG, & Pelckmans PA (1999). Neocuproine potentiates the activity of the nitrergic neurotransmitter but inhibits that of S-nitrosothiols. *Eur J Pharmacol* **381**, 151-159.

Demura Y, Ameshima S, Ishizaki T, Okamura S, Miyamori I, & Matsukawa S (1998a). The activation of eNOS by copper ion (Cu²⁺) in human pulmonary arterial endothelial cells (HPAEC). *Free Radic Biol Med* **25**, 314-320.

Demura Y, Ishizaki T, Ameshima S, Okamura S, Hayashi T, Matsukawa S, & Miyamori I (1998b). The activation of nitric oxide synthase by copper ion is mediated by intracellular Ca^{2+} mobilization in human pulmonary arterial endothelial cells. *Br J Pharmacol* **125**, 1180-1187.

Dicks AP & Williams DL (1996). Generation of nitric oxide from S-nitrosothiols using protein-bound Cu^{2+} sources. *Chem Biol* **3**, 655-659.

Dicks AP, Swift HR, Williams DL, Butler AR, Al-Sa'doni HH & Cox, BG (1996). Identification of Cu^{+} as the effective reagent in nitric oxide formation from S-nitrosothiols (RSNO). *J Chem Soc Perk Trans 2*, **4**, 481 – 487.

Drummer C, Kentsch M, Otter W, Heer M, Herten M, & Gerzer R (1997). Increased renal natriuretic peptide (urodilatin) excretion in heart failure patients. *Eur J Med Res* **2**, 347-354.

Eiserich JP, Baldus S, Brennan ML, Ma W, Zhang C, Tousson A, Castro L, Lusis AJ, Nauseef WM, White CR, & Freeman BA (2002). Myeloperoxidase, a leukocyte-derived vascular NO oxidase. *Science* **296**, 2391-2394.

Emery CJ (1995). Vasodilator action of the S-nitrosothiol, SNAP, in rat isolated perfused lung. *Physiol Res* **44**, 19-24.

Espiner EA, Richards AM, Yandle TG, & Nicholls MG (1995). Natriuretic hormones. *Endocrinol Metab Clin North Am* **24**, 481-509.

Faraci FM & Didion SP (2004). Vascular protection: superoxide dismutase isoforms in the vessel wall. *Arterioscler Thromb Vasc Biol* **24**, 1367-1373.

Feelisch M, Kotsonis P, Siebe J, Clement B, & Schmidt HH (1999). The soluble guanylyl cyclase inhibitor 1H-[1,2,4]oxadiazolo[4,3,-a] quinoxalin-1-one is a nonselective heme protein inhibitor of nitric oxide synthase and other cytochrome P-450 enzymes involved in nitric oxide donor bioactivation. *Mol Pharmacol* **56**, 243-253.

Field LR, Dilts R, Ravichandran PG, Lenhert & Carnahan GE (1978). An unusually stable thionitrite from N-acetyl-D,L-penicillamine; X-ray crystal and molecular structure of 2-(acetylamino)-2-carboxy-1,1-dimethylethyl thionitrite. *J. Chem. Soc. Chem. Commun* 1978, 249-250.

Fischmann TO, Hruza A, Niu XD, Fossetta JD, Lunn CA, Dolphin E, Prongay AJ, Reichert P, Lundell DJ, Narula SK, & Weber PC (1999). Structural characterization of nitric oxide synthase isoforms reveals striking active-site conservation. *Nat Struct Biol* **6**, 233-242.

Fleming I, Julou-Schaeffer G, Gray GA, Parratt JR, & Stoclet JC (1991). Evidence that an L-arginine/nitric oxide dependent elevation of tissue cyclic GMP content is involved in depression of vascular reactivity by endotoxin. *Br J Pharmacol* **103**, 1047-1052.

Forstermann U, Pollock JS, Schmidt HH, Heller M, & Murad F (1991). Calmodulin-dependent endothelium-derived relaxing factor/nitric oxide synthase activity is present in the particulate and cytosolic fractions of bovine aortic endothelial cells. *Proc Natl Acad Sci U S A* **88**, 1788-1792.

Freedman JE, Sauter R, Battinelli EM, Ault K, Knowles C, Huang PL, & Loscalzo J (1999). Deficient platelet-derived nitric oxide and enhanced hemostasis in mice lacking the NOSIII gene. *Circ Res* **84**, 1416-1421.

Friebe A, Schultz G, & Koesling D (1996). Sensitizing soluble guanylyl cyclase to become a highly CO-sensitive enzyme. *EMBO J* **15**, 6863-6868.

Friebe A & Koesling D (2003). Regulation of nitric oxide-sensitive guanylyl cyclase. *Circ Res* **93**, 96-105.

Fukai T, Folz RJ, Landmesser U, & Harrison DG (2002). Extracellular superoxide dismutase and cardiovascular disease. *Cardiovasc Res* **55**, 239-249.

Fulton D, Gratton JP, McCabe TJ, Fontana J, Fujio Y, Walsh K, Franke TF, Papapetropoulos A, & Sessa WC (1999). Regulation of endothelium-derived nitric oxide production by the protein kinase Akt. *Nature* **399**, 597-601.

Furchgott RF & Zawadzki JV (1980). The obligatory role of endothelial cells in the relaxation of arterial smooth muscle by acetylcholine. *Nature* **288**, 373-376.

Furlong B, Henderson AH, Lewis MJ, & Smith JA (1987). Endothelium-derived relaxing factor inhibits in vitro platelet aggregation. *Br J Pharmacol* **90**, 687-692.

Futaki N, Takahashi S, Yokoyama M, Arai I, Higuchi S, & Otomo S (1994). NS-398, a new anti-inflammatory agent, selectively inhibits prostaglandin G/H synthase/cyclooxygenase (COX-2) activity in vitro. *Prostaglandins* **47**, 55-59.

Gachhui R, Ghosh DK, Wu C, Parkinson J, Crane BR, & Stuehr DJ (1997). Mutagenesis of acidic residues in the oxygenase domain of inducible nitric-oxide synthase identifies a glutamate involved in arginine binding. *Biochemistry* **36**, 5097-5103.

Galijasevic S, Saed GM, Diamond MP, & Abu-Soud HM (2003). Myeloperoxidase up-regulates the catalytic activity of inducible nitric oxide synthase by preventing nitric oxide feedback inhibition. *Proc Natl Acad Sci U S A* **100**, 14766-14771.

Gandley RE, Tyurin VA, Huang W, Arroyo A, Daftary A, Harger G, Jiang J, Pitt B, Taylor RN, Hubel CA, & Kagan VE (2005). S-nitrosoalbumin-mediated relaxation is enhanced by ascorbate and copper: effects in pregnancy and preeclampsia plasma. *Hypertension* **45**, 21-27.

Garg UC & Hassid A (1989). Nitric oxide-generating vasodilators and 8-bromo-cyclic guanosine monophosphate inhibit mitogenesis and proliferation of cultured rat vascular smooth muscle cells. *J Clin Invest* **83**, 1774-1777.

Garthwaite J, Southam E, Boulton CL, Nielsen EB, Schmidt K, & Mayer B (1995). Potent and selective inhibition of nitric oxide-sensitive guanylyl cyclase by 1H-[1,2,4]oxadiazolo[4,3-a]quinoxalin-1-one. *Mol Pharmacol* **48**, 184-188.

Garvey EP, Oplinger JA, Furfine ES, Kiff RJ, Laszlo F, Whittle BJ, & Knowles RG (1997). 1400W is a slow, tight binding, and highly selective inhibitor of inducible nitric-oxide synthase in vitro and in vivo. *J Biol Chem* **272**, 4959-4963.

Gaston B, Reilly J, Drazen JM, Fackler J, Ramdev P, Arnelle D, Mullins ME, Sugarbaker DJ, Chee C, Singel DJ, & . (1993). Endogenous nitrogen oxides and bronchodilator S-nitrosothiols in human airways. *Proc Natl Acad Sci U S A* **90**, 10957-10961.

Gaston B, Sears S, Woods J, Hunt J, Ponaman M, McMahon T, & Stamler JS (1998). Bronchodilator S-nitrosothiol deficiency in asthmatic respiratory failure. *Lancet* **351**, 1317-1319.

Geiselhoringer A, Werner M, Sigl K, Smital P, Worner R, Acheo L, Stieber J, Weinmeister P, Feil R, Feil S, Wegener J, Hofmann F, & Schlossmann J (2004). IRAG is essential for relaxation of receptor-triggered smooth muscle contraction by cGMP kinase. *EMBO J* **23**, 4222-4231.

Ghosh DK & Stuehr DJ (1995). Macrophage NO synthase: characterization of isolated oxygenase and reductase domains reveals a head-to-head subunit interaction. *Biochemistry* **34**, 801-807.

Gocmen C, Gokturk HS, Ertug PU, Onder S, Dikmen A, & Baysal F (2000). Effect of neocuproine, a selective Cu(I) chelator, on nitrergic relaxations in the mouse corpus cavernosum. *Eur J Pharmacol* **406**, 293-300.

Goldman RK, Vlessis AA, & Trunkey DD (1998). Nitrosothiol quantification in human plasma. *Anal Biochem* **259**, 98-103.

Gomez AB, MacKenzie C, Paul A, & Plevin R (2005). Selective inhibition of inhibitory kappa B kinase-beta abrogates induction of nitric oxide synthase in lipopolysaccharide-stimulated rat aortic smooth muscle cells. *Br J Pharmacol* **146**, 217-225.

Gordge MP, Meyer DJ, Hothersall J, Neild GH, Payne NN, & Noronha-Dutra A (1995). Copper chelation-induced reduction of the biological activity of S-nitrosothiols. *Br J Pharmacol* **114**, 1083-1089.

Gorren AC, Schrammel A, Schmidt K, & Mayer B (1996). Decomposition of S-nitrosoglutathione in the presence of copper ions and glutathione. *Arch Biochem Biophys* **330**, 219-228.

Gow AJ, Buerk DG, & Ischiropoulos H (1997). A novel reaction mechanism for the formation of S-nitrosothiol in vivo. *J Biol Chem* **272**, 2841-2845.

Grasemann H, Gaston B, Fang K, Paul K, & Ratjen F (1999). Decreased levels of nitrosothiols in the lower airways of patients with cystic fibrosis and normal pulmonary function. *J Pediatr* **135**, 770-772.

Gross SS, Jaffe EA, Levi R, & Kilbourn RG (1991). Cytokine-activated endothelial cells express an isotype of nitric oxide synthase which is tetrahydrobiopterin-dependent, calmodulin-independent and inhibited by arginine analogs with a rank-

order of potency characteristic of activated macrophages. *Biochem Biophys Res Commun* **178**, 823-829.

Gryglewski RJ, Palmer RM, & Moncada S (1986). Superoxide anion is involved in the breakdown of endothelium-derived vascular relaxing factor. *Nature* **320**, 454-456.

Gu X & Bishop SP (1994). Increased protein kinase C and isozyme redistribution in pressure-overload cardiac hypertrophy in the rat. *Circ Res* **75**, 926-931.

Hagiwara M, Endo T, & Hidaka H (1984). Effects of vinpocetine on cyclic nucleotide metabolism in vascular smooth muscle. *Biochem Pharmacol* **33**, 453-457.

Hallstrom S, Gasser H, Neumayer C, Fugl A, Nanobashvili J, Jakubowski A, Huk I, Schlag G, & Malinski T (2002). S-nitroso human serum albumin treatment reduces ischemia/reperfusion injury in skeletal muscle via nitric oxide release. *Circulation* **105**, 3032-3038.

Hama N, Itoh H, Shirakami G, Suga S, Komatsu Y, Yoshimasa T, Tanaka I, Mori K, & Nakao K (1994). Detection of C-type natriuretic peptide in human circulation and marked increase of plasma CNP level in septic shock patients. *Biochem Biophys Res Commun* **198**, 1177-1182.

Hamilton IM, Gilmore WS, & Strain JJ (2000). Marginal copper deficiency and atherosclerosis. *Biol Trace Elem Res* **78**, 179-189.

Han B & Hasin Y (2003). Cardiovascular effects of natriuretic peptides and their interrelation with endothelin-1. *Cardiovasc Drugs Ther* **17**, 41-52.

Harris ED (2000). Cellular copper transport and metabolism. *Annu Rev Nutr* **20**, 291-310.

Hart TW (1985). *Tetrahedron Lett* **26**, 2013-2016.

Harrison SA, Reifsnnyder DH, Gallis B, Cadd GG, & Beavo JA (1986). Isolation and characterization of bovine cardiac muscle cGMP-inhibited phosphodiesterase: a receptor for new cardiotonic drugs. *Mol Pharmacol* **29**, 506-514.

Hartemink KJ, Groeneveld AB, de Groot MC, Strack van Schijndel RJ, van Kamp G, & Thijs LG (2001). alpha-atrial natriuretic peptide, cyclic guanosine monophosphate, and endothelin in plasma as markers of myocardial depression in human septic shock. *Crit Care Med* **29**, 80-87.

Harteneck C, Wedel B, Koesling D, Malkewitz J, Bohme E, & Schultz G (1991). Molecular cloning and expression of a new alpha-subunit of soluble guanylyl cyclase. Interchangeability of the alpha-subunits of the enzyme. *FEBS Lett* **292**, 217-222.

Hasegawa K, Fujiwara H, Doyama K, Mukoyama M, Nakao K, Fujiwara T, Imura H, & Kawai C (1993a). Ventricular expression of atrial and brain natriuretic peptides in dilated cardiomyopathy. An immunohistochemical study of the endomyocardial biopsy specimens using specific monoclonal antibodies. *Am J Pathol* **142**, 107-116.

Hasegawa K, Fujiwara H, Doyama K, Miyamae M, Fujiwara T, Suga S, Mukoyama M, Nakao K, Imura H, & Sasayama S (1993b). Ventricular expression of brain natriuretic peptide in hypertrophic cardiomyopathy. *Circulation* **88**, 372-380.

Hecker M, Mulsch A, & Busse R (1994). Subcellular localization and characterization of neuronal nitric oxide synthase. *J Neurochem* **62**, 1524-1529.

Heinecke JW (1999). Mechanisms of oxidative damage by myeloperoxidase in atherosclerosis and other inflammatory disorders. *J Lab Clin Med* **133**, 321-325.

Hemmens B, Goessler W, Schmidt K, & Mayer B (2000). Role of bound zinc in dimer stabilization but not enzyme activity of neuronal nitric-oxide synthase. *J Biol Chem* **275**, 35786-35791.

Heo J & Campbell SL (2004). Mechanism of p21Ras S-nitrosylation and kinetics of nitric oxide-mediated guanine nucleotide exchange. *Biochemistry* **43**, 2314-2322.

Hingorani AD, Cross J, Kharbanda RK, Mullen MJ, Bhagat K, Taylor M, Donald AE, Palacios M, Griffin GE, Deanfield JE, MacAllister RJ, & Vallance P (2000). Acute systemic inflammation impairs endothelium-dependent dilatation in humans. *Circulation* **102**, 994-999.

Hobbs A, Foster P, Prescott C, Scotland R, & Ahluwalia A (2004). Natriuretic peptide receptor-C regulates coronary blood flow and prevents myocardial ischemia/reperfusion injury: novel cardioprotective role for endothelium-derived C-type natriuretic peptide. *Circulation* **110**, 1231-1235.

Hobbs AJ (1997). Soluble guanylate cyclase: the forgotten sibling. *Trends Pharmacol Sci* **18**, 484-491.

Hobbs AJ (2002). Soluble guanylate cyclase: an old therapeutic target re-visited. *Br J Pharmacol* **136**, 637-640.

Hobbs AJ & Moncada S (2003). Antiplatelet properties of a novel, non-NO-based soluble guanylate cyclase activator, BAY 41-2272. *Vascul Pharmacol* **40**, 149-154.

Hogg N (1999). The kinetics of S-transnitrosation--a reversible second-order reaction. *Anal Biochem* **272**, 257-262.

Hogg N (2000). Biological chemistry and clinical potential of S-nitrosothiols. *Free Radic Biol Med* **28**, 1478-1486.

Huang PL, Huang Z, Mashimo H, Bloch KD, Moskowitz MA, Bevan JA, & Fishman MC (1995). Hypertension in mice lacking the gene for endothelial nitric oxide synthase. *Nature* **377**, 239-242.

Huo X, Abe T, & Misono KS (1999). Ligand binding-dependent limited proteolysis of the atrial natriuretic peptide receptor: juxtamembrane hinge structure essential for transmembrane signal transduction. *Biochemistry* **38**, 16941-16951.

Hussain MB, Hobbs AJ, & MacAllister RJ (1999). Autoregulation of nitric oxide-soluble guanylate cyclase-cyclic GMP signalling in mouse thoracic aorta. *Br J Pharmacol* **128**, 1082-1088.

Hussain MB, MacAllister RJ, & Hobbs AJ (2001). Reciprocal regulation of cGMP-mediated vasorelaxation by soluble and particulate guanylate cyclases. *Am J Physiol Heart Circ Physiol* **280**, H1151-H1159.

Ignarro LJ, Degnan JN, Baricos WH, Kadowitz PJ, & Wolin MS (1982). Activation of purified guanylate cyclase by nitric oxide requires heme. Comparison of heme-deficient, heme-reconstituted and heme-containing forms of soluble enzyme from bovine lung. *Biochim Biophys Acta* **718**, 49-59.

Ignarro LJ, Buga GM, Wood KS, Byrns RE, & Chaudhuri G (1987). Endothelium-derived relaxing factor produced and released from artery and vein is nitric oxide. *Proc Natl Acad Sci U S A* **84**, 9265-9269.

Ignarro LJ, Sisodia M, Trinh K, Bedrood S, Wu G, Wei LH, & Buga GM (2002). Nebivolol inhibits vascular smooth muscle cell proliferation by mechanisms involving nitric oxide but not cyclic GMP. *Nitric Oxide* **7**, 83-90.

Ikeda M, Kohno M, Yasunari K, Yokokawa K, Horio T, Ueda M, Morisaki N, & Yoshikawa J (1997). Natriuretic peptide family as a novel antimigration factor of vascular smooth muscle cells. *Arterioscler Thromb Vasc Biol* **17**, 731-736.

Ishihara H, Martin BL, Brautigan DL, Karaki H, Ozaki H, Kato Y, Fusetani N, Watabe S, Hashimoto K, Uemura D, & . (1989). Calyculin A and okadaic acid: inhibitors of protein phosphatase activity. *Biochem Biophys Res Commun* **159**, 871-877.

Itoh H, Yamamura S, Ware JA, Zhuang S, Mii S, Liu B, & Kent KC (2001). Differential effects of protein kinase C on human vascular smooth muscle cell proliferation and migration. *Am J Physiol Heart Circ Physiol* **281**, H359-H370.

Jalkanen S & Salmi M (2001). Cell surface monoamine oxidases: enzymes in search of a function. *EMBO J* **20**, 3893-3901.

Javesghani D, Hussain SN, Scheidel J, Quinn MT, & Magder SA (2003). Superoxide production in the vasculature of lipopolysaccharide-treated rats and pigs. *Shock* **19**, 486-493.

Jia L, Bonaventura C, Bonaventura J, & Stamler JS (1996). S-nitrosohaemoglobin: a dynamic activity of blood involved in vascular control. *Nature* **380**, 221-226.

John SW, Krege JH, Oliver PM, Hagaman JR, Hodgins JB, Pang SC, Flynn TG, & Smithies O (1995). Genetic decreases in atrial natriuretic peptide and salt-sensitive hypertension. *Science* **267**, 679-681.

Jourd'heuil D, Laroux FS, Kang D, Miles AM, Wink DA, & Grisham MB (1999). Stability of S-nitrosothiols in presence of copper, zinc-superoxide dismutase. *Methods Enzymol* **301**, 220-227.

Jourd'heuil D, Gray L, & Grisham MB (2000). S-nitrosothiol formation in blood of lipopolysaccharide-treated rats. *Biochem Biophys Res Commun* **273**, 22-26.

Jozkowicz A & Dulak J (2003). Effects of protoporphyrins on production of nitric oxide and expression of vascular endothelial growth factor in vascular smooth muscle cells and macrophages. *Acta Biochim Pol* **50**, 69-79.

Julou-Schaeffer G, Gray GA, Fleming I, Schott C, Parratt JR, & Stoclet JC (1990). Loss of vascular responsiveness induced by endotoxin involves L-arginine pathway. *Am J Physiol* **259**, H1038-H1043.

Kamata K, Chikada S, Umeda F, & Kasuya Y (1995). Effects of phorbol ester on vasodilation induced by endothelium-dependent or endothelium-independent vasodilators in the mesenteric arterial bed. *J Cardiovasc Pharmacol* **26**, 645-652.

Kamisaki Y, Saheki S, Nakane M, Palmieri JA, Kuno T, Chang BY, Waldman SA, & Murad F (1986). Soluble guanylate cyclase from rat lung exists as a heterodimer. *J Biol Chem* **261**, 7236-7241.

Kaposzta Z, Baskerville PA, Madge D, Fraser S, Martin JF, & Markus HS (2001). L-arginine and S-nitrosoglutathione reduce embolization in humans. *Circulation* **103**, 2371-2375.

Kashiba-Iwatsuki M, Kitoh K, Kasahara E, Yu H, Nisikawa M, Matsuo M, & Inoue M (1997). Ascorbic acid and reducing agents regulate the fates and functions of S-nitrosothiols. *J Biochem (Tokyo)* **122**, 1208-1214.

Kettle AJ, Gedye CA, Hampton MB, & Winterbourn CC (1995). Inhibition of myeloperoxidase by benzoic acid hydrazides. *Biochem J* **308** (Pt 2), 559-563.

Kharbanda RK, Walton B, Allen M, Klein N, Hingorani AD, MacAllister RJ, & Vallance P (2002). Prevention of inflammation-induced endothelial dysfunction: a novel vasculo-protective action of aspirin. *Circulation* **105**, 2600-2604.

Kharitonov VG, Sundquist AR, & Sharma VS (1995). Kinetics of nitrosation of thiols by nitric oxide in the presence of oxygen. *J Biol Chem* **270**, 28158-28164.

Kilbourn RG, Jubran A, Gross SS, Griffith OW, Levi R, Adams J, & Lodato RF (1990). Reversal of endotoxin-mediated shock by NG-methyl-L-arginine, an inhibitor of nitric oxide synthesis. *Biochem Biophys Res Commun* **172**, 1132-1138.

Kim D, Rybalkin SD, Pi X, Wang Y, Zhang C, Munzel T, Beavo JA, Berk BC, & Yan C (2001). Upregulation of phosphodiesterase 1A1 expression is associated with the development of nitrate tolerance. *Circulation* **104**, 2338-2343.

Kim HP, Ryter SW, & Choi AM (2005). CO as a Cellular Signaling Molecule. *Annu Rev Pharmacol Toxicol*.

Kim SJ, Chang YY, Kang SS, & Chun JS (1997). Phorbol ester effects in atypical protein kinase C zeta overexpressing NIH3T3 cells: possible evidence for crosstalk between protein kinase C isoforms. *Biochem Biophys Res Commun* **237**, 336-339.

Kirkeboen KA & Strand OA (1999). The role of nitric oxide in sepsis--an overview. *Acta Anaesthesiol Scand* **43**, 275-288.

Kishimoto I, Rossi K, & Garbers DL (2001). A genetic model provides evidence that the receptor for atrial natriuretic peptide (guanylyl cyclase-A) inhibits cardiac ventricular myocyte hypertrophy. *Proc Natl Acad Sci U S A* **98**, 2703-2706.

Klatt P, Pfeiffer S, List BM, Lehner D, Glatter O, Bachinger HP, Werner ER, Schmidt K, & Mayer B (1996). Characterization of heme-deficient neuronal nitric-oxide synthase reveals a role for heme in subunit dimerization and binding of the amino acid substrate and tetrahydrobiopterin. *J Biol Chem* **271**, 7336-7342.

Klevay LM (2000). Cardiovascular disease from copper deficiency--a history. *J Nutr* **130**, 489S-492S.

Kluge I, Gutteck-Amsler U, Zollinger M, & Do KQ (1997). S-nitrosoglutathione in rat cerebellum: identification and quantification by liquid chromatography-mass spectrometry. *J Neurochem* **69**, 2599-2607.

Knowles RG, Palacios M, Palmer RM, & Moncada S (1989). Formation of nitric oxide from L-arginine in the central nervous system: a transduction mechanism for stimulation of the soluble guanylate cyclase. *Proc Natl Acad Sci U S A* **86**, 5159-5162.

Ko FN, Wu CC, Kuo SC, Lee FY, & Teng CM (1994). YC-1, a novel activator of platelet guanylate cyclase. *Blood* **84**, 4226-4233.

Kobzik L, Reid MB, Bredt DS, & Stamler JS (1994). Nitric oxide in skeletal muscle. *Nature* **372**, 546-548.

Koide M, Kawahara Y, Tsuda T, & Yokoyama M (1993). Cytokine-induced expression of an inducible type of nitric oxide synthase gene in cultured vascular smooth muscle cells. *FEBS Lett* **318**, 213-217.

Koller KJ & Goeddel DV (1992). Molecular biology of the natriuretic peptides and their receptors. *Circulation* **86**, 1081-1088.

Komalavilas P & Lincoln TM (1994). Phosphorylation of the inositol 1,4,5-trisphosphate receptor by cyclic GMP-dependent protein kinase. *J Biol Chem* **269**, 8701-8707.

Komarek M, Bernheim A, Schindler R, Steden R, Kiowski W, & Brunner-La Rocca HP (2004). Vascular effects of natriuretic peptides in healthy men. *J Cardiovasc Pharmacol Ther* **9**, 263-270.

Komatsu Y, Nakao K, Suga S, Ogawa Y, Mukoyama M, Arai H, Shirakami G, Hosoda K, Nakagawa O, Hama N, & . (1991). C-type natriuretic peptide (CNP) in rats and humans. *Endocrinology* **129**, 1104-1106.

Kondo K, Umemura K, Miyaji M, & Nakashima M (1999). Milrinone, a phosphodiesterase inhibitor, suppresses intimal thickening after photochemically induced endothelial injury in the mouse femoral artery. *Atherosclerosis* **142**, 133-138.

Konorev EA, Kalyanaraman B, & Hogg N (2000). Modification of creatine kinase by S-nitrosothiols: S-nitrosation vs. S-thiolation. *Free Radic Biol Med* **28**, 1671-1678.

Kostka P, Xu B, & Skiles EH (1999). Degradation of S-nitrosocysteine in vascular tissue homogenates: role of divalent ions. *J Cardiovasc Pharmacol* **33**, 665-670.

Kowaluk EA, Poliszczuk R, & Fung HL (1987). Tolerance to relaxation in rat aorta: comparison of an S-nitrosothiol with nitroglycerin. *Eur J Pharmacol* **144**, 379-383.

Kowaluk EA & Fung HL (1990). Spontaneous liberation of nitric oxide cannot account for in vitro vascular relaxation by S-nitrosothiols. *J Pharmacol Exp Ther* **255**, 1256-1264.

Krotova KY, Zharikov SI, & Block ER (2003). Classical isoforms of PKC as regulators of CAT-1 transporter activity in pulmonary artery endothelial cells. *Am J Physiol Lung Cell Mol Physiol* **284**, L1037-L1044.

Kwiecien I, Sokolowska M, Luchter-Wasylewska E, & Wlodek L (2003). Inhibition of the catalytic activity of rhodanese by S-nitrosylation using nitric oxide donors. *Int J Biochem Cell Biol* **35**, 1645-1657.

Laber U, Kober T, Schmitz V, Schrammel A, Meyer W, Mayer B, Weber M, & Kojda G (2002). Effect of hypercholesterolemia on expression and function of vascular soluble guanylyl cyclase. *Circulation* **105**, 855-860.

Laher I & Zhang JH (2001). Protein kinase C and cerebral vasospasm. *J Cereb Blood Flow Metab* **21**, 887-906.

Lamzin VS, Dauter Z, & Wilson KS (1995). How nature deals with stereoisomers. *Curr Opin Struct Biol* **5**, 830-836.

Langford EJ, Brown AS, Wainwright RJ, de Belder AJ, Thomas MR, Smith RE, Radomski MW, Martin JF, & Moncada S (1994). Inhibition of platelet activity by S-nitrosoglutathione during coronary angioplasty. *Lancet* **344**, 1458-1460.

Le Cras TD, Xue C, Rengasamy A, & Johns RA (1996). Chronic hypoxia upregulates endothelial and inducible NO synthase gene and protein expression in rat lung. *Am J Physiol* **270**, L164-L170.

Lee MR, Li L, & Kitazawa T (1997). Cyclic GMP causes Ca²⁺ desensitization in vascular smooth muscle by activating the myosin light chain phosphatase. *J Biol Chem* **272**, 5063-5068.

Lefer AM & Ma XL (1993). Decreased basal nitric oxide release in hypercholesterolemia increases neutrophil adherence to rabbit coronary artery endothelium. *Arterioscler Thromb* **13**, 771-776.

Lemmon MA, Treutlein HR, Adams PD, Brunger AT, & Engelman DM (1994). A dimerization motif for transmembrane alpha-helices. *Nat Struct Biol* **1**, 157-163.

Leone AM, Palmer RM, Knowles RG, Francis PL, Ashton DS, & Moncada S (1991). Constitutive and inducible nitric oxide synthases incorporate molecular oxygen into both nitric oxide and citrulline. *J Biol Chem* **266**, 23790-23795.

Li H & Forstermann U (2000). Nitric oxide in the pathogenesis of vascular disease. *J Pathol* **190**, 244-254.

Li H, Wallerath T, & Forstermann U (2002). Physiological mechanisms regulating the expression of endothelial-type NO synthase. *Nitric Oxide* **7**, 132-147.

Li J, Billiar TR, Talanian RV, & Kim YM (1997). Nitric oxide reversibly inhibits seven members of the caspase family via S-nitrosylation. *Biochem Biophys Res Commun* **240**, 419-424.

Li YM & Casida JE (1992). Cantharidin-binding protein: identification as protein phosphatase 2A. *Proc Natl Acad Sci U S A* **89**, 11867-11870.

Liu L, Hausladen A, Zeng M, Que L, Heitman J & Stamler JS (2001). A metabolic enzyme for S-nitrosothiol conserved from bacteria to humans. *Nature* **410**, 490-494.

Llosas MD, Batlle E, Coll O, Skoudy A, Fabre M, & Garcia dH (1996). Evidence for a role of conventional protein kinase-C alpha in the control of homotypic contacts and cell scattering of HT-29 human intestinal cells. *Biochem J* **315** (Pt 3), 1049-1054.

Lopez MJ, Wong SK, Kishimoto I, Dubois S, Mach V, Friesen J, Garbers DL, & Beuve A (1995). Salt-resistant hypertension in mice lacking the guanylyl cyclase-A receptor for atrial natriuretic peptide. *Nature* **378**, 65-68.

Lucas KA, Pitari GM, Kazerounian S, Ruiz-Stewart I, Park J, Schulz S, Chepenik KP, & Waldman SA (2000). Guanylyl cyclases and signaling by cyclic GMP. *Pharmacol Rev* **52**, 375-414.

Luchner A, Stevens TL, Borgeson DD, Redfield M, Wei CM, Porter JG, & Burnett JC, Jr. (1998). Differential atrial and ventricular expression of myocardial BNP during evolution of heart failure. *Am J Physiol* **274**, H1684-H1689.

Luo D, Das S, & Vincent SR (1995). Effects of methylene blue and LY83583 on neuronal nitric oxide synthase and NADPH-diaphorase. *Eur J Pharmacol* **290**, 247-251.

Maack T, Suzuki M, Almeida FA, Nussenzveig D, Scarborough RM, McEnroe GA, & Lewicki JA (1987). Physiological role of silent receptors of atrial natriuretic factor. *Science* **238**, 675-678.

MacAllister R & Vallance P (1994). Nitric oxide in essential and renal hypertension. *J Am Soc Nephrol* **5**, 1057-1065.

MacMicking JD, Nathan C, Hom G, Chartrain N, Fletcher DS, Trumbauer M, Stevens K, Xie QW, Sokol K, Hutchinson N, & . (1995). Altered responses to bacterial infection and endotoxic shock in mice lacking inducible nitric oxide synthase. *Cell* **81**, 641-650.

Madhani M, Scotland RS, MacAllister RJ, & Hobbs AJ (2003). Vascular natriuretic peptide receptor-linked particulate guanylate cyclases are modulated by nitric oxide-cyclic GMP signalling. *Br J Pharmacol* **139**, 1289-1296.

Marcus LS, Hart D, Packer M, Yushak M, Medina N, Danziger RS, Heitjan DF, & Katz SD (1996). Hemodynamic and renal excretory effects of human brain natriuretic peptide infusion in patients with congestive heart failure. A double-blind, placebo-controlled, randomized crossover trial. *Circulation* **94**, 3184-3189.

Marin J & Rodriguez-Martinez MA (1997). Role of vascular nitric oxide in physiological and pathological conditions. *Pharmacol Ther* **75**, 111-134.

Marks DS, Vita JA, Folts JD, Keaney JF, Jr., Welch GN, & Loscalzo J (1995). Inhibition of neointimal proliferation in rabbits after vascular injury by a single treatment with a protein adduct of nitric oxide. *J Clin Invest* **96**, 2630-2638.

Marley R, Feelisch M, Holt S, & Moore K (2000). A chemiluminescence-based assay for S-nitrosoalbumin and other plasma S-nitrosothiols. *Free Radic Res* **32**, 1-9.

Marley R, Patel RP, Orie N, Ceaser E, Darley-Usmar V, & Moore K (2001). Formation of nanomolar concentrations of S-nitroso-albumin in human plasma by nitric oxide. *Free Radic Biol Med* **31**, 688-696.

Marques M, Millas I, Jimenez A, Garcia-Colis E, Rodriguez-Feo JA, Velasco S, Barrientos A, Casado S, & Lopez-Farre A (2001). Alteration of the soluble guanylate cyclase system in the vascular wall of lead-induced hypertension in rats. *J Am Soc Nephrol* **12**, 2594-2600.

Marsden PA, Heng HH, Scherer SW, Stewart RJ, Hall AV, Shi XM, Tsui LC, & Schappert KT (1993). Structure and chromosomal localization of the human constitutive endothelial nitric oxide synthase gene. *J Biol Chem* **268**, 17478-17488.

Marshall HE & Stamler JS (2001). Inhibition of NF-kappa B by S-nitrosylation. *Biochemistry* **40**, 1688-1693.

Massy ZA, Borderie D, Nguyen-Khoa T, Drueke TB, Ekindjian OG, & Lacour B (2003). Increased plasma S-nitrosothiol levels in chronic haemodialysis patients. *Nephrol Dial Transplant* **18**, 153-157.

Mathews WR & Kerr SW (1993). Biological activity of S-nitrosothiols: the role of nitric oxide. *J Pharmacol Exp Ther* **267**, 1529-1537.

Matsuoka H (2001). Endothelial dysfunction associated with oxidative stress in human. *Diabetes Res Clin Pract* **54 Suppl 2**, S65-S72.

Mazul-Sunko B, Zarkovic N, Vrkic N, Klinger R, Peric M, Bekavac-Beslin M, Novkoski M, Krizmanic A, Gvozdenovic A, & Topic E (2001). Pro-atrial natriuretic peptide hormone from right atria is correlated with cardiac depression in septic patients. *J Endocrinol Invest* **24**, RC22-RC24.

McFarlane SI, Winer N, & Sowers JR (2003). Role of the natriuretic peptide system in cardiorenal protection. *Arch Intern Med* **163**, 2696-2704.

McKenzie JC, Kelley KB, Merisko-Liversidge EM, Kennedy J, & Klein RM (1994). Developmental pattern of ventricular atrial natriuretic peptide (ANP) expression in chronically hypoxic rats as an indicator of the hypertrophic process. *J Mol Cell Cardiol* **26**, 753-767.

McNeill KL, Fontana L, Russell-Jones DL, Rajman I, Ritter JM, & Chowienczyk PJ (2000). Inhibitory effects of low-density lipoproteins from men with type II diabetes on endothelium-dependent relaxation. *J Am Coll Cardiol* **35**, 1622-1627.

Meffert MK, Haley JE, Schuman EM, Schulman H, & Madison DV (1994). Inhibition of hippocampal heme oxygenase, nitric oxide synthase, and long-term potentiation by metalloporphyrins. *Neuron* **13**, 1225-1233.

Megson IL, Morton S, Greig IR, Mazzei FA, Field RA, Butler AR, Caron G, Gasco A, Fruttero R, & Webb DJ (1999). N-Substituted analogues of S-nitroso-N-acetyl-D,L-penicillamine: chemical stability and prolonged nitric oxide mediated vasodilatation in isolated rat femoral arteries. *Br J Pharmacol* **126**, 639-648.

Megson IL, Holmes SA, Magid KS, Pritchard RJ, & Flitney FW (2000a). Selective modifiers of glutathione biosynthesis and 'repriming' of vascular smooth muscle photorelaxation. *Br J Pharmacol* **130**, 1575-1580.

Megson IL, Sogo N, Mazzei FA, Butler AR, Walton JC, & Webb DJ (2000b). Inhibition of human platelet aggregation by a novel S-nitrosothiol is abolished by haemoglobin and red blood cells in vitro: implications for anti-thrombotic therapy. *Br J Pharmacol* **131**, 1391-1398.

Mellion BT, Ignarro LJ, Myers CB, Ohlstein EH, Ballot BA, Hyman AL, & Kadowitz PJ (1983). Inhibition of human platelet aggregation by S-nitrosothiols. Heme-dependent activation of soluble guanylate cyclase and stimulation of cyclic GMP accumulation. *Mol Pharmacol* **23**, 653-664.

Mendelsohn ME, O'Neill S, George D, & Loscalzo J (1990). Inhibition of fibrinogen binding to human platelets by S-nitroso-N-acetylcysteine. *J Biol Chem* **265**, 19028-19034.

Michel JB, Feron O, Sacks D, & Michel T (1997). Reciprocal regulation of endothelial nitric-oxide synthase by Ca²⁺-calmodulin and caveolin. *J Biol Chem* **272**, 15583-15586.

Miller MR, Roseberry MJ, Mazzei FA, Butler AR, Webb DJ, & Megson IL (2000). Novel S-nitrosothiols do not engender vascular tolerance and remain effective in glyceryltrinitrate-tolerant rat femoral arteries. *Eur J Pharmacol* **408**, 335-343.

Miller MR, Hanspal IS, Hadoke PW, Newby DE, Rossi AG, Webb DJ & Megson IL (2003). A novel S-nitrosothiol causes prolonged and selective inhibition of platelet adhesion at sites of vascular injury. *Cardiovasc Res* **57**, 853-860.

Minamino N, Kangawa K, & Matsuo H (1990). N-terminally extended form of C-type natriuretic peptide (CNP-53) identified in porcine brain. *Biochem Biophys Res Commun* **170**, 973-979.

Mingone CJ, Gupte SA, Ali N, Oeckler RA, & Wolin MS (2006). Thiol oxidation inhibits nitric oxide-mediated pulmonary artery relaxation and guanylate cyclase stimulation. *Am J Physiol Lung Cell Mol Physiol* **290**, L549-L557.

Minor RL, Jr., Myers PR, Guerra R, Jr., Bates JN, & Harrison DG (1990). Diet-induced atherosclerosis increases the release of nitrogen oxides from rabbit aorta. *J Clin Invest* **86**, 2109-2116.

Misono KS (2000). Atrial natriuretic factor binding to its receptor is dependent on chloride concentration: A possible feedback-control mechanism in renal salt regulation. *Circ Res* **86**, 1135-1139.

Misono KS (2002). Natriuretic peptide receptor: structure and signaling. *Mol Cell Biochem* **230**, 49-60.

Mittermayer F, Pleiner J, Schaller G, Zorn S, Namiranian K, Kapiotis S, Bartel G, Wolfrum M, Brugel M, Thiery J, MacAllister RJ, & Wolzt M (2005). Tetrahydrobiopterin corrects Escherichia coli endotoxin-induced endothelial dysfunction. *Am J Physiol Heart Circ Physiol* **289**, H1752-H1757.

Miyagi M, Zhang X, & Misono KS (2000). Glycosylation sites in the atrial natriuretic peptide receptor: oligosaccharide structures are not required for hormone binding. *Eur J Biochem* **267**, 5758-5768.

Miyamoto A, Moriki H, Ishiguro S, & Nishio A (2004). In vitro application of endotoxin to thoracic aortas from magnesium-deficient rats enhances vascular hyporeactivity to phenylephrine. *J Am Coll Nutr* **23**, 518S-520S.

Miyazaki H, Matsuoka H, Cooke JP, Usui M, Ueda S, Okuda S, & Imaizumi T (1999). Endogenous nitric oxide synthase inhibitor: a novel marker of atherosclerosis. *Circulation* **99**, 1141-1146.

Mohr S, Hallak H, de Boitte A, Lapetina EG, & Brune B (1999). Nitric oxide-induced S-glutathionylation and inactivation of glyceraldehyde-3-phosphate dehydrogenase. *J Biol Chem* **274**, 9427-9430.

Molloy J, Martin JF, Baskerville PA, Fraser SC, & Markus HS (1998). S-nitrosoglutathione reduces the rate of embolization in humans. *Circulation* **98**, 1372-1375.

Moncada S, Rees DD, Schulz R, & Palmer RM (1991). Development and mechanism of a specific supersensitivity to nitrovasodilators after inhibition of vascular nitric oxide synthesis in vivo. *Proc Natl Acad Sci U S A* **88**, 2166-2170.

Moore PK, al Swayeh OA, Chong NW, Evans RA, & Gibson A (1990). L-NG-nitro arginine (L-NOARG), a novel, L-arginine-reversible inhibitor of endothelium-dependent vasodilatation in vitro. *Br J Pharmacol* **99**, 408-412.

Mori T, Chen YF, Feng JA, Hayashi T, Oparil S, & Perry GJ (2004). Volume overload results in exaggerated cardiac hypertrophy in the atrial natriuretic peptide knockout mouse. *Cardiovasc Res* **61**, 771-779.

Moriel P, Pereira IR, Bertolami MC, & Abdalla DS (2001). Is ceruloplasmin an important catalyst for S-nitrosothiol generation in hypercholesterolemia? *Free Radic Biol Med* **30**, 318-326.

Moroi M, Zhang L, Yasuda T, Virmani R, Gold HK, Fishman MC, & Huang PL (1998). Interaction of genetic deficiency of endothelial nitric oxide, gender, and pregnancy in vascular response to injury in mice. *J Clin Invest* **101**, 1225-1232.

Morrison KJ & Pollock D (1990). Impairment of relaxations to acetylcholine and nitric oxide by a phorbol ester in rat isolated aorta. *Br J Pharmacol* **101**, 432-436.

Munzel T, Sayegh H, Freeman BA, Tarpey MM, & Harrison DG (1995). Evidence for enhanced vascular superoxide anion production in nitrate tolerance. A novel mechanism underlying tolerance and cross-tolerance. *J Clin Invest* **95**, 187-194.

Murphy TV, Cross KM, Dunning PM, & Garland CJ (1994). Phorbol esters impair endothelium-dependent and independent relaxation in rat aortic rings. *Gen Pharmacol* **25**, 581-588.

Myers PR, Minor RL, Jr., Guerra R, Jr., Bates JN & Harrison DG (1990). Vasorelaxant properties of the endothelium-derived relaxing factor more closely resemble S-nitrosocysteine than nitric oxide. *Nature* **345**, 161-163.

Narhi LO & Fulco AJ (1987). Identification and characterization of two functional domains in cytochrome P-450BM-3, a catalytically self-sufficient monooxygenase induced by barbiturates in *Bacillus megaterium*. *J Biol Chem* **262**, 6683-6690.

Narindrasorasak S, Yao P & Sarkar B (2003). Protein disulfide isomerase, a multifunctional protein chaperone, shows copper-binding activity. *Biochem Biophys Res Commun* **311**, 405-414.

Naruko T, Ueda M, van der Wal AC, van der Loos CM, Itoh H, Nakao K, & Becker AE (1996). C-type natriuretic peptide in human coronary atherosclerotic lesions. *Circulation* **94**, 3103-3108.

Ndisang JF & Wang R (2003). Age-related alterations in soluble guanylyl cyclase and cGMP pathway in spontaneously hypertensive rats. *J Hypertens* **21**, 1117-1124.

Ndrepepa G, Braun S, Niemoller K, Mehilli J, von Beckerath N, von Beckerath O, Vogt W, Schomig A, & Kastrati A (2005). Prognostic value of N-terminal pro-brain natriuretic peptide in patients with chronic stable angina. *Circulation* **112**, 2102-2107.

Nedeljkovic ZS, Gokce N, & Loscalzo J (2003). Mechanisms of oxidative stress and vascular dysfunction. *Postgrad Med J* **79**, 195-199.

Nikitovic D & Holmgren A (1996). S-nitrosoglutathione is cleaved by the thioredoxin system with liberation of glutathione and redox regulating nitric oxide. *J Biol Chem* **271**, 19180-19185.

Nozaki K, Moskowitz MA, Maynard KI, Koketsu N, Dawson TM, Bredt DS, & Snyder SH (1993). Possible origins and distribution of immunoreactive nitric oxide synthase-containing nerve fibers in cerebral arteries. *J Cereb Blood Flow Metab* **13**, 70-79.

Ny L, Andersson KE, & Grundemar L (1995). Inhibition by zinc protoporphyrin-IX of receptor-mediated relaxation of the rat aorta in a manner distinct from inhibition of haem oxygenase. *Br J Pharmacol* **115**, 186-190.

O'Brien AJ, Wilson AJ, Sibbald R, Singer M, & Clapp LH (2001). Temporal variation in endotoxin-induced vascular hyporeactivity in a rat mesenteric artery organ culture model. *Br J Pharmacol* **133**, 351-360.

Oemar BS, Tschudi MR, Godoy N, Brovkovich V, Malinski T, & Luscher TF (1998). Reduced endothelial nitric oxide synthase expression and production in human atherosclerosis. *Circulation* **97**, 2494-2498.

Ohlstein EH, Wood KS, & Ignarro LJ (1982). Purification and properties of heme-deficient hepatic soluble guanylate cyclase: effects of heme and other factors on enzyme activation by NO, NO-heme, and protoporphyrin IX. *Arch Biochem Biophys* **218**, 187-198.

Okahara K, Kambayashi J, Ohnishi T, Fujiwara Y, Kawasaki T, & Monden M (1995). Shear stress induces expression of CNP gene in human endothelial cells. *FEBS Lett* **373**, 108-110.

Ottesen LH, Harry D, Frost M, Davies S, Khan K, Halliwell B, & Moore K (2001). Increased formation of S-nitrothiols and nitrotyrosine in cirrhotic rats during endotoxemia. *Free Radic Biol Med* **31**, 790-798.

Pagani ED, VanAller GS, O'Connor B, & Silver PJ (1993). Reversal of nitroglycerin tolerance in vitro by the cGMP-phosphodiesterase inhibitor zaprinast. *Eur J Pharmacol* **243**, 141-147.

Palmer RM, Ferrige AG, & Moncada S (1987). Nitric oxide release accounts for the biological activity of endothelium-derived relaxing factor. *Nature* **327**, 524-526.

Palmer RM, Ashton DS, & Moncada S (1988). Vascular endothelial cells synthesize nitric oxide from L-arginine. *Nature* **333**, 664-666.

Papapetropoulos A, Abou-Mohamed G, Marczin N, Murad F, Caldwell RW, & Catravas JD (1996). Downregulation of nitrovasodilator-induced cyclic GMP accumulation in cells exposed to endotoxin or interleukin-1 beta. *Br J Pharmacol* **118**, 1359-1366.

Papapetropoulos A, Marczin N, & Catravas JD (1998). Cross-tolerance between endogenous nitric oxide and exogenous nitric oxide donors. *Eur J Pharmacol* **344**, 313-321.

Parker JD & Gori T (2001). Tolerance to the organic nitrates: new ideas, new mechanisms, continued mystery. *Circulation* **104**, 2263-2265.

Pawloski JR, Swaminathan RV, & Stamler JS (1998). Cell-free and erythrocytic S-nitrosohemoglobin inhibits human platelet aggregation. *Circulation* **97**, 263-267.

Paya D, Gray GA, Fleming I, & Stoclet JC (1993). Effect of dexamethasone on the onset and persistence of vascular hyporeactivity induced by *E. coli* lipopolysaccharide in rats. *Circ Shock* **41**, 103-112.

Percival SS, Kauwell GP, Bowser E & Wagner M (1999). Altered copper status in adult men with cystic fibrosis. *J Am Coll Nutr* **18**, 614-619.

Petros A, Lamb G, Leone A, Moncada S, Bennett D, & Vallance P (1994). Effects of a nitric oxide synthase inhibitor in humans with septic shock. *Cardiovasc Res* **28**, 34-39.

Pieper GM & Peltier BA (1995). Amelioration by L-arginine of a dysfunctional arginine/nitric oxide pathway in diabetic endothelium. *J Cardiovasc Pharmacol* **25**, 397-403.

Pleiner J, Mittermayer F, Schaller G, MacAllister RJ, & Wolzt M (2002). High doses of vitamin C reverse *Escherichia coli* endotoxin-induced hyporeactivity to acetylcholine in the human forearm. *Circulation* **106**, 1460-1464.

Pollock JS, Klinghofer V, Forstermann U, & Murad F (1992). Endothelial nitric oxide synthase is myristylated. *FEBS Lett* **309**, 402-404.

Root P, Sliskovic I & Mutus B (2004). Platelet cell-surface protein disulphide-isomerase mediated S-nitrosoglutathione consumption. *Biochem J* **382**, 575-580.

Porter JG, Catalano R, McEnroe G, Lewicki JA, & Protter AA (1992). C-type natriuretic peptide inhibits growth factor-dependent DNA synthesis in smooth muscle cells. *Am J Physiol* **263**, C1001-C1006.

Potter LR & Garbers DL (1992). Dephosphorylation of the guanylyl cyclase-A receptor causes desensitization. *J Biol Chem* **267**, 14531-14534.

Potter LR & Garbers DL (1994). Protein kinase C-dependent desensitization of the atrial natriuretic peptide receptor is mediated by dephosphorylation. *J Biol Chem* **269**, 14636-14642.

Potter LR & Hunter T (1998a). Phosphorylation of the kinase homology domain is essential for activation of the A-type natriuretic peptide receptor. *Mol Cell Biol* **18**, 2164-2172.

Potter LR & Hunter T (1998b). Identification and characterization of the major phosphorylation sites of the B-type natriuretic peptide receptor. *J Biol Chem* **273**, 15533-15539.

Potter LR (1998). Phosphorylation-dependent regulation of the guanylyl cyclase-linked natriuretic peptide receptor B: dephosphorylation is a mechanism of desensitization. *Biochemistry* **37**, 2422-2429.

Potter LR & Hunter T (1999). A constitutively "phosphorylated" guanylyl cyclase-linked atrial natriuretic peptide receptor mutant is resistant to desensitization. *Mol Biol Cell* **10**, 1811-1820.

Potter LR & Hunter T (2000). Activation of protein kinase C stimulates the dephosphorylation of natriuretic peptide receptor-B at a single serine residue: a possible mechanism of heterologous desensitization. *J Biol Chem* **275**, 31099-31106.

Potter LR, Abbey-Hosch S, & Dickey DM (2006). Natriuretic peptides, their receptors, and cyclic guanosine monophosphate-dependent signaling functions. *Endocr Rev* **27**, 47-72.

Qian JY, Haruno A, Asada Y, Nishida T, Saito Y, Matsuda T, & Ueno H (2002). Local expression of C-type natriuretic peptide suppresses inflammation, eliminates shear stress-induced thrombosis, and prevents neointima formation through enhanced nitric oxide production in rabbit injured carotid arteries. *Circ Res* **91**, 1063-1069.

Radomski MW, Palmer RM, & Moncada S (1987). Endogenous nitric oxide inhibits human platelet adhesion to vascular endothelium. *Lancet* **2**, 1057-1058.

Ramasamy S, Parthasarathy S, & Harrison DG (1998). Regulation of endothelial nitric oxide synthase gene expression by oxidized linoleic acid. *J Lipid Res* **39**, 268-276.

Ramsay B, Radomski M, De Belder A, Martin JF, & Lopez-Jaramillo P (1995). Systemic effects of S-nitroso-glutathione in the human following intravenous infusion. *Br J Clin Pharmacol* **40**, 101-102.

Rand MJ & Li CG (1993). Differential effects of hydroxocobalamin on relaxations induced by nitrosothiols in rat aorta and anococcygeus muscle. *Eur J Pharmacol* **241**, 249-254.

Ratz PH, Berg KM, Urban NH, & Miner AS (2005). Regulation of smooth muscle calcium sensitivity: KCl as a calcium-sensitizing stimulus. *Am J Physiol Cell Physiol* **288**, C769-C783.

Rees DD, Palmer RM, & Moncada S (1989). Role of endothelium-derived nitric oxide in the regulation of blood pressure. *Proc Natl Acad Sci US A* **86**, 3375-3378.

Riegger GA, Elsner D, Kromer EP, Daffner C, Forssmann WG, Muders F, Pascher EW, & Kochsiek K (1988). Atrial natriuretic peptide in congestive heart failure in the dog: plasma levels, cyclic guanosine monophosphate, ultrastructure of atrial myoendocrine cells, and hemodynamic, hormonal, and renal effects. *Circulation* **77**, 398-406.

Roussos GG & Morrow BH (1966). Bovine intestinal xanthine oxidase: a metalloflavoprotein containing iron, copper, and flavin adenine dinucleotide. *Arch Biochem Biophys* **114**, 599-601.

Ruehlmann DO & Mann GE (2000). Rapid non-genomic vasodilator actions of oestrogens and sex steroids. *Curr Med Chem* **7**, 533-541.

Ruetten H, Zabel U, Linz W, & Schmidt HH (1999). Downregulation of soluble guanylyl cyclase in young and aging spontaneously hypertensive rats. *Circ Res* **85**, 534-541.

Rybalkin SD, Yan C, Bornfeldt KE, & Beavo JA (2003). Cyclic GMP phosphodiesterases and regulation of smooth muscle function. *Circ Res* **93**, 280-291.

Ryves WJ, Evans AT, Olivier AR, Parker PJ, & Evans FJ (1991). Activation of the PKC-isotypes alpha, beta 1, gamma, delta and epsilon by phorbol esters of different biological activities. *FEBS Lett* **288**, 5-9.

Sabrane K, Gambaryan S, Brandes RP, Holtwick R, Voss M, & Kuhn M (2003). Increased sensitivity to endothelial nitric oxide (NO) contributes to arterial normotension in mice with vascular smooth muscle-selective deletion of the atrial natriuretic peptide (ANP) receptor. *J Biol Chem* **278**, 17963-17968.

Sackner-Bernstein JD, Kowalski M, Fox M, & Aaronson K (2005). Short-term risk of death after treatment with nesiritide for decompensated heart failure: a pooled analysis of randomized controlled trials. *JAMA* **293**, 1900-1905.

Salamanca DA & Khalil RA (2005). Protein kinase C isoforms as specific targets for modulation of vascular smooth muscle function in hypertension. *Biochem Pharmacol* **70**, 1537-1547.

Saville B (1958). A scheme for the colorimetric Determination of Microgram Amounts of Thiols. *Analyst* **83**, 670-672.

Saxenhofer H, Raselli A, Weidmann P, Forssmann WG, Bub A, Ferrari P, & Shaw SG (1990). Urodilatin, a natriuretic factor from kidneys, can modify renal and cardiovascular function in men. *Am J Physiol* **259**, F832-F838.

Schini-Kerth VB, Boese M, Busse R, Fisslthaler B, & Mulsch A (1997). N-alpha-tosyl-L-lysine chloromethylketone prevents expression of iNOS in vascular smooth muscle by blocking activation of NF-kappa B. *Arterioscler Thromb Vasc Biol* **17**, 672-679.

Schmidt K, Klatt P, Graier WF, Kostner GM, & Kukovetz WR (1992). High-density lipoprotein antagonizes the inhibitory effects of oxidized low-density lipoprotein and lysolecithin on soluble guanylyl cyclase. *Biochem Biophys Res Commun* **182**, 302-308.

Schuschke DA, Reed MW, Saari JT, & Miller FN (1992). Copper deficiency alters vasodilation in the rat cremaster muscle microcirculation. *J Nutr* **122**, 1547-1552.

Scotland RS, Cohen M, Foster P, Lovell M, Mathur A, Ahluwalia A, & Hobbs AJ (2005a). C-type natriuretic peptide inhibits leukocyte recruitment and platelet-leukocyte interactions via suppression of P-selectin expression. *Proc Natl Acad Sci U S A* **102**, 14452-14457.

Scotland RS, Ahluwalia A, & Hobbs AJ (2005b). C-type natriuretic peptide in vascular physiology and disease. *Pharmacol Ther* **105**, 85-93.

Sebkhi A, Strange JW, Phillips SC, Wharton J, & Wilkins MR (2003). Phosphodiesterase type 5 as a target for the treatment of hypoxia-induced pulmonary hypertension. *Circulation* **107**, 3230-3235.

Serfass L & Burstyn JN (1998). Effect of heme oxygenase inhibitors on soluble guanylyl cyclase activity. *Arch Biochem Biophys* **359**, 8-16.

Shah AM (2000). Inducible nitric oxide synthase and cardiovascular disease. *Cardiovasc Res* **45**, 148-155.

Sharabi FM, Daabees TT, El Metwally MA, & Senbel AM (2005). Effect of sildenafil on the isolated rat aortic rings. *Fundam Clin Pharmacol* **19**, 449-456.

Shen YH, Wang XL, & Wilcken DE (1998). Nitric oxide induces and inhibits apoptosis through different pathways. *FEBS Lett* **433**, 125-131.

Singh RJ, Hogg N, Joseph J, & Kalyanaraman B (1996). Mechanism of nitric oxide release from S-nitrosothiols. *J Biol Chem* **271**, 18596-18603.

Singh RJ, Hogg N, Goss SP, Antholine WE, & Kalyanaraman B (1999). Mechanism of superoxide dismutase/H(2)O(2)-mediated nitric oxide release from S-nitrosoglutathione--role of glutamate. *Arch Biochem Biophys* **372**, 8-15.

Smith MP, Humphrey SJ, Kerr SW, & Mathews WR (1994). In vitro vasorelaxant and in vivo cardiovascular effects of S-nitrosothiols: comparison to and cross tolerance with standard nitrovasodilators. *Methods Find Exp Clin Pharmacol* **16**, 323-335.

Soeki T, Kishimoto I, Okumura H, Tokudome T, Horio T, Mori K, & Kangawa K (2005). C-type natriuretic peptide, a novel antifibrotic and antihypertrophic agent, prevents cardiac remodeling after myocardial infarction. *J Am Coll Cardiol* **45**, 608-616.

Sogo N, Campanella C, Webb DJ, & Megson IL (2000). S-nitrosothiols cause prolonged, nitric oxide-mediated relaxation in human saphenous vein and internal mammary artery: therapeutic potential in bypass surgery. *Br J Pharmacol* **131**, 1236-1244.

Sonnenburg WK, Rybalkin SD, Bornfeldt KE, Kwak KS, Rybalkina IG, & Beavo JA (1998). Identification, quantitation, and cellular localization of PDE1 calmodulin-stimulated cyclic nucleotide phosphodiesterases. *Methods* **14**, 3-19.

Sorenson E, Skiles EH, Xu B, Aleryani S, & Kostka P (2000). Role of redox-active iron ions in the decomposition of S-nitrosocysteine in subcellular fractions of porcine aorta. *Eur J Biochem* **267**, 4593-4599.

Stamler JS, Jaraki O, Osborne J, Simon DI, Keaney J, Vita J, Singel D, Valeri CR, & Loscalzo J (1992a). Nitric oxide circulates in mammalian plasma primarily as an S-nitroso adduct of serum albumin. *Proc Natl Acad Sci U S A* **89**, 7674-7677.

Stamler JS, Simon DI, Jaraki O, Osborne JA, Francis S, Mullins M, Singel D, & Loscalzo J (1992b). S-nitrosylation of tissue-type plasminogen activator confers vasodilatory and antiplatelet properties on the enzyme. *Proc Natl Acad Sci U S A* **89**, 8087-8091.

Stamler JS, Loh E, Roddy MA, Currie KE, & Creager MA (1994). Nitric oxide regulates basal systemic and pulmonary vascular resistance in healthy humans. *Circulation* **89**, 2035-2040.

Stamler JS, Jia L, Eu JP, McMahon TJ, Demchenko IT, Bonaventura J, Gernert K, & Piantadosi CA (1997). Blood flow regulation by S-nitrosohemoglobin in the physiological oxygen gradient. *Science* **276**, 2034-2037.

Stasch JP, Becker EM, Alonso-Alija C, Apeler H, Dembowski K, Feurer A, Gerzer R, Minuth T, Perzborn E, Pleiss U, Schroder H, Schroeder W, Stahl E, Steinke W, Straub A, & Schramm M (2001). NO-independent regulatory site on soluble guanylate cyclase. *Nature* **410**, 212-215.

Stasch JP, Alonso-Alija C, Apeler H, Dembowski K, Feurer A, Minuth T, Perzborn E, Schramm M, & Straub A (2002a). Pharmacological actions of a novel NO-independent guanylyl cyclase stimulator, BAY 41-8543: in vitro studies. *Br J Pharmacol* **135**, 333-343.

Stasch JP, Schmidt P, Alonso-Alija C, Apeler H, Dembowski K, Haerter M, Heil M, Minuth T, Perzborn E, Pleiss U, Schramm M, Schroeder W, Schroder H, Stahl E, Steinke W, & Wunder F (2002b). NO- and haem-independent activation of soluble guanylyl cyclase: molecular basis and cardiovascular implications of a new pharmacological principle. *Br J Pharmacol* **136**, 773-783.

Steinhilber ME, Cochrane KL, & Field LJ (1990). Hypotension in transgenic mice expressing atrial natriuretic factor fusion genes. *Hypertension* **16**, 301-307.

Stoclet JC, Muller B, Gyorgy K, Andriantsiohaina R, & Kleschyov AL (1999). The inducible nitric oxide synthase in vascular and cardiac tissue. *Eur J Pharmacol* **375**, 139-155.

Stone JR & Marletta MA (1994). Soluble guanylate cyclase from bovine lung: activation with nitric oxide and carbon monoxide and spectral characterization of the ferrous and ferric states. *Biochemistry* **33**, 5636-5640.

Stoupakis G & Klapholz M (2003). Natriuretic peptides: biochemistry, physiology, and therapeutic role in heart failure. *Heart Dis* **5**, 215-223.

Stuehr DJ, Cho HJ, Kwon NS, Weise MF, & Nathan CF (1991). Purification and characterization of the cytokine-induced macrophage nitric oxide synthase: an FAD- and FMN-containing flavoprotein. *Proc Natl Acad Sci U S A* **88**, 7773-7777.

Swift HR & Williams DL (1997). Decomposition of S-nitrosothiols by mercury(II) and silver salts *J. Chem. Soc., Perkin Trans 2*, 199: 1933-35.

Takahashi M, Ikeda U, Masuyama J, Funayama H, Kano S, & Shimada K (1996). Nitric oxide attenuates adhesion molecule expression in human endothelial cells. *Cytokine* **8**, 817-821.

Tewari K & Simard JM (1997). Sodium nitroprusside and cGMP decrease Ca²⁺ channel availability in basilar artery smooth muscle cells. *Pflugers Arch* **433**, 304-311.

Thiemermann C (1997). Nitric oxide and septic shock. *Gen Pharmacol* **29**, 159-166.

Travis MD, Stoll LL, Bates JN & Lewis SJ (1996). L- and D-S-nitroso-beta,beta-dimethylcysteine differentially increase cGMP in cultured vascular smooth muscle cells. *Eur J Pharmacol* **318**, 47-53.

Tremblay J, Desjardins R, Hum D, Gutkowska J, & Hamet P (2002). Biochemistry and physiology of the natriuretic peptide receptor guanylyl cyclases. *Mol Cell Biochem* **230**, 31-47.

Trujillo M, Alvarez MN, Peluffo G, Freeman BA & Radi R (1998). Xanthine oxidase-mediated decomposition of S-nitrosothiols. *J Biol Chem* **273**, 7828-7834.

Tsao LT & Wang JP (1997). Translocation of protein kinase C isoforms in rat neutrophils. *Biochem Biophys Res Commun* **234**, 412-418.

Tsikakos D, Sandmann J, Luessen P, Savva A, Rossa S, Stichtenoth DO, & Frolich JC (2001). S-Transnitrosylation of albumin in human plasma and blood in vitro and in vivo in the rat. *Biochim Biophys Acta* **1546**, 422-434.

Tsutamoto T, Kanamori T, Wada A, Miyauchi N, Murata T, & Kinoshita M (1992). Limitations of compensation by endogenous atrial natriuretic peptide in heart failure. *Jpn Circ J* **56**, 489-493.

Tyurin VA, Liu SX, Tyurina YY, Sussman NB, Hubel CA, Roberts JM, Taylor RN, & Kagan VE (2001). Elevated levels of S-nitrosoalbumin in preeclampsia plasma. *Circ Res* **88**, 1210-1215.

Uematsu M, Ohara Y, Navas JP, Nishida K, Murphy TJ, Alexander RW, Nerem RM, & Harrison DG (1995). Regulation of endothelial cell nitric oxide synthase mRNA expression by shear stress. *Am J Physiol* **269**, C1371-C1378.

Uriu-Adams JY & Keen CL (2005). Copper, oxidative stress, and human health. *Mol Aspects Med* **26**, 268-298.

Vallance P, Collier J, & Moncada S (1989). Effects of endothelium-derived nitric oxide on peripheral arteriolar tone in man. *Lancet* **2**, 997-1000.

Vallance P, Collier J, & Bhagat K (1997). Infection, inflammation, and infarction: does acute endothelial dysfunction provide a link? *Lancet* **349**, 1391-1392.

Vallance P & Chan N (2001). Endothelial function and nitric oxide: clinical relevance. *Heart* **85**, 342-350.

Vallet B (2003). Bench-to-bedside review: endothelial cell dysfunction in severe sepsis: a role in organ dysfunction? *Crit Care* **7**, 130-138.

Vo PA, Lad B, Tomlinson JA, Francis S, & Ahluwalia A (2005). autoregulatory role of endothelium-derived nitric oxide (NO) on Lipopolysaccharide-induced vascular inducible NO synthase expression and function. *J Biol Chem* **280**, 7236-7243.

Wallis RM, Corbin JD, Francis SH, & Ellis P (1999). Tissue distribution of phosphodiesterase families and the effects of sildenafil on tissue cyclic nucleotides, platelet function, and the contractile responses of trabeculae carneae and aortic rings in vitro. *Am J Cardiol* **83**, 3C-12C.

Wang TJ, Larson MG, Levy D, Benjamin EJ, Leip EP, Omland T, Wolf PA, & Vasan RS (2004). Plasma natriuretic peptide levels and the risk of cardiovascular events and death. *N Engl J Med* **350**, 655-663.

Way KJ, Katai N, & King GL (2001). Protein kinase C and the development of diabetic vascular complications. *Diabet Med* **18**, 945-959.

Williams DL (1996). S-nitrosothiols and role of metal ions in decomposition to nitric oxide. *Methods Enzymol* **268**, 299-308.

Williams SB, Cusco JA, Roddy MA, Johnstone MT, & Creager MA (1996). Impaired nitric oxide-mediated vasodilation in patients with non-insulin-dependent diabetes mellitus. *J Am Coll Cardiol* **27**, 567-574.

Witte K, Jacke K, Stahrenberg R, Arlt G, Reitenbach I, Schilling L, & Lemmer B (2002). Dysfunction of soluble guanylyl cyclase in aorta and kidney of Goto-Kakizaki rats: influence of age and diabetic state. *Nitric Oxide* **6**, 85-95.

Wolin MS, Wood KS, & Ignarro LJ (1982). Guanylate cyclase from bovine lung. A kinetic analysis of the regulation of the purified soluble enzyme by protoporphyrin IX, heme, and nitrosyl-heme. *J Biol Chem* **257**, 13312-13320.

Wong PS, Hyun J, Fukuto JM, Shirota FN, DeMaster EG, Shoeman DW, & Nagasawa HT (1998). Reaction between S-nitrosothiols and thiols: generation of nitroxyl (HNO) and subsequent chemistry. *Biochemistry* **37**, 5362-5371.

Wright A & Kanegasaki S (1971). Molecular aspects of lipopolysaccharides. *Physiol Rev* **51**, 748-784.

Wright SD, Ramos RA, Tobias PS, Ulevitch RJ, & Mathison JC (1990). CD14, a receptor for complexes of lipopolysaccharide (LPS) and LPS binding protein. *Science* **249**, 1431-1433.

Wu C, Wu F, Pan J, Morser J, & Wu Q (2003). Furin-mediated processing of Pro-C-type natriuretic peptide. *J Biol Chem* **278**, 25847-25852.

Wu CC, Ko FN, Kuo SC, Lee FY, & Teng CM (1995). YC-1 inhibited human platelet aggregation through NO-independent activation of soluble guanylate cyclase. *Br J Pharmacol* **116**, 1973-1978.

Xia Y & Zweier JL (1997). Superoxide and peroxynitrite generation from inducible nitric oxide synthase in macrophages. *Proc Natl Acad Sci U S A* **94**, 6954-6958.

Xian M, Chen X, Liu Z, Wang K, & Wang PG (2000). Inhibition of papain by S-nitrosothiols. Formation of mixed disulfides. *J Biol Chem* **275**, 20467-20473.

Xie QW, Cho HJ, Calaycay J, Mumford RA, Swiderek KM, Lee TD, Ding A, Troso T, & Nathan C (1992). Cloning and characterization of inducible nitric oxide synthase from mouse macrophages. *Science* **256**, 225-228.

Xie QW, Kashiwabara Y, & Nathan C (1994). Role of transcription factor NF-kappa B/Rel in induction of nitric oxide synthase. *J Biol Chem* **269**, 4705-4708.

Xiong Y, Fu YF, Fu SH, & Zhou HH (2003). Elevated levels of the serum endogenous inhibitor of nitric oxide synthase and metabolic control in rats with streptozotocin-induced diabetes. *J Cardiovasc Pharmacol* **42**, 191-196.

Xu KY, Huso DL, Dawson TM, Brecht DS, & Becker LC (1999). Nitric oxide synthase in cardiac sarcoplasmic reticulum. *Proc Natl Acad Sci U S A* **96**, 657-662.

Yamakage M, Hirshman CA, & Croxton TL (1996). Sodium nitroprusside stimulates Ca²⁺-activated K⁺ channels in porcine tracheal smooth muscle cells. *Am J Physiol* **270**, L338-L345.

Yamashita T, Kawashima S, Ohashi Y, Ozaki M, Rikitake Y, Inoue N, Hirata K, Akita H, & Yokoyama M (2000). Mechanisms of reduced nitric oxide/cGMP-mediated vasorelaxation in transgenic mice overexpressing endothelial nitric oxide synthase. *Hypertension* **36**, 97-102.

Yan W, Wu F, Morser J, & Wu Q (2000). Corin, a transmembrane cardiac serine protease, acts as a pro-atrial natriuretic peptide-converting enzyme. *Proc Natl Acad Sci U S A* **97**, 8525-8529.

Yano K, Bauchat JR, Liimatta MB, Clemmons DR, & Duan C (1999). Down-regulation of protein kinase C inhibits insulin-like growth factor I-induced vascular smooth muscle cell proliferation, migration, and gene expression. *Endocrinology* **140**, 4622-4632.

Yasue H, Yoshimura M, Sumida H, Kikuta K, Kugiyama K, Jougasaki M, Ogawa H, Okumura K, Mukoyama M, & Nakao K (1994). Localization and mechanism of secretion of B-type natriuretic peptide in comparison with those of A-type natriuretic peptide in normal subjects and patients with heart failure. *Circulation* **90**, 195-203.

Yasunari K, Kohno M, Murakawa K, Yokokawa K, Horio T, & Takeda T (1992). Phorbol ester and atrial natriuretic peptide receptor response on vascular smooth muscle. *Hypertension* **19**, 314-319.

Yoshizumi M, Tsuji H, Nishimura H, Masuda H, Kunieda Y, Kawano H, Kimura S, Sugano T, Kitamura H, Nakagawa K, & Nakagawa M (1999). Natriuretic peptides regulate the expression of tissue factor and PAI-1 in endothelial cells. *Thromb Haemost* **82**, 1497-1503.

Yuen PS, Potter LR, & Garbers DL (1990). A new form of guanylyl cyclase is preferentially expressed in rat kidney. *Biochemistry* **29**, 10872-10878.

Zai A, Rudd MA, Scribner AW & Loscalzo J (1999). Cell-surface protein disulfide isomerase catalyzes transnitrosation and regulates intracellular transfer of nitric oxide. *J Clin Invest* **103**, 393-399.

Zhang FX, Kirschning CJ, Mancinelli R, Xu XP, Jin Y, Faure E, Mantovani A, Rothe M, Muzio M, & Arditi M (1999). Bacterial lipopolysaccharide activates nuclear factor-kappaB through interleukin-1 signaling mediators in cultured human dermal endothelial cells and mononuclear phagocytes. *J Biol Chem* **274**, 7611-7614.

Zhao Y, Brandish PE, Ballou DP, & Marletta MA (1999). A molecular basis for nitric oxide sensing by soluble guanylate cyclase. *Proc Natl Acad Sci U S A* **96**, 14753-14758.

Zhou XB, Ruth P, Schlossmann J, Hofmann F, & Korth M (1996). Protein phosphatase 2A is essential for the activation of Ca²⁺-activated K⁺ currents by cGMP-dependent protein kinase in tracheal smooth muscle and Chinese hamster ovary cells. *J Biol Chem* **271**, 19760-19767.